MAJOR, MINOR AND TRACE ELEMENT GEOCHEMISTRY OF THE EAGLE FORD FORMATION, SOUTH TEXAS

by

SHARIVA T.R. DARMAOEN

Presented to the Faculty of the Graduate School of

The University of Texas at Arlington in Partial Fulfillment

of the Requirements

for the Degree of

MASTER OF SCIENCE IN GEOLOGY

THE UNIVERSITY OF TEXAS AT ARLINGTON

December 2013

Acknowledgements

There are many individuals to acknowledge for aiding in the preparation and submission of my thesis. I would like to thank my committee chair, Dr. Asish Basu, for assisting me in initially formulating my thoughts, sharing the wealth of his knowledge of geochemistry and his guidance until I reached my conclusions. I would like to thank Beau Tinnin for being a wonderful mentor, for introducing the topic of chemostratigraphy to me and for also taking the extra time necessary to serve as a member on my thesis committee. I would like to thank Dr. John Wickham for also being a member of my thesis committee and advising me throughout my graduate studies.

I would like to thank the geoscience management at Pioneer Natural Resources for allowing me to make use of their inorganic geochemical dataset, as well as core descriptions, XRD data, TOC data and GR logs. Thank you specifically to Neil Basu, Gervasio Barzola, Louis Goldstein, David Sanders and Skip Rhodes for supporting my thesis project. A special thank you to David Wood for analyzing more than 1000 samples of core and cuttings for this project. Thank you Nilotpal Ghosh for helping me prepare samples and get organized in the final stages of the thesis. Also, I would like to thank Gemma Hildred at Chemostrat, Inc. for her help with the methodology of their techniques.

I would like to thank Jillian Rowley and Tore Wiksveen for their help in getting organized for the thesis proposal. I would like to thank Paul Monahan for his constant support and for undertaking the graduate school journey with me. Finally, I would like to thank my family for rooting me on and giving me a reason to undertake this journey in the first place.

November 22, 2013

Abstract

MAJOR, MINOR AND TRACE ELEMENT GEOCHEMISTRY OF THE EAGLE FORD FORMATION, SOUTH TEXAS

Shariva T.R. Darmaoen, M.S.

The University of Texas at Arlington, 2013

Supervising Professor: Asish Basu

Major, minor and trace element concentrations analyzed through hand-held ED-XRF and several laboratory techniques characterize geochemical heterogeneity in strata that appear homogeneous within the Eagle Ford Formation. Two major facies were discovered in the study area; one that is rich in carbonates toward the southwest and another that increases in clay minerals toward the northeast. Both facies are enriched in proxies of micronutrients for planktonic organisms. Nutrients precipitated by two possible mechanisms; volcanic input or nutrient cycling from Large Igneous Provinces through upwelling of bottom waters. The provenance indicating rare earth element pattern for both facies deviate from average shale (i.e., average upper continental crust). Elemental data show a combined felsic to mafic source character and imply that volcanism was continuous throughout Eagle Ford time, affecting paleoredox conditions. The Eagle Ford was largely deposited under an anoxic bottom water column, yet cyclical redox variations mirrored changing bottom water column conditions.

Table of Contents

List of Figures

List of Tables

Chapter 1

Introduction

1.1 Project Objectives and Approaches

The objective of this thesis is to characterize lithostratigraphic facies of the South Texan Eagle Ford Formation using chemostratigraphy and to illustrate how events outside the depositional center affected sedimentation. Concentrations of major, minor and trace elements within the rocks of the Eagle Ford Formation characterize facies variations and aid in inferring paleodepositional conditions and a range of redox conditions. The cause of an anoxic to euxinic bottom water column and high rates of organic carbon burial during Eagle Ford time are widely hypothesized to be due to enhanced bioproductivity resulting from nutrient input into the Late Cretaceous ocean caused by a combination of upwelling mechanisms, volcanic gas output into the atmosphere or the increased occurrence of Large Igneous Provinces (LIPs) erupting flood basalt into the oceans (Brumsack, 2006; Sinton, 1996; Wignall, 2001; Kerr et al., 2003). The principal approaches in this research are outlined below:

1. Major elements are used to outline major carbonate- and clay-rich facies changes across the Eagle Ford study area.
2. Select minor and trace elements are indicative of a range of redox conditions (oxygenated to oxygen-deficient bottom water column) during Eagle Ford time.
3. Rare earth element concentrations and patterns can be used to decipher the provenance of Eagle Ford sediments.
4. The above approaches imply that volcanic ash deposition in the Eagle Ford depocenter in South Texas had an impact on water column conditions.

Major strides have been made to understand characteristics of the Eagle Ford Formation and its depositional controls. It is the objective of this thesis to bring combined research of other workers (Sinton, 1996; Wignall, 2001; Keller, 2005; Brumsack, 2006; Tribovillard et al., 2006;

Kearns, 2011) in conjunction with the extensive geochemical data of this study into a formative description of the origin and character of the sediments within the Eagle Ford Formation.

1.2 Introduction to Chemostratigraphy

Chemostratigraphy can be used to infer mineralogy, depositional environment, sediment provenance and to correlate strata between wells (Tinnin et al., 2013). Subtle geochemical changes can highlight heterogeneity in marine strata that may appear homogeneous (Tinnin et al., 2013). Major elements are used to map lateral facies changes along the Eagle Ford subsurface study area; multiple minor and trace element concentrations and ratios are used to infer paleodepositional conditions and rare earth elements (REEs) are used as indicators of sediment provenance.

Marine sediments are derived from different components of the geosphere by lithogenous, biogenous, hydrogenous and diagenetic processes (Calvert and Pedersen, 2007). Sageman and Lyons (2003) outlined various methods of element provenance that apply simultaneously to the Eagle Ford including detrital input, biogenic input or authigenic input. Terrigenous detritus has been weathered and transported from a continental crust source or could have been deposited as volcanic debris. Biogenic components, also the indicators of paleo-productivity, are derived from planktonic fauna in the oceans or terrestrial organisms. Authigenic material occurs naturally in the depositional environment the elements are found in (in situ), and precipitate at or near the sediment water interface as a function of Eh-pH, organic and inorganic processes (e.g. Sageman and Lyons, 2003; Brumsack, 2006). Chemical elements are transferred from the continental crust into clastic sediments as mechanical erosional products. Many elements such as REEs can be expected to have an average geochemical composition of their source, the average upper continental crust (Wedephol, 1971; Taylor and McLennan, 1985). Using the enrichment or depletion of major, minor and trace elements relative to their crustal abundances, inferences at paleodepositional conditions can be made (Tinnin et al., 2013). Grains in mudstone and claystone, in comparison to sandstone and conglomerate, possess

homogeneous elemental distributions and are more stable over wide areas; therefore providing greater potential for correlation (Cullers, 1995; Pearce et al., 1999).

Local variations in Total Organic Carbon (TOC) concentrations can also be correlated to trace metal deposition (Yao Tian et al., 2012). Organic-rich sediments contain high concentrations of trace elements depending on paleodepositional conditions (Brumsack, 2006; Tribovillard et al., 2006). Trace elements are adsorbed onto organic matter as well as on the surface of clay minerals that may be present (Taylor and McLennan, 1985; Horowitz, 1991; Tucker, 2001). The presence of elevated amounts of organic matter coeval with high trace metal concentrations can be used to define the boundaries of certain redox conditions (Tinnin et al., 2013). The study location featured in this thesis is in an area known for condensate/light oil Eagle Ford production where moderate amounts of TOC are present (Howard Weil Incorporated, 2011).

1.3 Study Location

The Eagle Ford Formation and its Late Cretaceous time equivalents were deposited during a 7 Ma time frame throughout the Middle Cenomanian to Late Turonian (~89-96 Mya) as a continuous unit stretching across Texas and into Louisiana (Figure 1.1) (Harbor, 2011; Matsutsuyu, 2011). Eagle Ford Formation outcrops extend from northeastern Texas to southwest Texas (Figure 1.2). Surface outcrops (road cuts) have been studied along U.S. Highway 90 in West Texas in Val Verde and Terrell counties by Donovan et al. (2012) as well as in Bell, Falls, Hill, Limestone, McLennan and Navarro counties in central Texas by Charvat (1985). Subsurface Eagle Ford in south Texas is found at subsea depths ranging from 4,000 feet to greater than 14,000 feet. It has been deduced from outcrops and subsurface interpretations that Eagle Ford rocks dip gently east and east-southeast toward the Gulf of Mexico Basin (Harbor, 2011).

The south Texas area of study is along the strike of the Early to Mid Cretaceous shelf edges, and at times, between the Edwards/Stuart City and Sligo shelf margins. The Edwards/Stuart City and Sligo reef margins are separated by a maximum distance of thirty miles and converge to the northeast near Live Oak and Bee counties; this created an accommodation

space and depocenter for a thick package of Eagle Ford sediments (Harbor, 2011). The bounds of this project are centered in Live Oak, Karnes and DeWitt counties just southeast of San Antonio, Texas (Figure 1.3). In this area of study the Eagle Ford Formation does not outcrop. All data are available from subsurface oil and gas wells as drill cuttings or core. The subsurface Eagle Ford has recently undergone much study in south Texas while its contemporary units have been examined in west Texas, near the Maverick Basin, and in east Texas (Charvat, 1985; Surles Jr., 1987; Donovan and Staerker, 2010; Harbor, 2011; Kearns, 2011; Donovan et al., 2012; Moran, 2013; Workman, 2013; McGarity, 2013).

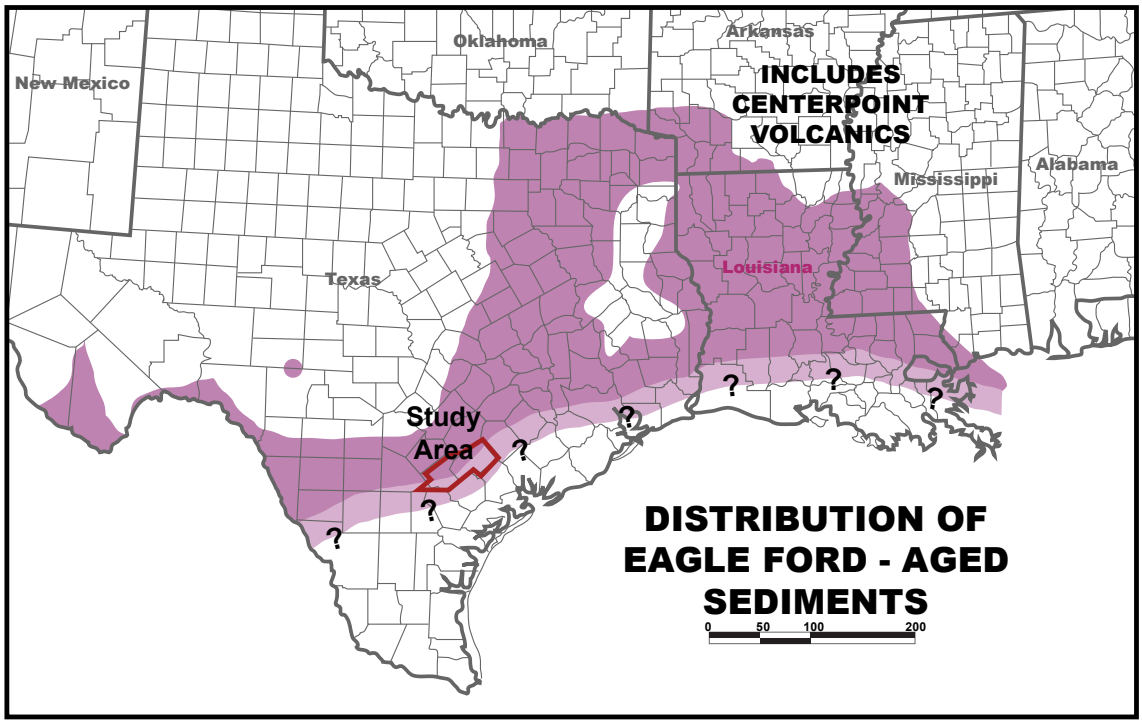

Figure 1.1 Distribution of the Eagle Ford Formation and its time equivalents

Modified from Adams and Carr, 2010 and references therein. Republished by permission of the Gulf Coast Association of Geological Societies, whose permission is required for further publication use.

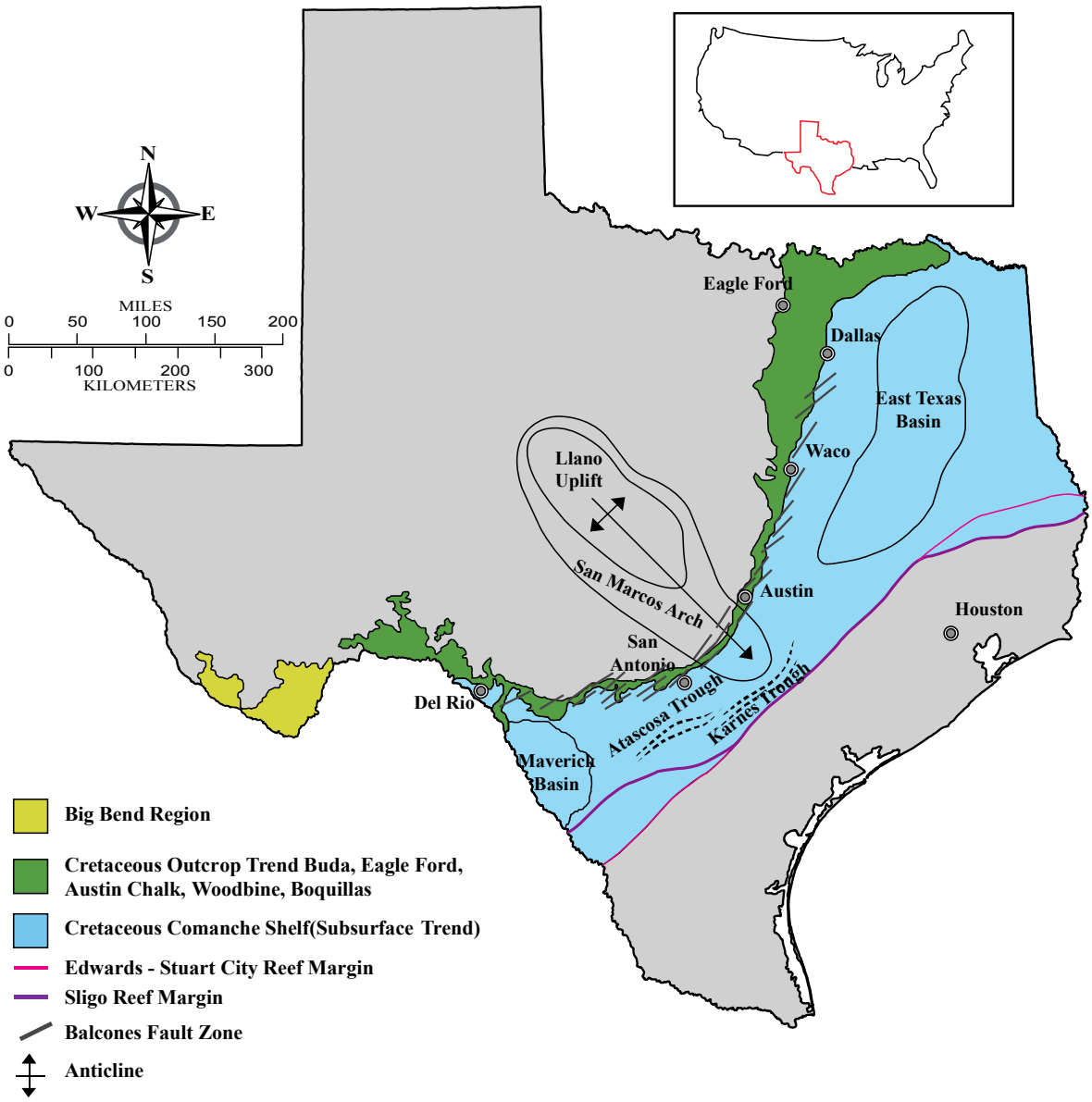

Figure 1.2 Generalized structural features near Late Cretaceous strata in Texas

Outcrops are outlined in dark green. Modified from Workman, 2013.

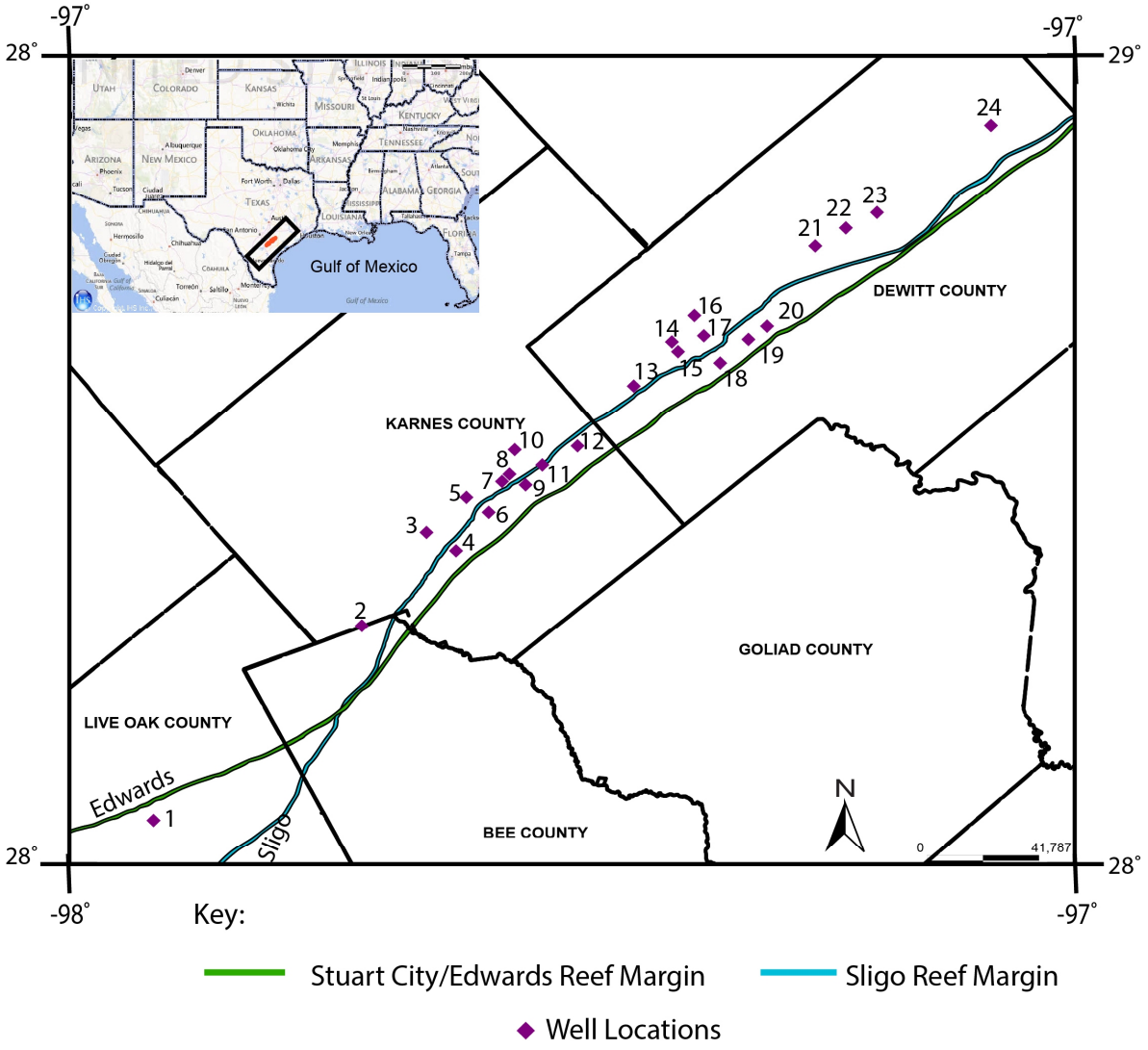

Figure 1.3 Study area and well locations in south Texas

Wells are located parallel to Early and Mid-Cretaceous shelf margins. Top left figure from IHS Enerdeq® Browser v2.3.5 through personal access of software.

1.4 Eagle Ford Oil and Gas Resources

Shale plays have seen rapid development across the United States since the early 2000s (Figure 1.4). The Eagle Ford Shale is one of the largest shale plays currently undergoing production and development.

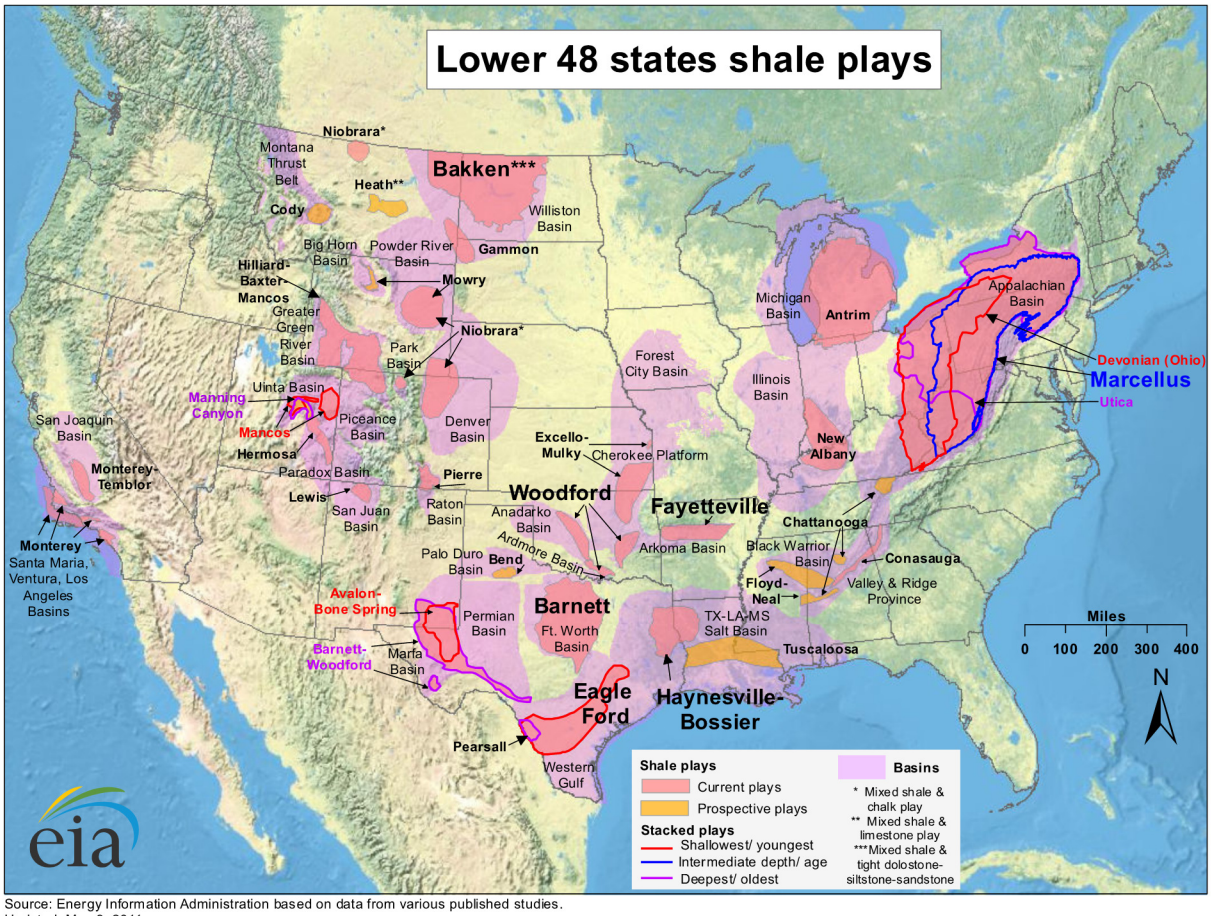

Source: Energy Information Administration based on data from various published studies.
Updated: May 9, 2011

Figure 1.4 Shale plays in the Lower 48 of the United States.

From the U.S. Energy Information Administration (EIA), 2011.

The Eagle Ford has proven to be a prolific unconventional oil and gas play since the first discovery well, the STS-241 #1H, was drilled in 2008 by Petrohawk in LaSalle County, Texas (Harbor, 2011). One way that unconventional plays differ from conventional plays is that the reservoir is also the source rock where hydrocarbons were generated. The requirements placed for conventional petroleum plays, including the presence of a trap and seal to prevent hydrocarbon migration, are interpreted differently. Unconventional reservoirs, unlike conventionals, are characterized by low matrix permeability (<0.1 millidarcy (mD)), yet do exhibit matrix porosities ranging from 5% to 14% (Jianwei Wang and Yang Liu, 2011; Workman, 2013).

The Eagle Ford Shale play is laterally extensive; roughly 50 miles wide and 400 miles long (Railroad Commission of Texas, 2013). Production to date spans twenty-one active fields in twenty-four counties (Figure 1.5). Production continues to grow as more development wells are planned. The Eagle Ford Formation is believed to be the source rock for the Austin Chalk, Olmos, Lobo and other formations in the East Texas Basin; wells from these formations are typically conventional oil and gas wells (Dawson, 2000; Howard Weil Incorporated, 2011). The Eagle Ford source rock has been economically producible largely in part to the combination of hydraulic fracturing and horizontal drilling technology, first successfully applied by Mitchell Energy in 1998 in the Barnett Shale (Bowker, 2007; Chazan, 2013).

In the first quarter of 2013 alone the Eagle Ford produced 512,355 billions of barrels (bbl) of oil per day and 1,945 million cubic feet (MMCF) of total natural gas (Railroad Commission of Texas, 2013). Eagle Ford oil production surpassed 600,000 bbl/day for the first time in May 2013 from a little less than 4,000 oil wells producing that amount (Dukes, 2013). The northern, shallower, portion of the play yields oil, condensate and wet gas while the deeper, southern portion of the play yields dry gas (Howard Weil Incorporated, 2011). Hydrocarbon yield changes as a function of increasing thermal maturity and increasing depth, from updip toward the basin (Figure 1.6) (Harbor, 2011).

The study area in Karnes, DeWitt and Live Oak counties provides some of the highest economic returns in the play area due to the Eagle Ford's position within the condensate/volatile oil window and because of the combination of high porosity, high brittleness and low clay content in certain areas. These combined parameters enhance the ability to successfully hydraulically fracture rocks (Howard Weil Incorporated, 2011). One of the reasons the Eagle Ford has been such a successful play is due to high organic matter content within the play area, varying from 1-7 wt. % TOC, depending on the locale, abundance of paleo bioproductivity and subsequent preservation of organic matter (Tucker, 2001; Hildred et al., 2011).

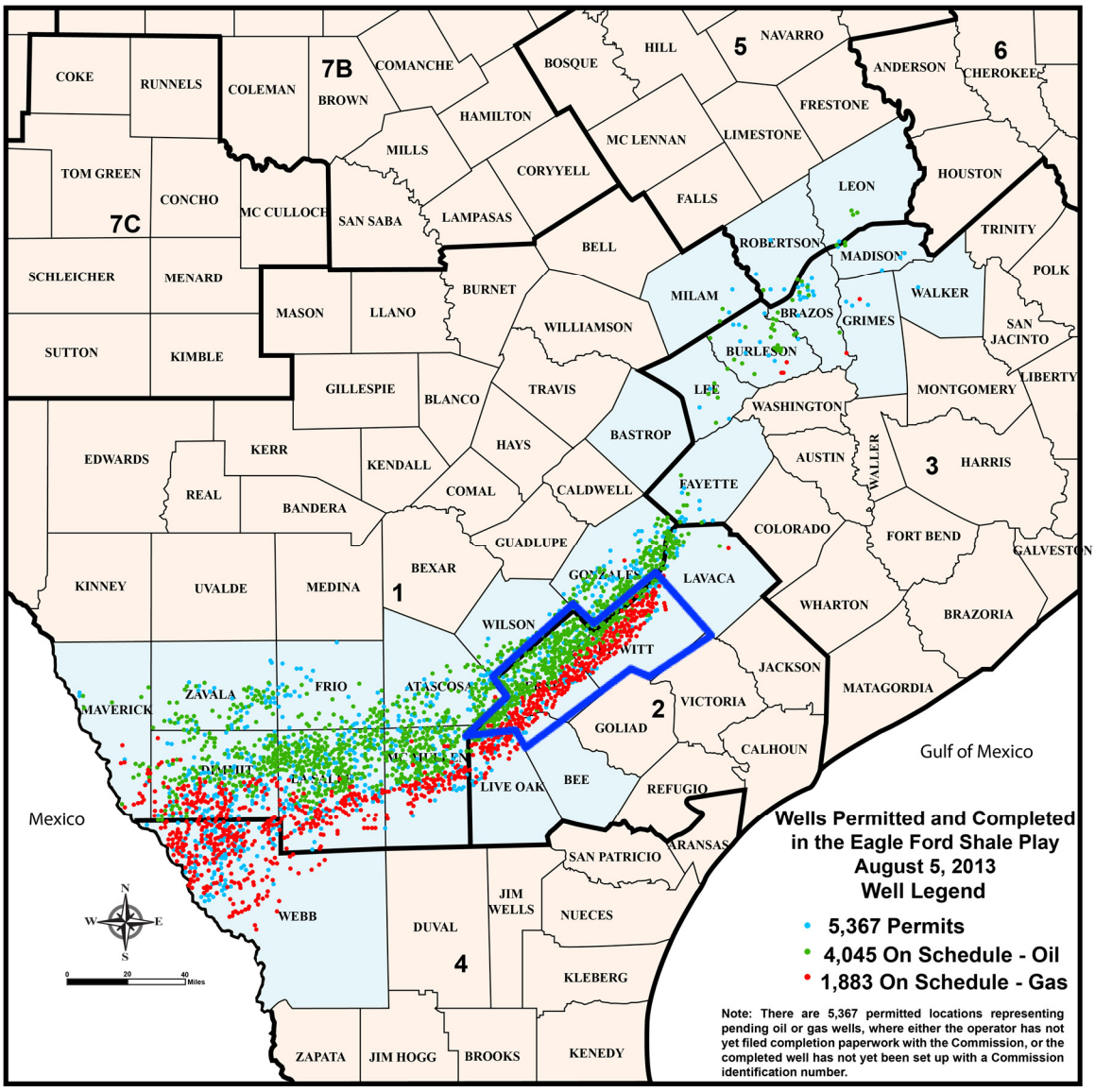

Figure 1.5 Drilling activity along the Eagle Ford Shale play trend

The study area is highlighted in the blue box. Modified from the Railroad Commission of Texas, 2013.

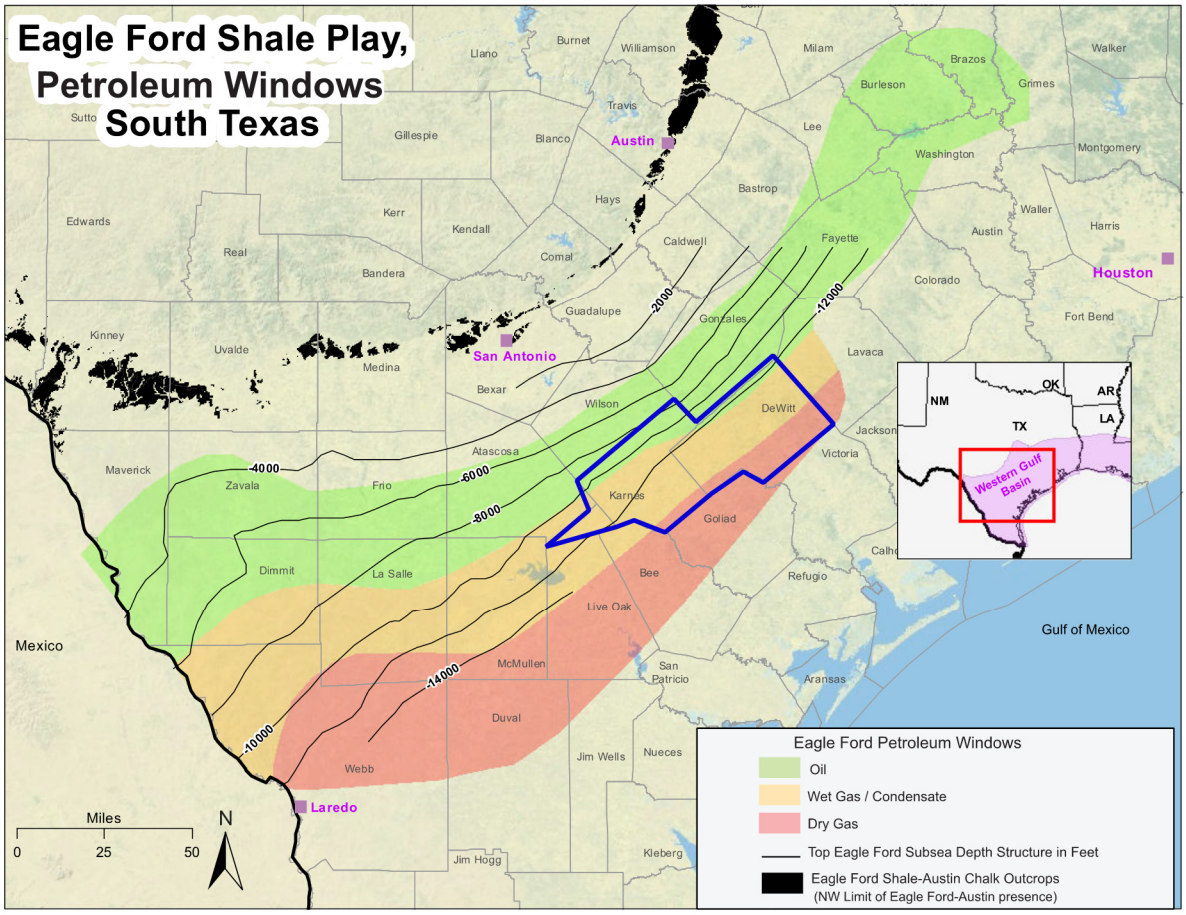

Figure 1.6 Petroleum windows of the Eagle Ford

The study area is highlighted in blue. Modified from the U.S. Energy Information Administration (EIA), 2010.

Gross Eagle Ford thickness ranges from less than 21 meters (70 feet) in the northeast to more than 201 meters (660 feet) in the western Maverick Basin (Howard Weil Incorporated, 2011). The Eagle Ford reservoir ranges from 43 meters (140 feet) to 137 meters (450 feet) thick, deepening from the northeast to the southwest with an average thickness of 76 meters (250 feet) (Howard Weil Incorporated, 2011; Railroad Commission of Texas, 2013). Wells completed in South Texas can reach as deep as 14,000 feet true vertical depth (TVD) and span 4,500 feet-9,000 feet. measured depth (MD) laterally (Howard Weil Incorporated, 2011).

Subsurface well control has provided a clear understanding of facies along the remnant Cretaceous reef margins (Sligo and Edwards/Stuart City) to oil and gas companies, and yet it is still undergoing investigation by academic institutions. The need to understand the subsurface equivalent of the Eagle Ford Shale better has been expressed; and even more specifically, the need to understand the factors controlling the success of hydrocarbon production from the Eagle Ford Shale (Yao Tian et al., 2012).

1.5 Previous Work

The Eagle Ford Formation has been studied by individual oil and gas companies as well as the academic community in outcrop and in the subsurface due to prolific oil and gas production and the need to better understand its source rock characteristics. To date there has been much discussion regarding detailed sedimentology and provenance for the subsurface extent of the Eagle Ford Formation and different parties have contributed different interpretations (Adams and Carr, 2010; Hentz and Ruppel, 2010; Donovan et al., 2012; Yao Tian et al., 2012). A review of selected works completed is appropriate in order to outline the understanding of the Eagle Ford Formation to date.

While the Eagle Ford was deposited from the Maverick Basin to the East Texas Basin, the nomenclature of the Eagle Ford surrounding the San Marcos Arch in South Texas is different from other depositional areas (Figure 1.7). Eagle Ford aged sediments are also found in Louisiana, southern Arkansas and Oklahoma, where the formation is known as the Tuscaloosa Shale. The Eagle Ford Formation was named after the town of Eagle Ford near Dallas in North Texas (Hill, 1901). The subsurface Eagle Ford sediments are found southeast of the outlined outcrop band (Figure 1.2). Harbor (2011) and Charvat (1985) give a thorough review of historical Eagle Ford Formation outcrop descriptions in central Texas.

Moreman (1942) divided the Eagle Ford Group into the Tarrant, the Britton and the Arcadia Park formations, from bottom to top, in north-central Texas. In east Texas, the Eagle Ford Group disconformably overlies the Woodbine Group (Woodbine sands, Maness Shale and

Pepper Shale), which was deposited by the Woodbine Delta (Dawson, 2000; Hentz and Ruppel, 2010). The Woodbine Delta prograded from the northeast to the southwest beyond the East Texas Basin and deposited fine-grained siliciclastic sediments, which may have reached as far southwest as the Eagle Ford depocenter shown in Figure 1.8 (Galloway, 2008).

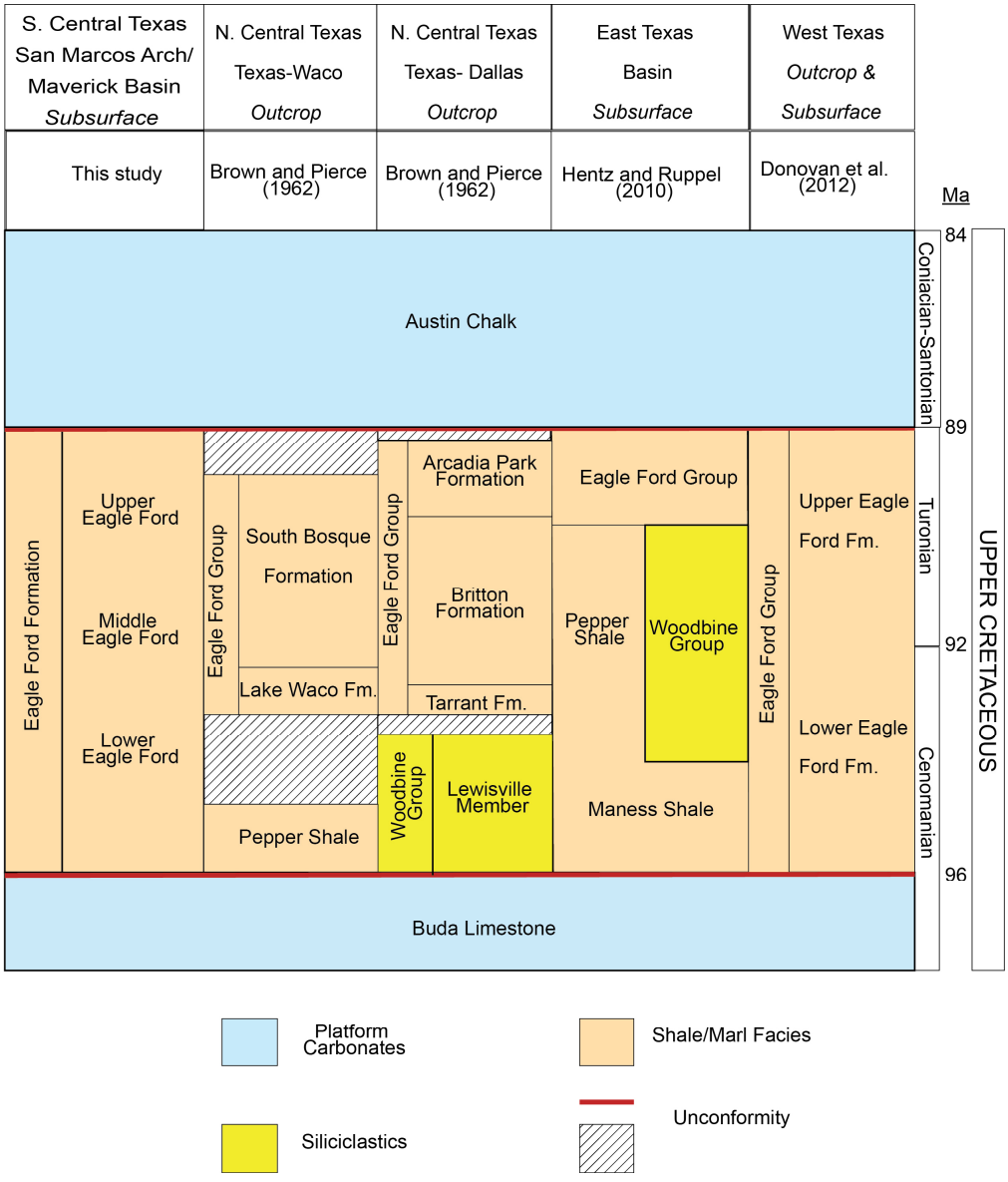

Figure 1.7 Regional stratigraphic column.

The Eagle Ford Formation and its Cretaceous time equivalents in Texas.
Not to scale. Modified from Adams and Carr, 2010, Moran, 2013, and Workman, 2013.

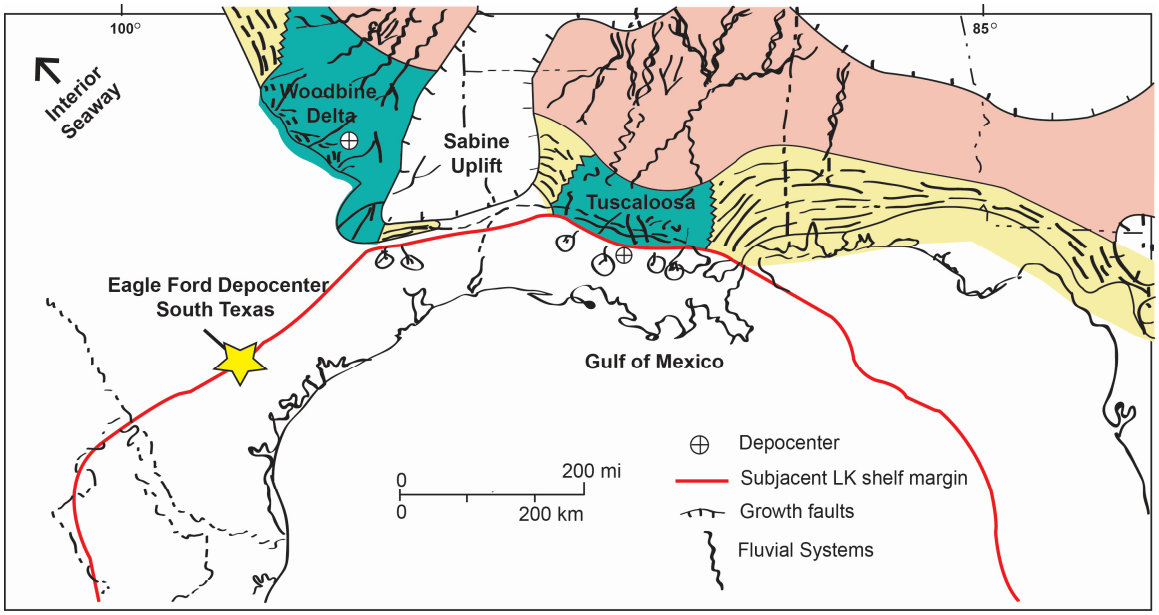

Figure 1.8 Late Cretaceous deltas

Prograding deltas carried terrigenous sediment toward the southwest. Modified from Galloway, 2008.

In central Texas, Colonel William Prather divided the Eagle Ford Group into two formations called the “South Bosque Marls” in 1902 (Charvat, 1985). Later the nomenclature was changed by Adkins and Lozo (1951) to the South Bosque Formation for the upper part and the Lake Waco Formation for the lower part of the Eagle Ford Group. In west Texas, Donovan and Staerker (2010) and Donovan et al. (2012) have given a description of outcrops and subsurface in the Eagle Ford equivalent Boquillas facies in Lozier Canyon in Terrell County as well as its sequence stratigraphic history. First, Donovan and Staerker (2010) named two members of the Boquillas Formation; the Rock Pens and Langtry members. Donovan et al. (2012) later changed the nomenclature to the Eagle Ford Group in order to tie the outcrops of West Texas to the subsurface of South Texas. The Eagle Ford Group in west Texas has been further subdivided into an Upper and Lower Eagle Ford formations with two members each. The Upper Eagle Ford Formation is composed of the Langtry Member above an Unnamed Member. The Lower Eagle

Ford Formation is composed of the Middle Shale Member and an Unnamed Member (e.g. Figure 5 in Donovan et al., 2012).

Donovan et al. (2012) also defined three transgressive-regressive cycles within the Boquillas Formation and correlated a sequence stratigraphic framework from outcrops in West Texas to subsurface Eagle Ford wells in south and central Texas. A major second-order transgression was identified but there are also smaller third-order cycles observed which depict the onset of a regression at the end of Eagle Ford time (Donovan et al., 2012). Vail et al. (1977) suggested that a major transgression reached a still stand at the Cenomanian-Turonian boundary; the onset of a regression that peaked in the mid-Turonian and returned to a transgression into late Turonian time (Figure 1.9).

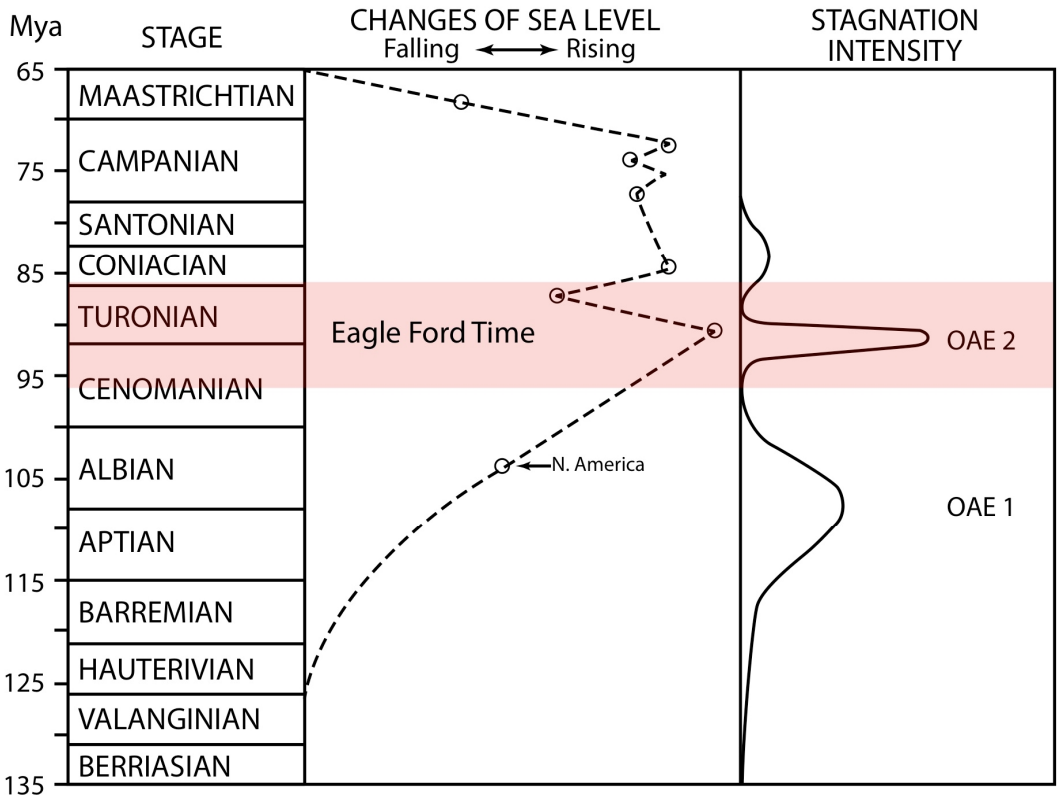

Figure 1.9 Generalized second-order sea level curve and water stagnation intensity curve for the Cretaceous period

Modified from Arthur and Schlanger (1979).

There are few published works that infer paleodepositional environments during Eagle Ford time in south Texas. Published interpretations for the depositional setting of the Eagle Ford in south Texas include models suggested by Donovan et al. (2012), which depict a carbonate platform exposed north of the Sligo and Edwards reef margins centered above the San Marcos Arch, a structural high. This platform affected the depositional area surrounding the south Texas submarine plateau that was restricted from the open ocean and allowed the deposition of organic-rich, calcareous mudstones. Hentz and Ruppel (2010) provide a lithostratigraphic framework which aims to create a more approximate picture of the gradation of the facies from the East Texas Basin to the Gulf Coast. Hentz and Ruppel (2010) suggest that the Eagle Ford Formation overlies the Maness/Pepper Shales toward the East Texas Basin. Their illustration depicts that north of our study area, stratigraphically above the San Marcos Arch, the contact between the Eagle Ford Shale and the Maness/Pepper Shales exists (Figure 1.10). The contact/interfingering of central Texas Eagle Ford facies to Woodbine facies toward northeast-central Texas have been generalized to be near the Brazos River near Waco (Charvat, 1985). The location of the contact between south Texas Eagle Ford facies and Woodbine influenced facies is still ambiguous yet Hentz and Ruppel (2010) defined that it exists near the paleohigh San Marcos Arch.

Regional studies and mapping have been completed with different interpretations on where the boundaries between the members within the Eagle Ford Formation lie and what the depth and thickness is across the Cretaceous margin trend (Adams and Carr, 2010; Donovan and Staerker, 2010; Yao Tian et al., 2012). In south Texas, a truncation of Eagle Ford sediments occurs proximal to the San Marcos Arch and thickening occurs toward the Maverick Basin; specifically the upper and lower Eagle Ford (Hentz and Ruppel, 2010). The opposite is also true in central Texas. The Eagle Ford thins southward and truncates onto the San Marcos Arch with an unconformity between the Eagle Ford and Austin Chalk (Harbor, 2011 and references therein). Yao Tian et al. (2012) divide the Eagle Ford into three members. Adams and Carr (2010) and

Donovan et al. (2012) divide the Eagle Ford into a lower and upper unit based on similar lithological characteristics. Authors choose their own subdivisions of the Eagle Ford based on the lithological changes seen in collected samples or wireline logs.

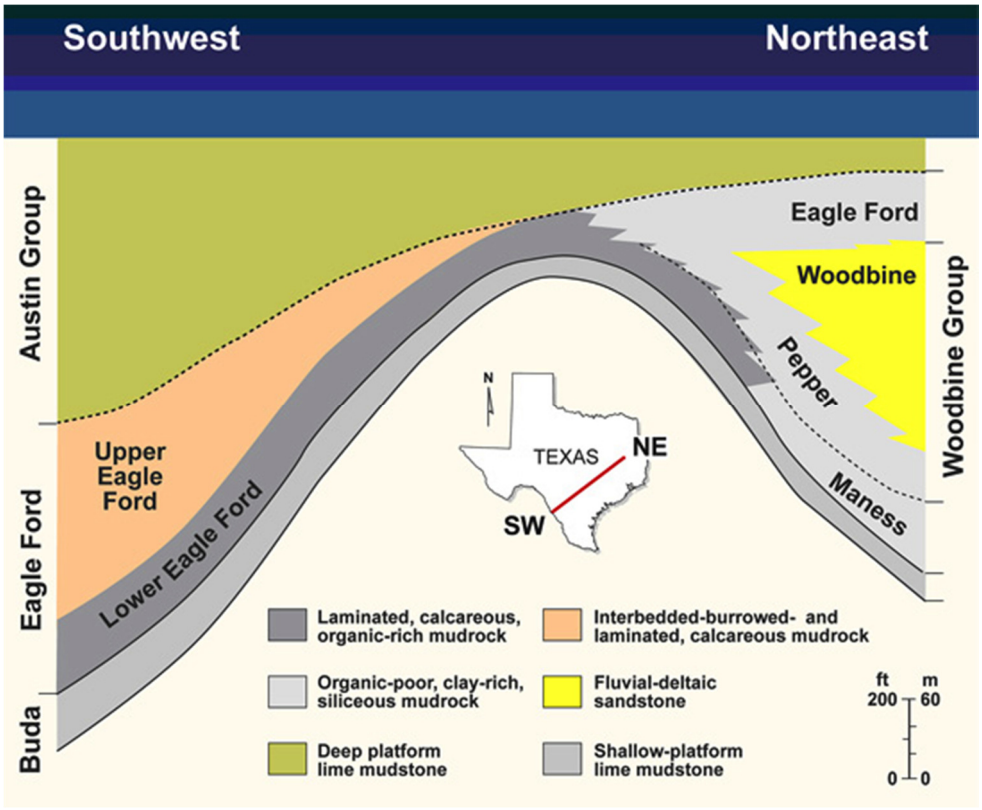

Figure 1.10 The contact of the Eagle Ford Formation and Woodbine Group

The contact overlies the anticlinal San Marcos Arch. Modified from Hentz and Ruppel, 2010. Republished by permission of the Gulf Coast Association of Geological Societies, whose permission is required for further publication use.

Microfacies descriptions give a clear petrographic description of Eagle Ford rocks. Dawson (2000), Harbor (2011), Workman (2013) and McGarity (2013) provide detailed microfacies descriptions based on petrographic and core studies. Locally, Harbor (2011) characterized the microfacies of the south Texas Eagle Ford Formation using core and wireline log data in fourteen counties analyzed by X-ray Fluorescence (XRF) and X-ray Diffraction (XRD). Harbor (2011) defined nine different subsurface Eagle Ford facies including massive argillaceous mudrock, laminated calcareous foraminiferal mudrock, laminated fossiliferous wackestone/

packstone, laminated foraminiferal and peloidal packstone, massive to burrowed kaolinitic claystone, laminated wackestone, disrupted bedded foraminiferal packstone, massive Inoceramid packstone, and bioturbated lime wackestone. Fairbanks and Ruppel (2012), Workman (2013) and McGarity (2013) found similar facies based on their own work. Laminated sediments with a lack of bioturbation have long been regarded as representative of deposits in a stagnant marine environment with little water circulation (Charvat, 1985; Arthur and Sageman, 1994). The general microfacies found in the Eagle Ford are laminated and not bioturbated in the lower Eagle Ford and massive and bioturbated in the upper Eagle Ford (Harbor, 2011).

A multitude of papers discuss general causes of ocean anoxia and source rock deposition that may be an effect of water stagnation (see Tribovillard et al. (2006) and Algeo et al. (2012) for an extensive review). Methods utilized to understand ocean anoxia consisted of interpreting major element, trace element, and stable isotope data collected from core or drill cuttings (e.g. Demaison and Moore, 1980; Calvert and Pedersen, 1993; Calvert et al., 1996; Turgeon and Brumsack, 2006; Poulson et al., 2006; Mort et al., 2007; Algeo and Rowe, 2012; Lezin et al., 2013). The findings from these authors conclude that enhanced bioproductivity is a precursor to an anoxic water column and is also directly linked to increased organic carbon burial and increased organic matter preservation. The Eagle Ford experienced periods dominated by anoxia in the water column and was also interrupted by shorter periods in which oxic to suboxic conditions dominated (Harbor, 2011).

Redox sensitive trace metals such as molybdenum (Mo) and uranium (U) are useful for determining levels of oxygen in a water column due to their low concentrations in oxic facies and authigenic enrichment under anoxic conditions (Algeo et al., 2012). Typical analogs for anoxic to euxinic basins are the Black Sea, the Cariaco Basin, or upwelled western margins of continents (e.g. Demaison and Moore, 1980; Brumsack, 2006). Anoxic basins have high Total Organic Carbon (TOC) and Mo concentrations enriched above average shale, making them ideal proxies for black shale deposition in different marine settings (Brumsack, 2006). Kearns (2011)

completed a major and trace element study of six cores from six counties within and near this thesis' study area using a hand-held ED-XRF. Moran (2013) analyzed the J.A. Leppard #1 core in Bee County and gave a description of the results obtained from hand-held ED-XRF analysis. Both authors expressed the usefulness of trace metals (Mo, V, Ni, Cu and U) as redox proxies and major elements as proxies for mineral composition (i.e., SiO_2 for quartz and Al_2O_3 for aluminum). These authors suggested that the Eagle Ford depocenter experienced cyclical anoxia and euxinia followed by oxic conditions. The Eagle Ford depocenter was also defined as having variable degrees of restriction from open marine settings and yet did experience upwelling events of different magnitudes (Moran, 2013; Kearns, 2011).

Biostratigraphic studies have identified planktonic foraminifera, ostracods, inoceramid bivalves, micritic peloids, accessory echinoderms, calcispheres, pelecypods, ammonites, and fish debris in outcrop (Charvat, 1985 and references therein; Dawson, 1997; Rowe et al., 2013). Benthic foraminifera are rare due to generally anoxic to euxinic water column conditions, yet it has also been suggested that benthonic invertebrates can live in dysaerobic zones where the oxygen concentrations range from 0.3 to 1.0 mL O_2/ L H_2O (Charvat, 1985, and references therein). Based on fauna found in samples from Eagle Ford outcrops, it was determined that the depositional environment showed an anaerobic to dysaerobic character (Charvat, 1985).

Herrin (1957) and Charvat (1985) have completed an extensive study on volcanic ash deposition within the Eagle Ford Formation in Central Texas. Ross et al. (1929) discussed water-laid volcanic rocks deposited in Arkansas, Oklahoma and northeast Texas during the Late Cretaceous as well as their possible source. Ross et al. (1929) showed that bentonite form by the alteration and devitrification of volcanic tuff and ash in an oxygen free environment, in the presence of water and in the presence of bicarbonates, sodium chloride, and possibly magnesium salts from seawater. Charvat (1985) has recognized the possibility of the volcanoes described in Ross et al. (1929) as being the source of ash in Eagle Ford rocks of central and southwest Texas but there is a need to prove this hypothesis. It is appropriate to note that ash

can travel large distances when carried by wind and that the source may be in an area that was previously not considered (Turgeon and Creaser, 2008) due to its distance from the Eagle Ford depocenter. Charvat (1985) completed a bentonite study on Eagle Ford outcrops in central Texas by analyzing fifty-four bentonite samples to determine their mineral composition using X-ray Diffraction (XRD). The mineralogy of the bentonite beds led Charvat (1985) to the conclusion that they were derived from the alteration of volcanic ash and formed in situ in a shallow marine environment.

Volcanoes centered in southwestern Arkansas (Hunter and Davies, 1979) or the Western Interior (Kauffman, 1977) are also hypothesized to be the source of the bentonite in central Texas. There is also the possibility of a source in west Texas in Uvalde County as igneous detritus was described by Adkins (1932). The proximity of the Eagle Ford depocenter to the Western Interior Seaway gives importance to studies on the Late Cretaceous epicontintental sea. The effect of the Sevier Orogeny can also not go unnoticed as it tectonically affected the regional study area.

Volcanism had a significant impact on black shale deposition during or preceding Ocean Anoxic Event 2 (OAE 2) and proving this theory has been attempted by authors on different basins (e.g., Sinton, 1996; Turgeon and Creaser, 2008; Keller, 2005). Kearns (2011) described the cause and effect relationship between increased volcanism during the Late Cretaceous with black shale deposition. His interpretation is that volcanism caused a chain reaction in the atmosphere and biosphere and led to the deposition of the Eagle Ford Shale. Further discussion on the impact of volcanism on the Eagle Ford is presented in later chapters.

The Eagle Ford Formation belongs to the group of black shales that have been deposited globally during Cenomanian-Turonian time. The Cenomanian-Turonian boundary occurs during Eagle Ford time and has been recorded in the sedimentary record. Ocean Anoxic Event 2 which precedes and occurs across the Cenomanian-Turonian boundary (Figure 1.9) is evident in a positive carbon isotope (δ^{13} C) excursion illustrated by Donovan et al. (2012) in the upper Eagle

Ford. The age of the Eagle Ford Group has mainly been based on biostratigraphic studies of ammonites, calcareous nannofossils and planktonic foraminifera (Ming-Jung Jiang, 1989). Charvat (1985) and references therein note that OAEs are really a series of local anoxic events that are connected by tectonics. Therefore, this study views the Eagle Ford Formation as a local depositional event that belongs to the greater OAE 2 phenomenon.

1.6 Significance of Study

This thesis provides a succinct geochemical dataset covering a linear distance of ~58 miles along a NE-SW strike line within three contiguous counties. The importance of this project is in the provision of well control that is much more detailed than previous studies. Harbor (2011), Kearns (2011), and Moran (2013) have published similar work with data sets of different magnitudes. Harbor (2011) and Kearns (2011) used a set of wells which covered fourteen and six counties, respectively. Moran (2013) studied one core in Bee County. This thesis would expand on the results of the authors' work using a multitude of core and cuttings data from twenty-four wells in total but concentrated over a smaller area. Core is difficult and costly to acquire yet cuttings are available for every well as a part of the drilling process. Cuttings can provide an individual stratigraphic framework as wells as complement other reservoir characterization parameters, such as XRD mineralogy studies (Tinnin et al., 2013; Pearce et al., 1999). Core, however, ultimately represents a homogeneous sample, which will give more precise results.

There is a clear facies shift in DeWitt County, seen in gamma ray logs as well as elemental data illustrated regionally by Hentz and Ruppel (2010) using wireline log data. This change can be illustrated by mapping major and trace elements. Another benefit of this data set is that it spans the entire vertical organic-rich section of the Eagle Ford Formation that falls mainly within the lower Eagle Ford Member. Since organic matter acts as a trace element sink (Horowitz, 1991), it is useful to have this data readily available. This thesis will add on to the existing knowledge about the south Texas equivalents of the Eagle Ford. Ambiguous facies and redox changes can be characterized using this geochemical dataset.

Chapter 2

Geologic Setting

2.1 Depositional Environment

The Eagle Ford's paleoposition in south Texas was medial to distal to the shoreline during the Late Cretaceous as shown in Figure 2.1. The shallow water shelf on which the Eagle Ford was deposited was surrounded by a deeper shelf to slope section basinward (Harbor, 2011). In the defined study area, the Eagle Ford was deposited on an extended shelf, at times locally restricted from the open ocean, between the Mid and Early Cretaceous aged Edwards/Stuart City and Sligo reef margins (Scott, 2010). While there are differing opinions on the conditions that existed as the Eagle Ford Formation was deposited, the general consensus based on fossil identification is that it was a shallow marine environment, ranging from inner to outer shelf, which was connected to the Cretaceous Interior Seaway (Surles Jr., 1987; Sageman and Arthur, 1994; Dawson, 2000; Moran, 2013). The water depth is estimated to have been between 50 meters (164 feet) and 200 meters (656 feet) deep above a submarine plateau formed on an extended shelf environment (Arthur and Sageman, 1994; Donovan et al., 2012; Tinnin et al., 2013).

There were several factors that affected the Eagle Ford's paleodepositional environment, including a global transgressive sequence resulting in sea level rise and shallow epeiric seas covering the North American continent (Figure 2.1). Although the main eustatic event during the Upper Cretaceous was a second-order transgressive sequence, third-order cycles of transgression and regression occurred, denoted by defined parasequence sets (Adams and Carr, 2010; Charvat, 1985; McGarity, 2013). The sequence stratigraphic history is beyond the scope of this work, but it is of importance because there are cyclical variations in the Eagle Ford that are not readily understood.

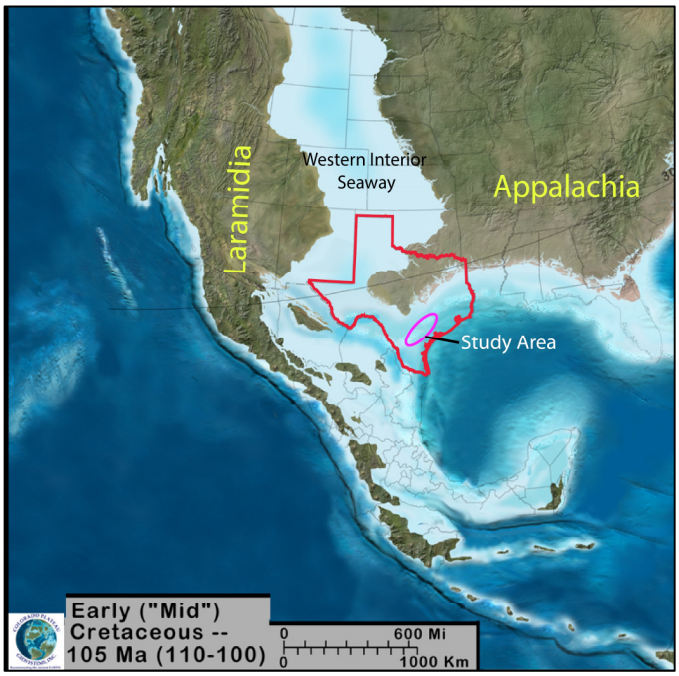

(a)

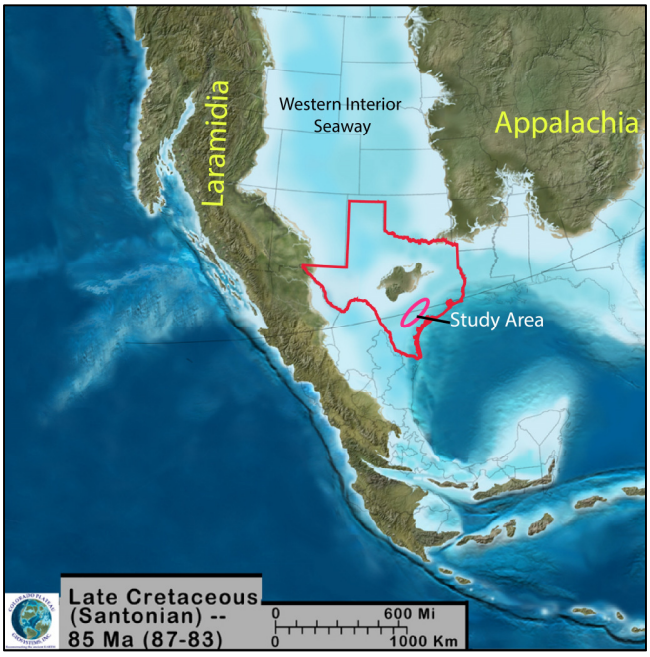

(b)

Figure 2.1 Paleogeographic North America around 105 Ma and 85 Ma

Modified from Blakey, 2013 and McGarity, 2013.

2.1.1 Tectonic Setting

The Cretaceous proto-Gulf of Mexico in southern North America was a passive margin with an extensive shelf whose position fluctuated with variations in sea level (Scott, 2010). Divergence of the Gulf Coast basin was caused by extensional processes during the early Jurassic separation of Pangaea. During the Late Cretaceous the Gulf Coast Basin subsided and created accommodation space for mixed-siliciclastic and carbonate sediments to be deposited (Scott, 2010).

Shales of the Eagle Ford have been described as fractured, fault-controlled fluvial-deltaic, shelf or slope (neritic) deposits (Scott, 2010). The tectonic features directly surrounding the Eagle Ford in south Texas include the San Marcos Arch, a paleo-topographic high, which is suggested to be an extension of the Mesoproterozoic Llano Uplift (Harbor, 2011; Smith and Gray, 2011). The San Marcos Arch trends southeast-northwest and separates the Maverick Basin and the East Texas Basin as shown in Figure 1.2 (Harbor, 2011). The Llano Uplift was exposed during Eagle Ford time and was a possible sediment source (Figure 2.1 b). The Maverick Basin in southwest Texas was an intra-shelf depocenter formed by tectonic basement structures which developed during the failed Rio Grande Rift (Donovan and Staerker, 2010; Harbor, 2011).

Salt withdrawal in the proto-Gulf of Mexico led to accommodation development due to faults trending southwest-northeast of the remnant Cretaceous reef margins (Figure 2.2) (Harbor, 2011). The fault systems surrounding Triassic/Jurassic salt include the Fashing Fault Zone/Karnes Trough, Charlotte Fault Zone, Luling Fault Zone, Talco Fault Zone, Rodessa Fault Zone and the Mt. Enterprise Fault Zone. Faulting initiated during the Late Jurassic to Early Cretaceous and remained active into the Cenozoic (Harbor, 2011 and references therein). The Miocene aged Balcones Fault Zone (~25 to 10 Ma) did affect the shape of the basin post-Eagle Ford time (Griffin, 2008 and references therein). All fault systems mentioned, with the exception of the Balcones, were active during Eagle Ford deposition and affected sedimentation and eventual outline of the Eagle Ford Formation (Harbor, 2011 and references therein). Faulting

resulted in landward-dipping grabens between the Luling and Balcones Fault Zones; faults are basinward and landward-dipping normal faults with graben development in between the Charlotte Fault System and Fashing Fault Zone/Karnes Trough (Harbor, 2011 and references therein).

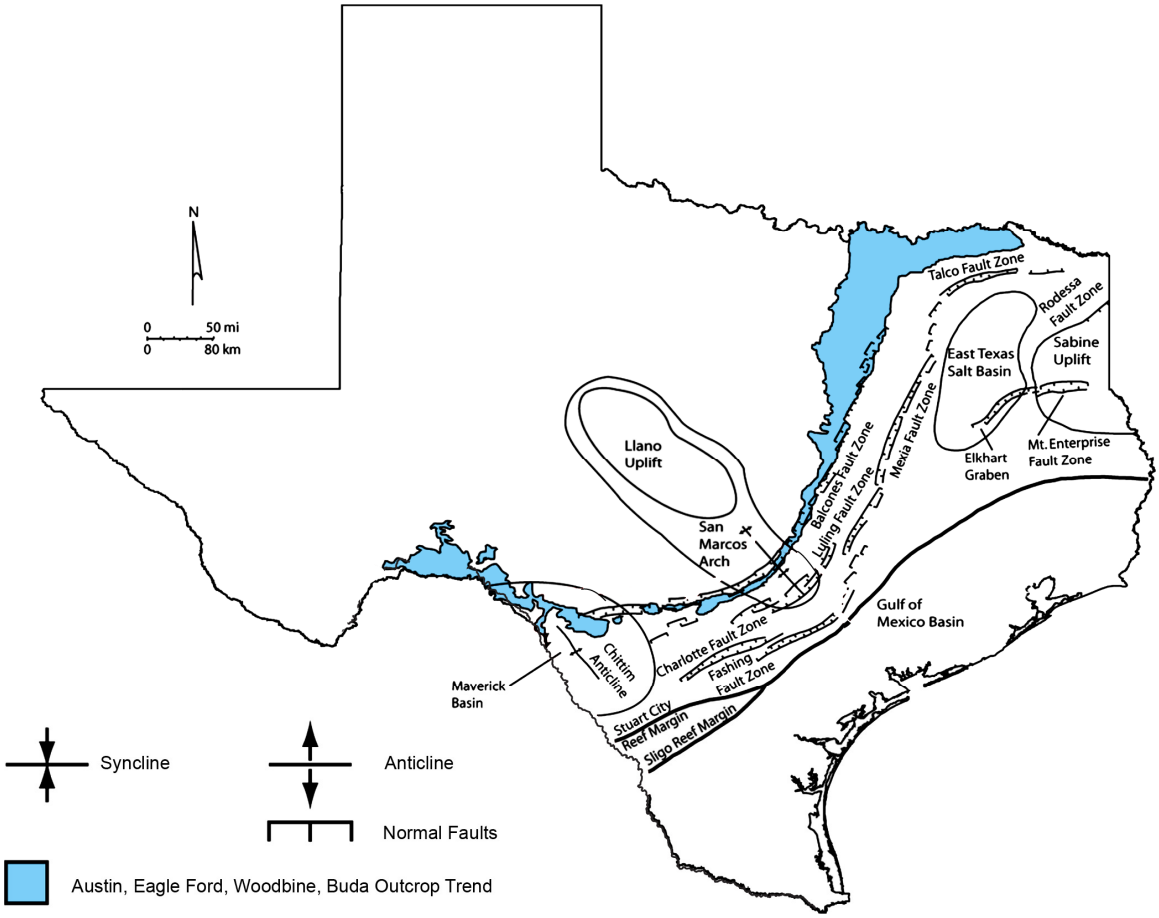

Figure 2.2 Structural features surrounding Late Cretaceous outcrops

Most faults are normal. Modified from Harbor, 2011.

2.1.2 Paleoclimate, Paleoproductivity and Organic Matter Deposition

The Eagle Ford was deposited during a time of increased bioproductivity on a global scale (e.g., Tethys Sea, Atlantic and Equatorial Pacific) contemporaneous with Oceanic Anoxic Event 2 (OAE 2) (Kuroda et al., 2007). OAE 2 occurred near the Cenomanian-Turonian boundary, which has been placed at 93.9 Ma by Walker et al., 2012. Ocean Anoxic Events

(OAEs) are geological time intervals characterized by extremely high burial rates of organic carbon that resulted in global deposition of black, organic-rich shales (Kuroda et al., 2007; Turgeon and Creaser, 2008). OAEs undergo a period of sluggish ocean circulation and may be caused by a voluminous release of methane from gas hydrates in marine sediments, massive volcanic events or water displacement caused from sea-floor spreading at mid-ocean ridges (Kuroda et al., 2007; Mort et al., 2010; Hetzel et al., 2011).

A popular theory for the cause of extreme organic carbon burial is massive subaerial volcanism, during the Cenomanian-Turonian, which triggered climatic changes and led to ocean anoxia (Kuroda et al., 2007). Surface volcanic activity released large amounts of CO_2 and other greenhouse gases (sulfur, chlorine and fluorine) into the atmosphere, resulting in elevated global temperatures and acidification of the oceans by forming acidic compounds in seawater (Wignall, 2001; Breyer et al., 2007; MacLeod, 2013). Thus the Late Cretaceous globe experienced a warmer Earth with no polar ice caps. The average sea-surface temperature (SST) in the Arctic Ocean is considered to have been approximately 15ºC, and the equator-to-pole SST gradient was ~15ºC (Breyer et al., 2007; Kearns, 2011 and references therein). The combination of warmer global temperatures and warm, shallow seas enabled planktonic organisms (primary producers) to flourish during the Late Cretaceous (Brumsack, 2006). The Late Cretaceous is also characterized by vast deposits of chalk and other carbonates as phytoplankton took up CO_2 from seawater and built their skeletons out of $CaCO_3$ (MacLeod, 2013). The carbonate fraction of the Eagle Ford is composed of the skeletal remains of these phytoplankton and other calcareous test-building fauna.

The extended shelf that the Eagle Ford was deposited on received cycles of upwelling that created lenses for enhanced bioproductivity (e.g., Sageman and Lyons, 2003; Kearns, 2011). While the basin had restricted areas such as the Karnes Trough, it did receive cool nutrient-rich water brought to the surface by localized upwelling events that may have driven bioproductivity (Brumsack, 2006). An increase in nutrient consumption of phosphorus and nitrogen by primary

producers (phytoplankton) caused planktonic blooms and led to rapid oxygen consumption. Sinton and Duncan (1997) suggested that submarine volcanism may have increased iron availability in the oceans and stimulated productivity. Productivity created a greater demand of nutrients and oxygen than could be supplied. In the photic zone phytoplankton produce organic matter by photosynthesis, which bacteria convert into energy by oxidizing the organic matter. There must be a constant supply of oxygen because a lack of oxygen would cause anoxic conditions throughout the ocean (Schijf, 1992). The subsequent death of planktonic organisms, that need oxygen to thrive, caused an increase in organic matter raining downward through the water column. Sulfate becomes the dominant oxidant in seawater producing H_2S as a byproduct of bacterial sulfate production in response to the microbial utilization of oxygen and reduction of sulfate (SO_4) into sulfide (SO_2) (Calvert and Pedersen, 2007). This caused an oxygen minimum zone (OMZ) below the photic zone, which extended beyond the inner shelf where high concentrations of organic matter were deposited and preserved (e.g., Brumsack, 2006).

The variations in organic content within Eagle Ford core are visible macroscopically. Generally, the richer the content of organic matter, the darker the Eagle Ford appears; hence its characterization as a black shale. Typical determinants for organic matter preservation include the lack of scavengers as well as a high rate of sedimentation (Demaison and Moore, 1980). This will inhibit anaerobic microbial decomposition of decaying phytoplankton remains (Burdige, 2007). If there is a low sedimentation rate and the circulation of water is restricted, a lack of oxygen reaches bottom water sediments and decomposition of organic material will not occur since there are few benthic fauna to decompose organic remains (Tucker, 2001). Regardless of the amount of oxygen present, organic matter production is controlled by nutrient availability and largely by absence of benthic fauna. Even when sediment or water is lacking in oxygen, few benthic fauna do remain since most benthic fauna are aerobic organisms. Yet some manage to survive and live in mixed redox sediments (Charvat, 1985; Burdige, 2007). The exact mechanism of nutrient input onto continental shelves is still under debate. The leading mechanisms under speculation include

upwelling of deep, cold, nutrient rich water onto continental shelves, volcanism or subaqueous flood basalt eruption during oceanic plate formation (Sinton, 1996; Brumsack, 2006).

2.1.3 Igneous Provinces and Volcanism

Volcanism which accompanied Late Cretaceous orogenic events was present in and surrounding North America while Eagle Ford deposition was taking place (e.g., Hunter and Davies, 1979). Pyroclastic debris were deposited in Gulf Coast sediments and appear as bentonite beds (Hunter and Davies, 1979) in subsurface cores. It is evident that volcanism was continuous as Eagle Ford outcrops and cores have bentonite layers deposited throughout. Contemporaneous volcanism was occurring in different regions around the globe yet the closest volcanic sources during Cenomanian-Turonian time were located in the Sevier highlands, in the locale that is present-day Oklahoma and Arkansas, Mexico and the Caribbean plateau (Kauffman, 1977; Hunter and Davies, 1979; Kerr, 1998; Turgeon and Creaser, 2008; Adams and Carr, 2010). While Eagle Ford sediments in northeastern Texas received volcaniclastic fan materials from a source in southwest Arkansas in the Murfreesboro-Nashville-Lockesburg area, it is uncertain were the precursor to volcanic ash in south Texas is sourced from (Ross et al., 1929; Hunter and Davies, 1979). Volcanic detritus sourced from southwestern Arkansas was deposited as ultrabasic (peridotitic) vents in southern Arkansas, southeastern Oklahoma and northeast Texas (Figure 2.3) (Hunter and Davies, 1979)

The Late Cretaceous Sevier Orogeny comprised of magmatic arc formation seen in Figure 2.4 (Kauffman, 1977). Most volcanism occurred west of the Western Interior Seaway margin beginning in the late Early Cretaceous and peaking in the Late Albian so that by the Middle Cenomanian when Eagle Ford deposition began, active tectonism and volcanism continued at a diminished rate (Kauffman, 1977). The Caribbean oceanic plateau, also depicted in Figure 2.4, in the South Atlantic Ocean, was wedged between North and South America during the Late Cretaceous (Sinton, 1996). The plateau was a Large Igneous Province (LIP) which formed by rapid flood basalt volcanism that began around ~90 Ma (Sinton, 1996). Oceanic

plateaus are the submarine equivalent of continental flood basalts. From Sinton's (1996) work using ^{40}Ar-^{39}Ar dating of samples from various exposures around flood basalt provinces within the plateau, it was determined that the bulk of the plateau formed between 91-88 Ma, contemporaneously with late Eagle Ford and early Austin Chalk deposition.

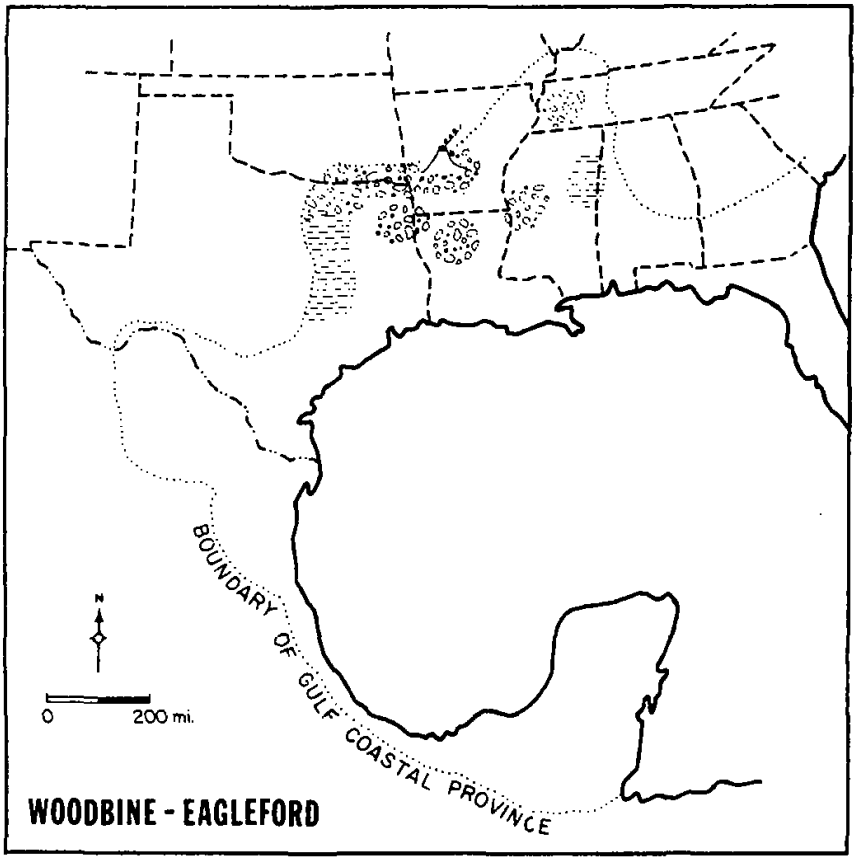

Figure 2.3 Volcanic sediment locations during Woodbine and Eagle Ford time

From Hunter and Davies, 1979. Bentonite in south Texas was relatively unpublished at the time of this publication. Republished by permission of the Gulf Coast Association of Geological Societies, whose permission is required for further publication use.

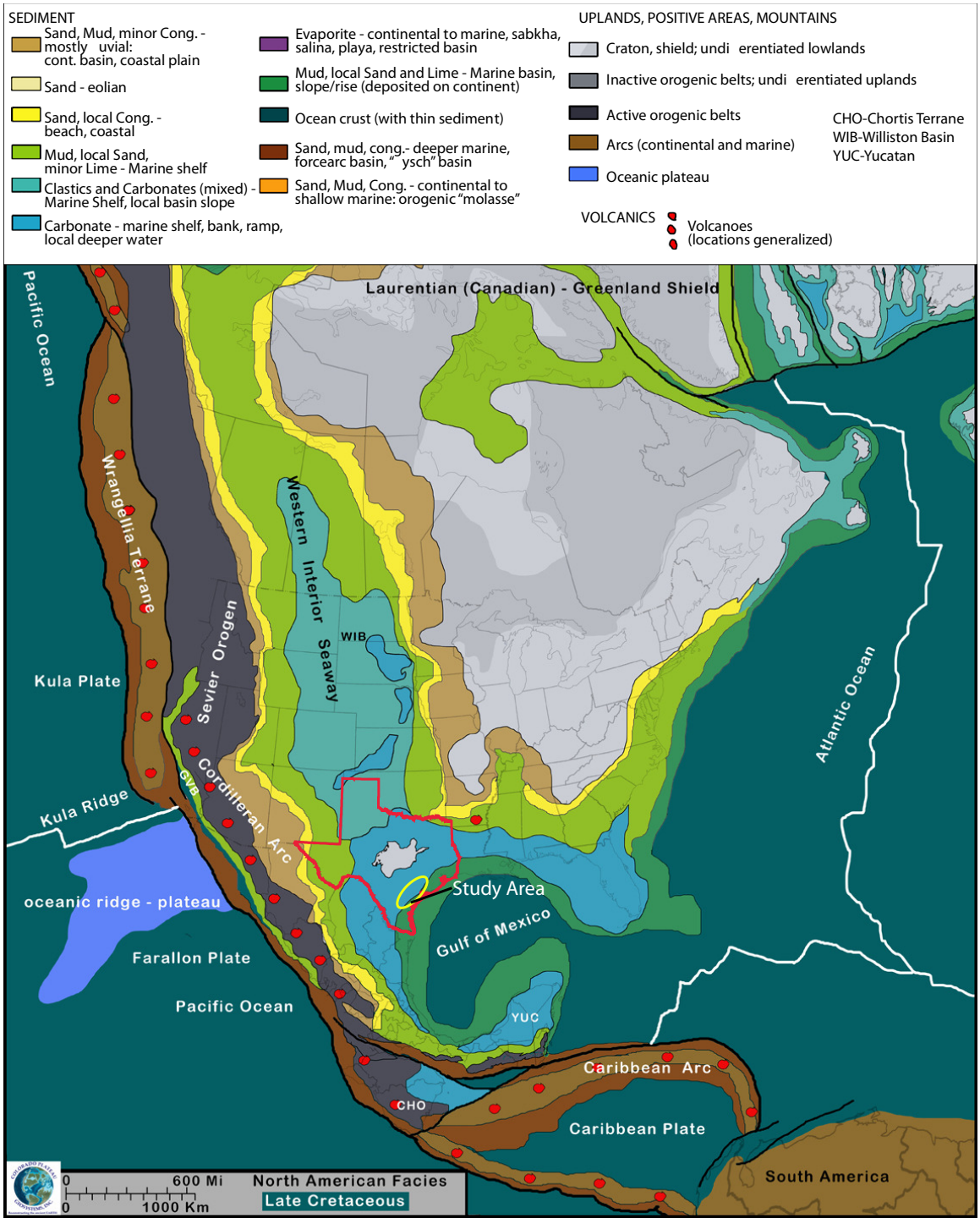

Figure 2.4 Late Cretaceous paleotectonism and sedimentation

The exposed Llano Uplift is highlighted in gray in central Texas. The Sevier Orogeny and Caribbean tectonism are highlighted as well. Modified from Blakey (2013).

There is a mismatch in timing of volcanism and flood basalt eruption with the bulk of Eagle Ford depositional time as most subaqueous flood basalt eruption occurred at the end of Eagle Ford time ~90 Ma (e.g., Sinton, 1996; Wignall, 2001). Further provenance studies are required to determine where the exact source of the Eagle Ford volcanic ash might be located. The presence of a great abundance of well-preserved bentonite beds throughout Eagle Ford and lower Austin Chalk core suggest that the environment received continuous volcaniclastic debris, which may have affected paleodepositional water conditions at the time of deposition. There are abundant bentonite beds in Austin Chalk core indicating that volcanism continued into Austin time; but may have been sourced from a different locale (Hunter and Davies, 1979; Breyer et al., 2007). There is evidence of volcanism believed to be Cretaceous in age in the Big Bend area of south Texas (Breyer et al., 2007); however, the Eagle Ford precedes this event. The Boquillas Formation (Eagle Ford time equivalent) in the Big Bend area does contain ash beds suggesting that volcanic ash reached Eagle Ford sediments outside of the study area as well.

Figure 2.5 depicts a response cycle due to Late Cretaceous climate changes. There is a theory suggesting that OAE 2 was triggered by a massive magmatic episode (Turgeon and Creaser, 2008). Sinton (1996) stated that there is a possibility that “massive, short-lived pulses of submarine magmatism produced hydrothermal plumes that may have consumed the dissolved oxygen in seawater and contributed to anoxia.” MacLeod (2013) discusses the possibility of excess CO_2 input from volcanism into the atmosphere may have resulted in the oceans not being able to remove the excess gas from the atmosphere. This would have caused CO_2 to accumulate in the atmosphere and sea surfaces; poisoning the phytoplankton due to acidification and causing extinction. The exact cause of marine anoxia during the Late Cretaceous has undergone much speculation. Characterizing the rock characteristics and geochemical make-up of the black shale in the Eagle Ford Formation may give insight into the effect of these mechanisms on the Eagle Ford depositional environment.

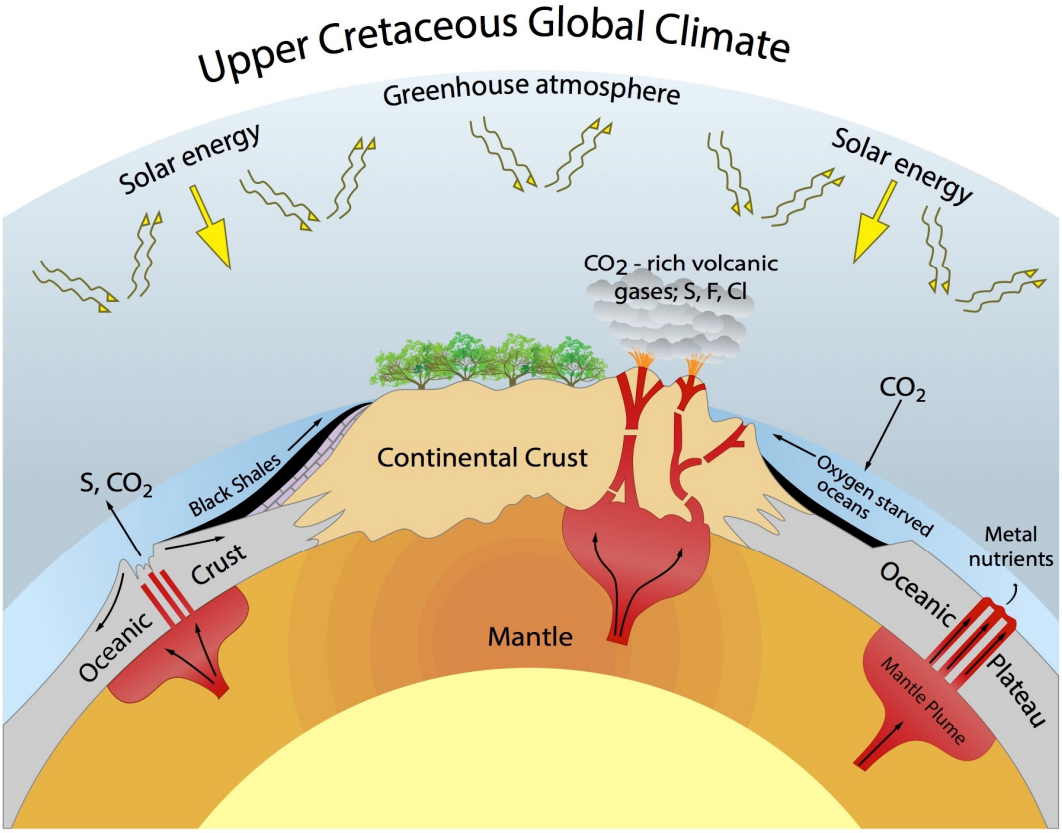

Figure 2.5 The effect of volcanism and LIPs

The Late Cretaceous experienced global warming which triggered a sequence of events culminating in black shale deposition. Modified from the British Geological Survey-NERC, accessed 2013. *Reproduced with the permission of the British Geological Survey ©NERC. All rights Reserved.*

2.2 Stratigraphy

2.2.1 Overview

The Eagle Ford Formation does not always fit the classification of shale. A shale is defined as a “argillaceous rock possessing lamination or fissility” (e.g., Moran 2013 and references therein). Strata in the Eagle Ford vary from organic rich calcareous marl to argillaceous marl and range from gray to black in color. The ideal classification for the Eagle Ford in south Texas would be marl unless fissility and an increased amount of clay are present. This conclusion is based on the amount of calcite found in Eagle Ford rocks based on XRD studies

completed by Core Laboratories. The Eagle Ford shows minor facies changes from well to well and it is difficult to use one classification for the rocks within. For the purpose of this study, the Eagle Ford will be referred to as the Eagle Ford Formation or shortened to the Eagle Ford based on the nomenclature of Hentz and Ruppel (2010) and Moran (2013).

Eagle Ford rocks are similar to hemipelagic facies, defined by Sageman and Lyons (2003) as finely laminated mudstones or bioturbated or massive mudstones. There are variable concentrations of silt-sized particles composed of quartz, authigenic pyrite or precipitated calcite present in hemipelagic facies (Sageman and Lyons, 2003). In outcrop, glauconite and biogenic phosphate have been observed (Dawson, 1997). Overall, sediments that make up the majority of the rocks within the Eagle Ford include a mixture of aluminosilicate and carbonate minerals, which have trapped organic matter. There are also lesser amounts of pyrite, siderite, feldspar, apatite and clays (illite/smectite, illite and kaolinite).

2.2.2 South Texas

2.2.2.1 Major Facies

The Eagle Ford Formation is overlain disconformably by the Austin Chalk and underlain unconformably by the Buda Limestone shown in Figure 2.6 (Dawson, 2000). The contact between the Eagle Ford Formation and Austin Chalk is an irregular burrowed surface at times while the contact between the Eagle Ford Formation and the Buda Formation is a sharp unconformity followed by a highly radioactive and clay-rich marl layer (Core Laboratories, personal communication). The Lower Cretaceous Buda Limestone was deposited throughout the late Albian (Adams and Carr, 2010). The top of the Buda is considered the boundary of the Comanche-Gulf Series and marks the beginning of Eagle Ford time (Reaser and Dawson, 1995). Buda outcrops can be found along the same trend as Eagle Ford in south, central, northeast, east and west Texas and northern Mexico (Figure 1.2). The Buda Limestone is mainly fossiliferous limestone with packages of marl and calcareous shale (Reaser and Dawson, 1995). The early Coniacian to early Campanian Austin Chalk is mainly composed of marl and chalk with areas in

northeast Texas composed of a mixture of chalk, clay and sand; all deposited upon a deep shelf below storm-wave base (Waters et al., 1955; Scott, 2010). Planktonic foraminifera as well as ammonites are found within the Austin Chalk. The base of the Austin Chalk sees an increase in trace fossils of pelecypods and *Thalassinoides* indicating a shift to more oxygenated bottom conditions compared to the Eagle Ford Formation (Dawson, 1997). Carbonate content also increases in the Austin Chalk and there is a general decrease in preserved organic matter as well as a decrease in pyrite (Dawson, 1997). The Austin Chalk has been a reservoir for petroleum, due to an abundance of organic matter, and has been targeted as a conventional play (Scott, 2010). The contact of the Eagle Ford and the Austin Chalk has been named the Turonian-Coniacian boundary (~89 Ma) (Dawson, 2000).

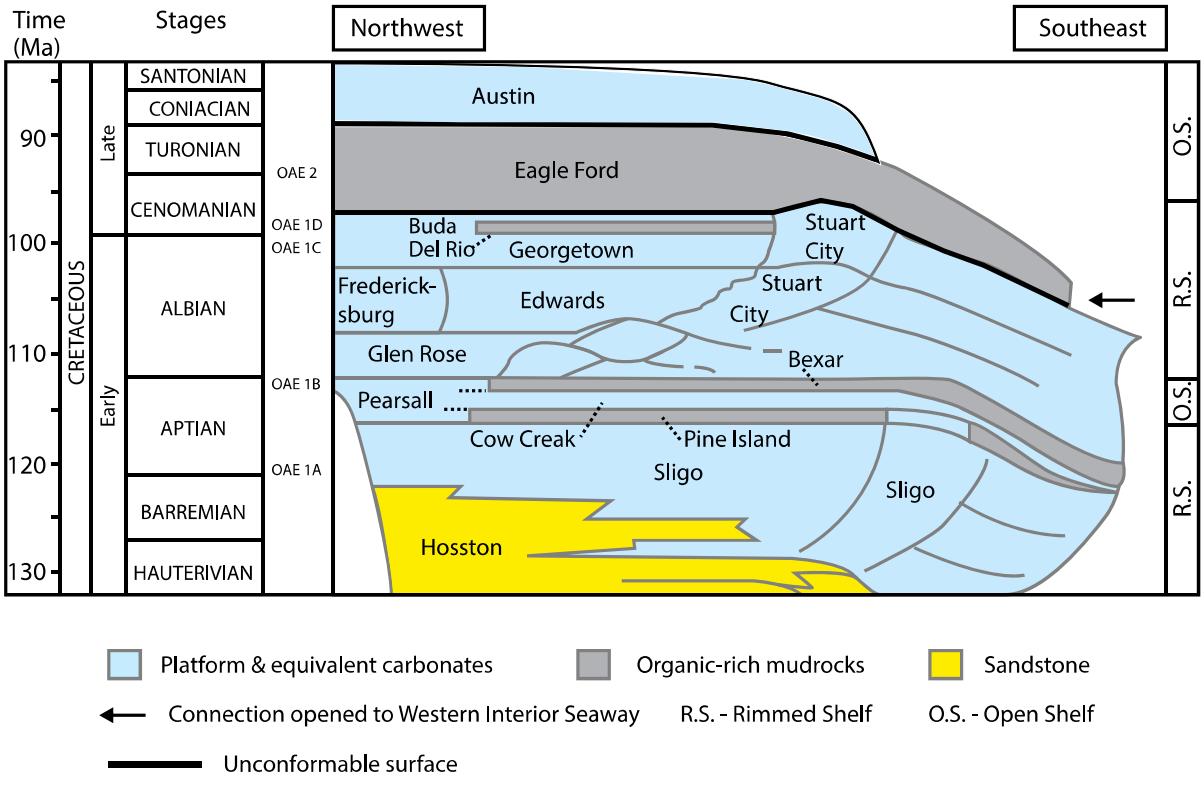

Figure 2.6 Lithofacies of South Texas and the Gulf Coast Basin

Modified from McGarity, 2013. OAE dates from Salacup, 2008.

The facies of the Eagle Ford Formation in south Texas record the onset of a major transgressive cycle at the contact of the Buda Limestone and Eagle Ford (Dawson, 2000). Minerals within the Eagle Ford can be grouped into clay phases, detrital silt, and carbonates (Dawson, 2000). The detrital component of the Eagle Ford Formation contains sediment that may have been brought in from deltas prograding from northeast to southwest as well as volcaniclastic sediments. Cyclic sedimentation with repetitive sequences of dark gray, organic-rich laminated marl interbedded with highly calcareous marl is visible in core. The cycles are defined coarsening upwards parasequence sets of dark gray, thinly laminated, organic-rich marls to foram-rich, locally bioturbated marls (Core Lab core description, personal communication). In intervals where the Eagle Ford Formation is rich in calcareous matter it is finely laminated and exhibits different degrees of fissility. The Eagle Ford Formation has been divided into the upper Eagle Ford member, the middle Eagle Ford member, and the lower Eagle Ford member for the purposes of this study. Boundaries between the Austin Chalk and Buda Limestone and within the Eagle Ford Formation were determined by geoscientists at Pioneer Natural Resources and are denoted by color categories (Figure 2.7). The Buda Limestone was picked below a hot gamma ray (GR) spike at the base of the lower Eagle Ford member. The middle Eagle Ford member was picked by an increase in gamma ray API and a reduction in the amount of carbonate stringers, signifying a more clay rich interval. The top of the Eagle Ford formation was picked as a coarsening upward sequence of carbonates followed by a hot GR marking the boundary of the Austin Chalk and the Eagle Ford. Boundaries were also verified using biostratigraphic studies of calcareous nannofossils.

The mineralogy of three cores (7, 12, and 20) from different locations along the trend have been described by Core Laboratories and Weatherford utilizing XRD analysis (Table 2.1). XRD derived mineralogy of the Eagle Ford includes calcite, quartz, apatite, plagioclase feldspar, orthoclase, pyrite, marcasite, siderite, various clay minerals such as illite and kaolinite, and minor amounts of dolomite. Generally the upper Eagle Ford member is richer in calcite, the middle

Eagle Ford and lower Eagle Ford members are richer in quartz and clay and have decreased calcite content. The lower Eagle Ford member grades from calcareous marl to finely laminated organic rich marl alternating with carbonate-rich stringers with depth (Tuttle, 2010).

Table 2.1 Select X-ray Diffraction (XRD) and TOC data for the Eagle Ford Formation

wt.%	Gross Eagle Ford	Upper Eagle Ford	Middle Eagle Ford	Lower Eagle Ford
	Mean (See Appendix B for sample count)			
TOC	4.16	2.77	3.97	4.98
Quartz	15.45	14.05	16.24	15.72
K-Feldspar	0.07	0.02	0.19	0.06
Orthoclase	0.74	0.00	0.74	0.74
Plagioclase	2.50	4.38	2.15	1.98
Pyrite	5.36	2.80	5.96	6.04
Marcasite	1.28	1.32	0.86	1.43
Apatite	0.81	0.02	1.21	0.83
Kaolinite	3.87	0.00	0.27	7.46
Illite	5.59	4.08	6.04	6.57
Chlorite	2.84	0.00	2.63	4.54
Mixed Layer Clay	8.33	6.10	8.48	9.89
Calcite	58.52	66.55	53.80	55.33
Dolomite	0.08	0.16	0.19	0.00

The carbonate stringers within Eagle Ford rocks are made up of the calcium carbonate ($CaCO_3$) tests of planktonic organisms (i.e., calcareous nannofossils and foraminifera), ostracods and Inoceramid bivalves. The middle Eagle Ford member has the highest concentration of total clay minerals and does not contain as many laterally continuous carbonate stringers as the lower Eagle Ford member. Illite/smectite and illite are the principal clay species with minor kaolinite also

present. Kaolinite is most abundant in the lower Eagle Ford member and has been found in foraminifera chambers. Chlorite is also most abundant in the lower Eagle Ford member. There are also biogenic phosphatic deposits near the upper Eagle Ford and Austin Chalk contact (Dawson, 1997). Lower Eagle Ford facies indicate a below storm wave base deposition and were deposited in poorly oxygenated and low energy waters (Dawson, 2000). The upper Eagle Ford member, however, was deposited in a well-oxygenated, shallow marine paleoenvironment denoted by a large diversity of organisms preserved in the section and observed bioturbation (e.g., Arthur and Sageman, 1994; Dawson, 2000). The upper Eagle Ford member was deposited during a regressive cycle with alternating deposition of marl, limestone and carbonaceous quartzose siltstones under higher energy (above storm wave base) conditions (Dawson, 2000).

Outcrop descriptions of the Eagle Ford Formation are similar to subsurface core descriptions including the presence of elevated TOC concentrations, low frequency of benthic foraminifera, minimal bioturbation and authigenic pyrite (Dawson, 2000). Kearns (2011) noted framboidal pyrite in SEM images within his thesis' study area. TOC values in Table 2.1 were derived from LECO analysis and indicate that the lower Eagle Ford member has the highest TOC values in wt. %. Finally, debris flows appear in outcrops and have been observed in the subsurface (Donovan et al., 2012). Hentz and Ruppel (2010) described debris flow facies as carbonate platform facies.

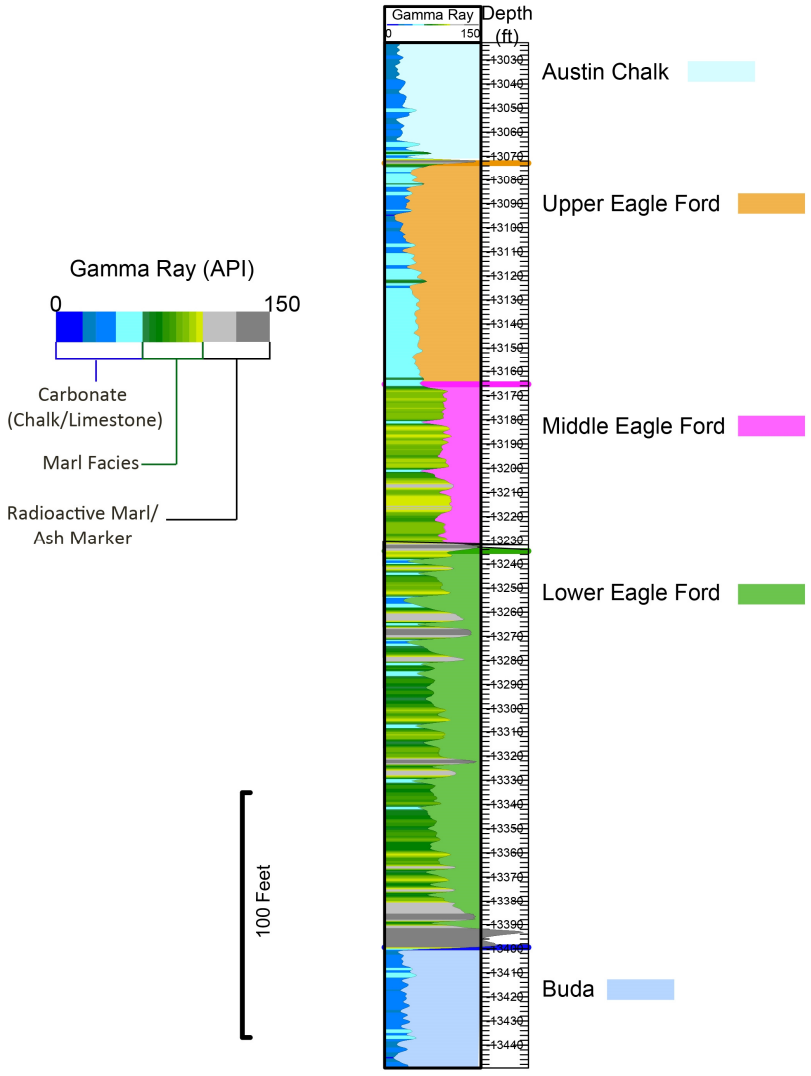

Figure 2.7 Type log of the Eagle Ford Formation

Gamma ray signatures highlight facies variations from a vertical well in Karnes County, Texas.

2.2.2.2 Bentonite

Bentonite is clay that has been altered from volcanic ash during diagenesis (Charvat, 1985). Clay minerals are formed by the hydrolytic decomposition of primary aluminosilicates during terrestrial weathering which result in the alteration of primary minerals and the formation of new aluminosilicate frameworks (Calvert and Pedersen, 2007). Smectite and its montmorillonite

family are formed at the onset of weathering of upper crustal rocks; illite is found at the intermediate stage of weathering and has been weathered from smectite; kaolinite occurs at the highest weathering rates (Calvert and Pedersen, 2007). Smectite is also found in bentonite of volcanic origin (Charvat, 1985). Eagle Ford rocks have an abundance of kaolinite, chlorite and illite/Smectite, determined by XRD analysis (Table 2.1). Determining the composition of bentonite in Eagle Ford rocks would be instrumental to understand the rate of weathering that bentonite clay has undergone and how they may have been deposited on the sea floor.

Charvat (1985) and references therein interpreted that ash layers were delivered to the study area as airborne ash, which settled through the water column at high rates of deposition. It was determined that bentonite was altered from wind-blown volcanic ash in a shallow marine environment during and after the deposition of the Eagle Ford in central Texas (Charvat, 1985). Bentonite samples from central Texas were deposited in a euxinic environment, and since the Eagle Ford shows indications of anoxic to euxinic bottom water conditions, it is theorized that volcanic ash may have been a precursor to reducing conditions (Charvat, 1985). Samples from the wells of interest in this thesis were interbedded with carbonates although they fluoresced a bright yellow under ultraviolet (UV) light (Figure 2.8). This suggests that ash deposition occurred simultaneously with carbonate deposition. There is a clear distribution of thin brown to gray/green ash beds that have been classified as bentonite within each member of the Eagle Ford Formation in South Texas (Figure 2.9).

Volcanic ash (altered to bentonite) has been found in Eagle Ford outcrops in the vicinity of Del Rio, West Texas in the form of more than 300 volcanic ash layers (Eldrett et al., 2013). McGarity (2013) has identified bentonite in subsurface Eagle Ford cores from South Texas. Beds range from tenths of a centimeter to up to fifteen centimeters thick and at times were replaced by pyrite; similar occurrences have been seen in bentonite from the study area (Figure 2.10). These beds are also interbedded with limestone (McGarity, 2013). Most bentonite in the study area vary from paper thin to a couple of centimeters with a thickness of less than five cm. Bentonite layers

were not deposited at the same depth interval in each core but they are all concentrated throughout the gross Eagle Ford Formation (Figure 2.11). Thicker bentonite beds are more frequent in Karnes County rather than DeWitt County. The largest concentration of thick bentonite layers in this study area was in the upper Eagle Ford member and Austin Chalk implying increased volcanism at the end of the Eagle Ford deposition well into Austin Chalk time (Late Turonian to Early Coniacian). The upper and lower contacts between bentonite and overlying/underlying lime mudstone, marl or shale beds are always sharp. This has also been noted in outcrops where there are no apparent transition zones (Charvat, 1985). The grains in Eagle Ford core are fine and may have altered ash scattered throughout, but this has been undetectable without magnification. Bentonite layers are distinguishable as thick beds but become difficult to identify when they are paper-thin.

The facies and tectonic setting of the Eagle Ford Formation is well documented yet chemostratigraphy can be employed to note detailed facies changes and paleoredox conditions. The following chapter evaluates the methodology necessary to obtain geochemical data.

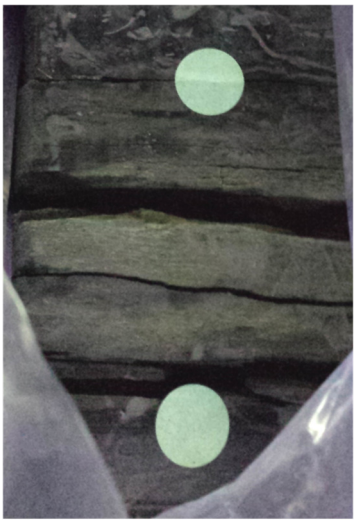

Figure 2.8 Bentonite under UV light

An 8 cm bentonite layer (altered volcanic ash) from well 8 fluoresced yellow under UV light.

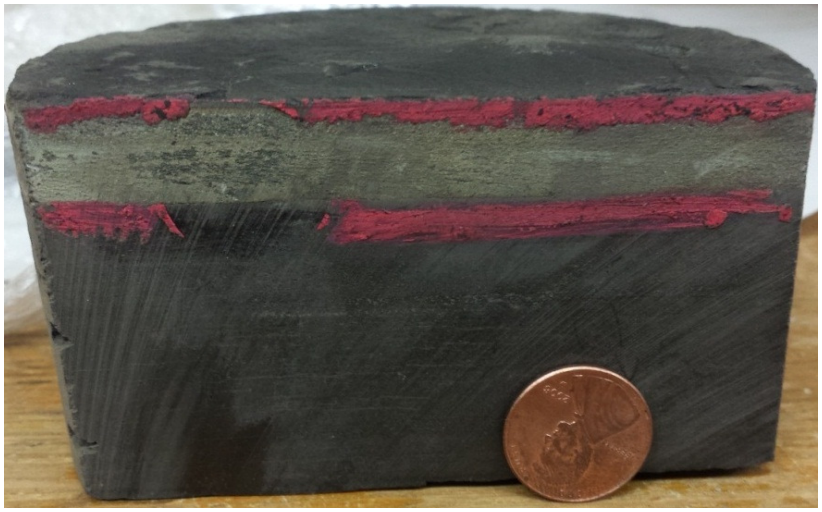

Figure 2.9 Bentonite layer

A sharp contact is visible above and below a 2 cm layer of bentonite from well 20.

\

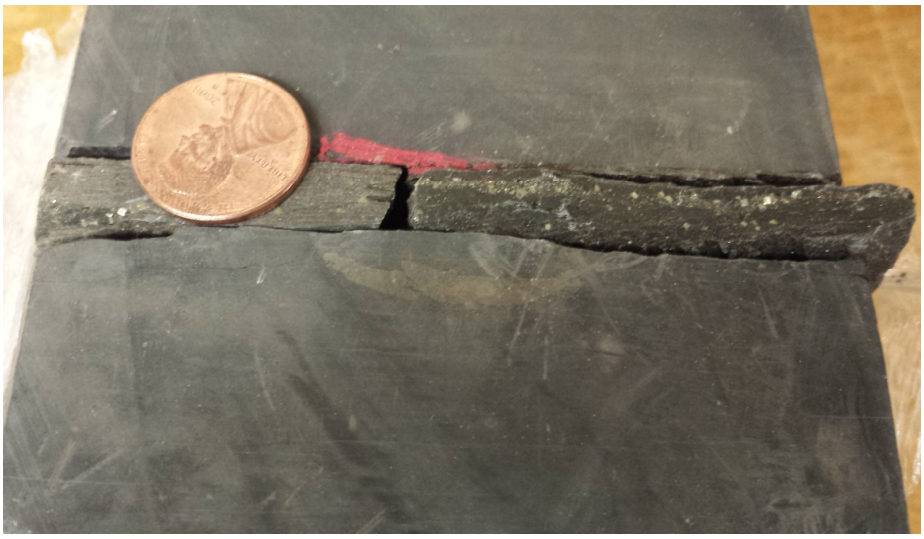

Figure 2.10 Abundant pyrite in bentonite

A 1cm layer of bentonite from well 1 with precipitated pyrite.

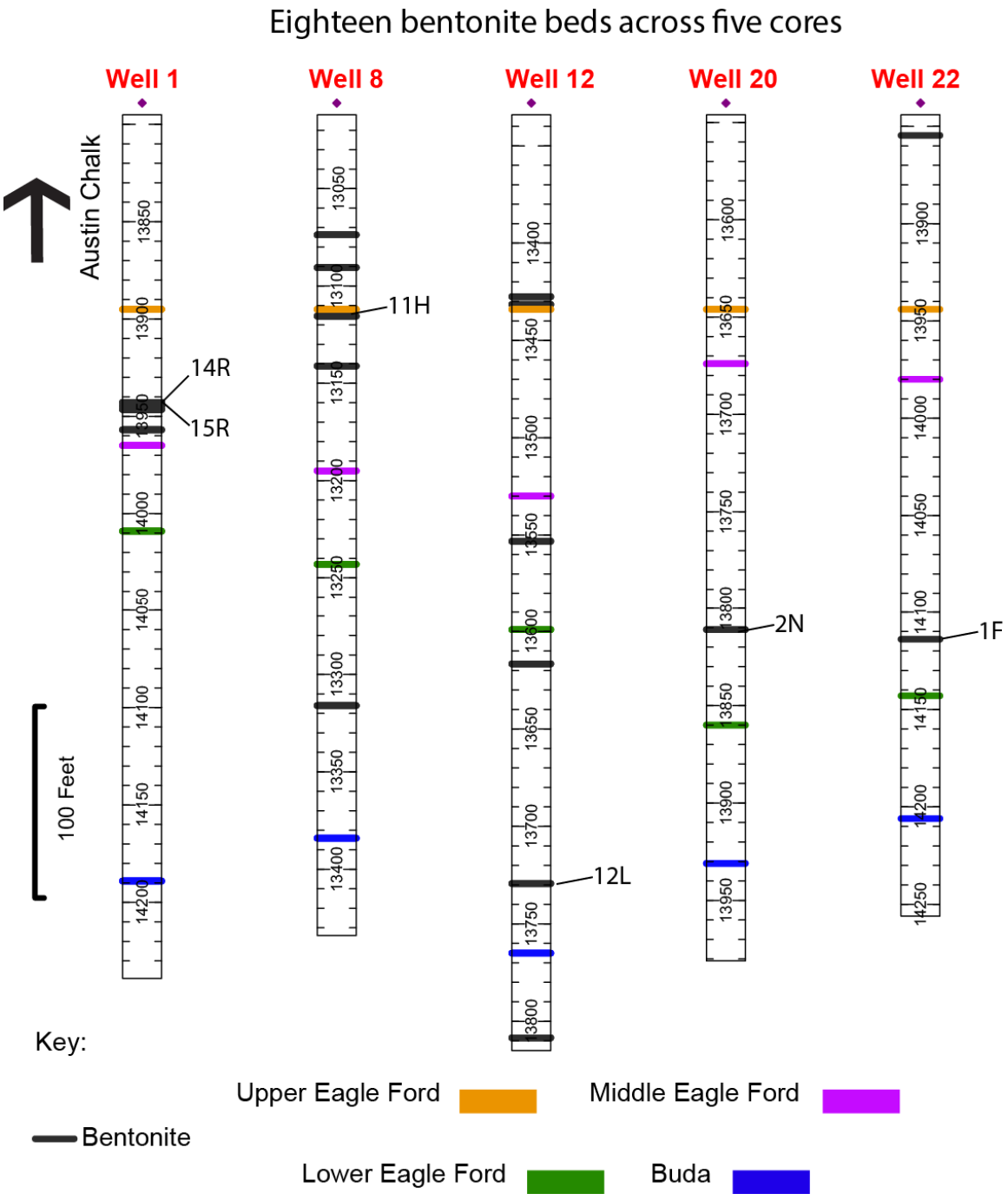

Figure 2.11 Bentonite throughout Eagle Ford core

A representation of the thickest bentonite beds visible under UV light. Thin bentonite beds are not depicted. Labeled samples were studied in this thesis. Wells are depth shifted to match the boundaries of each member within the Eagle Ford.

Chapter 3

Methods

3.1 Study Design

A representative area in south Texas is studied by analyzing drill cuttings and core for twenty-four Eagle Ford wells located in Karnes, DeWitt and Live Oak counties. Several methods were used to obtain geochemical data mainly because each method had its own benefits. The purpose of the hand-held Energy Dispersive-X-ray Fluorescence (ED-XRF) analysis was to illustrate the inorganic geochemistry of the Eagle Ford by collecting major, minor and trace element data for a large sample density of cuttings and core from twenty-two wells. This method allowed the largest amount of wells to be analyzed due to its rapid analysis and the portability of the device. A control upon the calibration of the hand-held ED-XRF was also obtained by analyzing the Green River Shale standard (SGR-1) and comparing recommended values against actual concentrations detected by the hand-held ED-XRF.

In order to interpret more precise measurements, a data set compiled through Inductively Coupled Plasma-Optical Emission Spectroscopy and Inductively Coupled Plasma-Mass Spectrometry (ICP-OES and ICP-MS) analysis by Chemostrat, Inc. in Houston, Texas was used. Major, minor and trace element patterns across the Eagle Ford trend were gathered for cuttings and core from seven wells. Most of the methodology was provided as a personal communication and the methodology from Hildred et al. (2011) was cited to further describe the analysis carried out. Trace elements, which were unable to be accurately measured or detected by the hand-held ED-XRF, were quantified using ICP-OES and ICP-MS analysis including Ba, U and V, and rare earth elements. Activation Laboratories in Ontario, Canada also collected elemental data for this study from bentonite beds in order to understand the effects of volcanic ash on the paleodepositional environment.

Table 3.1 outlines the main well list and number of samples analyzed for the hand-held ED-XRF method. Tables 3.3. and 3.4 list the wells and sample number for the Chemostrat, Inc.

and Activation Laboratories data sets, respectively. Depths are exact core depths in true vertical depth (TVD).

Table 3.1 Main well list

Well Number	Total Cuttings Samples EGFD (n)	Total Core Samples	Starting Depth (feet) TVD	Ending Depth (feet) TVD	Sample Interval range (feet)	Bentonite Core ID
1						x
2	8		13000	13180	10-40	
3	45		12665	12885	5	
4	55		13045	13315	5	
5	40		12955	13150	5	
6	58		13280	13580	5-10	
7	54	27	13090	13355	5	x
8	56		12995	13270	5	
9	13		13270	13570	10-30	
10	52		12755	13015	5-10	
11	11		13220	13500	20-30	
12	34	67	13410	13730	5-14	x
13	59		13600	13895	5-10	
14	10		13340	13570	10-40	
15	9		13370	13595	10-65	
16	52		13340	13595	5	
17	55		13575	13845	5	
18	72		13700	14060	5	
19						
20	53	53	13650	13930	3-17	x
21	46		13775	14005	5-10	
22	54		13900	14158	2-7	x
23	51		13860	14110	5	
24	5		13990	14175	25-60	

3.2 Hand-held ED-XRF

A hand-held ED-XRF provides quick analyses of core whether it is in the form of whole core, core chips, core cuttings or powdered samples. A selection of drill cuttings from a total of

twenty-two pilot wells were chosen to determine major and trace elemental data. A Bruker Elemental series IV-SD hand-held XRF was used to obtain elemental concentrations from a combination of cuttings and core from the wells in Table 3.1. Each well has a different sample count due to the way cuttings are preserved by the mudloggers who collect them (Table 3.1). The software that accompanies the hand-held ED-XRF analyzer is the S1 PXRF and is calibrated and provided by Bruker Elemental. The sample data is recorded within Excel based on a known calibration macro created by Rowe et al. (2012) and cited in Hughes (2011) and Kearns (2011). Their results imply that the hand-held ED-XRF data is a reliable tool to qualitatively and quantitatively measure elemental data within a sample. Twenty-six reference standards were used to calibrate the device by Dr. Harry Rowe for Bruker Elemental. Three cores (7,12 and 20), which are housed at Core Laboratories in Houston, TX and belong to Pioneer Natural Resources, were also analyzed to compare TOC data and XRD derived mineralogical weight percentages of the bulk rock. The hand-held ED-XRF analyzed twenty-eight elements (Si, Al, Ca, Mg, Na, K, Fe, Mn, Ti, P, S, Cr, Cu, Ni, Sr, Zn, Zr, Mo, Nb, Th, U,Y, Rb, Co, Pb, As, Sn, and Sb). Major elements are reported in weight percent (wt.%) and trace elements in parts per million (ppm).

3.2.1 Green River Shale Standard Comparison-SGR-1

The Green River Shale standard was used to determine the accuracy of results from the hand-held ED-XRF. The Green River Formation of Wyoming is an Eocene carbonaceous shale that is rich in oil. Sample for this reference material was collected from the Mahogany zone of the Green River Formation (Wilson, 2001). At the time of preparation, shale oil tests yield 51 to 57 gallons per ton. SGR-1 was approved as a standard by the U.S. Geological Survey (USGS). The mean concentration of three sample runs suggest that not all elemental results could be accurately measured and that it is necessary to quantify error before interpreting results (Table 3.2).

Table 3.2 Results of SGR-1 analysis

Element	SGR 1 Recommended Value (Wilson, 2001)	± 1 σ	Measured Value Mean of n=3	± 1 σ
SiO_2 (wt.%)	28.2	0.21	27.44	0.099
Al_2O_3	6.52	0.21	6.43	0.068
K_2O	1.66	0.10	1.89	0.007
Na_2O	2.99	0.13	0.67	0.007
Fe_2O_3	3.03 (Total)	0.14	3.32	0.005
CaO	8.38	0.17	12.66	0.035
MgO	4.44	0.2	1.54	0.083
P_2O_5	0.328	0.066	0.31	0.009
TiO_2	0.253	0.025	0.32	0.005
As(ppm)	67	5	80.36	9.45
Cr	30	3	41.70	8.27
Cu	66	9	58.57	5.25
Mn	267	34	385	3.83
Mo	35	0.90	37.49	0.93
Pb	38	4	29.92	5.71
Sb	3.4	0.40	13.58	7.20
Sr	420	30	387.38	4.83
Th	4.8	0.21	7.76	2.09
U	5.4	0.40	9.44	2.86
Zn	74	9	84.09	7.14
Ni	29		27.89	0.79

Table 3.2-*Continued*

Element	SGR 1 Recommended Value (Wilson, 2001)	± 1 σ	Measured Value Mean of n=3	± 1 σ
Sn (ppm)	1.9		2.50	0.43
Y	13		12.51	0.35
Zr	53		46.86	4.34
Ba	290	40	262.59	19.38
Co	12	1.5	8.47	2.50

The Eagle Ford Formation has some characteristics in common with the Green River Formation. They are both rich in organic carbon and contain an increased carbonate fraction. They were deposited under different depositional environments, however. Elements with a great amount of error were left out of the interpretation since their values are unreliable. SGR-1 was not included in the calibration for this particular tool. Nevertheless, select elements have been deemed useful based on the analysis of SGR-1 (Si, Al, Fe, P, Cu, Mo, Ni Sr, Y and Zn). Ca is included in the results to show the general stratigraphic variation in Ca concentrations along the trend.

3.2.2 Data Collection

All cuttings and core were analyzed by myself and David Wood of Pioneer Natural Resources at the company field office. Some samples were analyzed on a rotary table setup on which each sample remained stationary. The table rotated each sample and placed the sample cup flat above a 3x4 analyzer window (Figure 3.1). The sample amount was approximately five grams in a plastic sample cup with clear film on the bottom. The Bruker hand-held ED-XRF tool analyzes the surface of any sample that is placed directly above the analyzer window.

The energy required to obtain major elements in the low energy range between 1.25 to 7.06 keV was set by Hughes (2011) as 15 keV; the μA was 16. The voltage was set to 40keV at 5.68 μA to detect trace metals. A vacuum pump was used for the purpose of removing air

between the sampling window and the detector. The sample run time was 60 seconds for each sample, including major and trace elements individually, without a color filter.

3.2.2.1 Normalization

Elemental concentrations provided by the calibration are in weight percent. Major elements were normalized as oxides by dividing the atomic weight of their oxide molecule (e.g., Rollinson, 1993). Conversion factors are reported in Appendix A. Results for major elements were also normalized to a fraction of 100 wt.% bulk rock composition in order to compare wells to one another. Trace elements were multiplied by a factor of 10,000 to convert their concentration from weight percent to ppm. The tool returns negative numbers for elements that cannot be detected at times; negative numbers were all changed to a value of zero.

3.2.2.2 Relating Elemental Data (Correlation)

Microsoft's Excel software was used to create statistical relationships between major and trace elements and their mineral hosts analyzed by XRD. The Spearman's Rank Correlation Coefficient method was used to determine whether a positive anomaly existed between all elements of interest, minerals and additional remnant TOC data within the Data Analysis tool in Microsoft's Excel Software. The resultant relationships between elements, mineralogy and TOC will be reported in Chapter 4 for three cored wells (7, 12 and 20).

3.2.2.3 Application of Results

A case study has been undertaken using data derived from hand-held ED-XRF analysis to determine the chemostratigraphy of the lower Eagle Ford member. Lateral facies changes have been mapped out on a local scale within Karnes and DeWitt counties using Ca, Si and Al. Redox proxies (Mo) and paleoproductivity (P, Ni and Zn) proxies were also mapped. The average concentration of each element in each well was calculated and each well point on the map represents that mean value. Maps were hand-contoured around those data points.

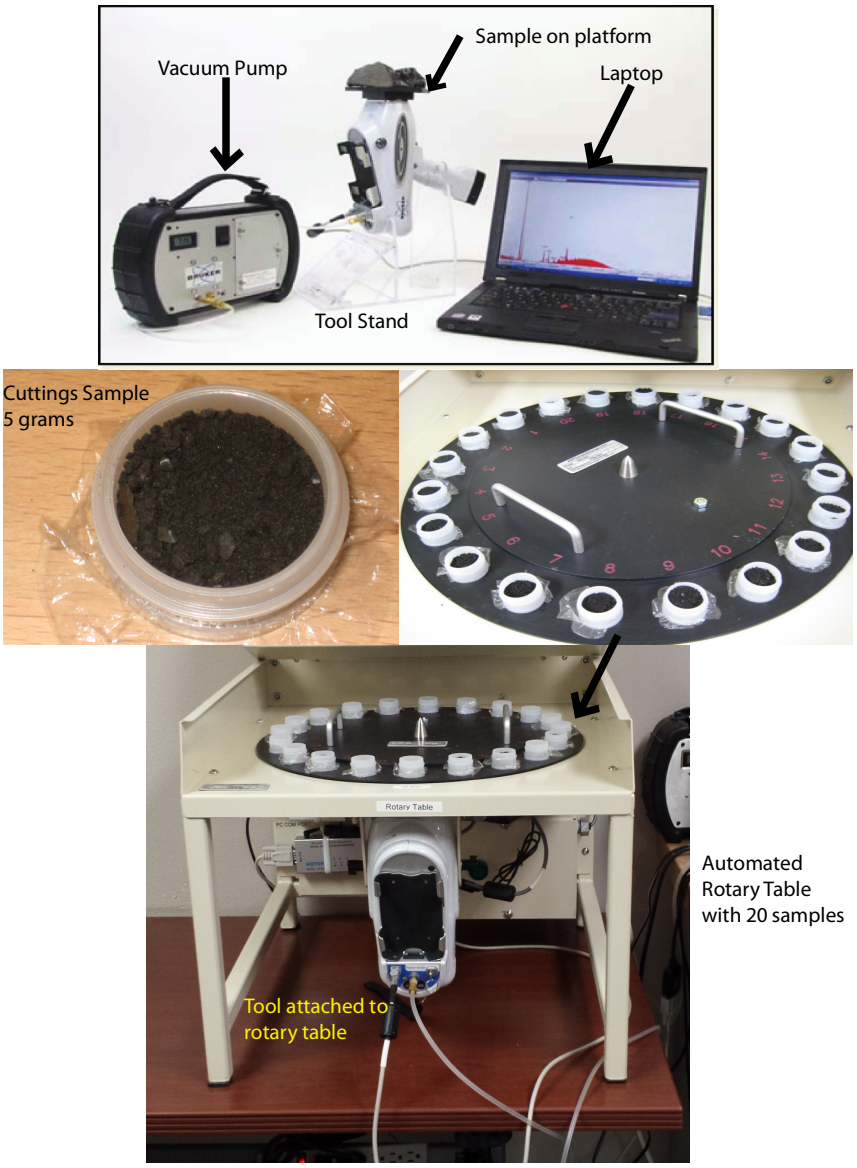

Figure 3.1 Rotary table set up at Pioneer's offices

The hand-held ED-XRF can analyze samples individually on a platform or using a rotary table. Loose tool picture provided and copyrighted by Bruker Elemental (personal communication).

3.3 Chemostrat, Inc. (ICP-OES and ICP-MS)

All samples from seven wells were analyzed by Chemostrat, Inc. (Table 3.3). All of the samples were drill cuttings except for core from the lower Eagle Ford member of well 20.

Table 3.3 List of wells and sample count

All samples analyzed by ICP-OES or ICP-MS analysis. See Appendix D for exact depths and sample interval.

Well	Total Eagle Ford Samples	Starting depth (ft.)	Ending depth (ft.)
3	37	12660	12885
12	27	13460	13750
16	42	13375	13625
17	20	13650	13840
19	62	13690	14000
20	74	13660	13930
24	8	14040	14220

First, samples were prepared by removing any surface contamination by washing the samples with solvent. Cuttings samples were hand-picked using a binocular microscope and then ground to a fine-grained powder using an agate mortar and pestle or re-circulating ball mill. Core samples were disaggregated using a plastic bag and a mallet and then ground with a ball mill. Chemostrat, Inc. notes that agate may result in a slight increase in the Si content of the sample, yet it will be negligible as mudstones already contain major concentrations of Si. Once samples were ground to a fine powder, they were dried at 105° C for twelve hours to remove moisture. Samples were analyzed using a combination of an ICP-OES and an ICP-MS device which returned forty seven elements; ten major elements reported as oxides in wt.%, (SiO_2, TiO_2, Al_2O_3, Fe_2O_3, MgO, MnO, CaO, Na_2O, K_2O, P_2O_5), twenty five trace elements in ppm (Ba, Be, Co, Cr, Cs, Cu, Ga, Hf, Mo, Nb, Ni, Pb, Rb, Sc, Sn, Sr, Ta, Tl, Th, U, V, W, Y, Zn, and Zr) and 14 rare earth elements in ppm (La, Ce, Pr, Nd, Sm, Eu, Gd, Tb, Ho, Dy, Er, Tm, Yb, and Lu). Samples were digested in acid using a combination of hydrofluoric and perchloric acid to create a solution and then sprayed into the ICP instruments as a fine aerosol. To ensure that all elements were detected by the ICP instruments, fusion of samples with an alkali flux and dissolution of the

resultant mix in dilute acid was completed. The flux was lithium metaborate ($LiBO_2$). $LiBO_2$ was mixed with the samples at a 5:1 ratio and heated to 1050°C. This resulted in a molten bead which was then dissolved in 2% nitric acid. Approximately 0.25 grams of sample were utilized per analysis.

The Li-ion fusion procedure followed by Hildred et al. (2011) was outlined by Jarvis and Jarvis (1992) and returned variable analytical error for certain elements. Five international rock standards were run every twenty unknown samples. The error for the major element data is 2% and 3% for high abundance trace element data measured using an ICP-OES (Ba, Cr, Sc, Sr, Zn and Zr). All remaining trace elements were analyzed by ICP-MS and the error was in the order of 5%. The precise nature of the results is the reason the ICP-MS and ICP-OES were used to analyze additional samples but the sample count was not as extensive as the hand-held ED-XRF cuttings analysis. That is why this data set is a supplement to the hand-held ED-XRF data. The limit of detection for the ICP-MS is one or two orders of magnitude lower than ICP-OES. Additional accuracy data from Chemostrat, Inc. is reported in Appendix B.

Chemostrat, Inc. checked the validity of the results compared to the depths that the cuttings came from by creating a chemical gamma log (ChemGR); a log composed of U, K, and Th signatures combined into one log. It was then checked against existing openhole gamma ray (GR) logs for the same well to ensure that no caved material from uphole is being analyzed. Figure 3.2 illustrates the resultant ChemGR profile for four wells that will be used for this dataset. When there is a good match between the red colored ChemGR profile and the wireline GR log, the assumption is that the cuttings are representative of the sequences drilled (Chemostrat, Inc., personal communication).

3.3.1 Normalization

Elements are reported un-normalized to 100% in wt. for major elements and were already reported in ppm for trace elements. Results normalized to 100% were interpreted specifically for Total Alkali-Silica (TAS) diagrams in Chapter 4 (Figure 4.41).

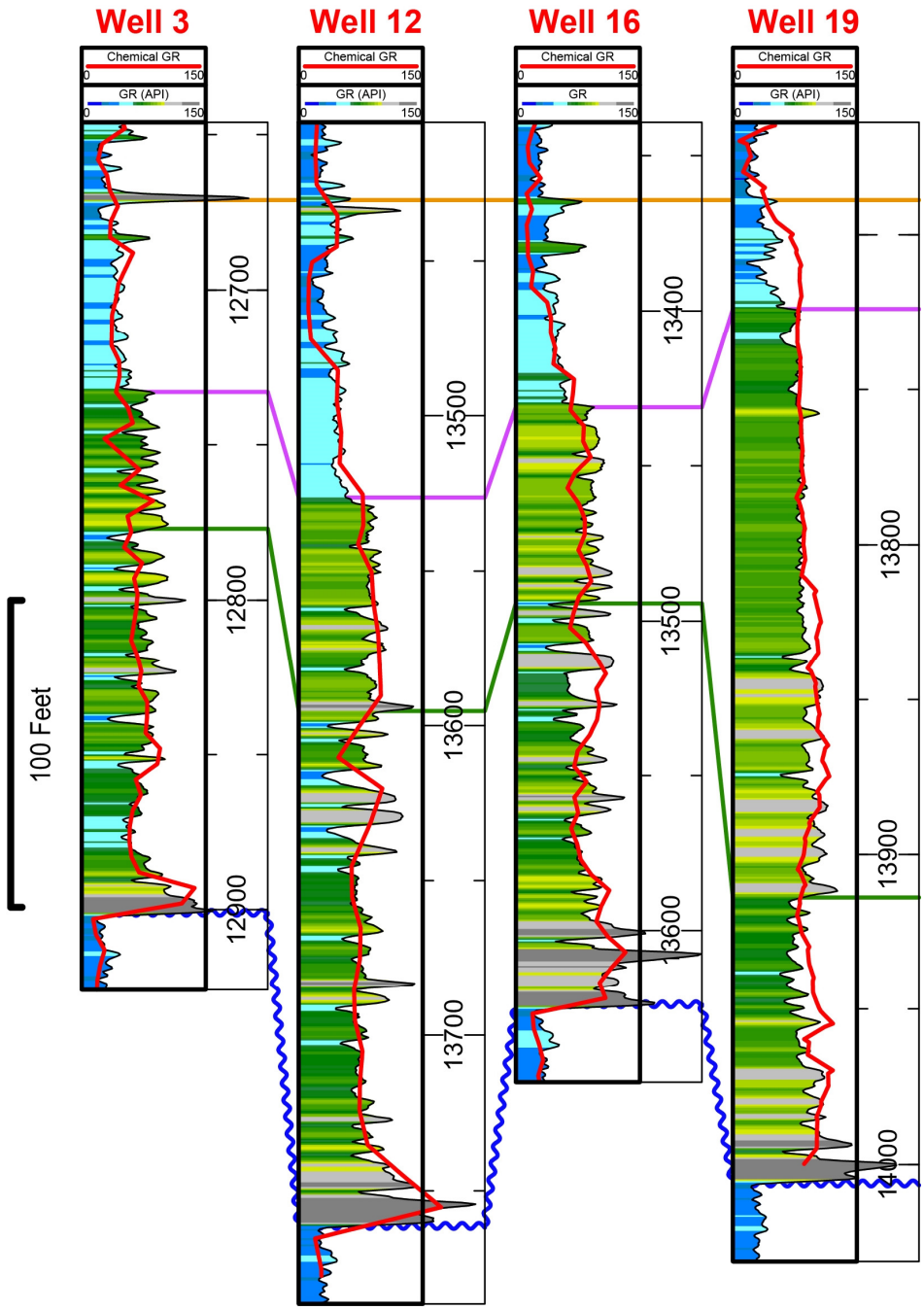

Figure 3.2 ChemGR log compared to an openhole GR log

The red ChemGR curve matches up to the gamma ray log.

3.3.2 Major, Minor and Trace Element Interpretation

IHS Petra® was used to create well logs from the raw spreadsheet data and plot major and trace elements in cross-sections to compare each side by side. Only select major and trace elements were plotted. All data was imported into Petra as a general ASCII file in columnar format. Logs were depth shifted to match gamma ray log signatures in each well using a CaO log from each well relative to the high carbonate Buda Limestone and Austin Chalk. The pilot well is a vertical well drilled to become familiar with the facies between the Coniacian Austin Chalk to the Lower Cretaceous Buda Limestone. Each log represents the Eagle Ford interval that cuttings were available for. Enrichment Factors (EFs) of select elements were normalized to average post-Archean Shale (PAS) to understand the degree of authigenic enrichment of the elements. EFs are calculated using the formula from Tribovillard et al. (2006); $EF = (Element/Al)_{sample} / (Element/Al)_{Standard\ shale}$. In place of a standard shale, average post-Archean Shale (PAS) concentrations from Taylor and McLennan (1985) were used.

3.3.3 Rare Earth Element Interpretation

Rare earth element concentrations from Eagle Ford cuttings were normalized to chondrite values from McDonough and Sun (1995). REEs were also compared to average REE concentrations from post-Archean Australian Shales (PAAS) compiled by Taylor and McLennan (1985) and references therein. REEs from Eagle Ford samples were normalized over PAAS samples to illustrate the similarities/differences between the two. PAAS samples have been suggested to be the average shale composition of upper continental crust by Taylor and McLennan (1985). Since sedimentary processes reflect sediment source provenance as weathering, erosion, transportation and deposition do not fractionate REEs from each other. One goal of this activity is to evaluate if Eagle Ford rocks are similar to upper continental crustal averages using these normalized plots. All plots are on a logarithmic scale with a base of 10. $(La/Lu)_N$ ratios were cross-plotted with $(Dy/Yb)_N$ ratios, both normalized to chondrite, to determine the slope of the Eagle Ford REE pattern.

3.4 Activation Laboratories Ltd.-Actlabs (INAA and ICP)

Additional analyses were completed to complement the hand-held ED-XRF and Chemostrat, Inc. (ICP-MS and ICP-OES) data sets in order to collect elemental data from bentonite. Ash layer (altered to bentonite) chemical signatures were not able to be isolated by the hand-held ED-XRF since cuttings represented an interval of ~five feet per sample. Seven bentonite samples were analyzed for trace metals by Activation Laboratories in Ontario, Canada (Table 3.4) and run through various types of analysis to determine their major and trace metal composition (results and amount of sample used reported in Appendix E).

Table 3.4 Bentonite studied

Well	Sample Number	Depth	Thickness	Formation member
1	14R	13914.8	4.5 cm	Upper Eagle Ford
1	15R	13916.7	3.5 cm	Upper Eagle Ford
8	11H	13090.5	21.7 cm	Lower Austin Chalk
12	3L	13400	5 cm	Lower Austin Chalk
12	7L	13701.8	0.3 cm	Lower Eagle Ford
20	1F	13814.4	2 cm	Middle Eagle Ford
22	2N	14068	2.5 cm	Middle Eagle Ford

Six grams of each core sample was sent to ActLabs and approximately 1 gram was used for each analysis. The Green River Shale Standard (SGR-1) was also included in the analysis as an unknown to determine the accuracy and precision of the instrumentation used. The results of the SGR-1 analysis are excellent for most elements and reported in Table 3.5.

Table 3.5 SGR-1 standard analysis by ActLabs

Element	SGR 1 Recommended Value (Wilson, 2001)	±1σ	Measured Value
SiO_2 (wt. %)	28.2	0.21	27.19
Al_2O_3	6.52	0.21	6.44
Fe_2O_3(T)	3.03	0.14	2.87

Table 3.5-*Continued*

Element	SGR 1 Recommended Value (Wilson, 2001)	±1σ	Measured Value
MnO	0.0267	0.003	0.032
MgO	4.44	0.20	4.38
CaO	8.38	0.37	8.27
Na_2O	2.99	0.13	2.91
K_2O	1.66	0.10	1.6
TiO_2	0.253	0.025	0.242
P_2O_5	0.328	0.066	0.27
As (ppm)	67	5	55
Ba	290	40	289
Cd	0.9		1.3
Co	12	1.5	13.8
Cr	30	3	35.3
Cu	66	9	69
Hf	1.4	0.14	1.6
Hg	0.3		< 1
Mo	35	0.9	36
Ni	29		33
Pb	38	4	40
Sb	3.4	0.5	3.3
S (wt. %)	1.53	0.11	1.67
Sc (ppm)	4.6	0.7	4.85
Se	3.5		< 0.5
Sr	420	30	384
Th	4.8	0.21	4.8
U	5.4	0.4	6.1
V	130	6	130
W	2.6	0.06	< 1
Y	13		9
Zn	74	9	73
Zr	53		42
La	20	1.8	20
Ce	36	4	34
Nd	16	1.7	11
Sm	2.7	0.3	2.55
Eu	0.56	0.09	0.46
Yb	0.94		1.01

Fifty elements were provided through this analysis; major and minor elements including Si, Al, Fe, Mn, Mg, Ca, Na, K, Ti, P and S, and trace elements including Au, Ag, As, Ba, Be, Bi, Br, Cd, Co, Cr, Cs, Cu, Hf, Hg, Ir, Mo, Ni, Pb, Rb, Sb, Sc, Se, Sr, Ta, Th, U, V, W, Y, Zn, Zr with eight rare earth elements including La, Ce, Nd, Sm, Eu, Tb, Yb, and Lu. The methodology of the actual analysis carried out is outlined by ActLabs (2013) on their website and the following outlines the methodology used for all samples as described therein. Pulverization was completed by Actlabs and involved cleaner sand between sample crushing to eliminate impurities from previously crushed samples and also to prevent sample contamination. For elements analyzed using the Instrumental Neutron Activation Analysis (INAA) method, a 1 gram aliquot was encapsulated in a polyethylene vial and irradiated with flux wires and an internal standard (1 standard for 11 samples) at a thermal neutron flux of 7×10^{12} n/ cm^2/s. After a 7 day decay to allow Na-24 to decay the samples are counted on a high purity Ge detector with resolution of better than 1.7 KeV for the 1332 KeV Co-60 photopeak. Using the flux wires, the decay-corrected activities are compared to a calibration developed from multiple certified international reference materials. The standard present is only a check on accuracy and is not used for calibration purposes. About 10-30% of the samples are rechecked by re-measurement. For values exceeding the upper limits, assays are recommended. One blank is analyzed per work order.

A 0.2 gram sample was mixed with a mixture of lithium metaborate/lithium tetraborate and fused in a graphite crucible to determine major element concentrations using an ICP instrument. The molten mixture was poured into a 5% nitric acid solution and shaken until dissolved (~ 30 minutes). The samples were run for major oxides and selected traces on a combination simultaneous/sequential Thermo Jarrell-Ash Enviro II ICP. Calibration was achieved using a variety of international reference materials.

Base metals and selected trace elements are prepared differently. Samples were analyzed using a Varian Vista ICP. A 0.25 gram sample is digested with four acids beginning with hydrofluoric, followed by a mixture of nitric and perchloric acids and then heated using precise programmer controlled heating in several ramping and holding cycles which takes the samples to

dryness. After dryness is attained, samples are brought back into solution using hydrochloric acid. With this digestion certain phases may be only partially solubilized. These phases include zircon, monazite, sphene, gahnite, chromite, cassiterite, rutile and barite. Ag greater than 100 ppm and Pb greater than 5,000 ppm should be assayed as high levels may not be solubilized. Only sulphide sulfur will be solubilized. An in-lab standard (traceable to certified reference materials) or certified reference materials are used for quality control.

3.4.1 Normalization

Elements are reported normalized close to 100% in wt. for major elements and were already reported in ppm for trace and rare earth elements (Au reported in ppb). CaO and Loss on Ignition (LOI) concentrations, both in wt. %, were subtracted and data re-normalized to 100% for a Total Alkali-Silica (TAS) diagram.

3.4.2 Rare Earth Element Interpretation

Similar to the interpretation of Chemostrat, Inc. data, rare earth element concentrations from bentonite results were normalized over chondrite values from McDonough and Sun (1995) and also compared to REE concentrations from post-Archean Australian Shales (PAAS) compiled by Taylor and McLennan (1985) and references therein.

Chapter 4

Results

The results of the methodology will be reviewed systematically in this chapter. In the study design it was mentioned that there were clear goals for undertaking each method of analysis. Hand-held ED-XRF analysis was chosen as the quickest tool to analyze cuttings from twenty-two Eagle Ford wells. Data were collected to illustrate the extent of redox variations and facies changes along the trend of the study area. Laboratory derived data were used to compare with hand-held ED-XRF data since it was measured more precisely using both ICP and INAA techniques. The laboratory dataset is not as comprehensive as the hand-held ED-XRF analysis as it is restricted to a smaller subset of wells (Tables 3.3 and 3.4).

This chapter includes the geochemical results of each analysis and applications of those results in the form of maps, cross-sections, scatter plots and enrichment/depletion diagrams. Organic matter and redox proxies (Mo, V, Cr, Ni, Cu, Co, Zn, and U), detrital proxies (Si, Al, Ti, Fe, Pb) and a carbonate proxy (Ca) are presented for the environmental conditions during the deposition of the Eagle Ford. Indicators for the level of oxygenation in the water column during deposition are also presented (P and Mn). Additionally, the Enrichment Factor (EF) of select elements will be presented. EFs illustrate the degree of enrichment or depletion of an element within the Eagle Ford relative to average post-Archean shale (PAS) concentrations. Finally, data are plotted in various normalized diagrams to determine the provenance of sediments within the Eagle Ford. The general thickness of each member of the Eagle Ford in the study area is illustrated when the GR log is flattened along the upper Eagle Ford contact with the Austin Chalk (Figure 4.1).

4.1 Hand-held ED-XRF

Cuttings from twenty-two wells and core from three wells were analyzed for major, minor and trace elements by a Bruker Elemental Series IV hand-held ED-XRF (

Table 3.1). Mean concentrations of an element for each well were mapped across the trend of the lower Eagle Ford because of its changing characteristics across the study area.

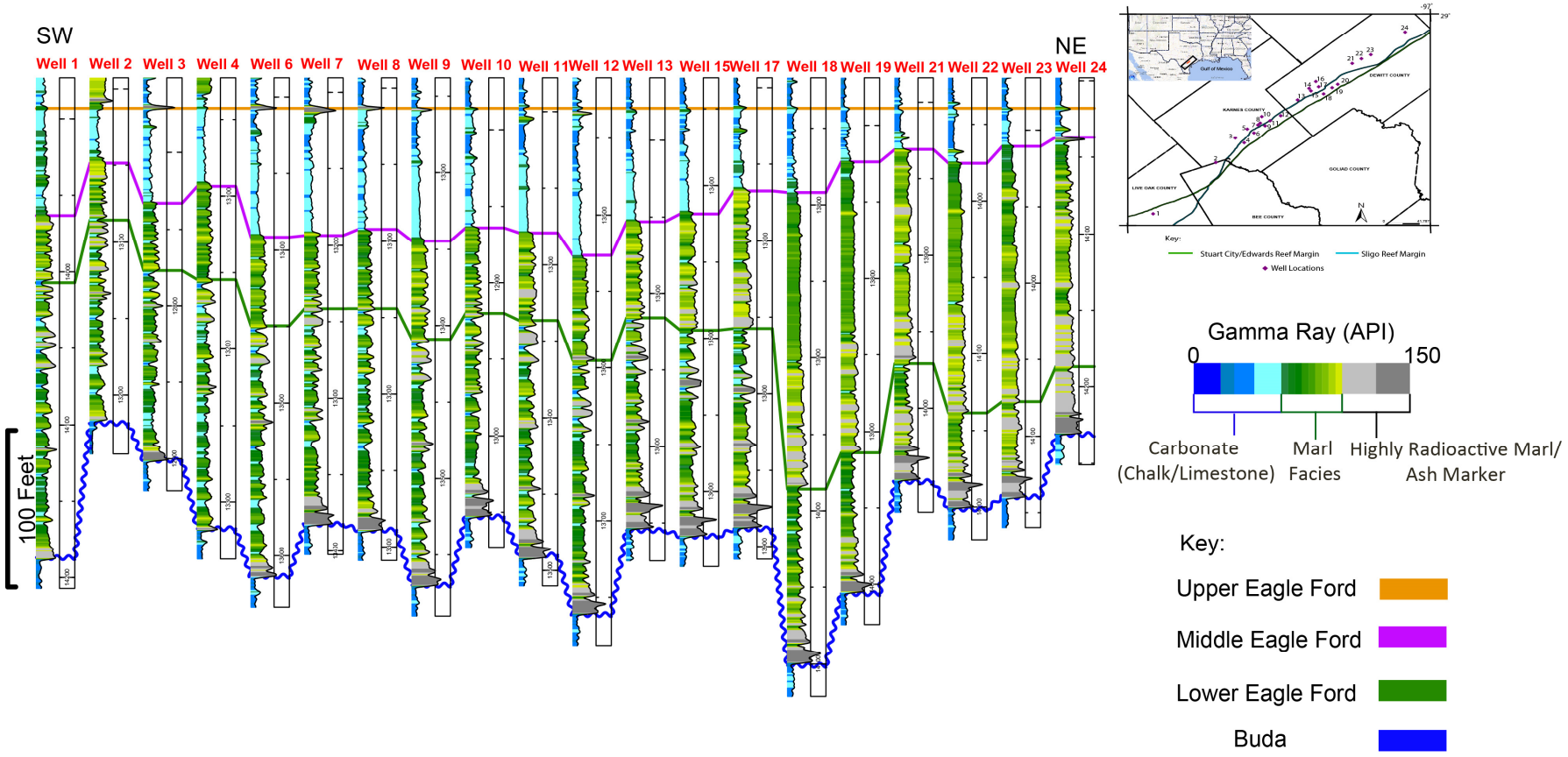

Figure 4.1 General Eagle Ford thickness along strike of the study area

Twenty out of twenty-four of the wells studied. Map of Texas from IHS Enerdeq® Browser v2.3.5 through personal access of software.

4.1.1 Elemental Relationships (Correlation)

Normally XRD analysis is used to determine mineralogy within a rock but the hand-held ED-XRF is a supplement as individual elements can be used as proxies for their mineral hosts (Tucker, 2001; Rowe et al., 2012). Elements have either an affinity for other elements or repel others and statistically, these relationships within the Eagle Ford have been proven to be useful. Correlation coefficients between elements and their mineral hosts indicate that the relationships derived from studies on shales worldwide by Wedephol (1971), Tribovillard et al. (2006) and Brumsack (2006) also apply to the Eagle Ford (Table 4.1). Correlation coefficients have been calculated for elements and their corresponding mineral hosts using Spearman's Rank Coefficient Correlation to provide the basis of those elements' use as proxies. All samples came from three cores (7, 12, and 20). A positive correlation of 1 indicates a perfect linear relationship; -1 would represent the opposite trend, indicating those variables have no affinity for one another and are independent of each other. They will also not be present in large concentrations in the same mineral phase. Si, Al, Na, K, S, and Fe have strong positive correlations with one another, Ti, total clay minerals and quartz (Table 4.1). Ca shows the opposite trend and has a negative correlation with siliciclastic elements and clay minerals. Mn only has a positive correlation with Ca and total carbonate minerals. P correlates well with Fe yet has a weak correlation with others. TOC has also been correlated with all elemental data (

Table 4.2). There were 115 samples which had corresponding TOC analysis completed by LECO in a laboratory setting, taken from the same depth as samples analyzed by hand-held ED-XRF. Those that have been cited as organic matter/nutrient proxies have the best positive association with TOC; including Cu, Ni, Mo, Cr and Zn in decreasing order.

Table 4.1 Correlation coefficients for major elements and minerals

Variable sample amount match for the hand-held ED-XRF data and XRD data (see Appendix B).

Wt.%	*%SiO_2*	*%Al_2O_3*	*%CaO*	*%Na_2O*	*%K_2O*	*%Fe_2O_3*	*%MnO*	*%TiO_2*	*%P_2O_5*	*%Quartz*	*%Total Clays*	*%Total Carbonate*
SiO_2	1.00											
Al_2O_3	0.82	1.00										
CaO	-0.95	-0.92	1.00									
Na_2O	0.76	0.86	-0.81	1.00								
K_2O	0.88	0.82	-0.89	0.75	1.00							
Fe_2O_3	0.40	0.54	-0.62	0.41	0.54	1.00						
MnO	-0.68	-0.60	0.77	-0.45	-0.61	-0.62	1.00					
TiO_2	0.70	0.81	-0.84	0.71	0.79	0.79	-0.65	1.00				
P_2O_5	-0.12	-0.04	-0.05	-0.12	0.04	0.50	-0.19	0.28	1.00			
Quartz	0.66	0.31	-0.53	0.40	0.45	0.13	-0.37	0.34	-0.09	1.00		
Total Clays	0.60	0.81	-0.75	0.69	0.71	0.63	-0.57	0.79	0.14	0.20	1.00	
Total Carbonate	-0.75	-0.72	0.81	-0.65	-0.80	-0.19	0.61	-0.62	0.20	-0.62	-0.93	1.00

Table 4.2 Correlation coefficients for TOC and select elements

One hundred and fifteen samples were correlated with hand-held ED-XRF data and TOC data (see Appendix B).

	TOC
TOC wt.%	1
Cu (ppm)	0.69
Ni	0.68
Mo	0.67
Cr	0.65
Zn	0.49

4.1.2 Lower Eagle Ford Maps

4.1.2.1 Major and Minor Elements

Major elements are useful to define facies variations since they make up greater abundances in crustal rocks. Major elements are also useful for differentiating between clastic sediments and authigenic sediments as well between marine carbonates and siliciclastic rocks. Along a SE-NW strike from Karnes County into DeWitt County there is an increase in detrital silt and clay, whereas a high concentration of carbonate minerals usually makes up the bulk rock composition (Figure 4.2-4.4). Ca will be used as a proxy for marine carbonate deposition although it can also be bound within clay minerals in small concentrations. Ca is enriched in Karnes County and southwest DeWitt County; its concentration decreases basinward and also towards northeast DeWitt County where a higher concentration of quartz and clay are found. Silica (Si) can either be detrital or biogenic. Si occurs as the basic building block of the aluminosilicates including clay and feldspar, and makes up pure quartz (Calvert and Pedersen, 2007). Biogenic silica also makes up the opaline skeletons of diatoms and silicoflagellates, in addition to radiolarians (Calvert and Pedersen, 2007). A small biogenic component has been discovered in radiolarians through Scanning Electron Microscope (SEM) imaging on cuttings from the lower Eagle Ford member. Quartz and therefore Si occurs primarily in silt and clay fractions in Eagle Ford rocks. The detrital component of quartz is greatest in northeast DeWitt County. Al is the best proxy for clay minerals and has been used to quantify the terrigenous/detrital fraction in marine rocks as its authigenic enrichment under normal seawater conditions is low (Brumsack, 2006). Al is a proxy for the deposition of aluminosilicates in addition to silica thus it will show high concentrations were these sediments dominated. Al content is enriched in northeast DeWitt County where a high concentration of clastic material is found (Figure 4.4). Al is diluted where there is a greater concentration of carbonate deposition.

Phosphorus (P) is used as a paleoproductivity proxy because it is a limiting macronutrient for algal growth along with fixed nitrogen in modern oceans (Calvert and Pedersen, 2007). It is normally brought in with oxygen-rich water through upwelling. P is the main element in apatite,

which can be present in the form of individual grains or phosphate concretions (Brumsack, 2006). P shows an increase in concentration basinward and a decrease in concentration updip from the Lower Cretaceous shelf edges (Figure 4.5).

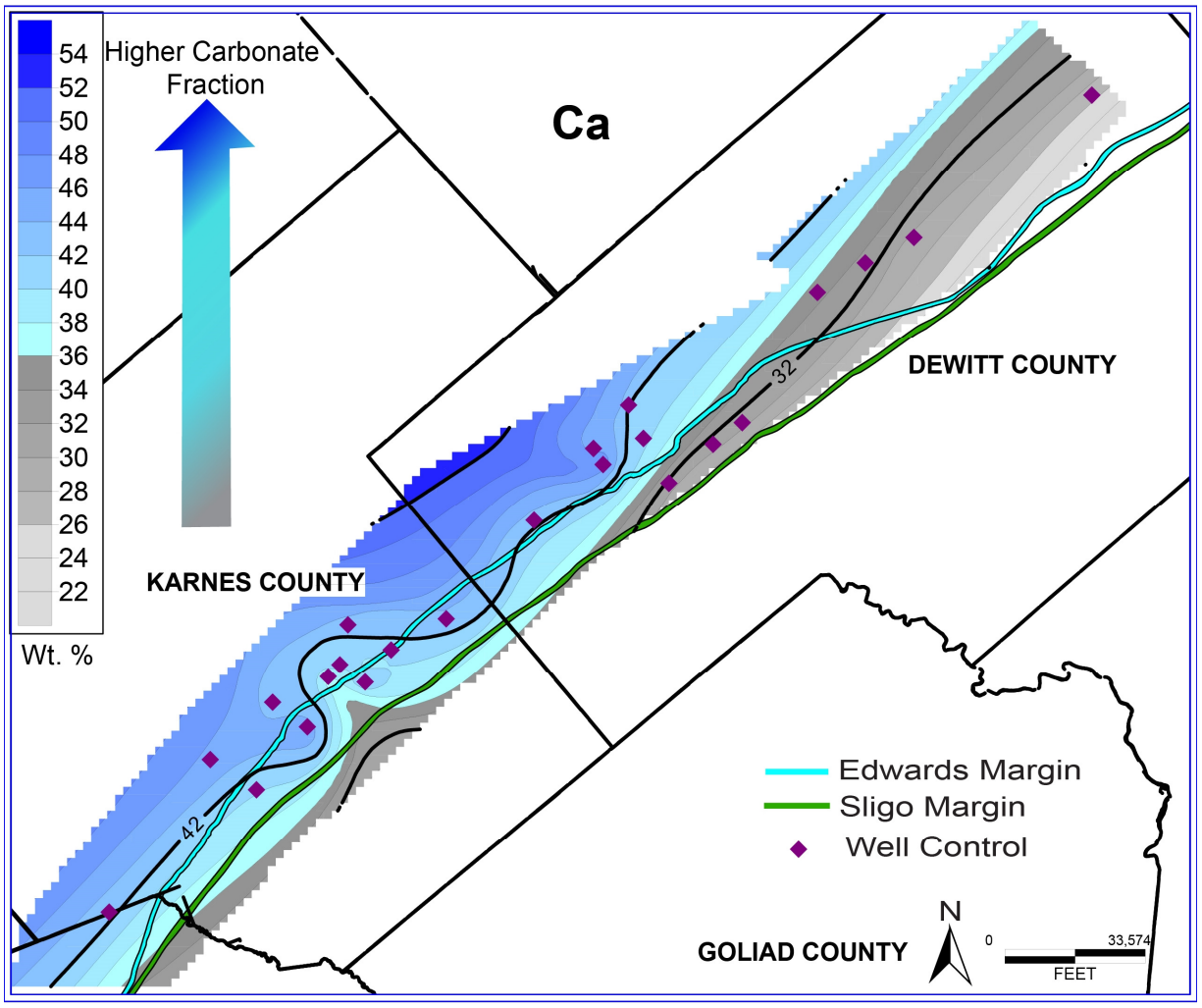

Figure 4.2 Lower Eagle Ford distribution of calcium

Ca concentrations increase updip of the shelf margins within the carbonate fraction.

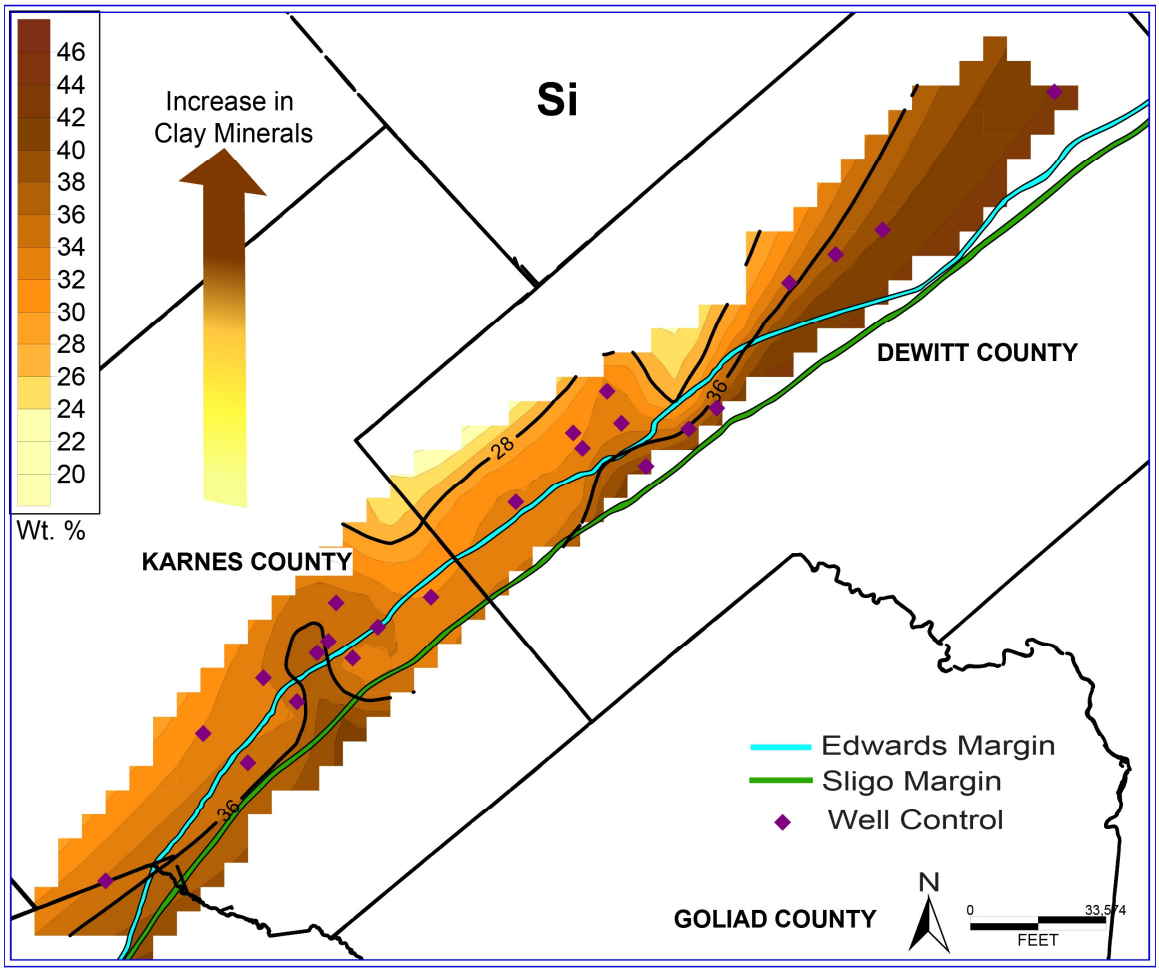

Figure 4.3 Lower Eagle Ford distribution of silica

Si concentrations are highest in northeast DeWitt County as well as basinward and imply an increase in clay minerals.

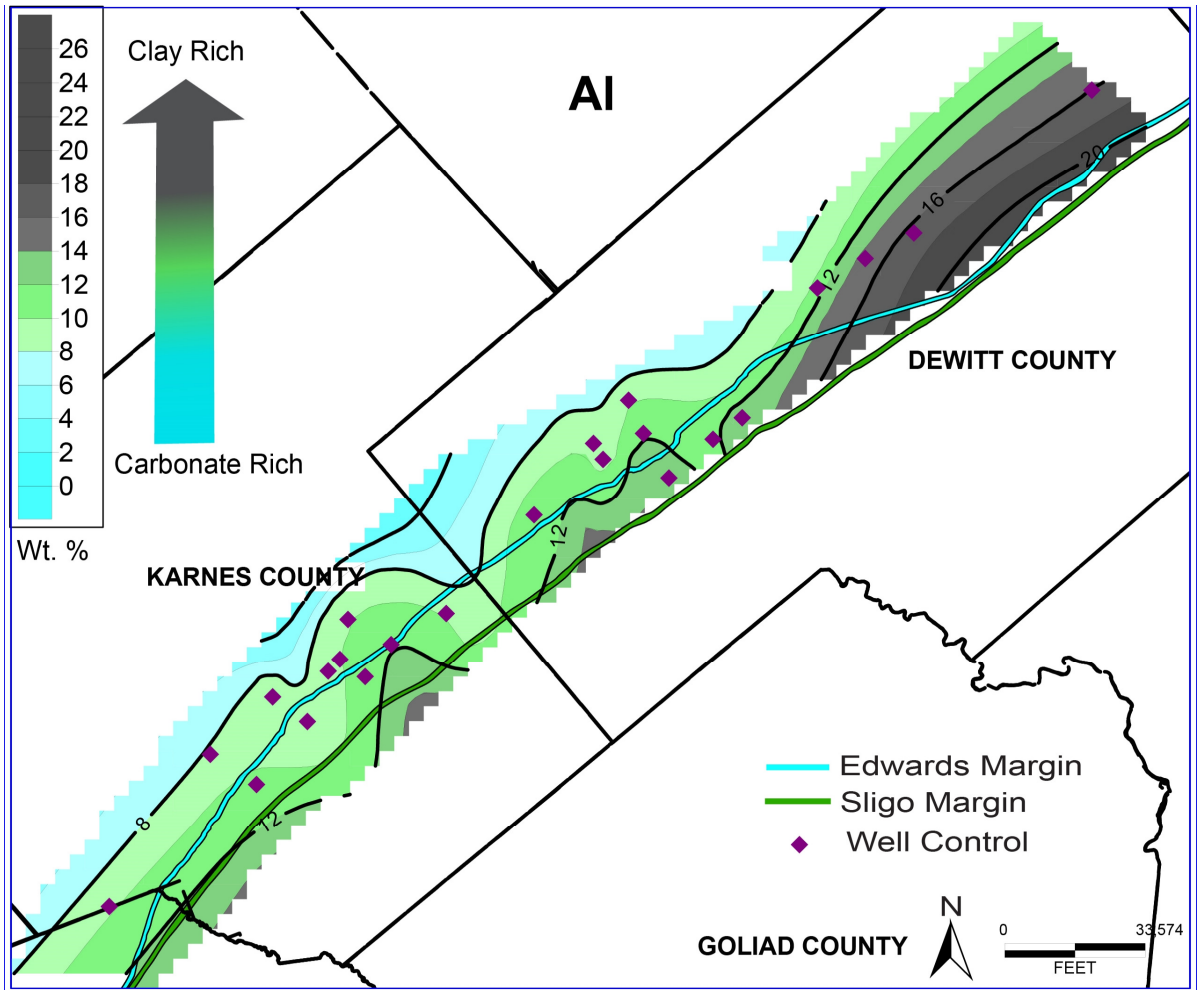

Figure 4.4 Lower Eagle Ford distribution of aluminum

Al concentrations are highest in northeast DeWitt County as well as basinward where there is a higher amount of clay minerals. Al concentrations decrease where the carbonate minerals make up the bulk of the rock.

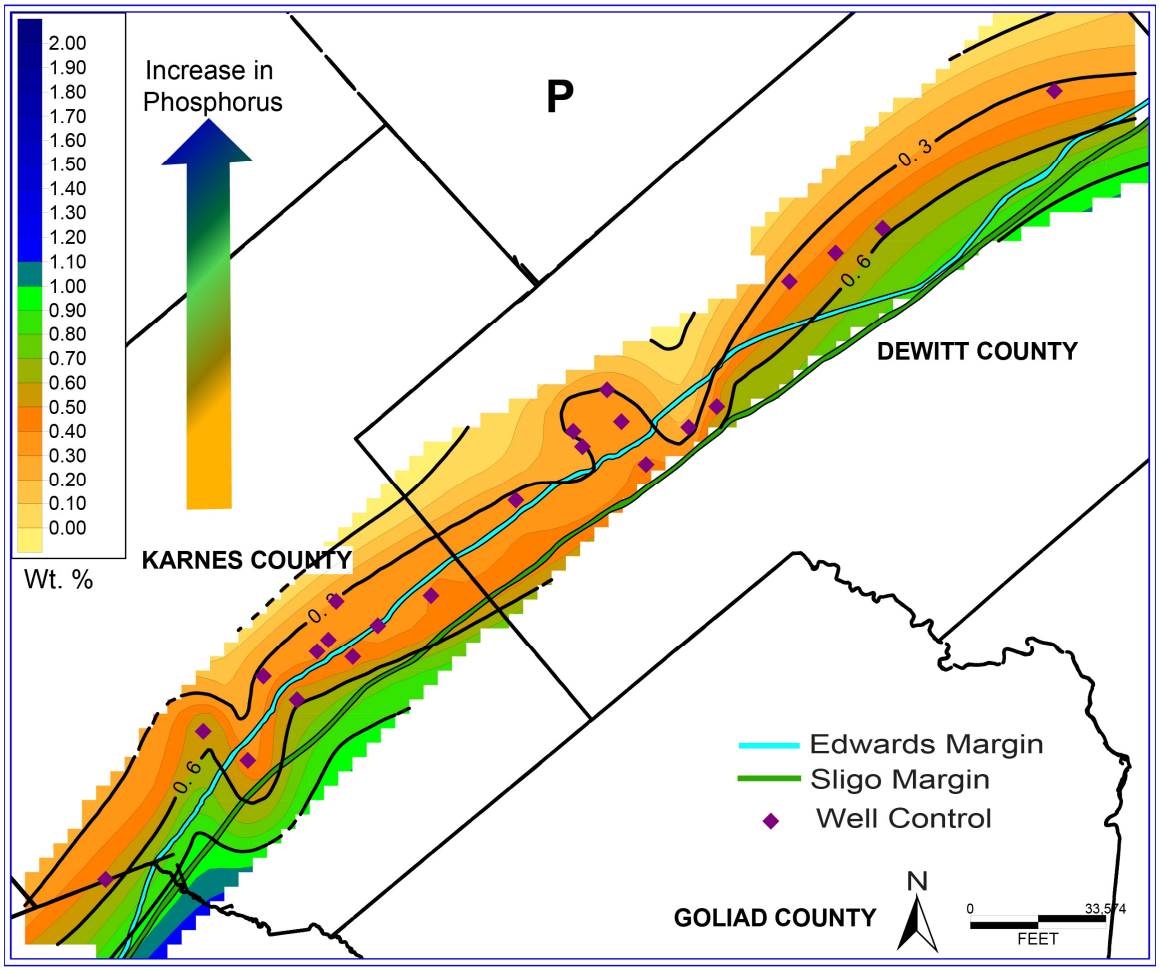

Figure 4.5 Lower Eagle Ford distribution of phosphorus

P concentrations are greatest downdip of the shelf margins and decrease updip.

4.1.2.2 Redox Sensitive Trace Metals and Nutrient Proxies

Trace metals are useful as paleoredox proxies (Mo) or can be used as organic matter proxies since some are nutrients for planktonic organisms (Ni and Zn) (Tribovillard et al., 2006). Water column anoxia can be traced using redox sensitive metals such as Mo. Mo is useful as a proxy for paleoanoxia when its concentrations are enriched above average shale concentrations (Yan Zheng et al., 2000; Wedephol, 1971). Mo is found in low concentrations in oxygenated water and high concentrations of Mo are found when free H_2S is present in the water column under euxinic conditions (Brumsack, 2006). Mo can be used to define the cycles of oxic, anoxic and

euxinic conditions depending on its abundance in the rock (Kearns, 2011). Some values may be greater than 20 ppm in the whole rock which can be classified as euxinic and fall as low as 1 ppm which would be classified as oxic (Kearns, 2011). Mo concentrations range between 0-90 ppm within the lower Eagle Ford member with an average of 20 ppm. The cut-offs and scale from a combination of Yan Zheng et al.'s (2000), Kearns' (2011) and Tinnin et al.'s (2013) work have been scaled as a relative gradient to determine changes from an oxic to anoxic and euxinic environment. Mapping mean concentrations for each well drilled in the lower Eagle Ford member presents an environmental shift from an anoxic environment to a more oxygen-rich environment from the southwest to northeast as well as basinward (Figure 4.6).

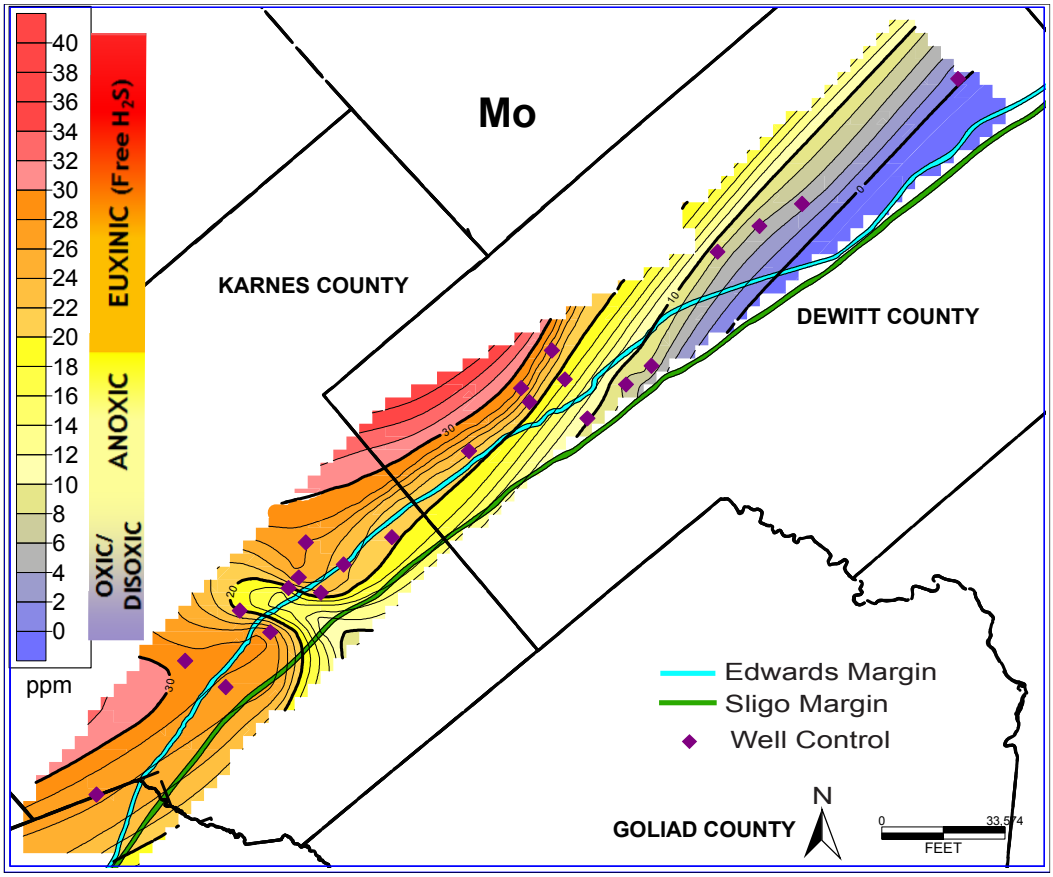

Figure 4.6 Lower Eagle Ford distribution of molybdenum

Mo concentrations are low in northeast DeWitt County indicating that this area was oxygen rich during depositional time. Higher Mo concentrations in southwest DeWitt County and Karnes County persist since the bottom water column was more anoxic to euxinic.

Concentrations of other nutrient proxies such as Ni and Zn also vary across the trend. Both elements are present in moderate to high concentrations (Figures 4.7 and 4.8). Ni and Zn are used as productivity proxies since they are micronutrients (Tribovillard et al., 2006). Where Ni and Zn are present in high concentrations, nutrient deposition or precipitation is expected to be high.

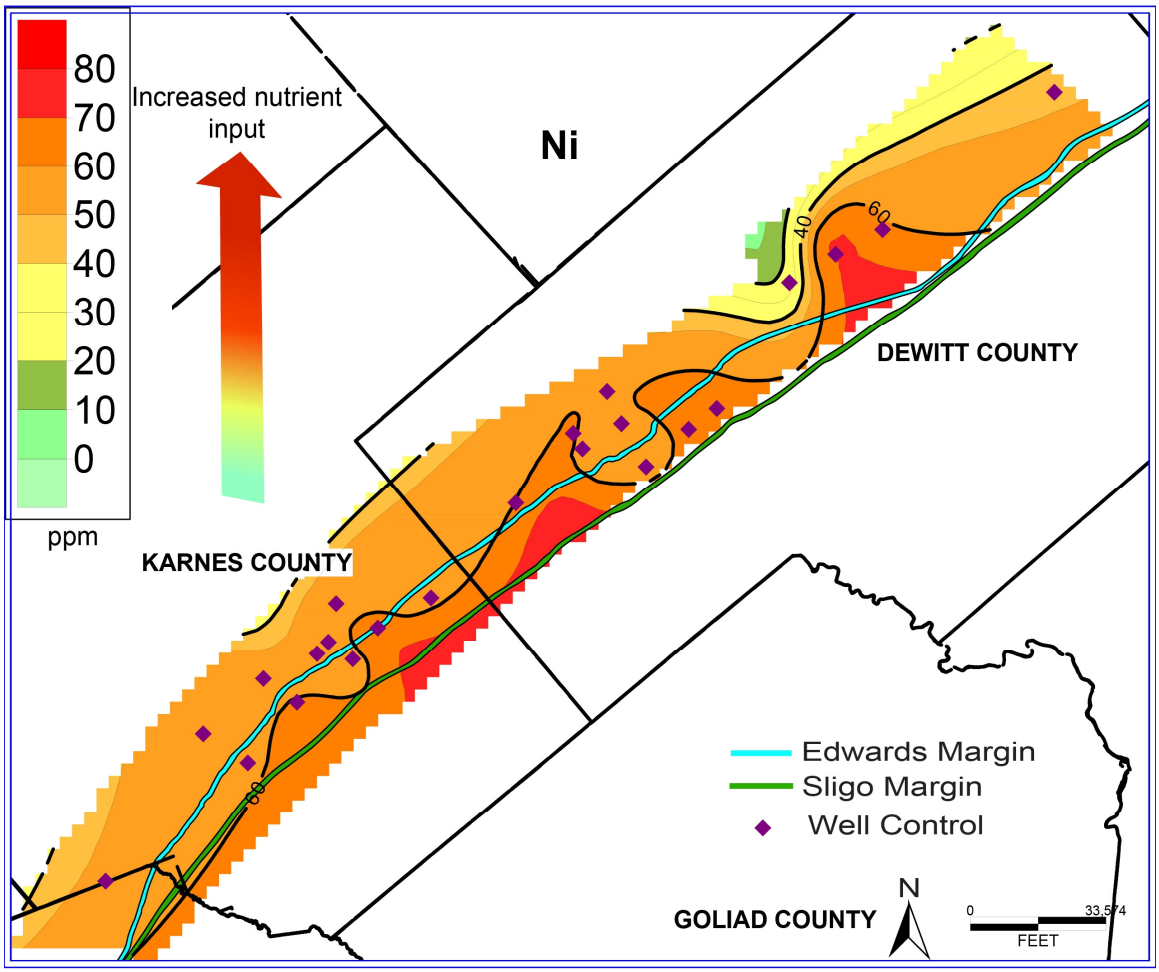

Figure 4.7 Lower Eagle Ford distribution of nickel

Individual Ni concentrations were relatively high overall but increase basinward.

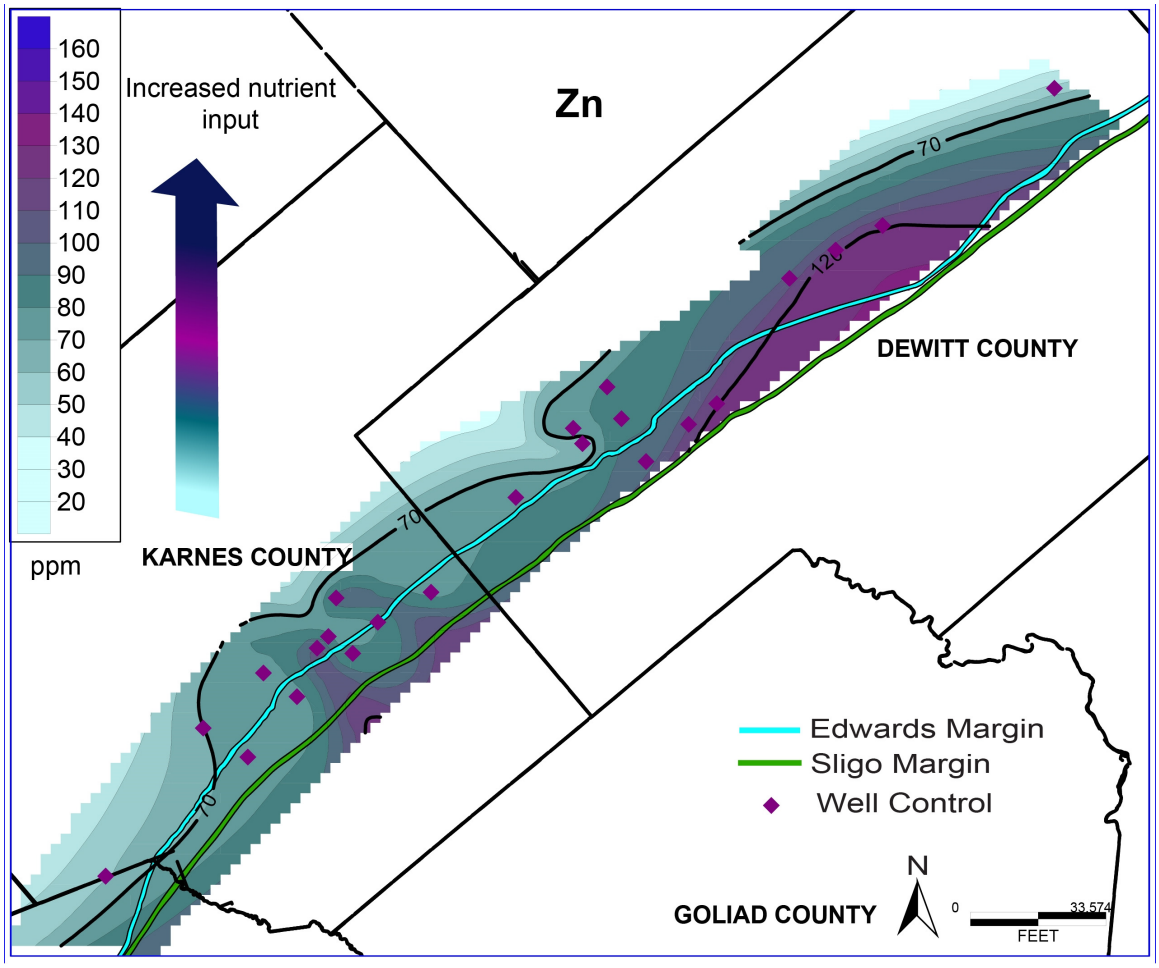

Figure 4.8 Lower Eagle Ford distribution of zinc

Individual Zn concentrations increase basinward and decrease updip of the shelf margins.

4.1.2.3 Maps of Enrichment Factors

The Enrichment Factor (EF) for certain elements was also calculated to create a separation between authigenic and detrital sediments within the lower Eagle Ford member. First, elements are normalized over Al from Eagle Ford samples, and then that ratio is normalized to average shale concentrations for the same elements. Elements were normalized over Al mainly because Al is conservative and stable and estimates the “background” contribution of an element derived from crustal sources (Calvert and Pedersen, 2007). Al is abundant in weathering profiles and is present due to the in situ formation of clay minerals and its mechanical erosion from

continental rocks, which eventually are transported onto the sea floor (Calvert and Pedersen, 2007). The EF of an element is greater than 1 if an element is enriched or less than 1 if the element is depleted relative to average shale. The post-Archean shale (PAS) reference from Taylor and McLennan (1985) was used as the model for average shale.

EF P was mapped in order to compare its similarity to phosphorus concentrations in average PAS. Sediments in the Eagle Ford are enriched greater than 20 times that of an average PAS (Figure 4.9). Although P is deposited across the Eagle Ford trend, P can be solubilized under reducing conditions and is not well preserved in oxygen-deprived sediment (Poulson et al., 2006; Tribovillard et al., 2006). There is a low abundance of P where the Eagle Ford experiences reducing conditions. The maps of Mo or EF Mo are useful guides to identify these areas.

EF Mo was mapped to determine the enrichment and depletion of Mo along the trend relative to average PAS. Where EF Mo values are low, Mo is depleted and the Eagle Ford was deposited under oxygen rich conditions. Mo is depleted in northeast DeWitt County and enriched in southwest DeWitt and Karnes Counties (Figure 4.10). The EF of Mo can reach as high as 60 times the concentration of Mo in an average PAS suggesting the lower Eagle Ford member was deposited under highly euxinic conditions in Karnes County and SW DeWitt County based on the scale derived by Yan Zheng et al. (2000).

Mapping EF of Ni and Zn illustrates a different pattern than the un-normalized elements. When normalizing over Al, EF Ni concentrations appear higher updip from the shelf margins. This is unlike Ni and Zn individually, which are higher basinward. These maps reflect the need to normalize to Al to remove the influence of the elements' fraction in clay minerals. Ni and Zn are bound to organic matter and can also be retained in the sediment in association with pyrite under reducing conditions (Tribovillard et al., 2006). EF Ni and EF Zn are enriched 3 and 6 times an average PAS, respectively (Figures 4.11 and 4.12). Thus there was a high availability of nutrients during the deposition of the lower Eagle Ford member.

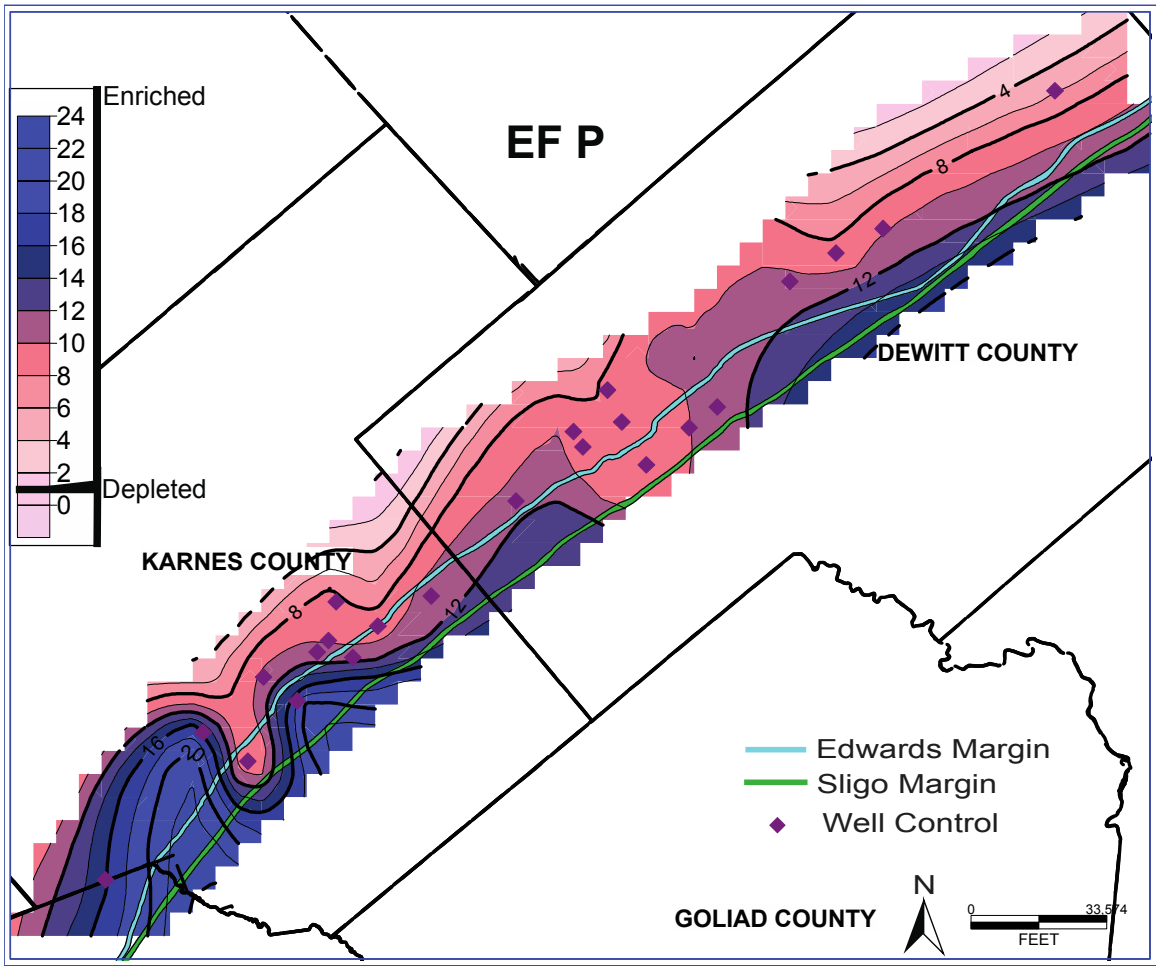

Figure 4.9 The Enrichment Factor of phosphorus in the lower Eagle Ford

The EF of P suggests that the Eagle Ford was enriched overall relative to average shale but more so downdip of the shelf margins.

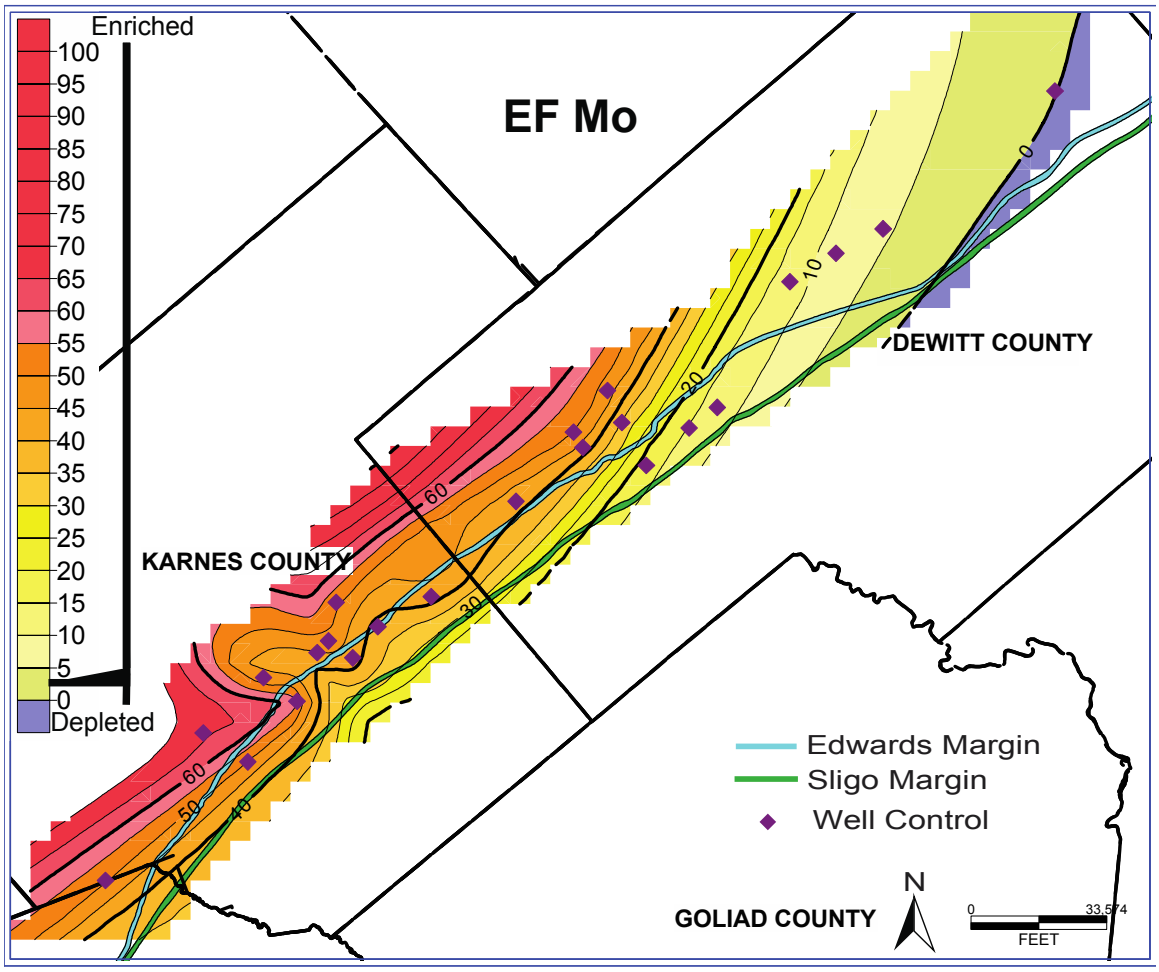

Figure 4.10 The Enrichment Factor of molybdenum in the lower Eagle Ford

The EF of Mo is similar to mean concentrations of Mo alone. The Eagle Ford is depleted in Mo in northeast DeWitt County relative to average shale and greatly enriched toward the southwest.

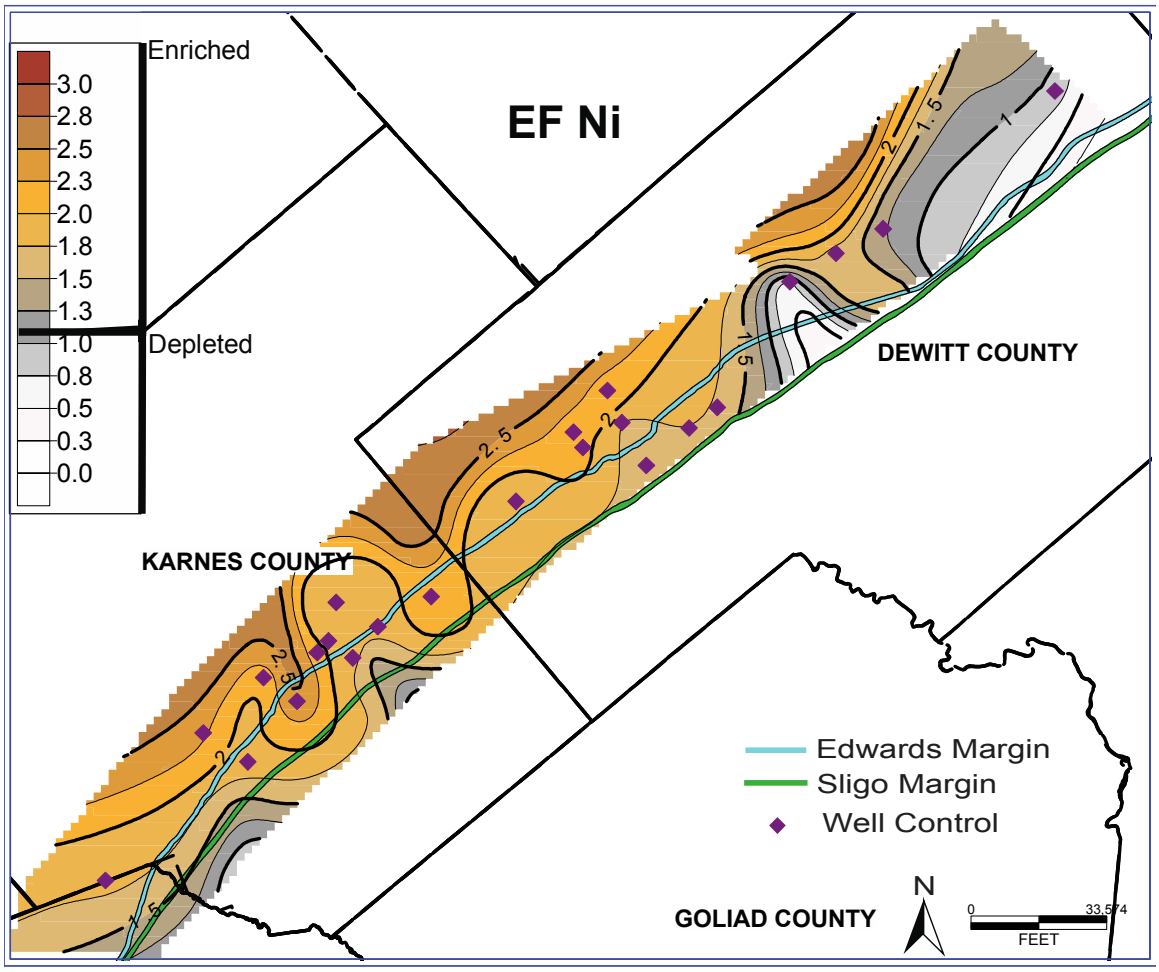

Figure 4.11 The Enrichment Factor of nickel in the lower Eagle Ford

The EF of Ni was mapped and illustrates that there is a dilution of nickel in carbonate rich sediments. Removing the effect of aluminum (clay minerals) reveals that nickel is actually enriched authigenically updip of the shelf margins relative to average shale.

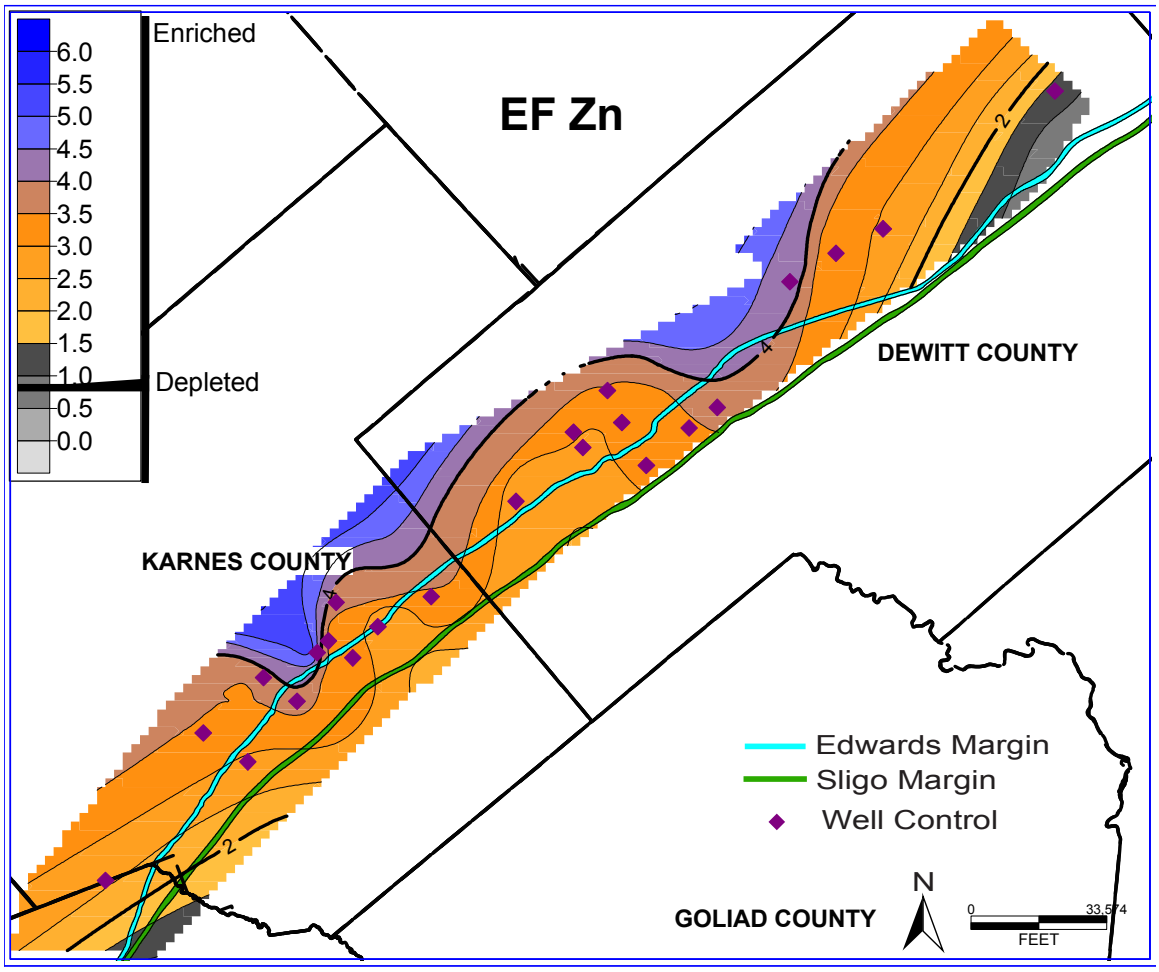

Figure 4.12 The Enrichment Factor of zinc in the lower Eagle Ford

The EF of Zn shows the same effect as the EF of Ni. Zinc is slightly enriched updip of the shelf margins and depleted downdip relative to average shale.

4.2.2.4 Summary

Maps in the previous section illustrate facies changes as well as changes in paleoredox conditions and nutrient availability within the lower Eagle Ford member. Mapping the mean EF for select elements illustrates the anoxic nature of the Eagle Ford relative to terrigenous average shale such as a PAS. In the following section, cross-sections will illustrate temporal changes throughout the depth of the entire Eagle Ford Formation based on more precise analytical methods through ICP-OES and ICP-MS techniques. Rare earth elements will also be employed to illustrate the major change in facies, as well as to understand the provenance of sediments

within the Eagle Ford. The Eagle Ford Formation has been compared to average shale and the findings reflect that the rocks within the Eagle Ford were deposited under different conditions than average shale. It is best to evaluate major elements, trace elements and REEs individually.

4.2 Chemostrat, Inc.: ICP-OES and ICP-MS

A total of forty-seven elements have been analyzed through laboratory ICP-OES and ICP-MS techniques. The precise measurement of elemental data enables the values derived to be used to illustrate the changes in facies in the Eagle Ford throughout its depositional time. Paleoredox conditions are illustrated by using major, minor and trace metals and sediment provenance can be illustrated using the rare earth elements.

4.2.1 Major, Minor and Trace Elements

It has already been illustrated from elemental data maps of the lower Eagle Ford member that there is a change in nutrient and redox proxies toward the northeast of the study area. The following cross-sections aim to illustrate that there is also a change with depth (temporally) in the depositional environment of the Eagle Ford Formation. Results from seven wells have been plotted along a southwest to northeast strike (Figure 4.13). Figures 4.14-4.20 represent aluminum-normalized samples from each well and depict how select minor and trace elements (Mo, Ni, Cu, Zn, P, Fe, Co and Mn) change along the strike of the study area. Elements were normalized to remove the effect of any part of the element bound in clay minerals. The Element/Al log represents the authigenic component for each element. The gamma ray (GR) log and a color-coded Mo log, using the scale from Tinnin et al., 2013, have been added to each cross-section to help the reader recognize which facies changes they are observing. The first pattern to note is that the GR signature increases toward the northeast showing a decrease in carbonate content and an increase in argillaceous minerals. Another pattern that emerges is cyclical anoxia within the bottom water column and also cyclical deposition of nutrient proxies such as Ni, Cu and Zn. P also increases concentrations in a cyclical manner suggesting there were pulses of increased upwelling throughout the deposition of the Eagle Ford instead of a continuous pattern. There was a steady supply of nutrients carried in as Ni, Cu, and Zn

concentrations are high in the upper Eagle Ford member. Co is seen as a micronutrient necessary in the biological processes of algae (Brumsack, 2006 and references therein). Co can be effective as a paleoredox proxy but not to the extent of Mo or V (Tribovillard et al., 2006). Co is better interpreted as a nutrient proxy. Other nutrients such as Ni, Cu and Zn mimic the Mo pattern at times suggesting that these elements are contained within a mineral phase that contain S, as these are all chalcophilic elements. Sulfur concentrations increase as anoxic to euxinic conditions persist based on the high concentrations of all chalcophiles.

Mn is actively recycled between oxidized and reduced states and brought in by fluvial systems either dissolved or in particulate form (Brumsack, 2006; Calvert and Pedersen, 2007). Mn is largely depleted in the Eagle Ford. P is more sensitive to pulses of increased upwelling, yet Mn does show cyclical variations. The Eagle Ford shows the relationships between Mn and redox as described by Brumsack (2006). There is a pattern that suggests high concentrations of Mn in oxygen rich waters and low concentrations in anoxic water. In the Eagle Ford, Mn concentrations are low throughout the Eagle Ford Formation and high in the Buda and Austin Chalk formations. The upper Eagle Ford member was deposited under an oxygenated and upwelling environment shown in increased Mn concentrations. Since the upper Eagle Ford was deposited during a third-order regression cycle (Donovan et al., 2012), sea level would have been falling during this time and sediment prograding toward the basin.

Contacts at the end and beginning of Eagle Ford time can be seen in elemental logs. At the contact of the Eagle Ford and the Buda Limestone anoxia increases greatly and an oxygenated environment is replaced by an anoxic environment shown in the sharp increase in Mo. This is a typical chemostratigraphic marker depicting the beginning of Eagle Ford time in South Texas. The transition from the upper Eagle Ford member to the Austin Chalk is more gradational as carbonates fine into the overlying Austin Chalk and increase in concentration. The Austin Chalk was also deposited under an oxygenated water column as Mo concentrations decrease and Mn concentrations increase.

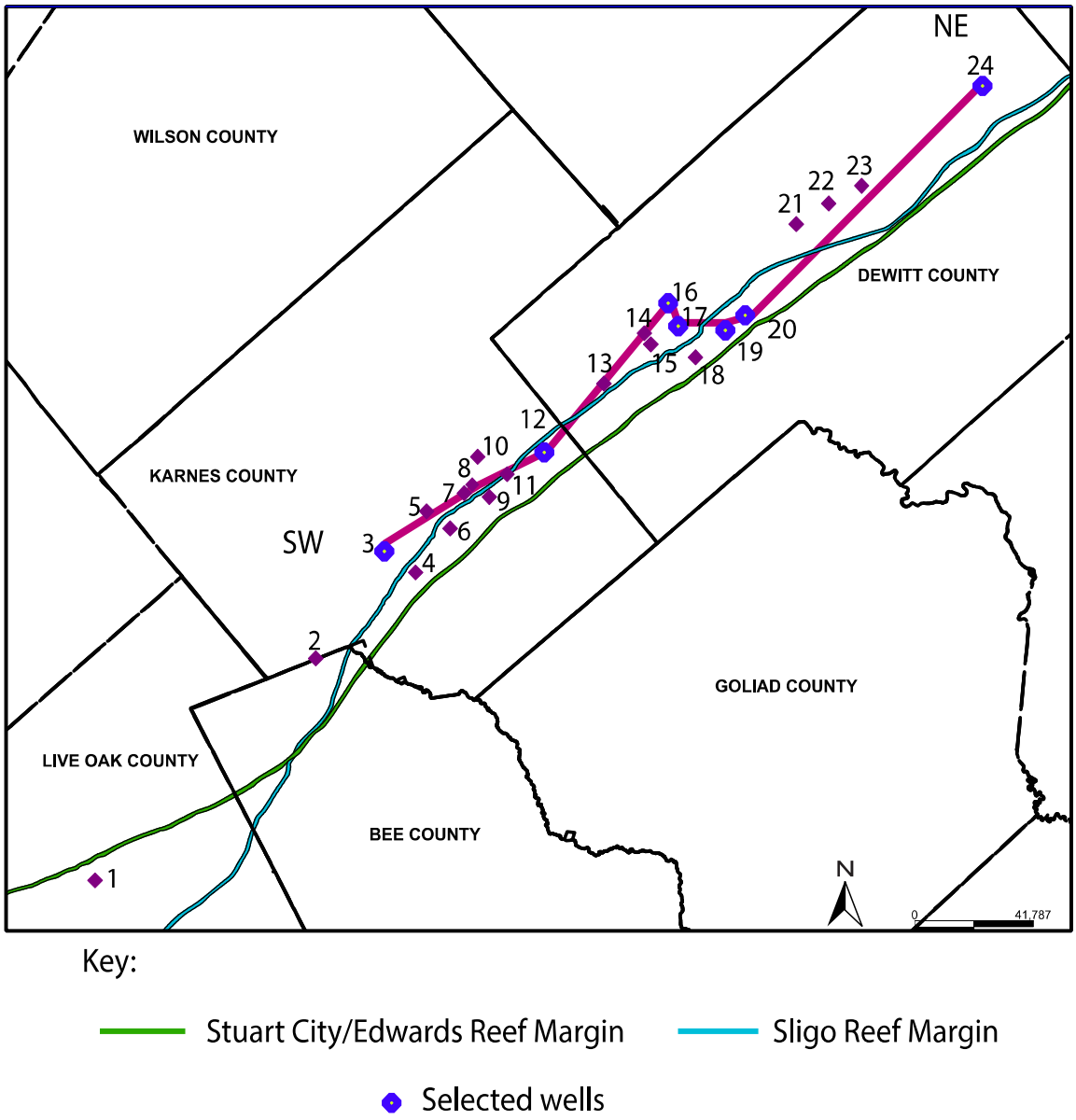

Figure 4.13 Strike line of wells with wet geochemical data

A subset of seven wells is presented.

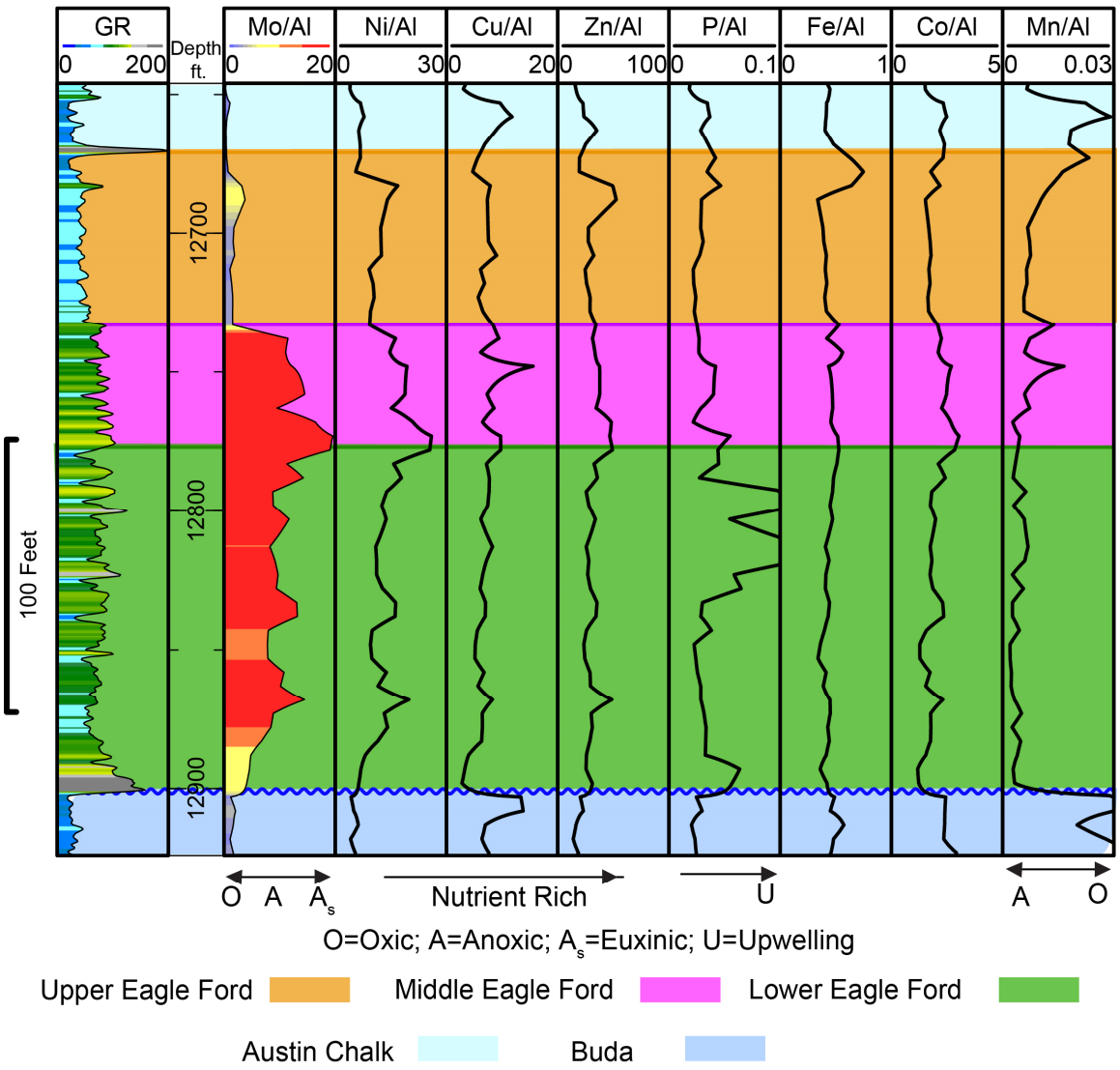

Figure 4.14 Minor and trace element patterns in well 3

Molybdenum concentrations are highest in the middle and lower Eagle Ford showing mainly anoxic bottom water conditions during Eagle Ford time. Phosphorus shows a cyclical upwelling pattern. The GR signature implies that there are several carbonate stringers interbedded with marl and mudstone in this location.

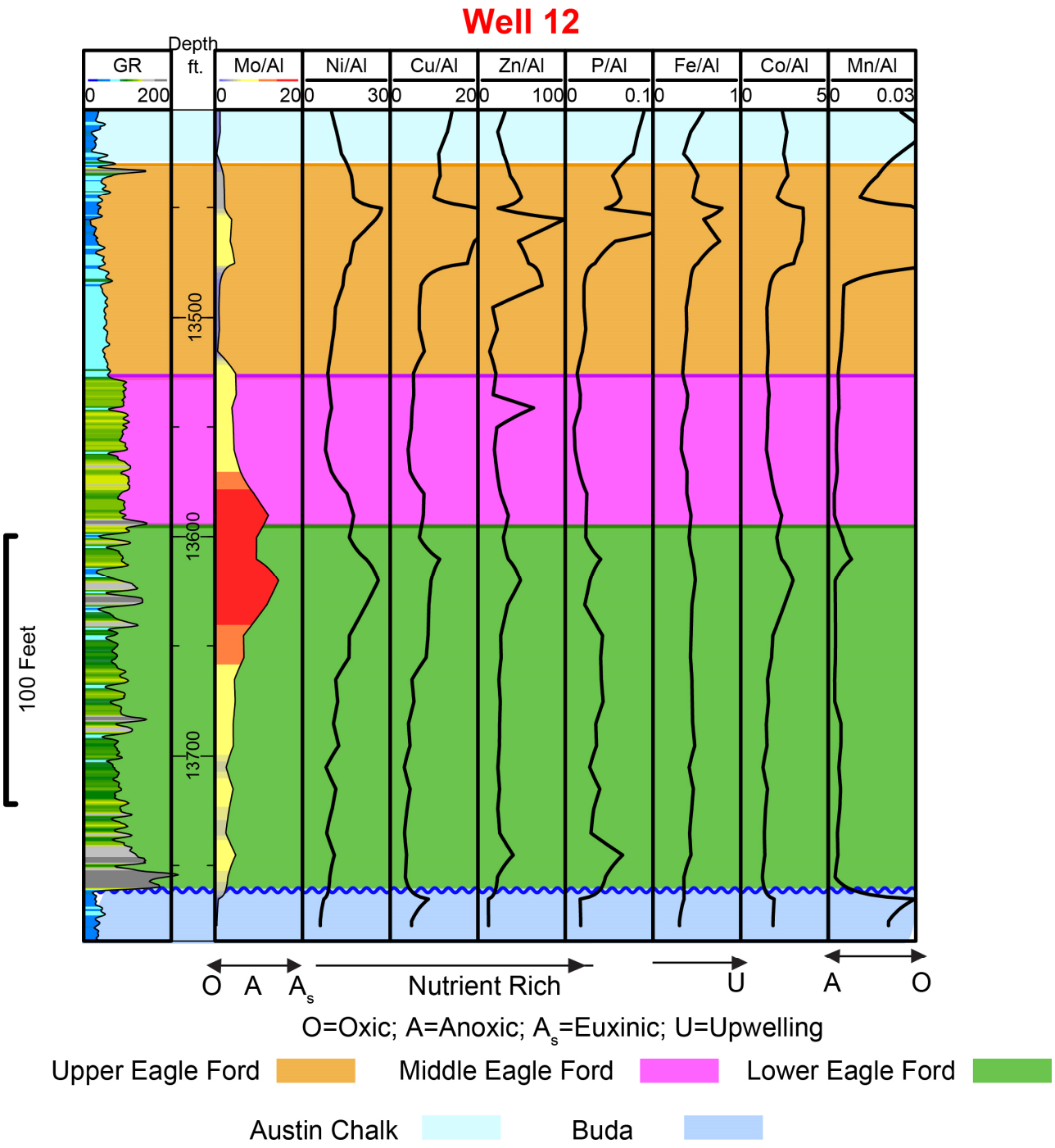

Figure 4.15 Minor and trace element patterns in well 12

As seen in well 3, nutrient proxy concentrations vary slightly within the lower Eagle Ford and decrease in the Austin Chalk and Buda Limestone. Manganese concentrations decrease where an anoxic environment is encountered.

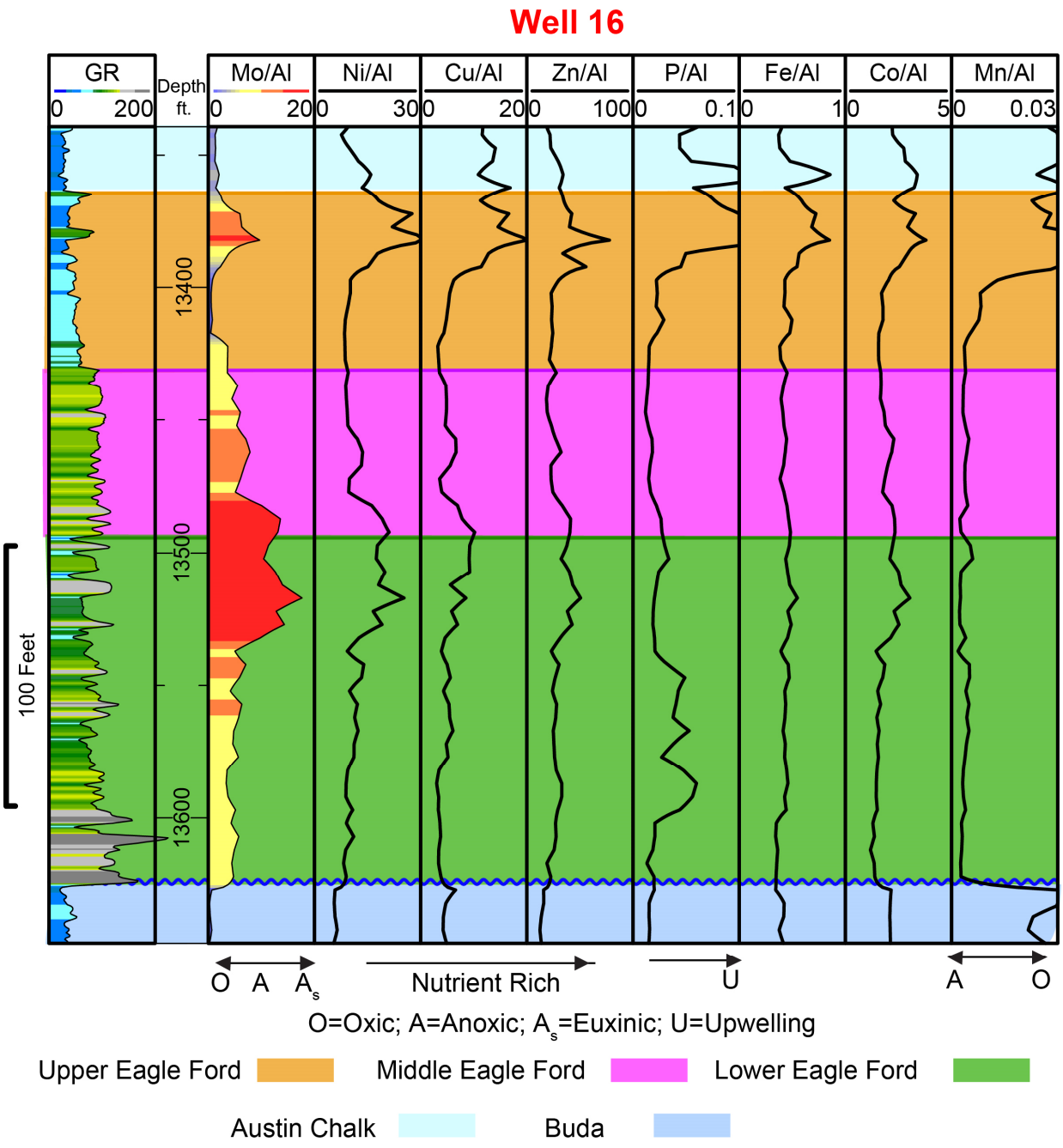

Figure 4.16 Minor and trace element patterns in well 16

Nutrient proxies mimic Mo. Phosphorus decreases in concentration in the middle Eagle Ford. In this well it is evident that Mn concentrations sharply increase in the Buda, the upper Eagle Ford member and the Austin Chalk.

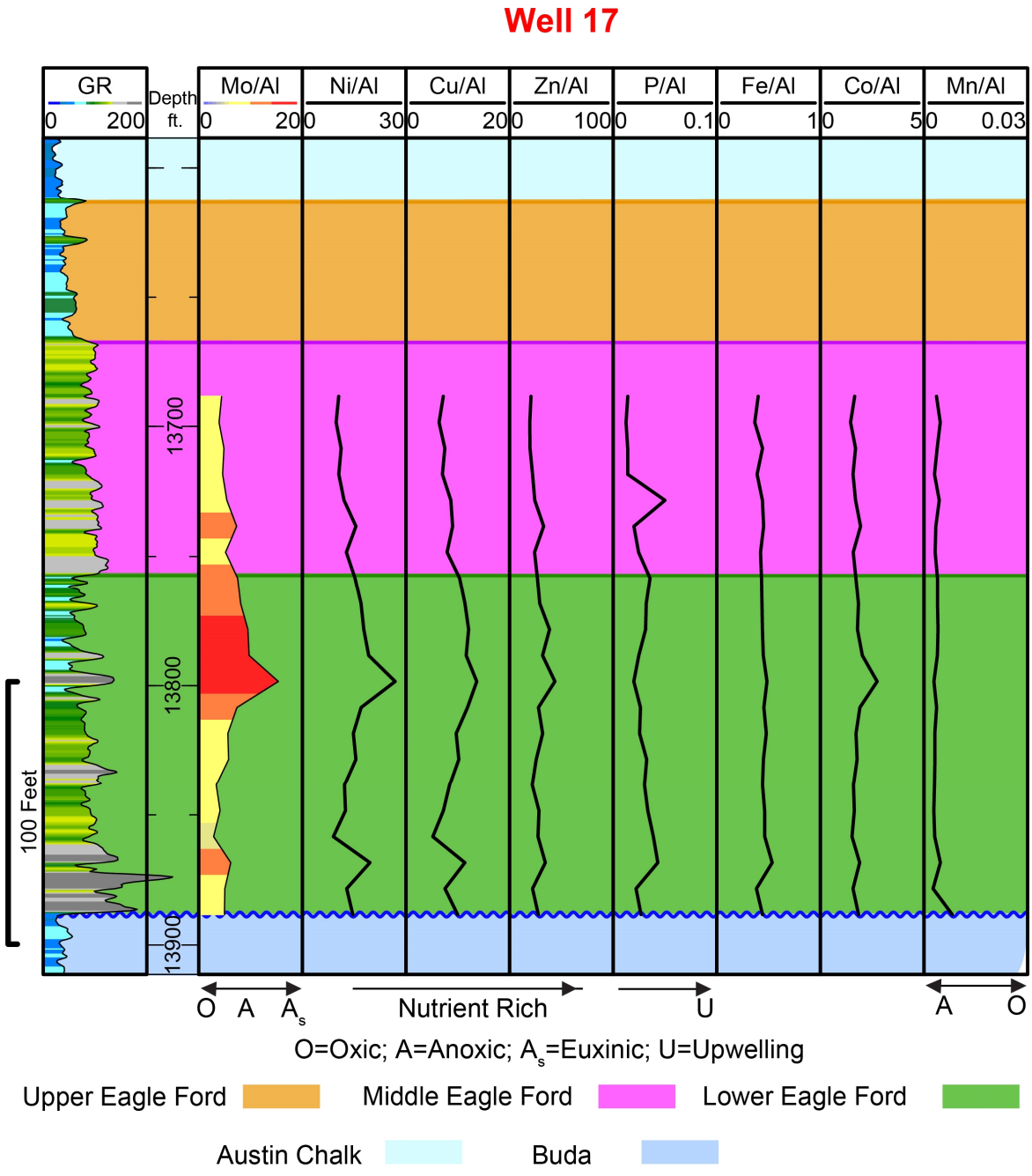

Figure 4.17 Minor and trace element patterns in well 17

This well has samples from only the middle and lower Eagle Ford members. Varying degrees of anoxia persisted throughout the deposition of the Eagle Ford in this well's location. Nutrient proxies also mimic Mo patterns.

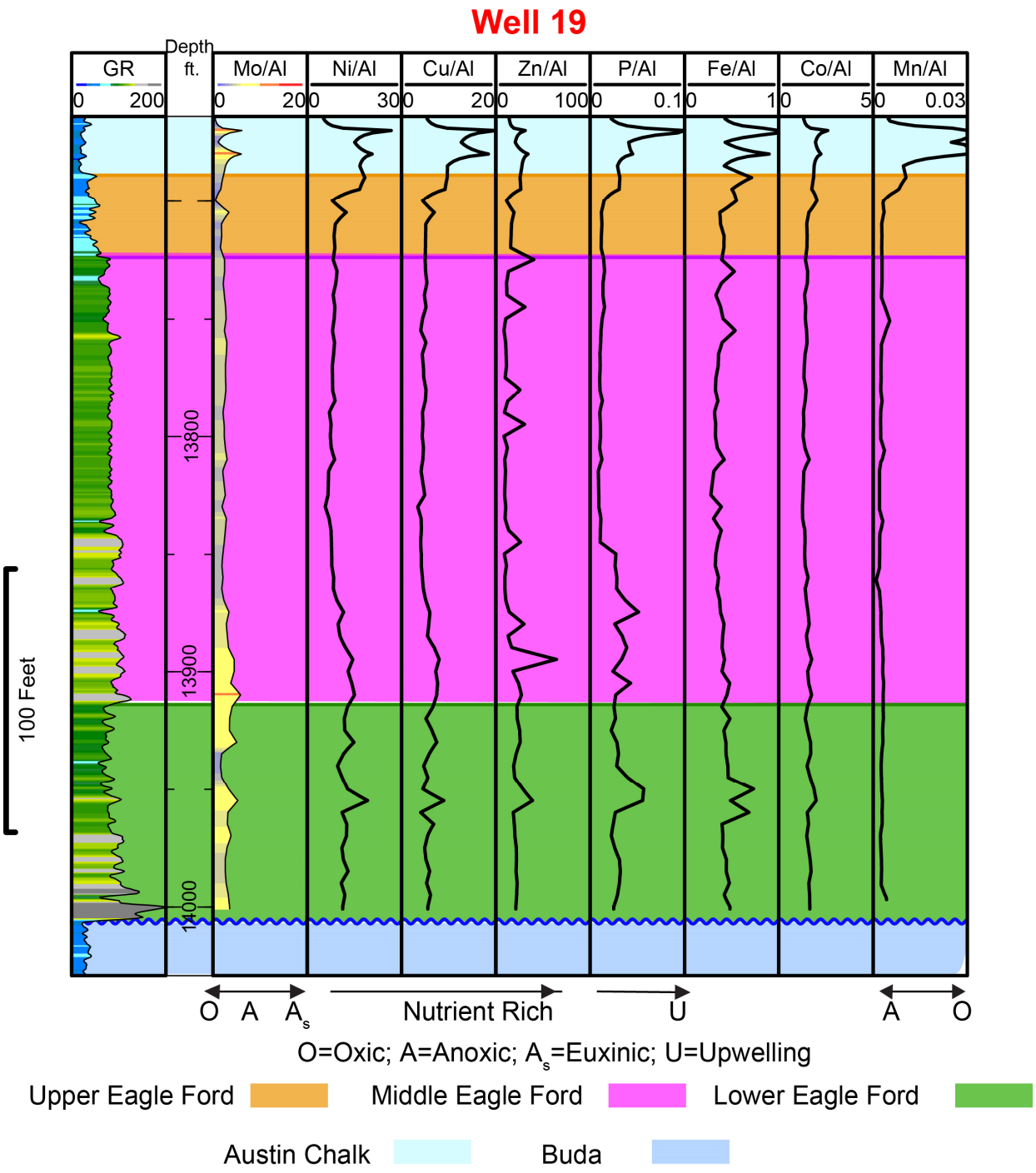

Figure 4.18 Minor and trace element patterns in well 19

Mo concentrations decrease downdip of the shelf margins, visible in this well. Phosphorus concentrations are relatively high throughout the lower and middle Eagle Ford and decrease in the upper section of the middle Eagle Ford.

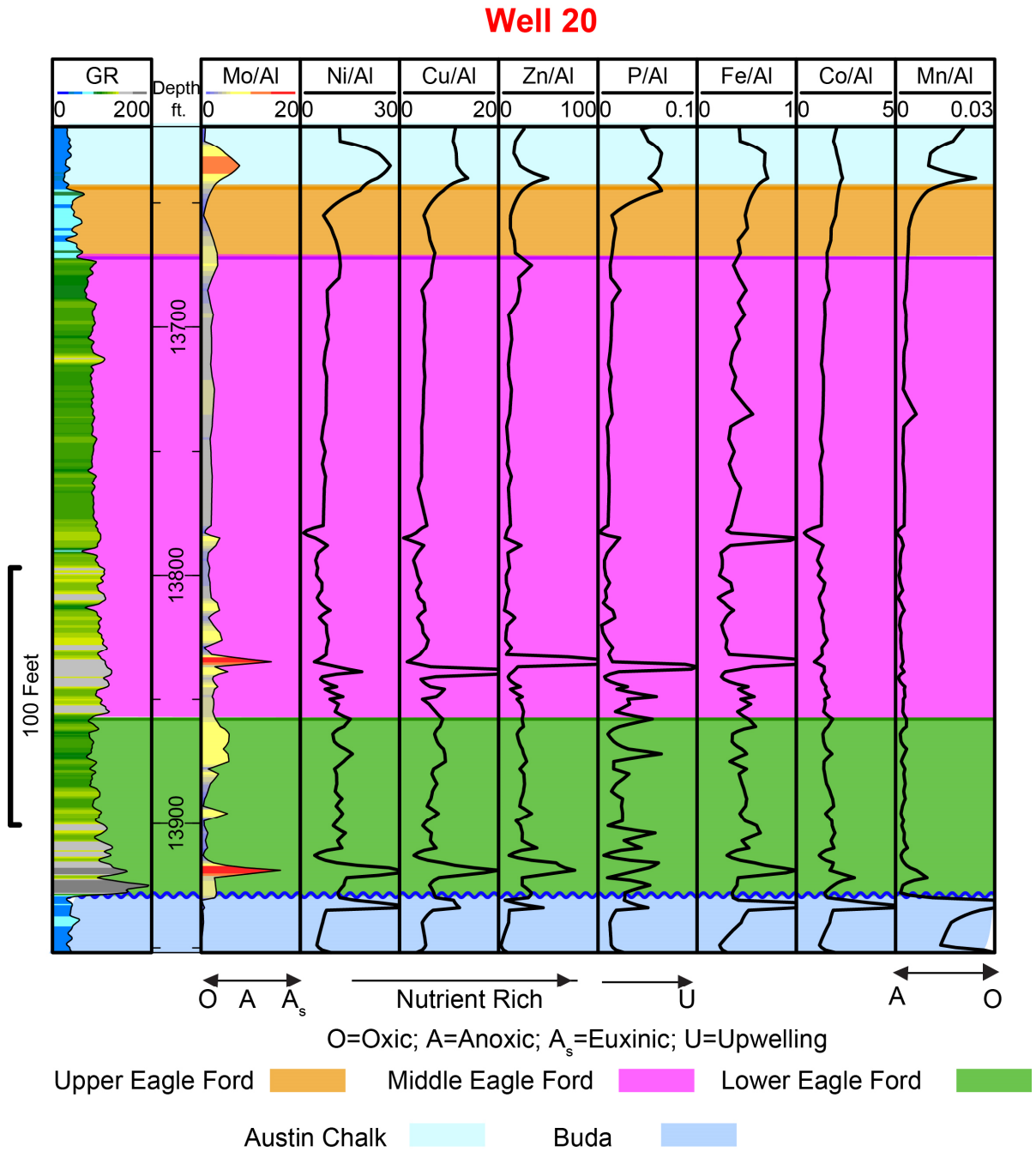

Figure 4.19 Minor and trace element patterns in well 20

Elemental concentrations show high variability in samples from this well due to an increased sample rate. The water column during deposition of the Eagle Ford was dysoxic to anoxic, yet experienced cyclical upwelling. Nutrient proxies mimic Mo, also seen in previous figures.

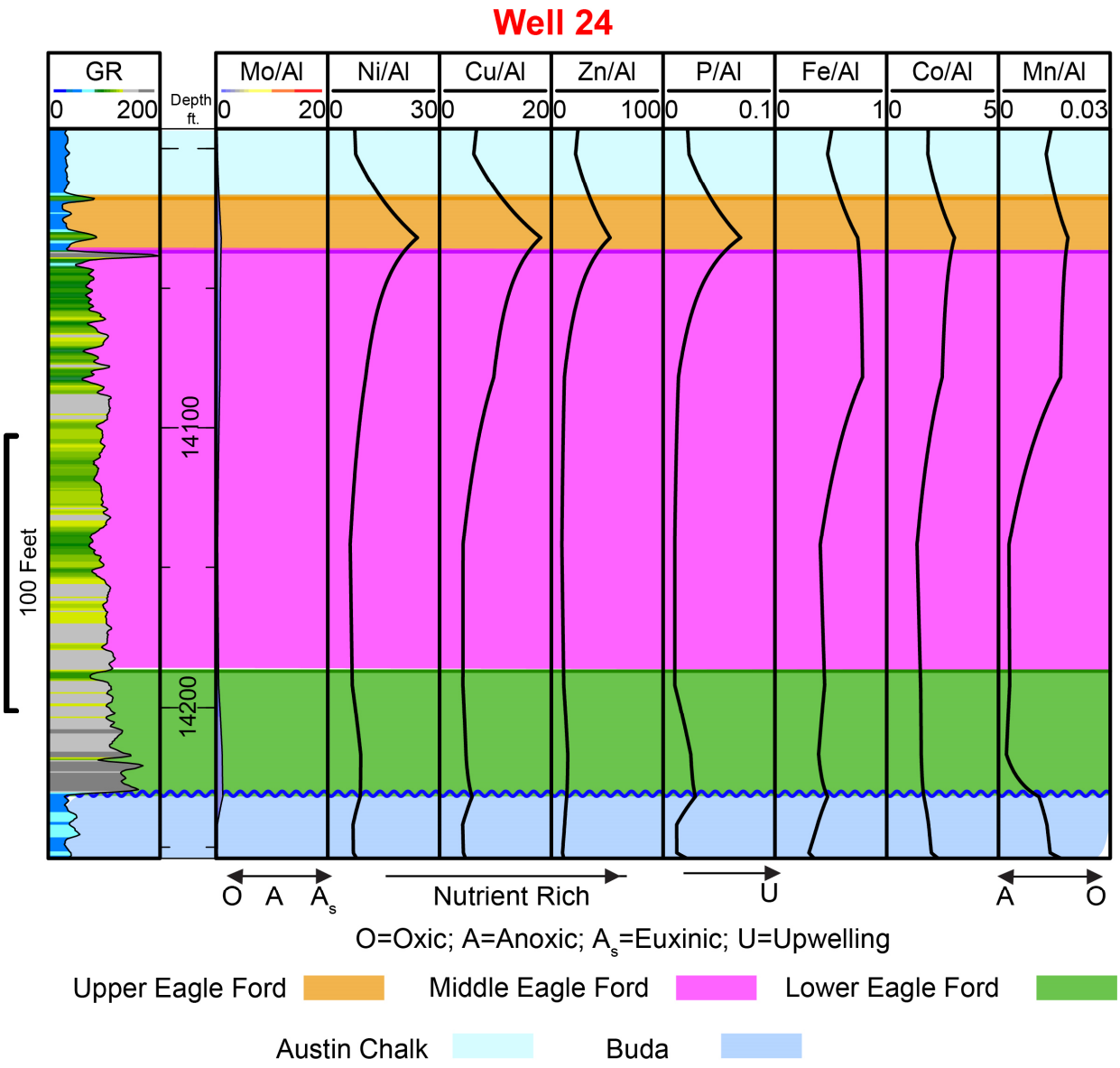

Figure 4.20 Minor and trace element patterns in well 24

Molybdenum concentrations sharply decrease in the northeast of DeWitt County in agreement with the maps of Mo and the EF of Mo. Manganese increases in concentration suggesting an oxygenated water column during deposition. The GR signature has progressively shown a decrease in carbonate stringers as argillaceous marl becomes the dominant lithology.

4.2.2 Enrichment Factors

Enrichment Factors of multiple elements from the Chemostrat, Inc. data set were normalized to average PAS (Taylor and McLennan, 1985). An EF of greater than 1 means that, that element is enriched in the Eagle Ford relative to the average PAS. An EF less than 1 indicates that, that element is depleted relative to the average PAS. Average values from analogs including mean Cenomanian-Turonian (C/T) black shale and anoxic and upwelling environments (represented by results from Namibian mud lens samples) compiled by Brumsack (2006) were also compared to each member of the Eagle Ford Formation as well as the gross Eagle Ford (Figures 4.21 and 4.22).

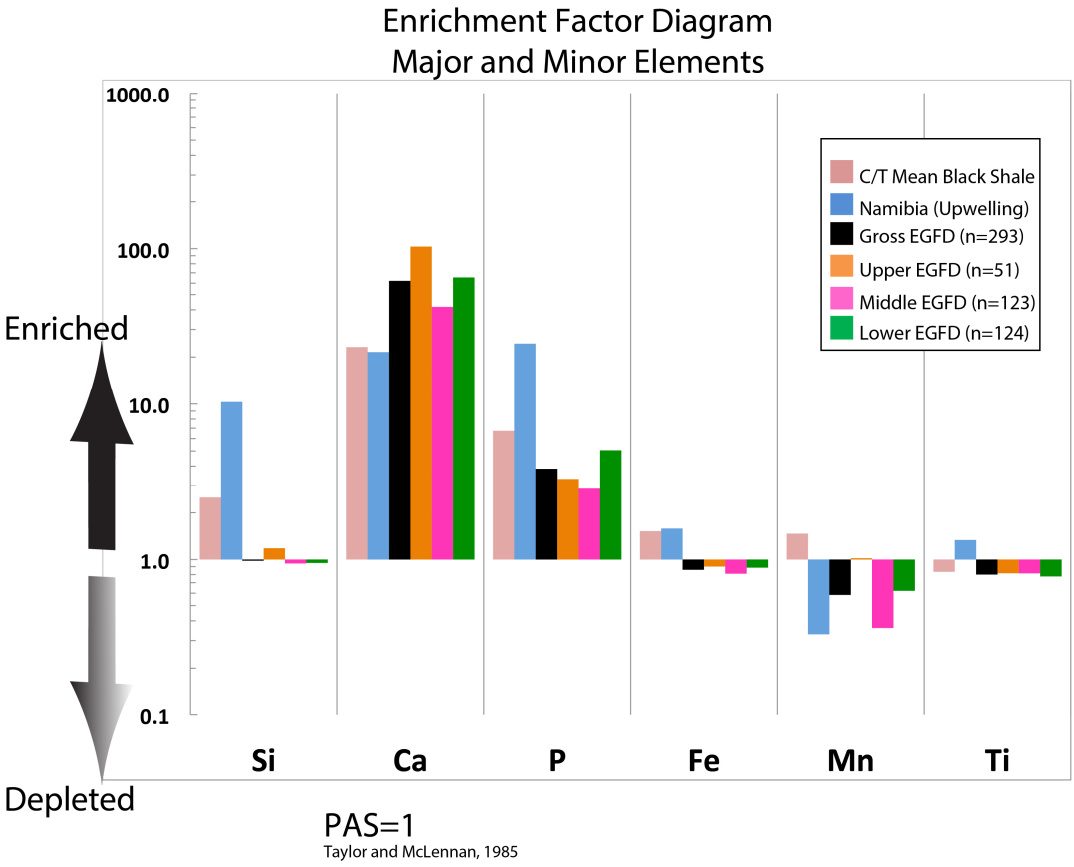

Figure 4.21 Enrichment Factors of major and minor elements

Ca is greatly enriched in the gross Eagle Ford. Si, Fe and Ti are slightly depleted and much more similar to average shale. Mn shows more depletion in conjunction with an enrichment of P.

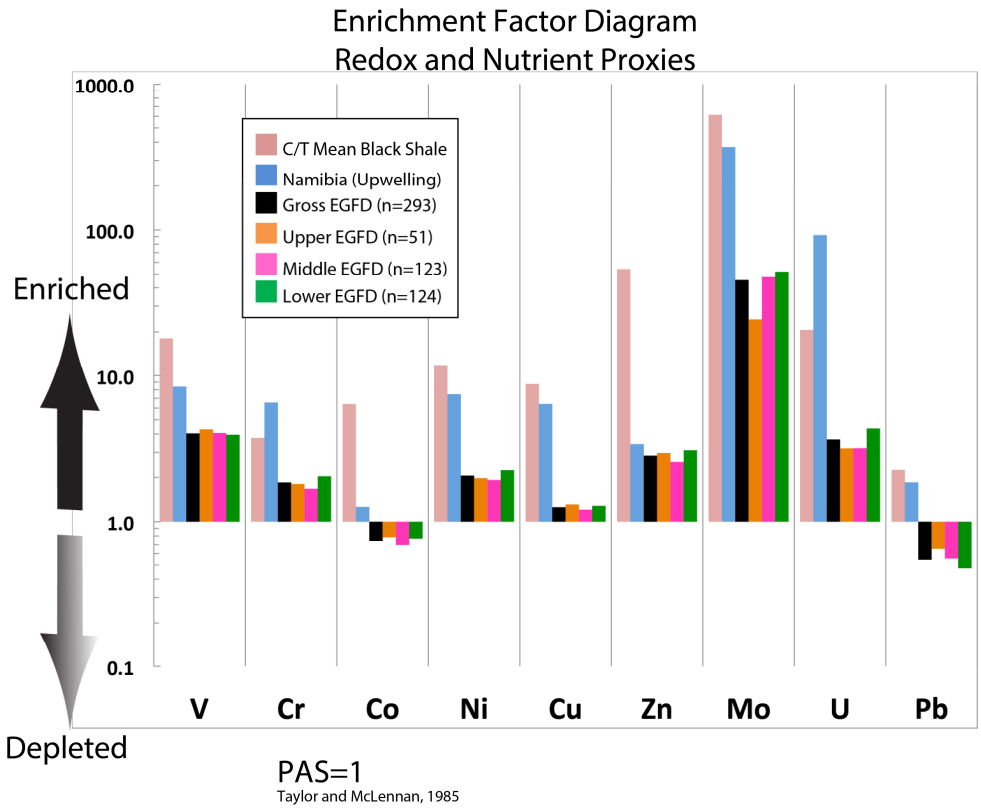

Figure 4.22 Enrichment Factors of redox and nutrient proxies

Nutrient proxies as well as redox proxies are enriched in the Eagle Ford. Pb and Co are depleted relative to average shale.

Si is depleted in most members of the Eagle Ford with the exception of the upper Eagle Ford due to limited clastic input. Ca is enriched in the entire Eagle Ford Formation. C/T mean black shale from Brumsack (2006) represents an average of varying depositional environments yet is enriched in Ca and Si. P is enriched in all settings, yet there is a greater degree of enrichment in an upwelling environment. Fe is depleted in the Eagle Ford Formation in relation to a terrigenous PAS. Fe is slightly enriched in an upwelling environment and in mean C/T black shale. Fe can be a nutrient but it is mainly concentrated in clastic rocks (Calvert and Pedersen, 2007), which is why it could be depleted in the Eagle Ford relative to average shale. Mn is depleted in the Eagle Ford as well as in the analog of an upwelling environment, yet it is slightly enriched in mean C/T black shale. Brumsack (2006) has suggested that the EF of Mn can be

enriched slightly above a factor of 1 in mean C/T black shale. The EF of Mn is similar to an average PAS in the upper Eagle Ford as it was deposited in more oxic conditions. Ti is also depleted in the Eagle Ford Formation as well as average C/T black shale while Ti is slightly enriched in the upwelling environment analog.

Cr, Cu, Ni, Zn and U are all nutrient proxies (Tribovillard et al., 2006) which are enriched in Eagle Ford sediments. Average shale is deposited near shore or on land and upper continental rocks do not have large concentrations of these nutrients. Both Mo and V are highly enriched in the Eagle Ford Formation, particularly in the middle and lower Eagle Ford members. U is enriched in the Eagle Ford due to its affinity for organic matter. U forms organometallic complexes under reducing conditions (Tribovillard et al., 2006). Finally, Pb is hosted in clay minerals as well as sulfides (Calvert and Pedersen, 2007). Pb concentrations do vary in the Eagle Ford but are authigenically depleted in relation to average PAS for the gross Eagle Ford. Enrichment Factors show an overall pattern of the authigenic enrichment of redox, organic matter and paleoproductivity proxies. The bulk of Eagle Ford rocks are composed of carbonate minerals yet aluminosilicate elements and trace metals are also present in other mineral phases.

4.3 Rare Earth Element Results

After consideration of the major and trace elements in this study, the provenance of Eagle Ford sediments still needs clarification. Rare earth element (REE) patterns were studied to further understand the facies changes within the Eagle Ford Formation. Normalizing REE concentration data of Eagle Ford samples to chondrite concentrations from McDonough and Sun (1995), as well as average post-Archean Australian Shale (PAAS) concentrations from Taylor and McLennan (1985), was followed. REE normalized patterns were plotted to evaluate the provenance of the sediments within the Eagle Ford. Thulium (Tm) data was left out of the analysis because there were errors seen within the data which may be due to two reasons; interference of another element's energy detected during ICP-MS analysis or the normalization value provided by Taylor and McLennan (1985) was too low for Tm concentrations in the Eagle Ford.

4.3.1 Chondrite Normalized REEs

The chondrite REE pattern parallels bulk earth abundances and is used as a standard to normalize REE data of rocks around the world. Normalizing Eagle Ford samples to chondrite values has revealed individual REE patterns for samples from seven wells. The subscript (N) is used to indicate that a sample has been normalized to chondrite. The chondrite normalized REE pattern for average PAAS concentrations are plotted along with those of the Eagle Ford in order to illustrate the correlation between the two “shales”. These plots are shown in figures 4.23 to 4.29.

Most samples are depleted in Ce shown by a negative anomaly of Ce and are also relatively depleted in all the REEs relative to PAAS. There are other distinct differences between the REE distributions of the seven wells analyzed. Wells 3, 12 and 16, show REE patterns that are much flatter than PAAS and also depleted in heavy rare earth elements (HREEs) such as Er to Lu and light rare earth elements (LREEs) such as La to Nd relative to PAAS (Figures 4.23-4.25). Wells 3, 12, and 16 show a combination of sedimentary patterns which parallel PAAS and samples which do not parallel PAAS. Samples which do parallel PAAS are characterized by a depletion of Eu which forms a distinct negative Eu anomaly relative to PAAS. They are also enriched in LREE and show a flat to negative HREE distribution. Samples which do not parallel the PAAS REE pattern have no Eu anomaly and are unlike PAAS as they are enriched In Eu relative to PAAS.

Four wells show REE patterns which parallel PAAS characterized by their negative Eu anomaly, LREE enrichment relative to chondrite and fairly flat to slightly positive middle rare earth elements (MREEs), such as Sm to Ho, and HREEs (Sethi et al., 1998). The rare earth element patterns for wells 17, 19, 20 and 24 have been plotted along with their closest match, the rare earth elements pattern for PAAS (Figures 4.26-4.29). The location of these wells falls in an area with high concentrations of Al and Si and they appear to have a greater influence of sediments from the upper continental crust.

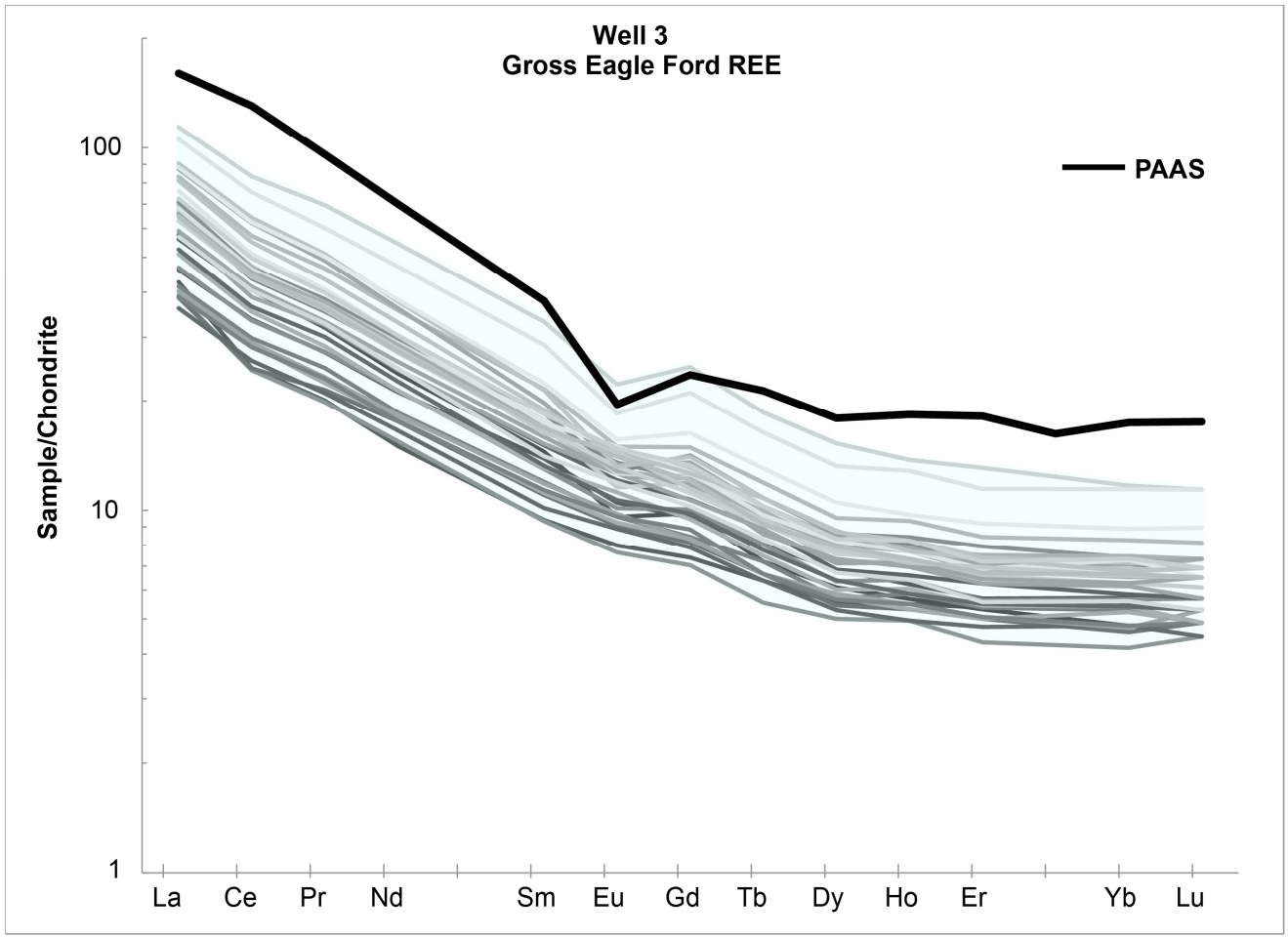

Figure 4.23 Well 3 Chondrite normalized

There is a negative Ce anomaly in most samples and variations in the degree of the negative Eu anomaly. The negative Eu anomaly is absent in many samples. The slope of the HREE is either flatter than PAAS or more negative.

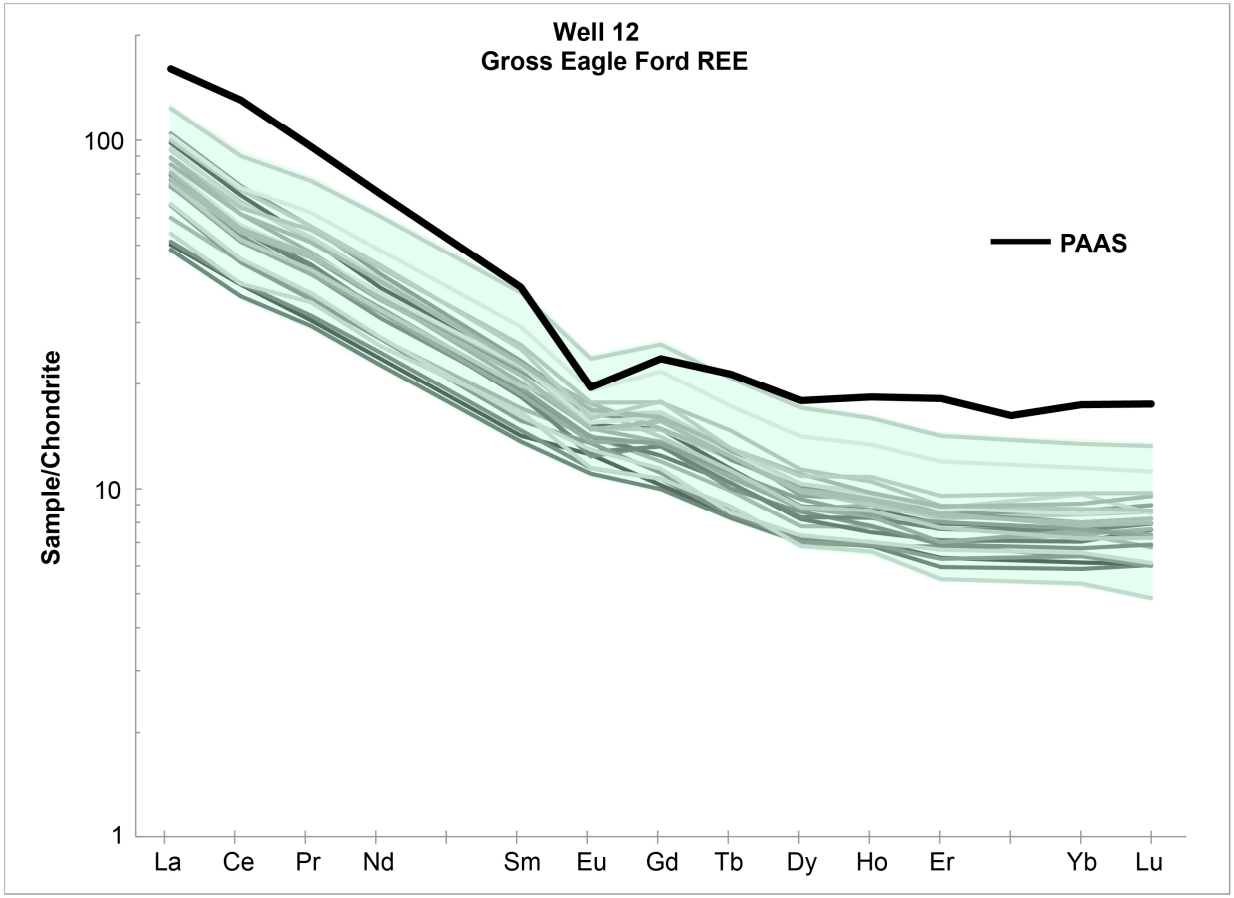

Figure 4.24 Well 12 Chondrite normalized

There is a lack of a negative Eu anomaly in many samples with lower concentrations of REEs than PAAS, also illustrated in the previous well. Also, the negative Ce anomaly is ubiquitous although its degree varies.

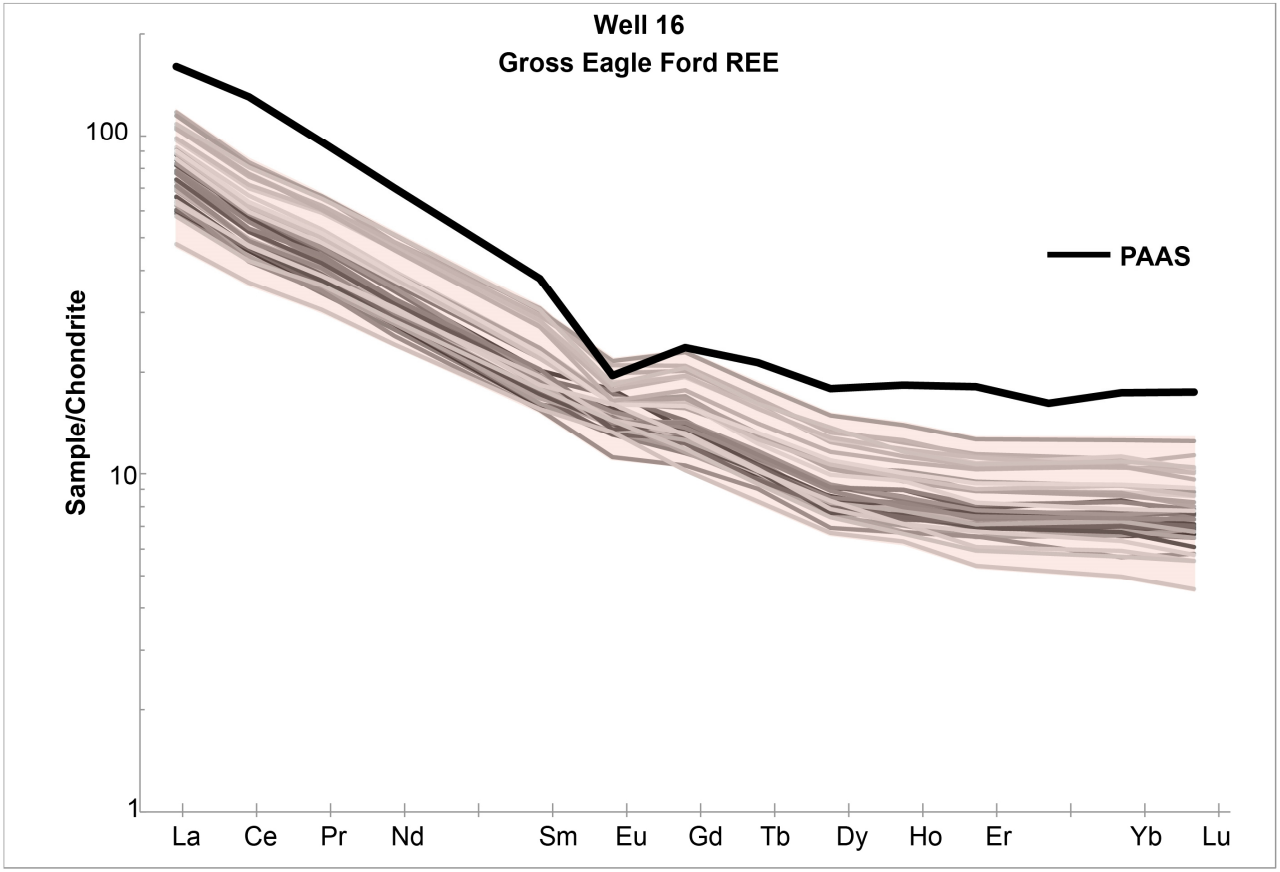

Figure 4.25 Well 16 Chondrite normalized

The REE patterns in this well are similar to the preceding two figures (wells 3 and 12) showing a mixed character in the Eu anomaly. Ce has a negative anomaly of varying degrees. The slope of the HREEs is much more negative than PAAS for these samples.

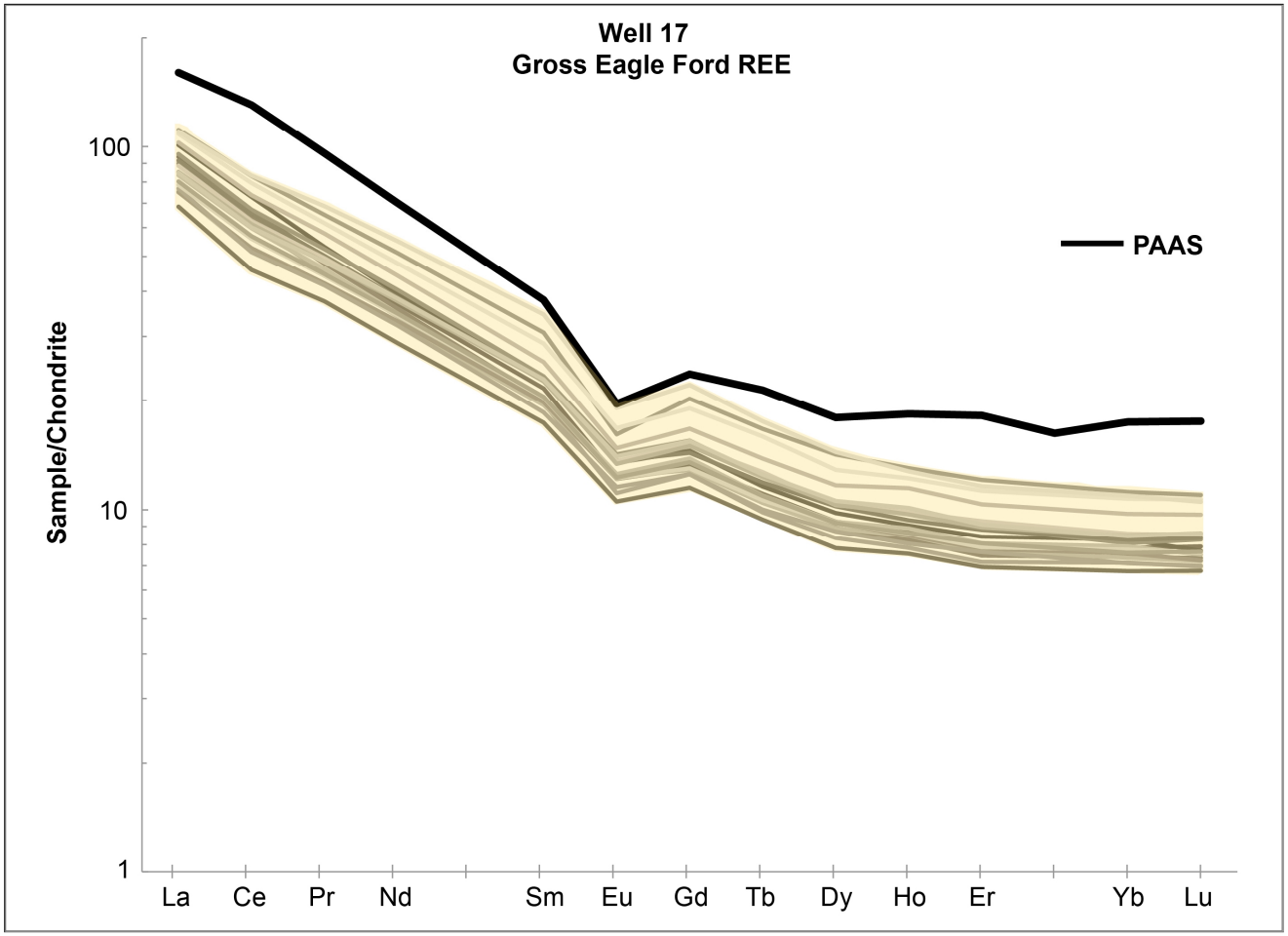

Figure 4.26 Well 17 Chondrite normalized

Samples from this well contain a distinct negative Eu anomaly. The strong negative Ce anomaly previously shown is absent in several samples. The slope of the HREEs is either flatter or slightly positive relative to PAAS.

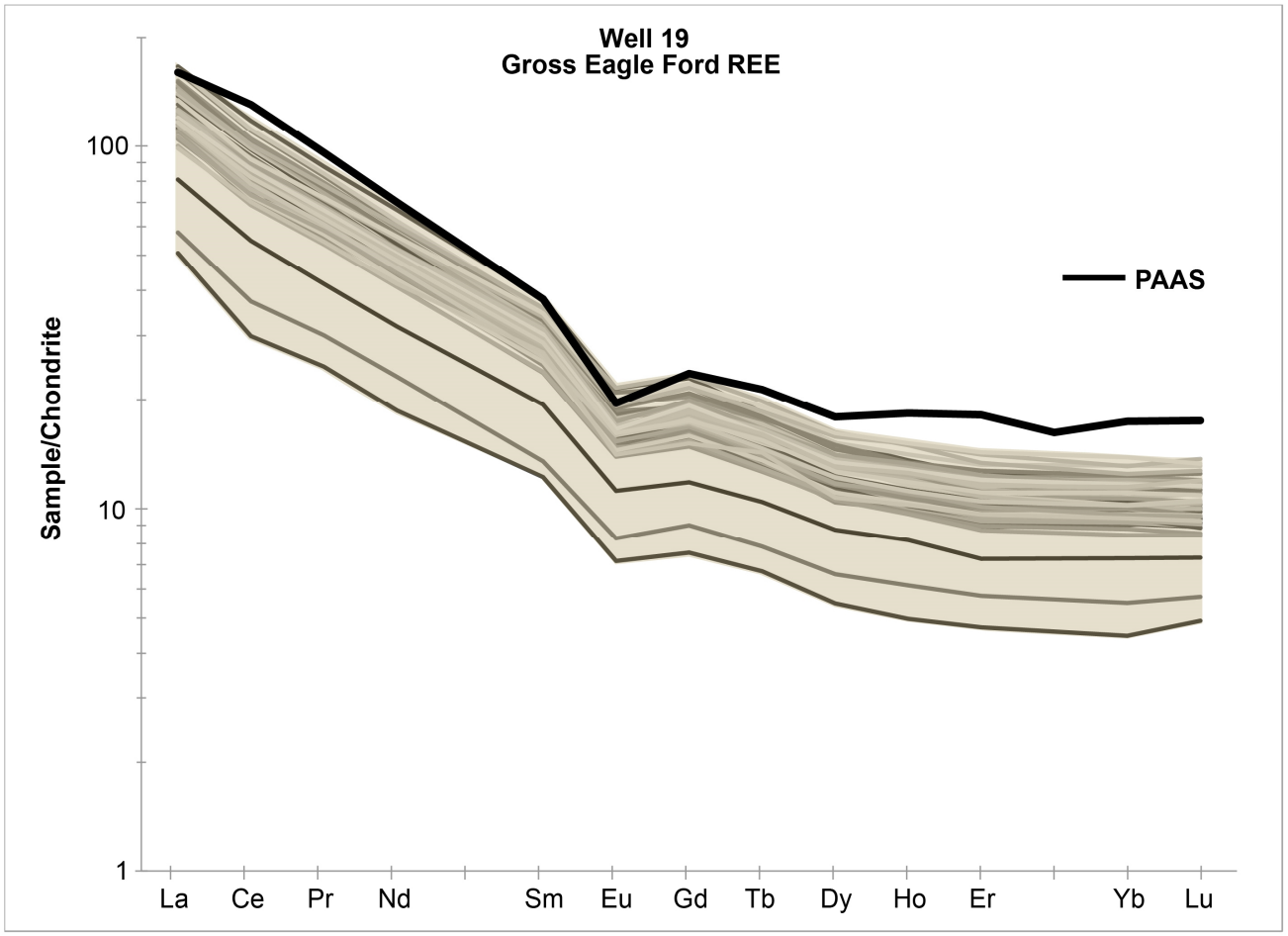

Figure 4.27 Well 19 Chondrite normalized

As shown in the previous figure, the negative Ce anomaly varies while the negative Eu anomaly is closer to that of average PAAS due to an increase in REE concentrations.

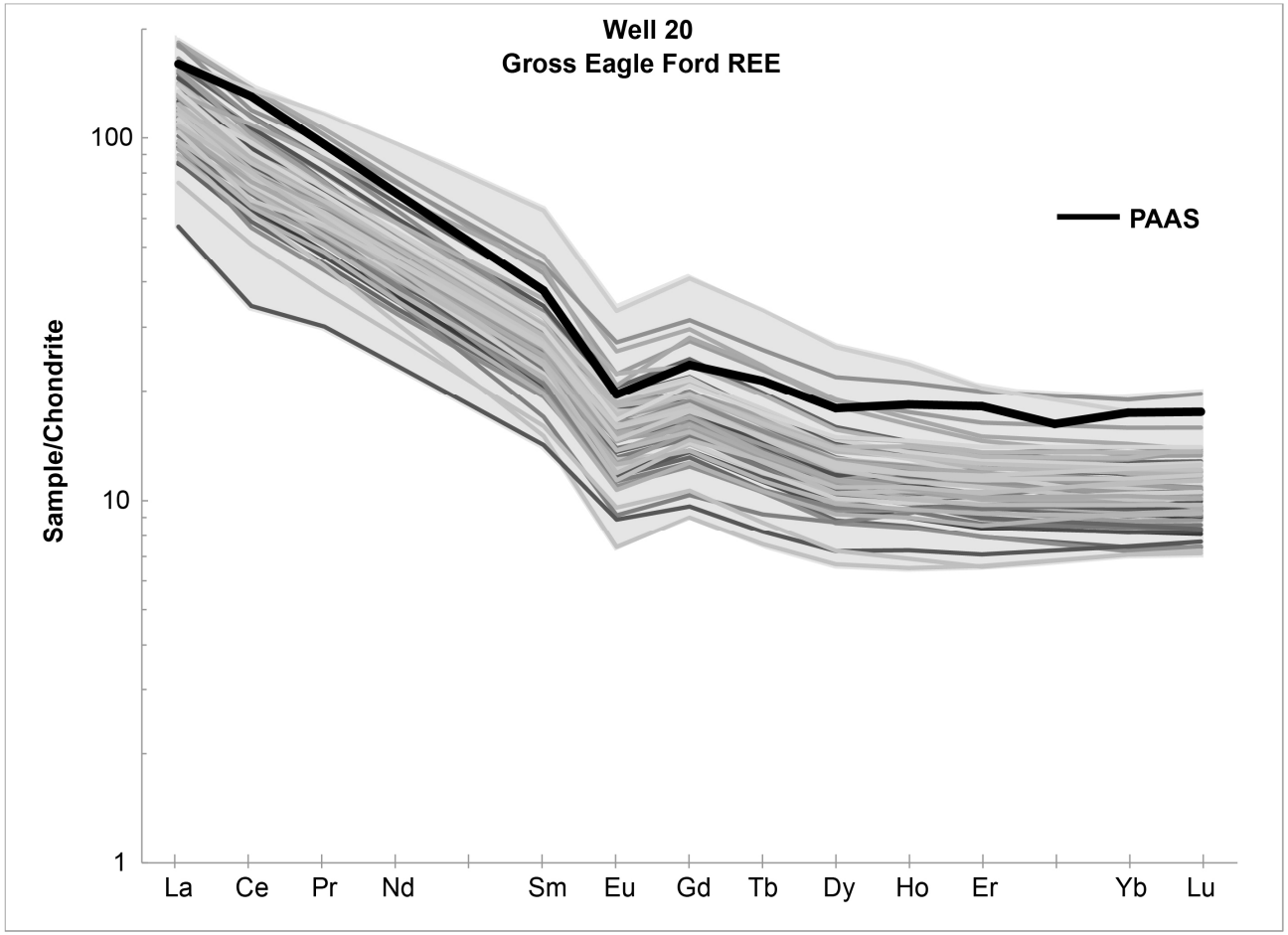

Figure 4.28 Well 20 Chondrite normalized

The patterns of samples from this well also depict varying degrees of a negative Ce anomaly and a distinct negative Eu anomaly. The slopes of the REE curves are variable between samples. This is best seen in Figure 4.37.

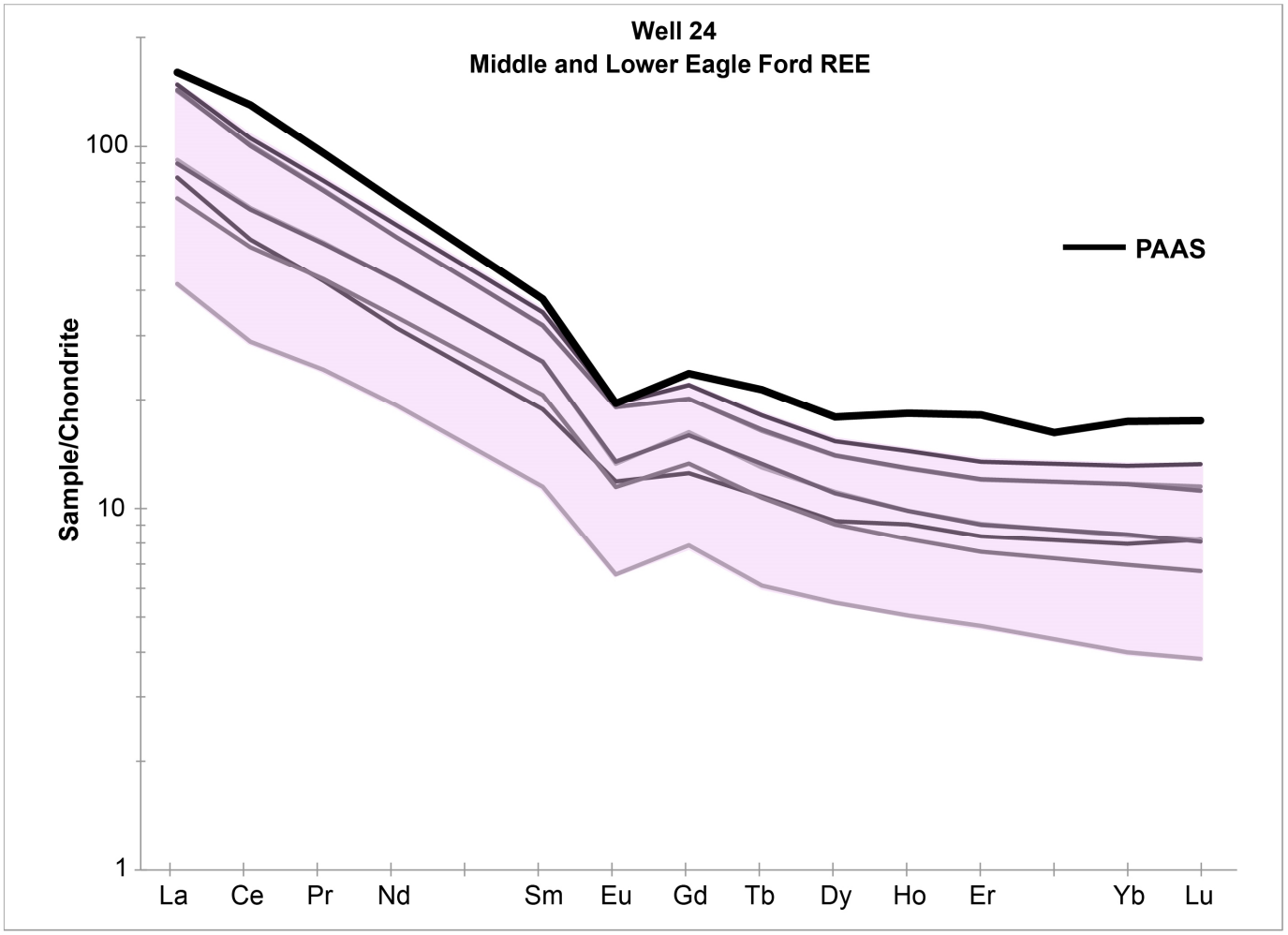

Figure 4.29 Well 24 Chondrite normalized

Samples from this well are similar to those in wells 17, 19 and 20 with variable negative Ce anomalies and a distinct negative Eu anomaly.

4.3.2 PAAS Normalized REEs

REE results were normalized to post-Archean Australian Shale (PAAS) to illustrate the similarities and differences between sediments in the Eagle Ford and average shale concentrations. PAAS represents average shale that originates from weathered granitic rock which makes up the bulk upper continental crust of the earth (Taylor and McLennan, 1985). Average PAAS is indicated by a straight line with a value of 1 in Figures 4.30-4.36. Similar to samples normalized to chondrite, there is a separation between samples from wells that are closely related to PAAS and wells that are unlike PAAS. Samples which have an exaggerated, positive Eu anomaly in these PAAS-normalized plots can be placed into one category, and samples which have softer positive Eu anomalies relative to PAAS into another. Wells 3, 12, and 16 show a strong positive anomaly for Eu, indicating an enrichment of Eu relative to average PAAS (Figures 4.30 to 4.32). Wells 17, 19, 20 and 24 show patterns somewhat closer to PAAS although most samples are depleted in certain REEs including a fairly constant negative Ce anomaly (Figures 4.33 to 4.36). The positive anomaly for Eu softens in these wells indicating a slight enrichment of Eu in these samples relative to PAAS. Samples which parallel PAAS are diluted by carbonate content and therefore have lower concentrations when normalized. It can be noted that samples from the Eagle Ford seem to parallel PAAS when normalized to chondrite, yet they are different in their elemental abundances. For example, samples are distinctly different from PAAS due to their negative Ce anomaly, enrichment in Eu and variable HREE slope. The following figures depict a deviation from PAAS for all samples from the Eagle Ford.

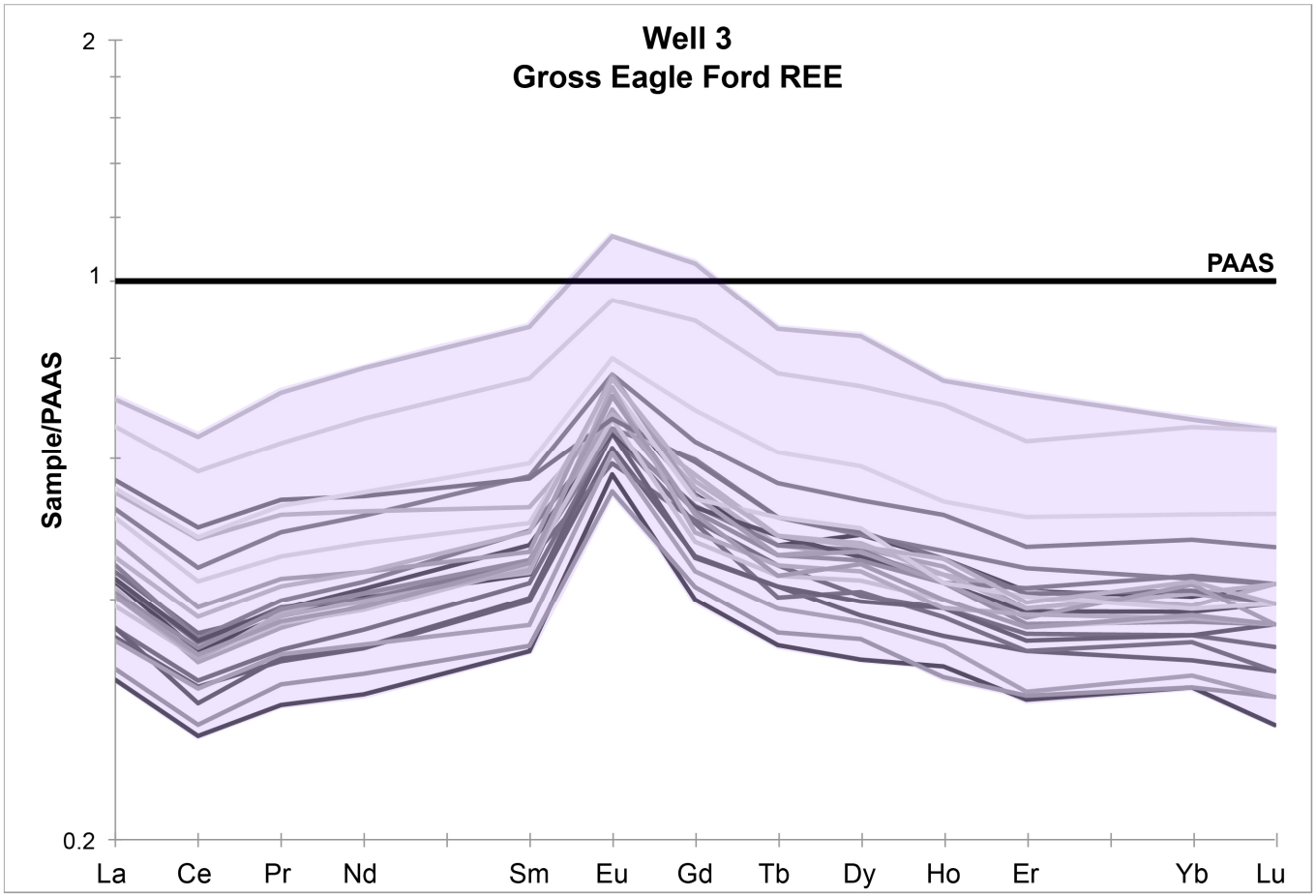

Figure 4.30 Well 3 PAAS normalized

There is a distinct enrichment of Eu in this well as well as the ubiquitous negative Ce anomaly that was also present in chondrite normalized plots. Samples from this well completely deviate from PAAS (i.e. average upper continental crustal rocks).

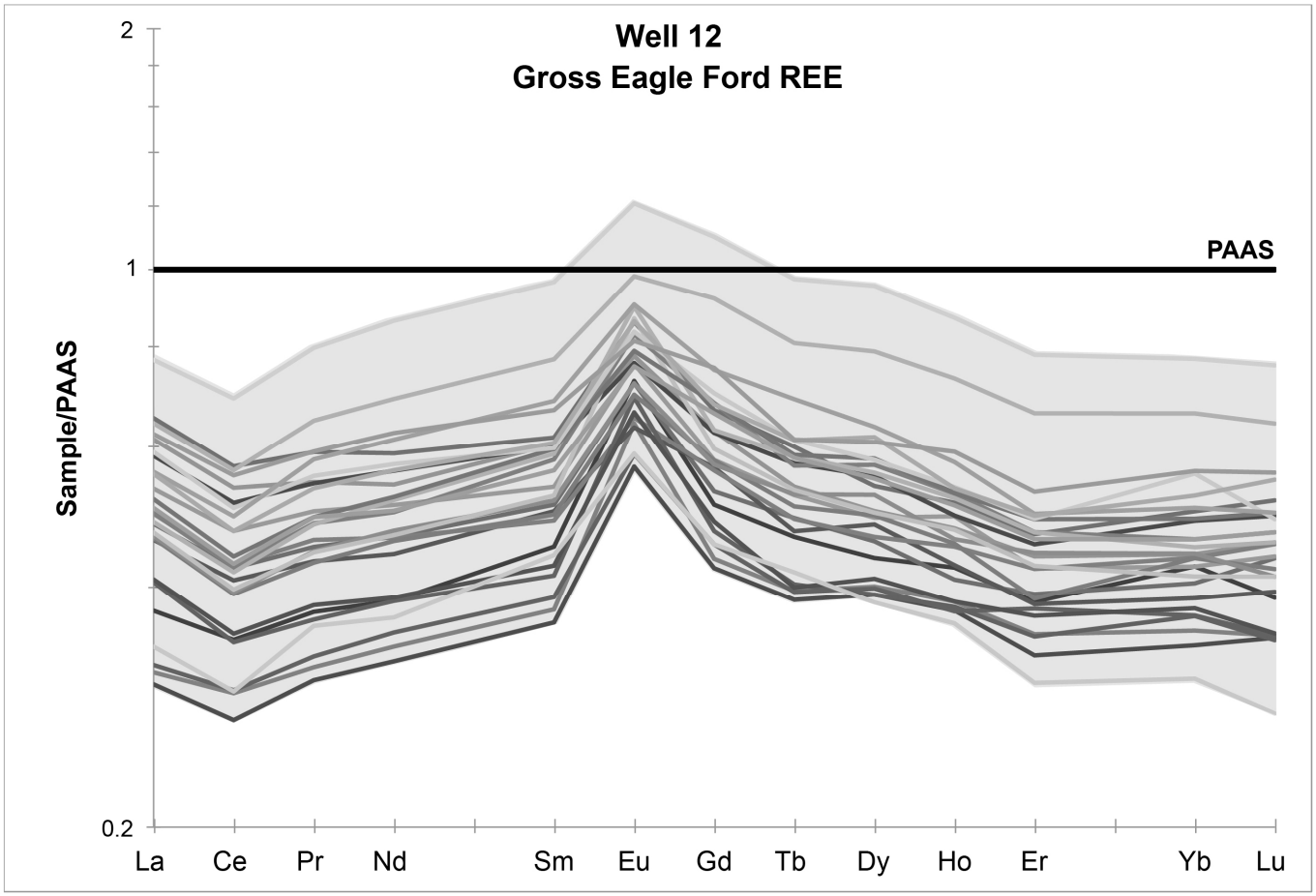

Figure 4.31 Well 12 PAAS normalized

There is a distinct enrichment of Eu in this well as well as the negative Ce anomaly as seen in the previous figure. There is much variability in the HREEs relative to PAAS.

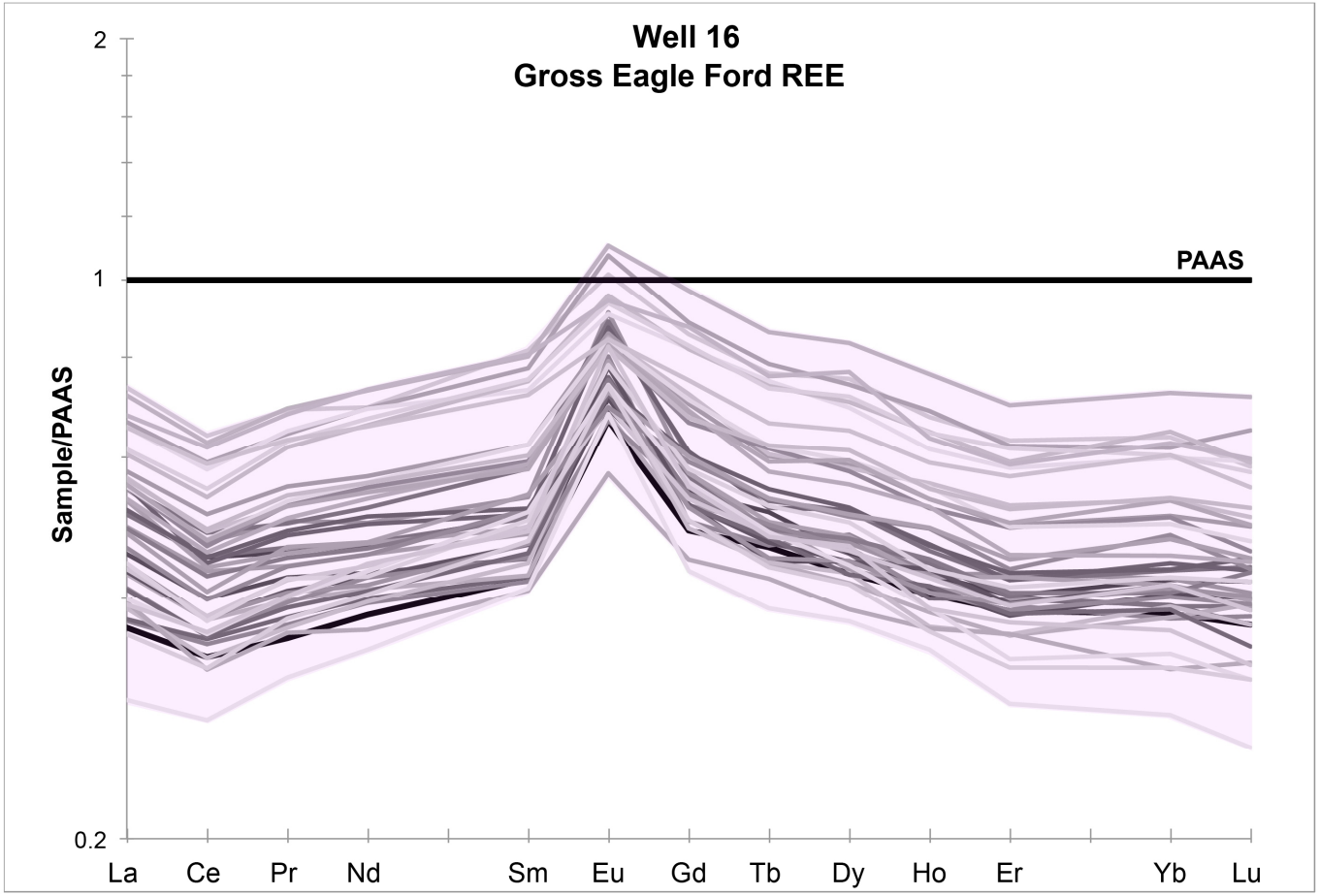

Figure 4.32 Well 16 PAAS Normalized

Samples from this well show is a distinct enrichment of Eu as the two previous figures do, as well as a negative Ce anomaly and negative HREE slope relative to PAAS.

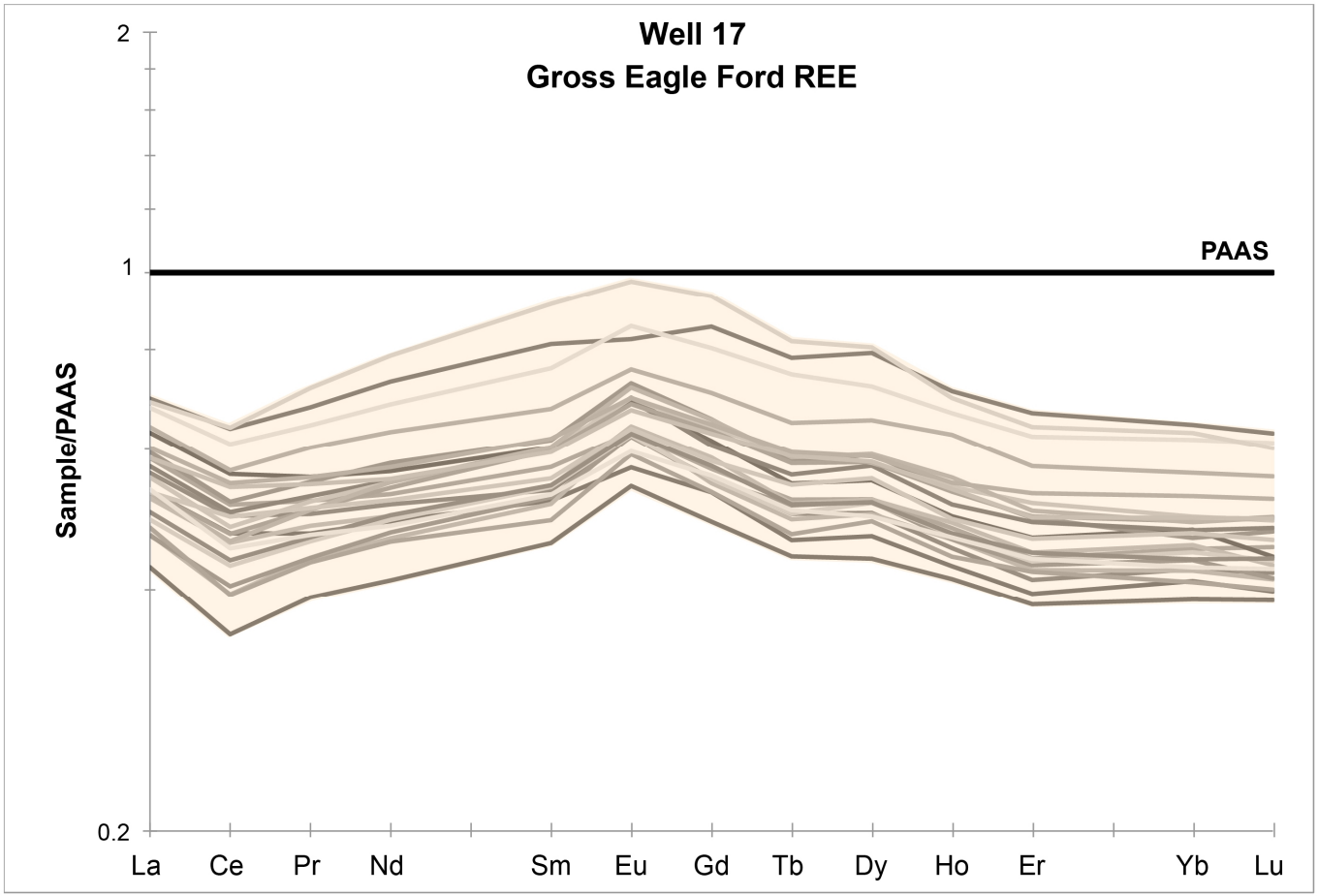

Figure 4.33 Well 17 PAAS normalized

The positive Eu anomaly softens in this well, yet is still slightly enriched in Eu relative to PAAS. Samples also have a negative Ce anomaly relative to PAAS.

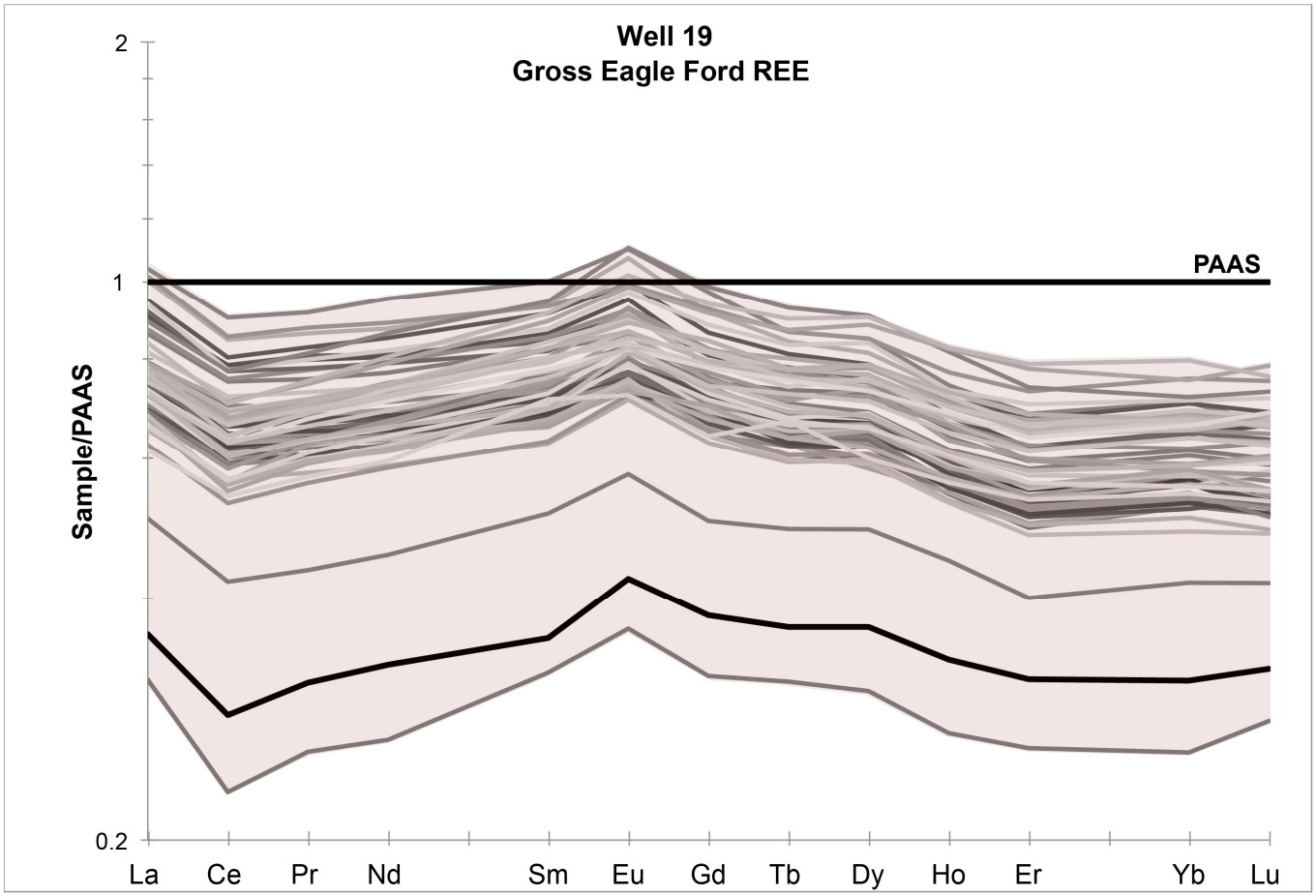

Figure 4.34 Well 19 PAAS normalized

The positive Eu anomaly softens in this well, yet is still enriched in Eu relative to PAAS. Most samples also increase in REE abundance relative to PAAS and are far removed from upper crustal patterns. Samples also have a negative Ce anomaly relative to PAAS. There is a strong variation in slope in the HREEs creating a contrasting pattern with PAAS.

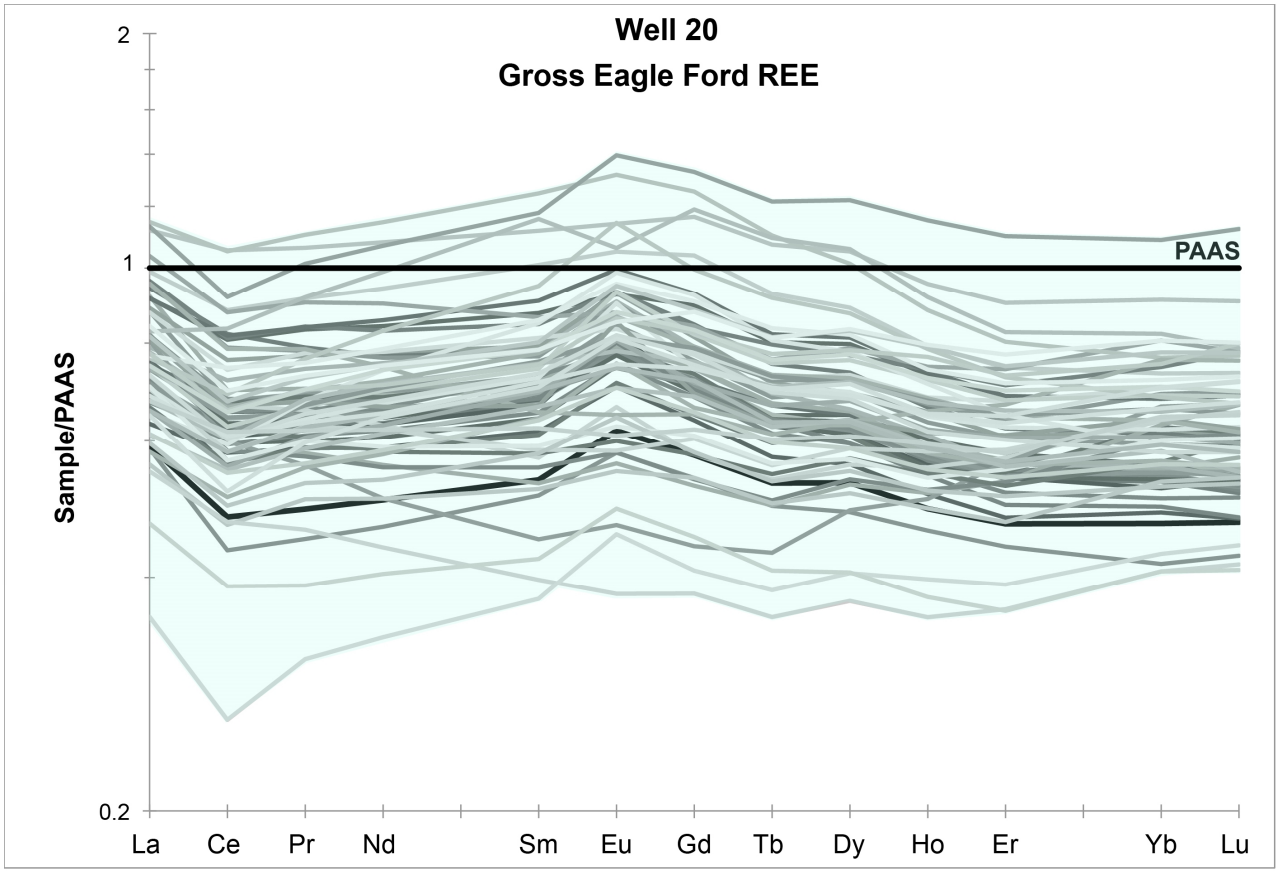

Figure 4.35 Well 20 PAAS normalized

Samples from this well show high variability to each other. Some samples have a positive Eu anomaly while others are flatter and have no Eu anomaly. Samples from this well are distinctly different from PAAS due to their negative Ce anomaly, slight enrichment in Eu and variable HREE slope.

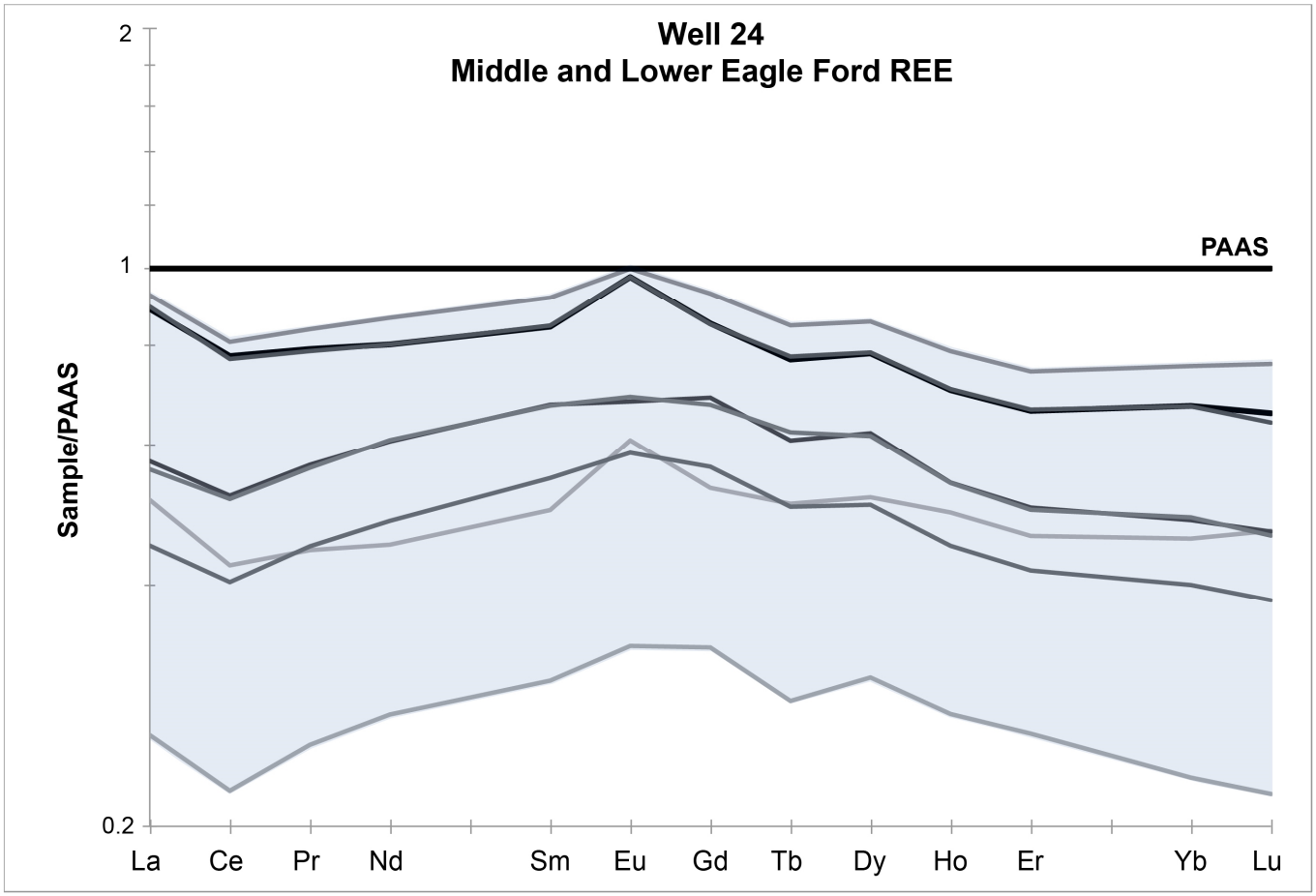

Figure 4.36 Well 24 PAAS normalized

Samples from this well show the negative Ce anomaly typical of Eagle Ford REE patterns. Some samples are slightly enriched in Eu while others are flatter and much more similar to PAAS, albeit of lower abundance. There is also a strong HREE depletion relative to PAAS in some samples as the HREEs have a negative slope.

4.3.3 $(La/Lu)_N$ vs. $(Dy/Yb)_N$

$(La/Lu)_N$ and $(Dy/Yb)_N$ ratios for samples from each of the seven wells of the Eagle Ford Formation normalized to chondrite values were cross-plotted. As mentioned previously, the subscript (N) denotes chondrite normalization. Light REEs (LREEs) such as Lanthanum (La) can be compared to heavy REEs (HREEs) such as Lutetium (Lu) in order to compare the contrast or similarity in their concentration patterns. The purpose for this plot is to measure the enrichment of LREEs in relation to HREEs in Eagle Ford sediments. The chondrite normalized ratio of Dysprosium and Ytterbium ($(Dy/Yb)_N$) represents the slope of the MREE to HREE pattern (Davidson et al., 2013). A greater $(Dy/Yb)_N$ ratio value increases the slope of the pattern. A ratio of 1.0 is a horizontal line, and a ratio below 1.0 indicates a negative slope in the general REE plot that is chondrite normalized. $(Dy/Yb)_N$ ratios average 1.17 indicating a slightly positive, yet nearly flat slope. Eagle Ford sediments have $(La/Lu)_N$ ratios averaging 10.8 indicating a negative slope for this ratio seen previously in Figures 4.23 to 4.29. Chondrite normalized REE plots show that Eagle Ford sediments are more enriched in LREEs rather than HREEs.

The $(La/Lu)_N$ vs. $(Dy/Yb)_N$ cross-plot for PAAS indicates an enrichment of $(La/Lu)_N$ and an enrichment of $(Dy/Yb)_N$ relative to PAAS (Figure 4.37). $(La/Lu)_N$ ratios for samples from the Eagle Ford Formation range from 7-16 showing high variability. The average ratio from average shale such as PAAS is 9.17. The $(Dy/Yb)_N$ ratio for PAAS is 1.03. Eagle Ford samples range from a min of 0.7 to a max of 1.4 for $(Dy/Yb)_N$. Most samples cluster around a $(Dy/Yb)_N$ ratio 1.2. Samples have been plotted together with PAAS in Figure 4.37. Most Eagle Ford samples are unlike PAAS as they have a steeper negative slope for $(La/Lu)_N$ and a flatter, less negative slope for $(Dy/Yb)_N$.

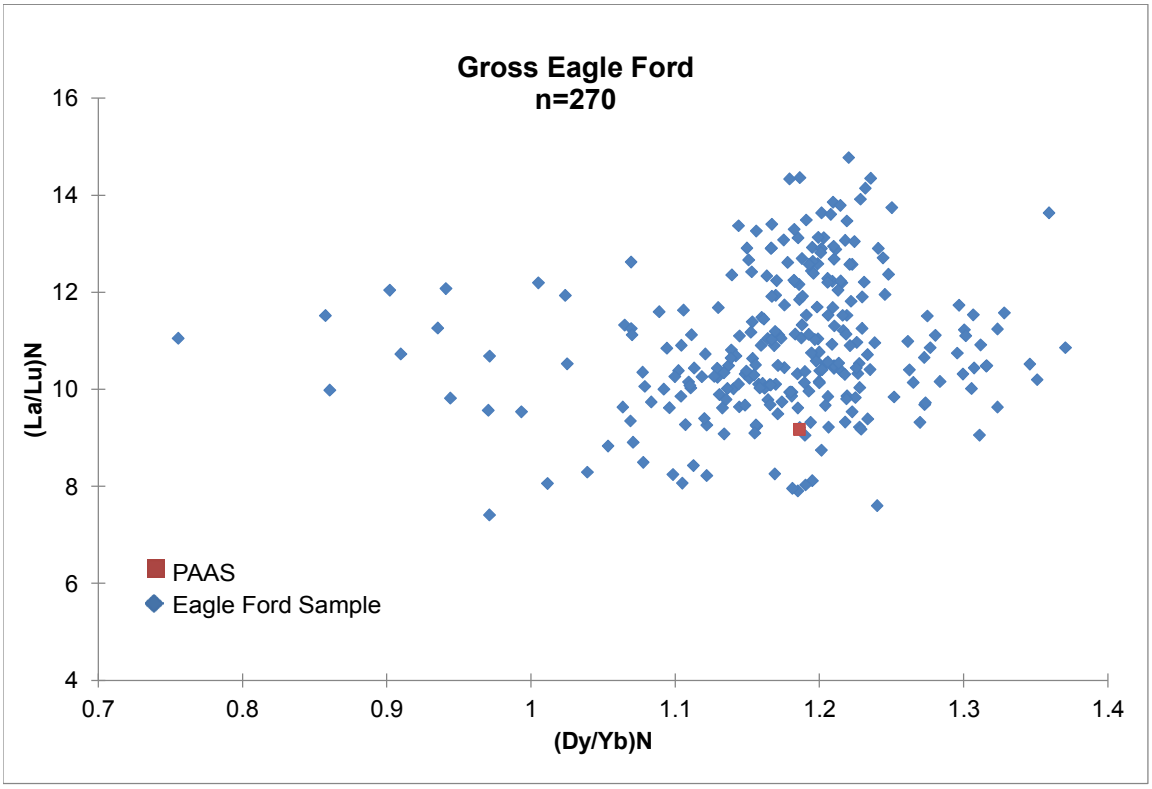

Figure 4.37 $(La/Lu)_N$ and $(Dy/Yb)_N$ scatter plot

Most samples from the Eagle Ford are unlike PAAS due to their higher $(La/Lu)_N$ and variable $(Dy/Yb)_N$ ratios.

4.4 Bentonite

Seven bentonite samples selected from eighteen of the thickest bentonite beds across five cores (depicted in Figure 2.11) were analyzed and found to be composed mainly of Si, Al and K (raw data in Appendix E). Ca is a minor element within these bentonite samples. Figure 4.38 and Figure 4.39 show the relationship of the REEs from these samples relative to chondrite and PAAS. Samples exhibit different characteristics when normalized to chondrite. Samples 2N, 14R and 15R exhibit a pattern of sediment from a mafic source when normalized to chondrite. Samples 1F, 3L, 7L and 11H exhibit a large negative Eu anomaly relative to chondrite and have a positive Eu anomaly relative to PAAS. All samples deviate from PAAS (Figure 4.39).

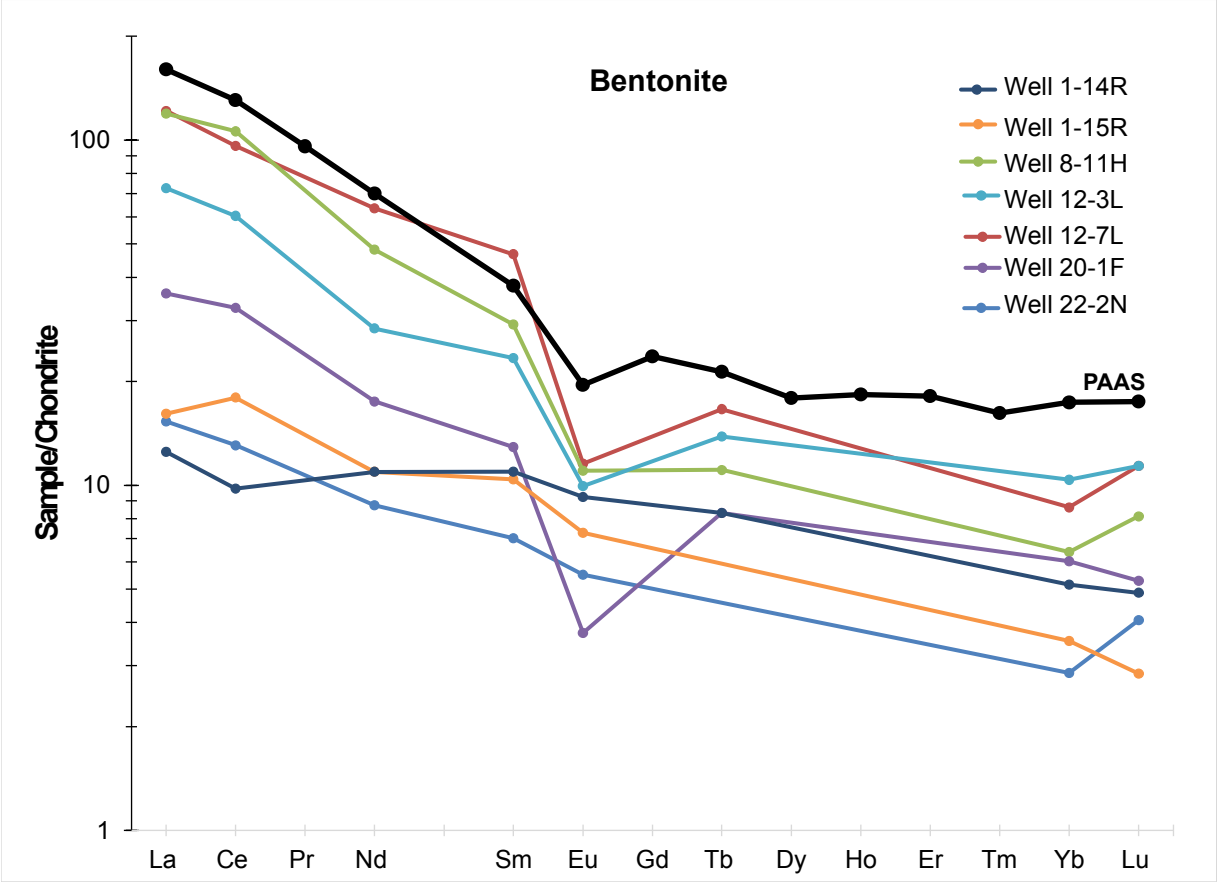

Figure 4.38 Bentonite normalized to chondrite

Samples 14R, 15R and 2N plot without a negative Eu anomaly relative to PAAS. The remaining samples have a greater depletion of Eu than PAAS. The Ce anomaly shows variability between samples, at times positive and at times negative. Most of the HREE were not analyzed.

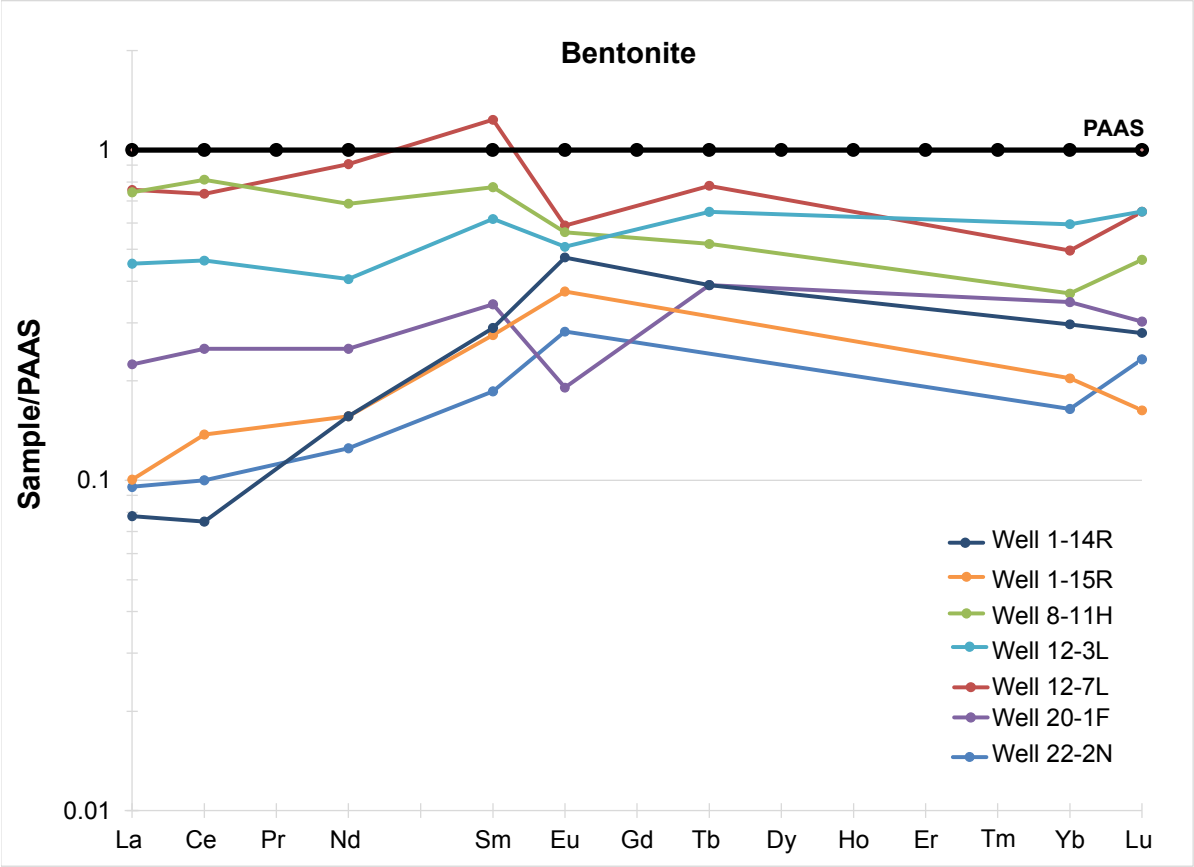

Figure 4.39 Bentonite normalized to PAAS

All samples vary greatly from PAAS. Samples 14R, 15R and 2N have a positive Eu anomaly relative to PAAS and positive LREE slope with varying Ce anomalies. All remaining samples have a negative Eu anomaly relative to PAAS and flat to positive LREE patterns.

4.5 Total Alkali-Silica Rock Classification Diagrams

When removing the effect of the Ca dilution, one can determine what the possible rock classification is for all samples. Bentonite (altered volcanic ash) had very low concentrations of Ca and seemed to be unaffected by the mixing of carbonate minerals and volcanic ash during depositional time (see raw data in Appendix E). Bentonite samples have been plotted in Figure 4.40. All samples from seven wells (3, 12, 16, 17, 19, 20 and 24) are plotted in Figure 4.41 with concentrations re-normalized to 100% after the removal of CaO and LOI, both in wt.%. Samples cluster within the andesite to dacite category in LeBas et al.'s (1986) SiO_2 vs. Na_2O+K_2O (Total Alkali-Silica) diagram for regular Eagle Ford marl samples while they vary from basalt to different types of basaltic andesite for bentonite samples.

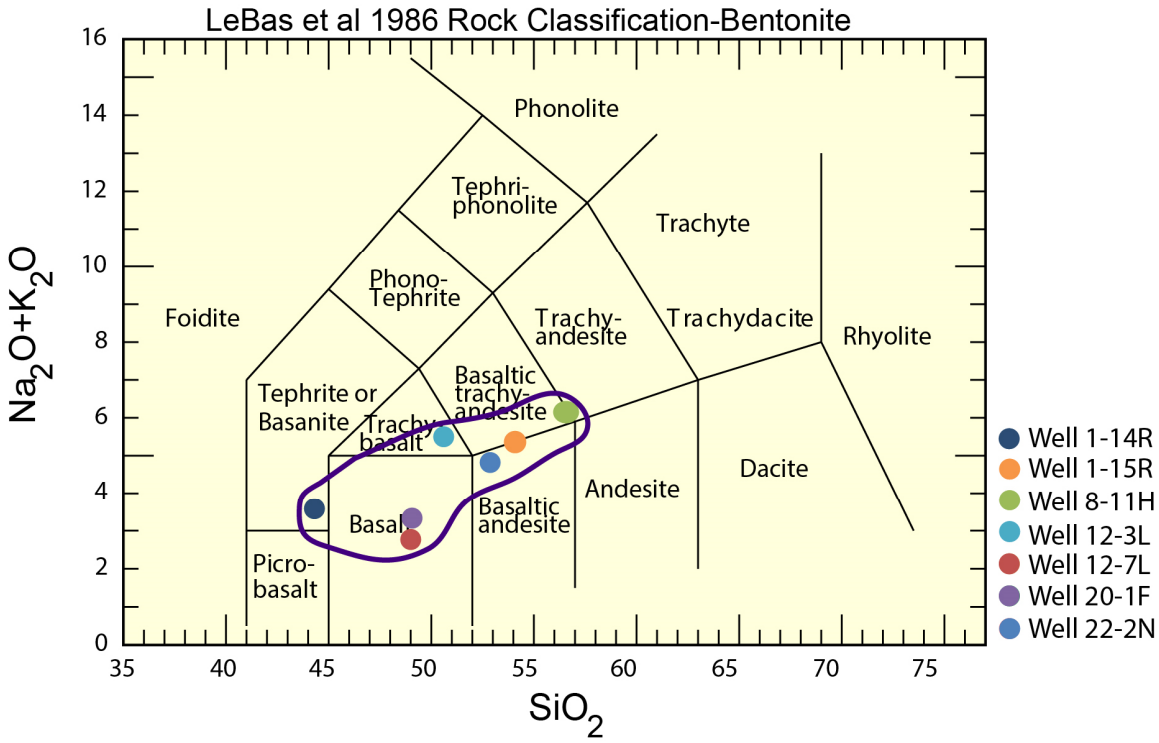

Figure 4.40 Bentonite samples Rock Classification Diagram

Bentonite samples plot as various types of basalt and basaltic andesite based on their silica, sodium, and potassium content. A positive trend implies an increase in Na_2O+K_2O as SiO_2 increases.

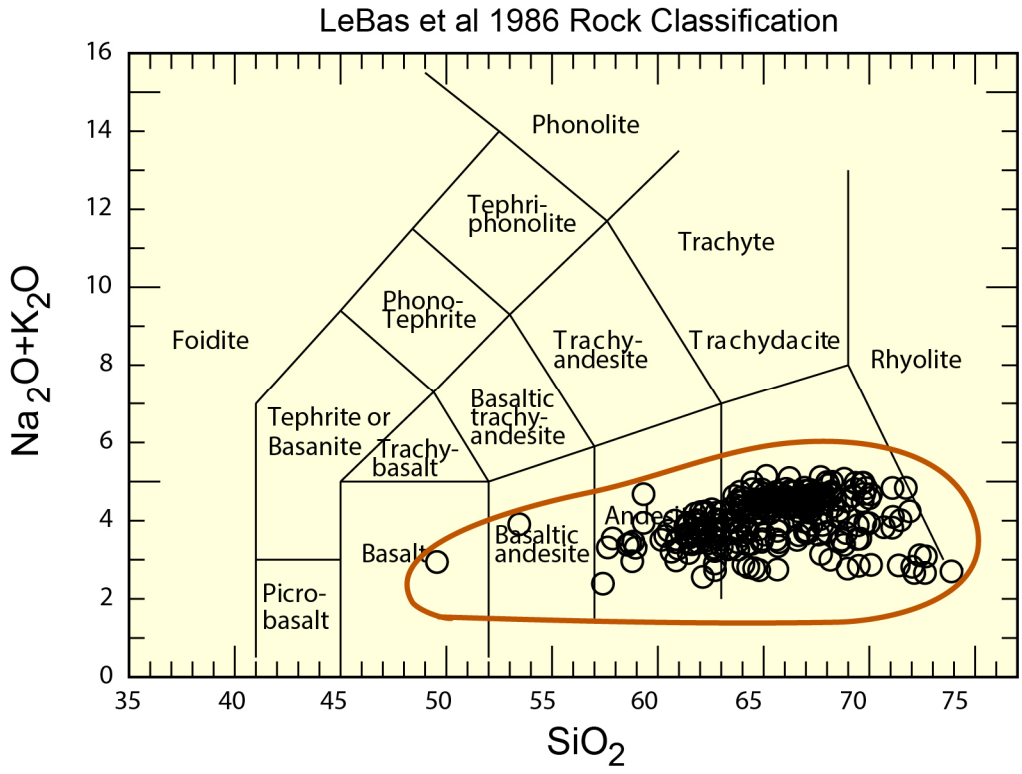

Figure 4.41 Rock Classification Diagram for wet geochemical samples

Ca-subtracted samples cluster as andesite or dacite indicating an intermediate to basic source. Outliers represent basalt or basaltic andesite due to a decrease in silica content and decreased sodium and potassium content in those samples.

4.6 Summary

The results of multiple element analyses of the Eagle Ford Formation in south Texas has shown that facies changes along the paleohigh San Marcos Arch feature are evident and that redox conditions also change along the trend of the study area as well as temporally. Chapter 5 elaborates on the possible causes for the behavior of major elements and trace metals and the implications on the depositional environment of the Eagle Ford. The elemental composition of Eagle Ford rocks provides information about mineralogy, sediment source, organic production and sea-floor and sedimentary oxygenation (e.g., Calvert and Pedersen, 2007). Major, minor, and trace elements have been powerful proxies for understanding the paleodepositional conditions that the Eagle Ford was formed under.

Chapter 5

Discussion

The main goal of this thesis was to illustrate that there is a facies change from Karnes to DeWitt counties, south Texas, seen in major, minor, and trace elements. The vertical depth profile also illustrates the change in depositional influences throughout Eagle Ford time (Figures 4.14-4.20). The Eagle Ford Formation is not a heterogeneous rock facies. Complex geochemical processes affected sedimentation during depositional time. These processes are presented in the sedimentary record in the form of major and minor element geochemical variations recorded in associated mineral phases.

The Eagle Ford can be divided into two distinct facies in the study area. One that is carbonate rich and deposited under an anoxic water column, and another that is richer in quartz and aluminosilicates and deposited under a more oxic/dysoxic water column. The provenance of the sediments within all the members of the Eagle Ford is discussed through the interpretation of REE patterns. Rare earth element patterns also show two separate facies across the trend. One that is similar to an average shale (PAAS), which represents the upper continental crust, and another, which has signatures of an intermediate/mafic source. Samples normalized to PAAS all deviate from its pattern suggesting that samples from the Eagle Ford were either of volcanic origin or subject to dilution from detrital sediment input and biogenic carbonate production. In order to provide a plausible explanation for the separation of these facies, a review of the relationships between elements and their mineral hosts will be provided, followed by an explanation of the geochemical processes occurring during Eagle Ford sedimentation.

5.1 Elemental Relationships (Correlation)

Correlation coefficients were calculated for major elements and primary minerals found within Eagle Ford rocks from three cores (wells 8, 12, and 20) (Table 4.1). Clay minerals have strong correlations with Si, Al and K suggesting that these elements are bound within the crystal structure of aluminosilicate minerals such as illite. Elements which go into heavy minerals such as

Ti correlate positively with clay species and will be used as proxies for detrital input. Si and Fe have a strong positive relationship with each other indicating they are concurrently present in some mineral phases such as chlorite. There is a small fraction of elements such as Si, Fe and Al that are authigenic but their strong positive correlation with Ti indicates they are more detrital.

Fe and S have a positive linear relationship though not strong. The relationship between Fe and S will mostly be concentrated within pyrite, yet there is a fraction of Fe bound in chlorite as suggested by the positive correlation between Fe and Al; also possibly in montmorillonite families such as nontronite. The presence of pyrite throughout the core supports the abundant presence of FeS_2. Fe has also been considered as a nutrient for biologic processes (Sinton and Duncan, 1997). Similarly, Ca is found in carbonate minerals such as calcite and dolomite and shows a positive correlation with these minerals, both represented as Total Carbonate samples. Dolomite, by itself, is rare in the Eagle Ford Formation (see Table 2.1 for concentrations).

Proxies for TOC include Cu, Mo, Ni, Cr and Zn. The correlation for each well may produce a different result, yet the elements mentioned have the strongest affinity for TOC. Mainly Cu, Ni, Mo and Zn can be used as proxies for organic matter within the Eagle Ford Formation.

5.2 Elemental Interpretation

5.2.1 Major, Minor and Trace Elements.

5.2.1.1 Major Facies

The sources of sediments are continents, the sea floor and the water column which ultimately determine the relative proportions of elements which are bound in constituent phases in sedimentary rocks (Calvert and Pedersen, 2007). It is useful to discuss how elements are used as proxies and how they can be related back to their source. Taylor and McLennan (1985) published a model based on a granitic upper crust which has weathered into mudrocks deposited far from their source (distal). Focus will be placed on proximal and distal Eagle Ford sediments and how they are different along the trend of the study area. Immobile elements were chosen to be proxies for environmental conditions during Eagle Ford time.

Elements that are immobile and resistant to weathering preserve a record of upper crustal composition (Taylor and McLennan, 1985). Pearce et al. (1999) and references therein note the differences between immobile and stable elements compared to elements that are associated with diagenetic activity. Pearce et al. (1999) classify inorganic Ca, Na, K, Pb, Rb and Sr as diagenetic materials weathered from feldspars and unstable. Most elements are soluble but elements such as Al, K, Rb and Nb are adsorbed onto clay minerals and retained making them useful as non-authigenic clay proxies. Clay-bound elements such as Al and K also have a strong positive correlation with terrigenous Si and Ti (Table 4.1).

In the case of the Eagle Ford Shale, clay richness varies along the trend. The Eagle Ford receives pro-deltaic sedimentation carried southward from the Woodbine Delta, possibly as suspended particulates. A fraction of Si can also be biogenic as siliceous tests are present, yet rare. The high concentrations of Si and low abundance of siliceous tests indicate that Si was mainly detrital. Titanium (Ti) is a heavy element and will be enriched in terrigenous sediments. Ti has been used as a lithogenous proxy because it is hosted principally in Ti-bearing heavy minerals in sediments and sedimentary rocks that are transported with the silt and fine sand fractions of marine sediments. Ti can also be hosted in biotite, amphiboles, pyroxenes and some clay minerals (Calvert and Pedersen, 2007). Ti, Al and Si have a strong positive correlation (Table 4.1). This indicates that Al and Si are mainly detrital. Al has a low abundance in seawater and is brought in by fluvial or eolian sources (Brumsack, 2006). The increased concentration of Si and Al along the San Marcos Arch shows that deltaic sediments were possibly carried as far southwest as the Eagle Ford depocenter (Figure 5.1).

Ca is the most abundant element in Eagle Ford rocks from Karnes County. Where Ca increases there are more carbonate minerals present. Microfacies interpretations identify that skeletal grains made up of $CaCO_3$ from planktonic nannofossils (i.e., coccolithophores) and planktonic foraminifera make up the bulk of the carbonate fraction in the Eagle Ford. There are also accessory grains of calcareous echinoids, ostracods and bivalves present. Precipitated

calcite crystals have also been found in core. There is a detrital component of Ca in feldspars and clay minerals within the Eagle Ford but that makes up a much smaller fraction compared to calcareous skeletal grains.

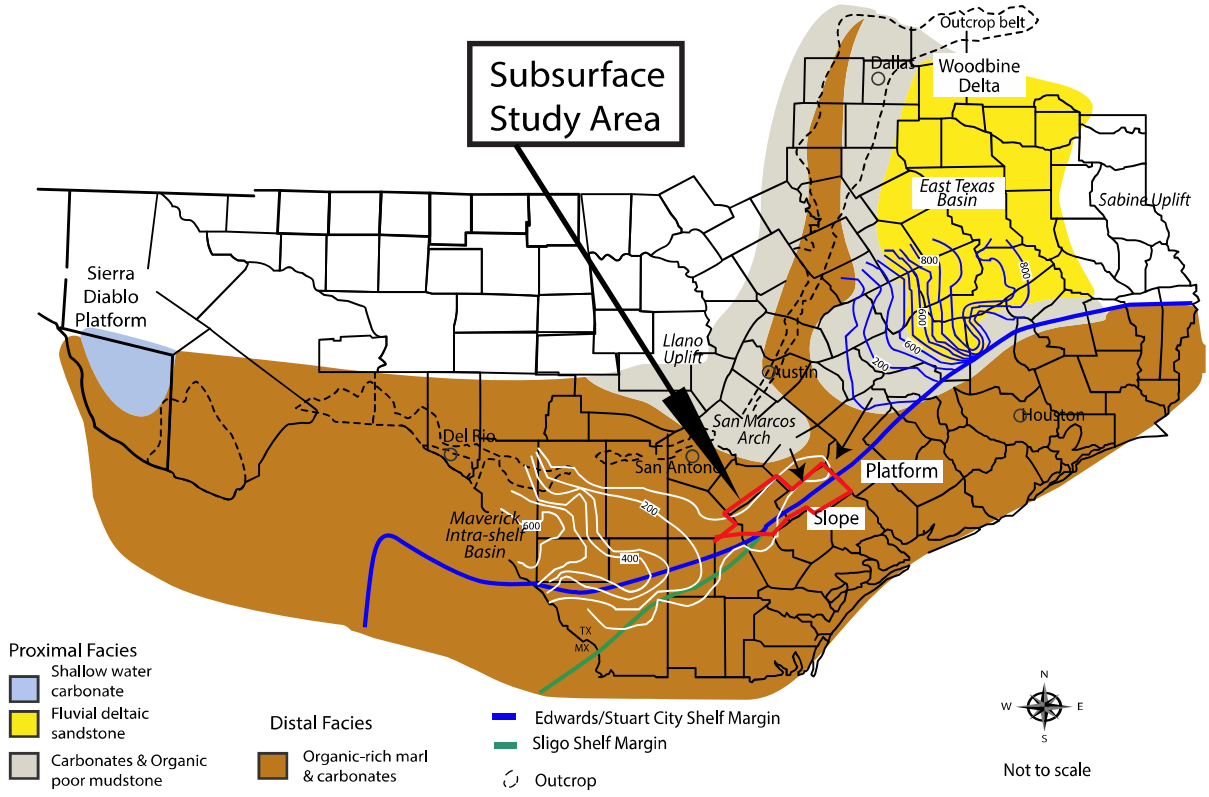

Figure 5.1 Woodbine and Eagle Ford facies in South Texas

Fine-grained fluvial deltaic sediments prograded toward the south mixing with organic rich marls near the study area. Modified from Ruppel et al., 2012.

5.2.1.2 Enrichment Factors

Average shale is typically deposited near shore under an oxygenated water column which allows for most organic matter to be oxidized (Wedephol, 1971; Arthur and Sageman, 1994). Samples from average shale are clay rich and include silt-sized quartz (Tucker, 2001). Taylor and McLennan (1985) as well as Wedephol (1971) sampled shale standards from around the world and determined average values that can be expected in average shale such as PAS. The reason a carbonate rich rock such as the Eagle Ford is compared to post-Archean Shale

(PAS) is because average shale serves as a background for sedimentation under normal seawater conditions.

Enrichment Factor (EF) values of 1 indicate a similarity to an average shale which is typically deposited in a near shore, oxygen rich environment (Wedephol, 1971; Moran, 2013). The relative enrichment of trace elements (Mo, Ni, Cr, Cu, U and Zn) above an average shale indicate that organic matter acted as a trace metal sink as anoxic conditions persisted in the water column throughout Eagle Ford time. These trace metals authigenically enriched in the water column under anoxic conditions and all except U form sulfides in the presence of high concentrations of sulfur (S) (Tribovillard et al., 2006).

Enriched P and depleted Mn and Co are proxies upwelling and simultaneous anoxic conditions (Brumsack, 2006). The EF of P was mapped across the trend to illustrate the enrichment of P above an average PAS. Phosphate rich black shale facies are representative of production during anoxic bottom conditions during high sea level stands in an offshore environment (Charvat, 1985 and references therein). Upwelling events bring in P and nitrogen with cold, oxygen rich water to continental shelves. Enriched P concentrations in the Eagle Ford suggest upwelling may have also played a role in bringing in nutrients to the Eagle Ford depocenter.

Since the Eagle Ford experiences a depletion in Mn and enrichment of P (Figure 4.21), it can be inferred that upwelling took place as the Eagle Ford was deposited although it was cyclical and not constant. Pulses of oxygen- and nutrient-rich water reached the Eagle Ford depocenter throughout time rejuvenating the water column with oxygen. Mn is also redox-sensitive, present in low concentrations in generally anoxic conditions and high concentrations in oxic conditions. There are cycles within core which depict a foraminifer rich zone gray in color followed by an organic matter rich zone black in color (see Rowe et al., 2013). It can be implied that these cycles are the result of cyclical oxygen input and deficiency as the water column went from oxygenated to anoxic. Mn and Ca have a strong positive association with one another and may be an

indicator for the precipitation of $MnCO_3$ the mineral rhodocrosite, or that Mn^{2+} is present in the $CaCO_3$ phase (Kearns, 2011). Ca has a positive association mainly with Total Carbonate minerals (0.81) and Mn (0.77) seen in Table 4.1 Correlation coefficients for major elements and minerals Most Ca is biogenic (Kearns, 2011).

The upper, middle and lower Eagle Ford members contain elements that behave similarly during Eagle Ford time as they are either enriched or depleted in all members. In comparison to mean C/T black shale, the Eagle Ford is either enriched or depleted in all elements similarly except Mn, Co and Pb (Figures 4.21 and 4.22). Mn, Co and Pb are enriched in mean C/T black shale with respect to average PAS concentrations. C/T black shale are more enriched in redox proxies such as Cr, Ni, Cu, Zn, Mo and U. This is speculated to be due to the variation in black shale depositional environments which span different types of basin restriction. The Eagle Ford is weakly restricted from the open ocean and may not be as enriched in trace metals as other C/T black shale which were deposited under different degrees of restriction (Moran, 2013). In comparison to anoxic and upwelling environments such as the Namibian extended shelf, the Eagle Ford is also less enriched in trace metals. The Eagle Ford Formation underwent localized influences as well as effects from global occurrences which is why it can be compared to mean C/T black shale or upwelled sediments. There is a degree of difference between the Eagle Ford and those two analogs.

5.2.1.3 Paleoproductivity and Redox Changes

Trace metals are either present in seawater in a soluble form or can be adsorbed onto particles. Under reducing conditions metallic ions of elements are adsorbed onto organic material, can form organometallic complexes, or precipitated as iron sulfides (Tribovillard et al., 2006). Trace elements that have been used as proxies for dysoxic and anoxic bottom waters are present in greater than average quantities indicating that the water column directly overlying these sediments was oxygen deficient and reducing. The Eagle Ford experienced trace metal enrichment greater than the elements' natural occurrence in seawater (e.g., Calvert and

Pedersen, 2007). The elements that are most useful to determine redox facies are Mo, S, V, Ni, Cu, Co, Th and U. Tribovillard et al. (2006) consider U, Mo, Ni and Cu as elements least vulnerable to primary and secondary complications and suggest their use as paleoredox proxies. Ba is also an important element but drilling mud contamination (drilling mud composition of barite, $BaSO_4$) led to ambiguous errors when analyzing cuttings; this element was therefore left out of the interpretation.

Redox sensitive trace metals tend to be soluble under oxic conditions and less soluble under reducing conditions, which explains why certain trace metals are authigenically enriched in oxygen-depleted facies (Tribovillard et al., 2006). Euxinic conditions existed within the Eagle Ford in a cyclic pattern as high concentrations of redox-sensitive trace metals demonstrate temporally. The variation in trace element concentrations throughout the Eagle Ford Formation indicates that the water column directly overlying the Eagle Ford depocenter was transformed from an oxic-upwelling environment, indicated by spikes in P concentrations, to an anoxic and also euxinic environment in a cyclic pattern, indicated by Mo (Figures 4.14-4.20). Trace element data indicates a cycling of alternating transgressive/regressive sequences as supported by Donovan and Staerker (2010), Lock et al. (2010) and Harbor (2011). Influences from outside sources have also played a role; including detrital input diluting trace element concentrations or volcanism increasing the availability of trace metals.

Although trace metals are of low abundance in crustal rocks, they are sensitive to geochemical changes in seawater and sediment pores (Calvert and Pedersen, 2007). Brumsack (2006) elaborates on trace metal deposition onto continental shelves and the subsequent development of an oxygen minimum zone (OMZ) if they are present in great quantities. Planktonic blooms occur cyclically when there is renewed availability of nutrients including trace metals in the water column they live in (Brumsack, 2006). Figure 5.2 illustrates the sediment capture of trace metals under an anoxic water column with high productivity at the sea surface above an extended shelf which experiences upwelling. Sporadic H_2S in the water column is

present as a byproduct of oxygen consumption by microbial organisms (sulfur-reducing bacteria) as decaying organic matter is oxidized or as they reduce excess inorganic sulfate into sulfide (e.g., Barton and Fauque, 2009).

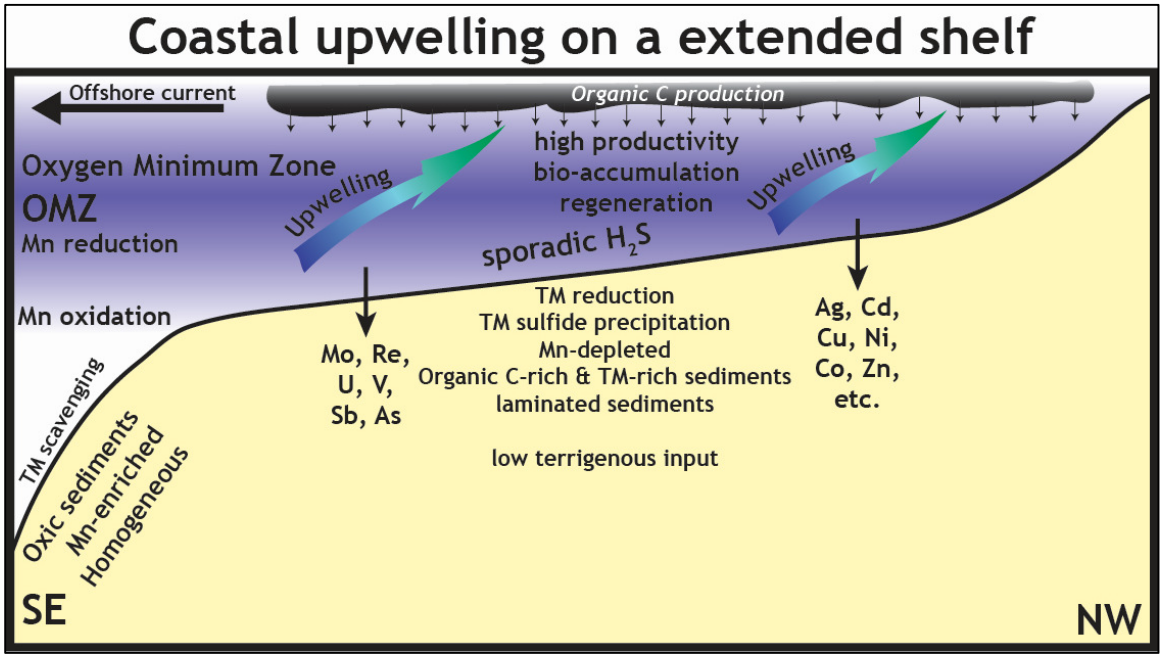

Figure 5.2 The process of sedimentary trace metal capture

Trace metals are captured into sediment as they come out of solution under anoxic conditions when free H_2S is present within the water column and form sulfides. Surface productivity is a result of nutrient input and a cyclical supply of oxygen by upwelling of bottom waters. Modified from Brumsack (2006).

Trace elements can also depict facies changes but are more specific proxies for environmental conditions as well as the geochemical makeup of the rock. Mo has been the favored trace element to understand changes in redox within the Eagle Ford in south Texas although V has been used by Tinnin et al. (2013) to describe anoxia as well. From analysis of Mo concentrations it appears that peak anoxic to euxinic conditions existed at the beginning of Eagle Ford time through the deposition of the lower part of the upper Eagle Ford (Figures 4.14-4.20). Although the Eagle Ford has been linked to global OAE 2 deposition, Mo concentrations in drill cuttings and core suggest that anoxia preceded the defined OAE 2 boundary (Kearns, 2011). Mo is found in high concentrations when it is removed from seawater under anoxic to euxinic

environments (Yan Zheng et al., 2000). Mo reservoirs are found in seawater and in detrital clastics or Mo can be authigenically precipitated (Poulson et al., 2006). The exact mechanism under which Mo becomes enriched under anoxic conditions is speculated to be diagenetic (Brumsack, 2006; Calvert and Pedersen, 2007). Mo in seawater or from detrital sources is relatively low compared to authigenic Mo. In terrigenous materials such as granites and their mechanical erosional products, mudrocks, the average Mo isotope composition is close to 0% and found mainly as MoO_3. MoO_3 is also found in association with Mn-oxyhydroxides (Yan Zheng et al., 2000; Poulson et al., 2006). When Mo isotope concentrations increase under oxic environments Mo is found as MoO_4^{2-} (Poulson et al., 2006).

Trace metal fixation is a term referred to by Brumsack (2006) to explain the bacterial sulfate reduction and its relationship with trace metals. Trace metals such as Mo, Zn, and Cu form sulfides when they are available in increased concentrations due to their solubility decrease in sulfidic waters (Brumsack, 2006 and references therein). H_2S is generally not enriched under normal circumstances in seawater; sulfur and therefore pyrite acts as a sink for Mo and As and have an effect on Co, Cu, Mn and Ni (Brumsack, 2006). This explains why these trace elements are enriched in the Eagle Ford Formation where large abundances of pyrite are encountered. Concentrations of MoO_4^{2-} are then converted to MoS_4^{2-} in an anoxic to euxinic water column where sulfide concentrations exceed 100μM (Figure 5.3) (Poulson et al., 2006). The relationship between trace metal enrichment due to sulfur generation have been explained by Sageman and Lyons (2003), Poulson et al. (2006), Brumsack (2006) and Tribovillard et al. (2006) leading Mo to be used as the main proxy to define sulfur rich zones within the Eagle Ford.

Cu, Zn, Co and Ni can be used as a paleoproductivity indicator and when their values in ppm are higher than the average gray shale and there is a high abundance of organic matter present (Brumsack, 2006; Tribovillard et al., 2006). These elements are mainly chalcophiles in the earth's crust (White, 2013). It can be suggested that since these elements are chalcophiles and are found with abundant organic matter, that these elements' concentrations will be high in

anoxic conditions. After nutrients drive enhanced bioproductivity, organic carbon rich sediments will be well preserved under an anoxic environment (Brumsack, 2006). Figures (4.14-4.20) illustrate that the logs for these elements often mirror Mo.

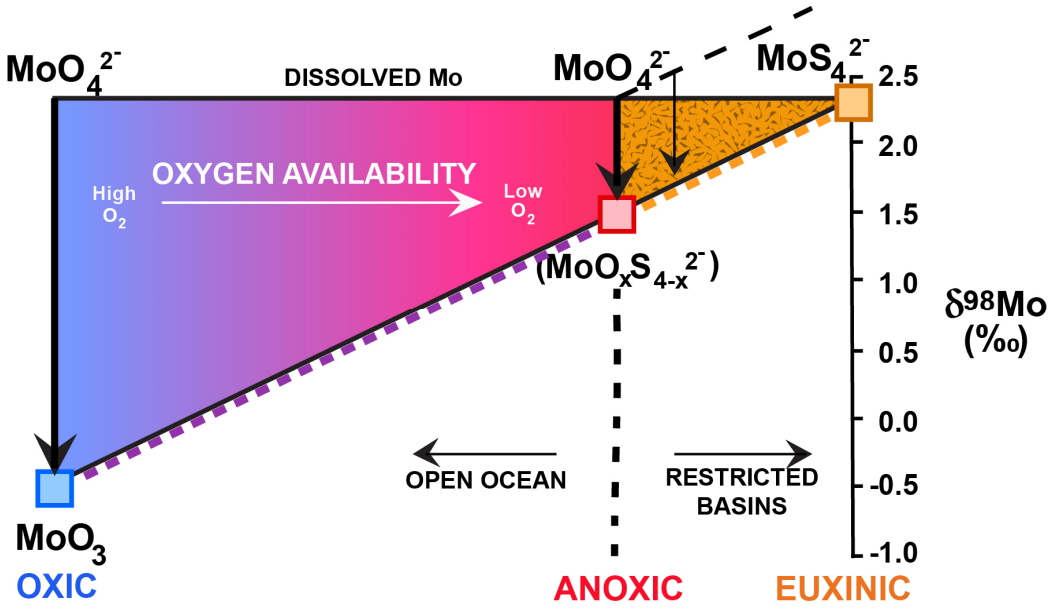

Figure 5.3 Mo relationships with respect to oxygen and sulfur

From Poulson et al. (2006). As Mo isotope concentrations increase and sulfur is introduced to the water column, chemical reactions bind molybdenum with sulfur and the water column becomes more oxygen-deficient and sulfur-rich.

The presence of these nutrients in great abundances when normalized to average shale can suggest two things. One being that nutrients were the precursor to enhanced bioproductivity and were brought in by upwelling. Cycles of anoxic to euxinic water conditions may have been the result of planktonic blooms that caused the widening of the oxygen minimum zone above the shelf. Another suggestion is that Ni, Zn, and Cu are also enriched in mantle rocks and that the source of these elements in the Eagle Ford depocenter could have been volcanic ash. Nutrient cycling from subaqueous flood basalt centers have also been discussed by Sinton (1996). Figure 5.4 illustrates a generalized model for nutrient output into seawater and volcanic gas output by Large Igneous Province (LIP) activity, which results in warmer global temperatures, sea level rise, a stratified water column, planktonic blooms, and black shale deposition.

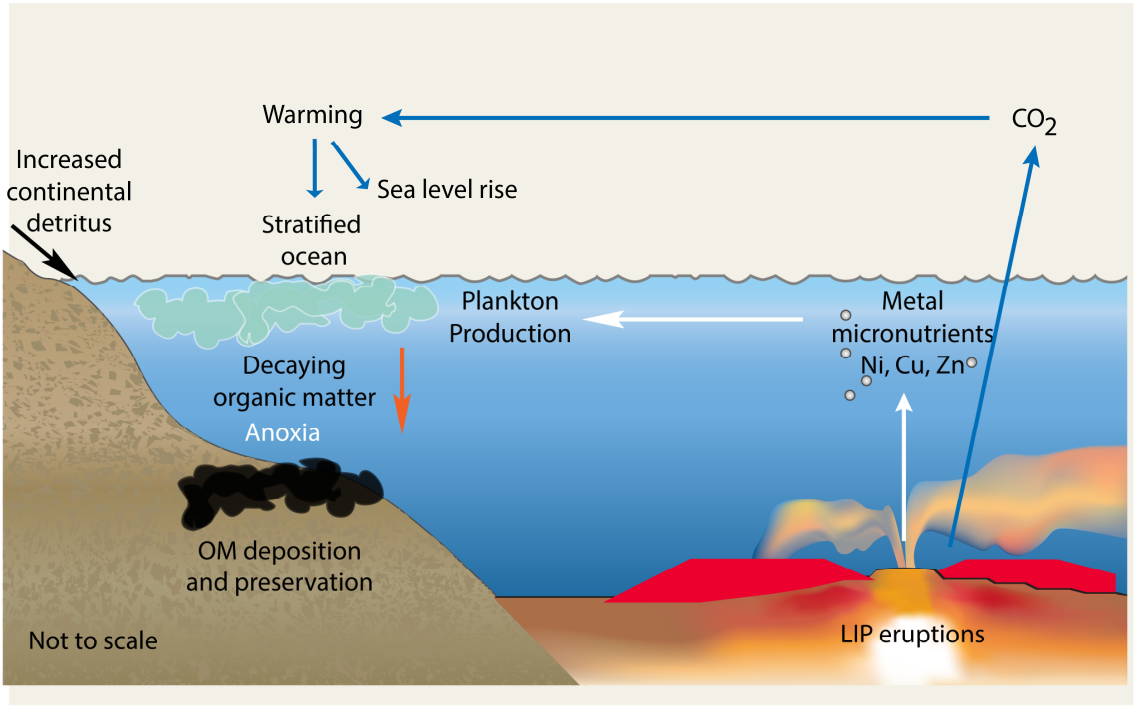

Figure 5.4 The effect of LIPs on black shale deposition

Metal micronutrients are released into the ocean in addition to sulfur and CO_2 as LIPs erupt. These reactions drive planktonic production and possibly lead to an anoxic water column, organic matter deposition and organic matter preservation. Modified from Bralower, 2008.

5.2.1.4 Summary

Major and trace elements have shown that the Eagle Ford Formation is rich in nutrients brought in by upwelling or volcanic ash deposition. Mo has shown that reducing conditions persisted starting at the beginning of Eagle Ford time while a transgressive system covered a broader area of the shelf. The upper Eagle Ford member was deposited under different conditions as a third-order regression commenced and oxic conditions took over. Not only did redox processes change during the span of Eagle Ford time, the conditions along the shelf margin were also variable. In Karnes County and southwest DeWitt County conditions were reducing resulting in greater carbonate deposition while in northeast DeWitt County more oxygenated conditions persisted and there was a greater influence of detrital sediments. Rare earth elements will be used to differentiate between the sources of these two different facies.

5.2.2 Rare Earth Elements

Taylor and McLennan (1985) and references therein stated that sedimentary processes undergo homogenizing effects and that nearly constant REE distributions in sedimentary rocks should reflect upper continental crust abundances. REEs are considered the least soluble trace elements and are relatively immobile as they undergo weathering, metamorphism or hydrothermal alteration (e.g., Rollinson, 1993). Typical average shales from around the world (North America, Europe and Australia) have reflected the composition of crustal rocks in their REE patterns (Taylor and McLennan, 1985 and references therein). Post-Archean Australian Shale (PAAS) values have been adopted to represent a typical upper continental crust pattern and represent average shale according to Taylor and McLennan (1985). Sedimentary REE patterns appear to be uniform in spite of diversity in the composition of igneous rocks, leading researchers to believe that they are useful indicators of average provenance compositions for the exposed continental crust and also tectonically active settings (McLennan, 1989). The REE patterns of rocks within the Eagle Ford Formation can in turn be used to determine the source of sediments. PAAS also represent normal, oxygen rich conditions in the water column while samples unlike PAAS are indicative of a deviation from those normal conditions.

REE patterns from Eagle Ford samples normalized to chondrite values from McDonough and Sun (1995) show that seven wells analyzed by Chemostrat, Inc. can be grouped into two categories (Figures 4.23-4.29). The first category includes wells 17, 19, 20 and 24 (Figures 4.26-4.29). Samples from these wells show slight differences relative to chondrite normalized PAAS and are slightly depleted in REEs overall. There are two possibilities that explain the low abundances of REEs in Eagle Ford rocks relative to $PAAS_N$. The first suggestion is that when this occurs it represents fluvial sand input (see Figure 2.8 in Taylor and McLennan (1985)). The suggestion is that coarser grained sedimentary rocks will have overall lower abundances of REEs (Taylor and McLennan, 1985 and references therein). Silt fractions have lower abundances due to the dilution of quartz, a mineral with lower REE abundances (McLennan, 1989). Another

suggestion is the amount of carbonate present in Eagle Ford rocks due to its marine depositional setting. Taylor and McLennan (1985) suggest that low concentrations of REEs are present in rocks that are enriched in calcite above 10 ppm, as is the case with the Eagle Ford. The bulk of the REEs reside in the silt and clay size fraction and dilution from carbonates should not affect their distribution (McLennan, 1989 and references therein). The only effect that should occur is the reduction in the absolute abundances of the REEs in carbonate rocks by a factor of 20% of average shale; the pattern should still parallel the upper crustal pattern as their provenance (McLennan, 1989). Carbonate minerals also have low REE abundances as the REEs are taken from seawater during skeletal growth of marine organisms. Seawater has low REE abundances overall (Figure 5.5) (Elderfield and Greaves, 1982). The PAAS normalized seawater REE pattern is characterized by a depletion in LREEs and an enrichment of MREEs and HREEs indicating input of recycled coexisting minerals. This creates a dilution effect which lowers overall abundances for all REEs when the pattern of marine carbonate-rich rocks is plotted.

There is also a ubiquitous negative Ce anomaly in all Eagle Ford REE patterns, which is indicative of Ce depletion common to marine rocks deposited under anoxic conditions (e.g. Taylor and McLennan, 1985; McLennan, 1989). Under oxic conditions Ce^{3+} in seawater is oxidized and forms Ce^{4+} that combines with oxygen to form CeO_2 (Wilde et al., 1996). This leads to an enrichment of Ce (a positive Ce anomaly) in sediments, and depletion (a negative Ce anomaly) when the water column is anoxic. When black shale is deposited under a suboxic water column or reducing conditions, the bond between CeO_2 is broken and Ce^{3+} is precipitated back in to water column, leaving a negative Ce anomaly in the sediment, seen in most Eagle Ford samples (Wilde et al., 1996).

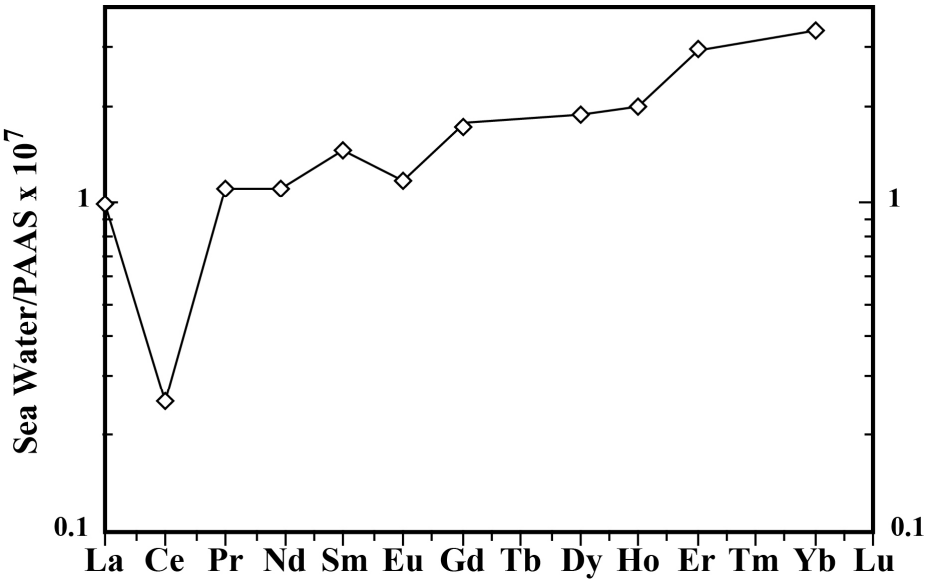

Figure 5.5 Atlantic seawater REE pattern

PAAS normalized Atlantic seawater from 900 m of depth. Modified from Elderfield and Greaves, 1982 and Mazumdar et al., 1999.

Ce is a useful paleoredox indicator in addition to Mo. Ce and other REEs come in with terrigenous sediments (Rollinson, 1993) and Mo precipitates authigenically under reducing conditions. When the Ce anomaly (Ce*) is normalized to PAAS and plotted with Mo, the elements' relationship in anoxic conditions are evident (Figure 5.6). The formula for Ce* is cited in Kato et al. (2006) as $[2Ce^*/ (La^* + Pr^*)]^{1/2}$. A Ce* of less than 1 indicates that Ce is depleted. None of the samples within the Eagle Ford have a Ce* equal or greater than 1 yet some do peak above 0.98. Ce* shows greater sensitivity to cyclical redox changes and indicates that most samples were deposited under a generally anoxic water column. Under more oxic conditions Ce concentrations are higher and Mo concentrations are lower. In some samples of the Eagle Ford, Ce is more depleted than in others indicating a more oxic environment is expected. The reverse happens under anoxic conditions; Ce concentrations decrease and Mo concentrations increase. This results in a negative correlation between both elements.

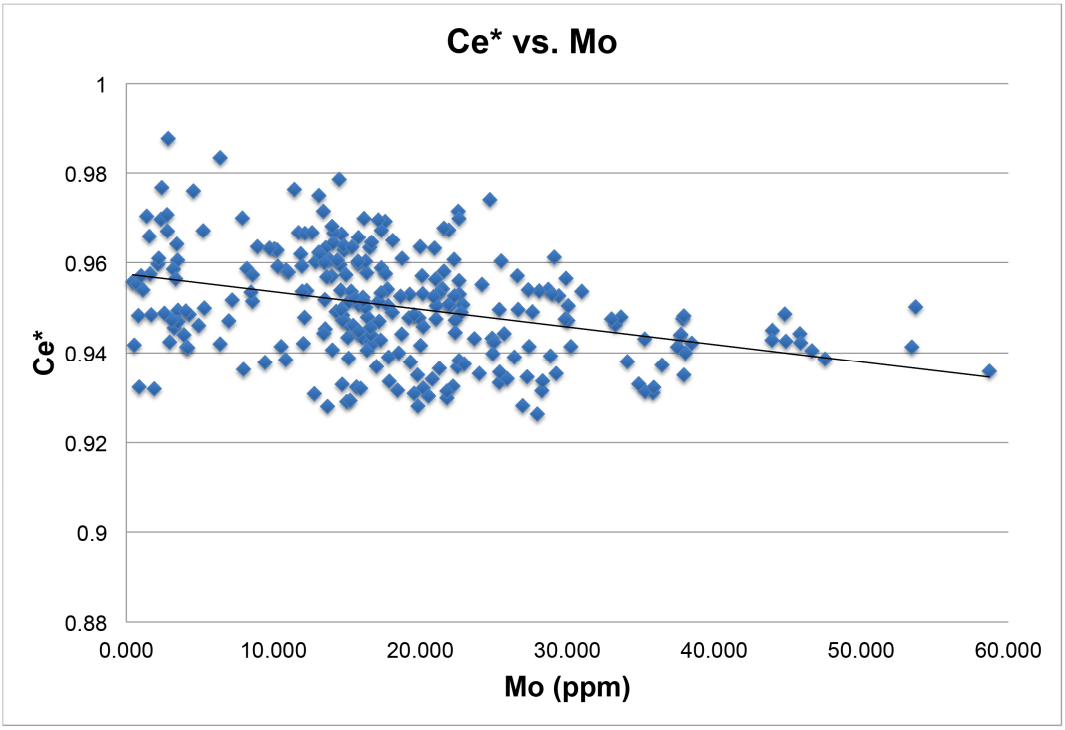

Figure 5.6 Ce anomaly plotted against Mo.

There is a negative relationship between Ce* and Mo. This diagram suggests that all samples were deposited under varying degrees of oxygen deficient water column conditions.

Other rare earth elements also have distinct patterns for Eagle Ford samples. Wells 17, 19, 20 and 24 are characterized by a negative Eu anomaly similar to granitic rocks such as PAAS. Eu is depleted in the sediments from these four wells due to the relative absence of plagioclase feldspar, which was fractionated out of the source melt, weathered out or could have been lost during transportation (McLennan, 1989). Eagle Ford rocks in northeast DeWitt County contain a greater aluminosilicate fraction due to the input of recycled clastic material derived from granitic sources such as the Llano Uplift or a different continental source. The general composition of the Llano Uplift is comprised of two suites of igneous rocks. The first, fine-grained granitic enclaves that are felsic in composition (70-75 wt.% SiO_2) and a second enclave of intermediate composition, most like mafic crustal rocks (Smith and Gray, 2011). The Woodbine delta also brought continental sediments into the ocean as suspended particulate matter.

Nevertheless, Eagle Ford samples from the four wells mentioned above are similar to the average PAAS pattern that is normalized to chondrite, depicting a greater influence from input from an upper continental sediment source (Figures 4.26-4.29). Rare earth elements support the notion that the location of these wells is receiving sediment input by currents as reworked sediment coming from the northeast as mechanically broken down fine grained detritus from the continent (i.e. original granite/granodiorite source). REEs are recycled in the weathering profile (McLennan, 1989). This is how they can be indicative of the source (provenance) of the sediments they are found in. REE values can be compared to PAAS averages to estimate where the increase in clastic sediments occurs within the Eagle Ford Formation in addition to mapping aluminosilicate fractions.

Wells 3, 12 and 16 which have a combination of REE patterns; some samples depict a negative Eu anomaly and some samples have no Eu anomaly relative to chondrite (Figures 4.23-4.25). Eu is enriched in sediment that has plagioclase because Eu^{2+} is retained in plagioclase (where it substitutes for $Ca^{2+)}$ of source rocks and it is anomalous when plagioclase in weathered out. A negative Eu anomaly implies that plagioclase was removed in different degrees during weathering. The enrichment of Eu with respect to PAAS patterns could be attributed to the presence of plagioclase in the source rock, also suggesting that these sediments were deposited near their source and did not undergo much weathering. The source for sediment with no negative Eu anomaly is possibly volcanic input comprised from a mafic source or element cycling from Large Igneous Provinces (LIPs). Elements from a mafic source could have been brought into the Eagle Ford depocenter during sedimentation, most likely by subaerial volcanic ash deposition in the water column. Sinton (1996) proposes that upwelling brought bottom waters carrying mafic material from subaqueous flood basalt plateau formation to continental shelves during the Late Cretaceous. There is greater evidence that volcanic ash deposition was the main mechanism for the deposition of mafic material.

If the only difference between the two types of REE patterns found between wells in the northeast and the southwest is the variation in the degree of a Eu anomaly, this may be the reason for the differentiation between carbonate-rich, anoxic sedimentation and oxygenated, siliciclastic sedimentation. The only contradiction in this suggestion is that these patterns hold true for sediments across the Eagle Ford members although redox conditions change from anoxic to oxic (i.e. the gradation from the lower Eagle Ford member to the middle Eagle Ford member and the upper Eagle Ford member). This suggests that an outside influence is responsible for the change in facies seen in the Eagle Ford.

The pattern exhibited by all wells appears to be volcanic in origin mixed with detrital clays. McLennan (1989) has stated that it is possible for "sediments deposited at active continental margins to show REE patterns intermediate between a typical andesite pattern and PAAS, or in some cases indistinguishable from PAAS"; which is the case in the Eagle Ford. The typical andesite pattern defined by McLennan (1989) is a lower REE abundance than PAAS and without a negative Eu anomaly. They also show less fractionation. In LeBas et al.'s (1986) TAS diagram all samples plot in the andesite and dacite categories while bentonite samples across five wells plot as basalt and various types of basaltic-trachy andesite. One outlier plots as tephrite/basanite (Figure 4.40). The bulk samples for seven wells from the Eagle Ford range from andesite to dacite and rhyolite based on their SiO_2, Na_2O and K_2O contents when CaO is removed (Figure 4.41). This is due to the combination of mixing volcanic ash with detrital aluminosilicates (such as clay minerals, rich in Si, Na and K) during deposition and weathering of clay minerals into kaolinite, which results in a loss of Na and K and an increase in Si.

To demonstrate the differences in Eagle Ford fractionation relative to PAAS, $(La/Lu)_N$ ratios were cross-plotted against $(Dy/Yb)_N$ ratios (Figure 4.37). REEs increase in compatibility from La to Lu as well as increase in atomic number from lower to higher to the right of the diagram. Incompatible trace elements such as La and Ce tend to concentrate in the melt rather than the solid and are partitioned into the melt during partial melting of the mantle source rock

during fractional crystallization (Winter, 2010). Fractional crystallization involves the physical separation of the solid (crystals) from the melt. Bulk composition and magma compositional changes (differentiation) can be determined from fractional melting and crystallization of the magma. All samples from the Eagle Ford show a higher degree of fractionation in comparison with PAAS. Incompatible LREEs favor fractionating first. Compatible trace elements such as Yb and Lu concentrate favorably in solid minerals due to their smaller ionic radius and are more likely to substitute for a major element in a mineral (Winter, 2010). La is an incompatible element showing that the source of the sediments within the Eagle Ford are highly fractionated due to a more negative $(La/Lu)_N$ slope (Figure 4.37).

Ocean Island Basalt, Normal Mid Ocean Ridge Basalt (N-MORB), many andesites and basalts have REE patterns much lower than PAAS and show a lower degree of fractionation. LREE-depleted basalts have HREE patterns with near flat to slightly negative slopes with $(Dy/Yb)_N$ ratios near 1 (Barrat, 2004). $(Dy/Yb)_N$ can be interpreted to determine if a sample has a greater MREE or HREE abundance. A slope greater than 1 indicated that those samples have a greater concentration of MREEs than HREEs. Since Dy and Yb are less incompatible during the crystallization of an ultramafic or a basaltic liquid they are sensitive to the original melt that they originated from. A strong HREE enrichment is indicated by a $(Dy/Yb)_N$ ratio significantly lower than 1 (Barrat, 2004). Samples from the Eagle Ford are above a ratio of 1 in most cases indicating that the Eagle Ford has a greater abundance of MREEs in addition to LREEs (Figure 4.38). The implications this has for the Eagle Ford, and any rock showing this characteristic, is that most samples are enriched in elements which had been partitioned in silicate melts originally rather than due to coexisting minerals since deposition (Frey, 2009).

5.3 Summary

In summary, the environment surrounding the Eagle Ford depocenter in south Texas was a unique environment characterized by an accumulation of biogenic calcite, high trace metal availability and influence by outside factors such as deposition of recycled clastic sediment,

volcanic ash deposition and upwelling of nutrient-rich water. These factors are all interrelated and affected the accumulation of silt, mud and carbonate along the trend. It has been illustrated that the Eagle Ford Formation has a high abundance of carbonate minerals as well as aluminosilicates, but that there is a separation between the two facies along the trend. In northeast DeWitt County the increased input of silt-sized quartz and clay minerals revealed that continental sediments prograded south toward the Gulf under an oxic to dysoxic water column; either carried in as fine-grained particulate matter from the Woodbine Delta or weathered from the Llano Uplift. Eagle Ford sedimentation in Karnes County and southwest DeWitt County occurred under a mostly anoxic water column with greater concentrations of carbonate minerals deposited.

An understanding of the provenance of Eagle Ford sediments would aid in understanding the character of these rocks and why a facies change exists in the first place. Rare earth element patterns suggest that sediments from the southwest area along the Eagle Ford trend came from an intermediate to mafic source and sediments from the northeastern area were a mixture of a felsic source, including recycled clastics. Little variation in REE patterns that depict a intermediate to mafic source throughout the gross Eagle Ford suggest that volcanism was continuous throughout Eagle Ford depositional time, with pulses of increased volcanism where thicker bentonite layers (altered volcanic ash) are preserved. The discovery that a large number of samples appear to be volcanically derived or remnants of flood basalt eruptions is useful because it has been speculated for a number of years that the origin of Cenomanian-Turonian black shales involves volcanism (Sinton, 1996; Kerr, 1998; Wignall, 2001; Sageman et al., 2006; Turgeon and Creaser, 2008).

Planktonic organisms were affected by the environmental conditions as seen in an increase in organic matter burial when nutrient input increased. Enhanced bioproductivity caused an oxygen minimum zone to expand above the shelf with the greater demand of oxygen by planktonic organisms exceeding the supply (Kearns, 2011). An anoxic water column preserved this organic matter, as there were few benthic fauna to oxidize it. The regular output of hydrogen

sulfide into the water column can be attributed to sulfur brought in by volcanic ash as sulfate, then converted by sulfur-reducing bacteria to sulfide (Barton and Fauque, 2009). This reaction resulted in the authigenic enrichment of trace elements such as Mo, Ni, Cu and Zn. The cause for enhanced bioproductivity has also been attributed to upwelling from deeper waters, which brings cold nutrient rich waters onto continental shelves (e.g., Demaison and Moore, 1980; Brumsack, 2006). Chemical elements derived from volcanic eruptions are also a source of nutrients (Sinton, 1996; Kerr et al., 2003). A suggestion can be made that these two methods of nutrient input are related.

This thesis has shown that the Eagle Ford system was not restricted from outside influences and was affected by the factors that others have speculated lead to the deposition of black shale on a global scale. The following chapter summarizes the major highlights of this research.

Chapter 6

Conclusions

This thesis has illustrated how major, minor and trace elements were used to characterize the stratigraphic facies changes and provenance of sediments within the Eagle Ford Formation in south Texas. The major findings are outlined in the following sections.

6.1 Major Conclusions

The transgressive lower member of the Eagle Ford Formation was deposited in an oxygen depleted paleoenvironment illustrated by high Mo concentrations, the abundance of framboidal pyrite in core (Harbor, 2011) and high concentrations of proxies for organic matter (i.e., Cu, Ni and Zn). In addition to the abundant pyrite found in Eagle Ford core, Mo concentrations suggest that there was free H_2S in the water column during Eagle Ford deposition but that it was cyclically deposited. Mo needs free sulfur in the water column to be converted from MoO_4^{2-} to MoS_4^{2-} (Poulson et al., 2006). The regressive upper member of the Eagle Ford Formation was deposited in an oxygen rich environment as characterized by low Mo concentrations and a decrease in the concentrations of organic matter proxies.

Major clastic facies changes from Karnes County to northeast DeWitt County have been illustrated using Si, Ca and Al. There is an increase in silt-sized quartz and aluminosilicate minerals as facies change in northeast DeWitt County from carbonate-rich facies in the southwest. Toward northeast DeWitt County the Eagle Ford has a greater abundance of clay and grades into moderately organic, argillaceous silty marl. In central Karnes and north-central Live Oak counties, calcite is the most abundant mineral and occurs as skeletal fossil remains or recrystallized calcite cement. In Karnes County, the Eagle Ford can be described as organic-rich marl. This gradation along the San Marcos Arch area is directly visible in well logs, core, and drill cuttings. The results of this study substantiate Hentz and Ruppel's (2010) model that the lower to middle Eagle Ford members begin to grade into organic-poor mudstones, including Woodbine facies such as the Maness/Pepper Shales, along the San Marcos Arch area.

The deposition of the Eagle Ford coincides with Cenomanian-Turonian marine black shale deposition worldwide (Dawson, 2000) yet there is still ambiguity over the exact age of the C/T boundary within the Eagle Ford Formation. Trace element concentrations, specifically Mo, show that anoxia preceded the Cenomanian-Turonian boundary (or OAE 2 event), which is expected to have occurred within the upper Eagle Ford based off carbon isotope (δ^{13} C) data from Donovan et al. (2012). Validity can be given to two models for the causes of ocean water anoxia preceding OAE 2 since there is evidence for both within Eagle Ford sediments. It has been confirmed that the Eagle Ford Formation is a prolific source rock because of its organic richness preserved by an anoxic water column. Enhanced bioproductivity, triggered by upwelling of nutrient rich waters, is supported by high concentrations of phosphorus along the edge of the Eagle Ford depocenter; as well as an area of anoxia and euxinia updip from the shelf edge depicted by variations in high Mo concentrations. In addition to upwelling, volcanism was a precursor to enhanced bioproductivity aided by the eruption of subaqueous flood basalts at the end of Eagle Ford time. Both mechanisms brought in nutrients (minor and trace metals) and affected paleoredox water column conditions.

The presence of abundant bentonite (clay weathered from volcanic ash) in Eagle Ford core indicates that volcanic ash was deposited contemporaneously with Eagle Ford sediments. The claim that volcanism affected Cenomanian-Turonian (C/T) black shale deposition is supported by the rare earth element pattern findings of sediments originating from a felsic to mafic source throughout all wells. Rare earth element (REE) patterns show a variable provenance of Eagle Ford sediments. Some samples parallel the upper continental crust pattern of average post-Archean Australian shales (PAAS). Other samples appear volcanic due to their lack of a negative Eu anomaly and Eu enrichment relative to PAAS-due to the presence of plagioclase feldspar. Overall, samples from the Eagle Ford show a mixed source character including subaerial volcanic ash and detrital sediment input possibly from the Llano Uplift or a different continental source. Ca rich sediments will still have a negative Eu anomaly according to

McLennan (1989) suggesting that Ca dilution would not affect the REE pattern of these rocks. Volcanic gas output may have caused acidification of the oceans during C/T time and caused extinctions of marine organisms which resulted in the deposition of vast amounts of organic rich black shale, but this thesis does not contain an extensive study of those effects. The exact source of Eagle Ford sediment and the type of volcanic material in the bentonite beds within remains undetermined and requires further study.

6.2 Limitations

Each quantitative analysis has limitations which must be contended with. The following best describe where there could be room for improvement in the defined study:

1. The density of each element in a sample varies and affects the energy peak detected by the hand-held ED-XRF during fluorescence. Error quantification is important, especially if the samples are not homogeneous.
2. Cuttings represent a range of depths and it is not possible to pinpoint the exact depth that they came from. However, it is possible to visually inspect which member of the Eagle Ford Formation they came from as illustrated using the ChemGR log in Figure 3.2.
3. Understanding geochemical processes within black shale facies is a relatively new undertaking with regard to understanding the provenance of these sediment. Many methods typically used for clastics such as sandstone without a large carbonate fraction are being modified for carbonate and organic rich rocks. There are limitations to this as a large amount of Ca and a reduction in Si skews the data and could misrepresent the original source (e.g., Rollinson, 1993). Ca can be removed from the data and concentrations of remaining elements can be interpreted. Significant REE studies on Cenomanian-Turonian black shales are still lacking and the need to interpret a full suite of elements is necessary.
4. Because of the possibility of contamination and high variability of the lithology of

Eagle Ford rocks it is best to focus on the stratigraphic variation in all elements including Enrichment Factors (EFs), rather than absolute values (see Tribovillard et al., 2006 for an explanation on elemental variability).

6.3 Recommendations

The data set provided for this study has great potential and there are many topics that can be explored in the future:

1. Removing the carbonate fraction within these rocks and only interpreting results of remaining major, minor and trace elements.
2. Study the effect of Ca dilution in Eagle Ford rocks due to ocean acidification caused by volcanic gas output during the Upper Cretaceous.
3. A geochemical analysis of bentonite in both the Eagle Ford Formation and the Austin Chalk in order to understand their relation to volcanism or subaqueous flood basalt eruption during the Cenomanian to Santonian.
4. A study on benthic foraminifera to determine if anoxia reached the sediment-water interface and resulted in a lack of benthic fauna.
5. Isotope studies to understand the impact of volcanic ash on black shale, particularly of the Eagle Ford Formation, better. Sulfur isotopes would be useful to determine if sulfur was volcanically sourced.
6. XRD analysis on bentonite samples to determine their mineralogical composition in comparison to the mineralogy of bentonite from central Texas as described by Charvat (1985).
7. The identification of the Cenomanian-Turonian boundary in Eagle Ford core using carbon isotopes.
8. Interpret a full suite of elements utilizing Spider Diagrams to better understand the whole rock chemistry of samples. Increasing the amount of samples in the study area overall, or sampling at a higher frequency within, would also be useful.

Appendix A

Supporting Formulas

Clay Mineral Formulas

Illite (KAl2(SiO3AlO10)(OH)2

Kaolinite (Al2Si2O5(OH)4)

Smectite (Na, Ca)0.33(Al, Mg)2(Si4O10)(OH)2*n(H2O)

Chlorite (Mg, Fe)3(Si, Al)4O10(OH)2-(Mg, Fe)3(OH)6)

Moran (2013)

Conversion Factors Uaed

Element (wt.%)	Element Oxide Molecule (wt.%)	Conversion Factor
Si	SiO_2	0.4675
Al	Al_2O_3	0.5292
Ca	CaO	0.7147
Mg	MgO	0.6031
Na	Na_2O	0.7419
K	K_2O	0.8301
Fe	Fe_2O_3	0.6994
Mn	MnO	0.7745
Ti	TiO_2	0.5995
P	P_2O_5	0.4364
S	SO_2	0.500478

To calculate the element oxide of a sample:

Element% of your sample/Conversion Factor=Oxide%

Oxide%*Conversion Factor=Element%

Enrichment Factor Formula

EF= (Element/Al) $_{\text{your sample}}$ / (Element/Al) $_{\text{Average Shale of choice}}$

e.g., Tribovillard et al. (2006)

EF>1 is an enriched element

EF<1 is depleted based on average shale values

REE Normalization Values

Sources: [1] McDonough and Sun, 1995; [2] Taylor and McLennan, 1985

REE	C1 Chondrite[1]	PAAS[2]
La	0.237	38
Ce	0.613	80
Pr	0.0928	8.9
Nd	0.457	32
Pm	-	-
Sm	0.148	5.6
Eu	0.0563	1.1
Gd	0.199	4.7
Tb	0.0361	0.77
Dy	0.246	4.4
Ho	0.0546	1
Er	0.16	2.9
Tm	0.0247	0.4
Yb	0.161	2.8
Lu	0.0246	0.43

Calculations

Ce^* (Ce anomaly) = $[2Ce^*/ (La^* + Pr^*)]^{1/2}$ –Elements normalized to PAAS

Kato et al. (2006) and references therein

ChemGR= (K_2O*0.83*16.32)+(Th*3.93)+(U*8.08)

Chemostrat, Inc. (personal communication)

FeO to Fe_2O_3: Multiply by 1.1113

Fe_2O_3 to FeO: Multiply by 0.8998

Winter (2010)

Appendix B

Elemental Data Tables

Hand Held XRF Data Mean Statistics

Major, Minor and Trace Elements from twenty-two wells

	Gross Eagle Ford n=892			Upper Eagle Ford n=204			Middle Eagle Ford n=301			Lower Eagle Ford n=387			PAS Taylor& McLennan 1985
Element (wt.%)	Min	Max	Mean	Min	Max	Mean	Min	Max	Mean	Min	Max	Mean	
SiO2	13.91	49.32	34.48	15.37	40.19	28.48	13.91	49.32	37.86	23.16	46.95	35.02	62.8
Al2O3	0.00	19.87	10.31	2.90	13.52	7.22	0.00	19.81	11.85	5.86	19.87	10.75	18.9
CaO	16.88	73.75	41.52	32.30	73.75	52.81	16.88	71.14	35.98	19.80	58.54	39.87	1.3
MgO	0.00	3.35	1.23	0.15	2.39	1.34	0.00	3.35	1.19	0.00	2.61	1.22	2.2
Na2O	0.00	2.70	1.34	0.49	2.09	1.34	0.00	2.70	1.32	0.80	2.57	1.36	1.2
K2O	0.22	3.68	1.37	0.22	2.13	0.90	0.36	3.68	1.73	0.42	2.52	1.33	3.7
Fe2O3	2.03	16.85	3.73	2.03	4.95	3.17	2.23	16.85	4.05	2.35	6.50	3.79	6.5 (FeO)
MnO	0.01	0.19	0.06	0.04	0.19	0.06	0.01	0.16	0.05	0.03	0.19	0.05	0.11
TiO2	0.00	1.69	0.40	0.09	0.54	0.31	0.00	1.69	0.46	0.00	0.80	0.40	1.0
P2O5	0.00	2.46	0.36	0.00	0.67	0.30	0.16	1.95	0.32	0.19	2.46	0.43	0.16
SO2	1.28	12.11	5.16	1.28	9.53	4.07	1.28	11.86	5.12	2.89	12.11	5.78	-
Cr (ppm)	0.00	575.00	21.04	0.00	265.00	9.54	0.00	575.00	21.77	0.00	133.00	26.54	110

	Gross Eagle Ford n=892			Upper Eagle Ford n=204			Middle Eagle Ford n=301			Lower Eagle Ford n=387			PAS Taylor& McLennan 1985
Element (wt.%)	Min	Max	Mean	Min	Max	Mean	Min	Max	Mean	Min	Max	Mean	
Cu	1.00	238.00	40.00	1.00	150.00	29.80	10.00	165.00	39.61	20.00	238.00	45.68	50
Ni	15.00	111.00	50.00	15.00	73.00	37.05	17.00	86.00	49.30	15.00	111.00	57.38	55
Sr	426.44	1222.00	742.15	601.0	1222.0	812.34	547.69	1191.0	749.80	426.44	1155.00	699.19	200
Zn	0.00	451.00	73.86	0.00	346.00	47.80	7.00	389.00	73.30	17.00	451.00	88.04	85
Zr	7.00	128.89	58.04	7.00	86.22	38.09	22.00	128.89	70.02	13.00	110.75	59.25	210
Mo	0.00	90.00	14.53	0.00	30.00	4.95	0.00	58.00	13.12	0.00	90.00	20.67	1.0
Nb	2.00	11.60	5.58	2.00	7.00	4.65	3.00	11.60	6.31	2.00	9.96	5.49	19
Th	3.00	10.51	5.08	3.00	6.23	3.93	3.00	10.51	5.97	3.00	8.79	5.00	14.6
U	0.00	28.00	8.25	0.00	22.00	7.19	0.00	27.00	9.36	0.00	28.00	7.96	3.1
Y	8.00	30.00	16.75	9.00	24.00	15.49	8.00	28.00	16.45	8.00	30.00	17.63	27
Rb	6.00	124.37	45.34	6.00	66.00	26.81	12.00	124.37	60.09	9.00	103.26	43.64	160
Co	0.00	47.00	4.90	0.00	7.00	2.80	0.00	47.00	5.89	0.00	15.00	5.23	23
Pb	7.00	48.00	13.86	7.00	30.00	11.90	8.00	29.00	14.02	8.00	48.00	14.77	20
As	2.00	245.00	9.06	2.00	54.00	5.24	2.00	65.00	8.64	2.00	245.00	11.40	-

	Gross Eagle Ford n=892			Upper Eagle Ford n=204			Middle Eagle Ford n=301			Lower Eagle Ford n=387			PAS Taylor& McLennan 1985
Element (wt.%)	Min	Max	Mean	Min	Max	Mean	Min	Max	Mean	Min	Max	Mean	
Sn	2.00	2.26	2.01	2.00	2.22	2.01	2.00	2.26	2.02	2.00	2.24	2.01	4.0
Sb	3.00	12.00	7.38	3.00	11.00	7.11	4.00	11.00	7.31	4.00	12.00	7.57	-

XRD Sample count

Measured mineral/TOC (wt.%)	Gross Eagle Ford	Upper Eagle Ford	Middle Eagle Ford	Lower Eagle Ford
TOC	106	26	26	54
Quartz	133	26	37	70
K-Feldspar	91	26	18	47
Orthoclase	42	0	19	23
Plagioclase	133	26	37	70
Pyrite	133	26	37	70
Marcasite	91	26	18	47
Apatite	107	18	33	56
Other Minerals	42	0	19	23
Kaolinite	91	26	18	47
Illite	26	8	4	14
Chlorite	91	26	18	47
Mixed Layer Clay	26	8	4	14
Calcite	91	26	18	47
Dolomite	91	26	18	47
Total Carbonate Minerals	42	0	19	23
Total Clays	133	26	37	70

Chemostrat, Inc. ICP-MS and ICP-OES Data Statistics

Accuracy Data provided by Chemostrat, Inc. (personal communication)

ICP-OES	Unit	Element	*Limits of Quantification*	% Accuracy offset from Standards
	%	Al2O3	*0.06*	-3.74
	%	SiO2	0.30	-0.22
	%	TiO2	0.02	-3.19
	%	Fe2O3	0.05	-3.21
	%	MnO	0.00	-2.26
	%	MgO	0.11	-3.58
	%	CaO	0.30	0.81

	%	Na2O	0.10	-0.02
	%	K2O	0.02	-0.24
	%	P2O5	0.00	0.73
	ppm	Ba	4.94	5.70
	ppm	Be	0.51	1.73
	ppm	Ce	7.08	-1.79
	ppm	Cr	3.86	2.14
	ppm	Cu	3.16	2.99
	ppm	La	2.95	4.44
	ppm	Nb	3.61	2.20
	ppm	Ni	2.85	1.70
	ppm	Sc	1.05	2.59
	ppm	Sr	4.24	-2.11
	ppm	V	5.82	6.09
	ppm	Y	1.18	1.00
	ppm	Zn	4.79	4.06
	ppm	Zr	3.12	-2.59
ICP-MS	Unit	Element	*Limits of Quantification*	% Accuracy offset from Standards
	ppm	Be*	2.61	-1.29
	ppm	V	5.21	3.23
	ppm	Cr	4.82	0.19
	ppm	Co	1.91	-1.31
	ppm	Ni*	7.38	-1.52
	ppm	Cu	3.52	0.15
	ppm	Zn	7.42	-5.48
	ppm	Ga	1.51	-4.42
	ppm	Rb	1.38	0.89
	ppm	Sr	4.00	0.50
	ppm	Y	0.96	9.28
	ppm	Zr	2.73	4.71
	ppm	Nb	1.04	8.38
	ppm	Mo*	2.50	5.20
	ppm	Sn	0.98	-4.91
	ppm	Cs	0.43	1.98

	ppm	Ba	5.27	6.57
	ppm	La	2.42	4.89
	ppm	Ce	1.83	2.25
	ppm	Pr	0.70	2.24
	ppm	Nd	1.28	2.89
	ppm	Sm	0.56	3.30
	ppm	Eu	0.28	4.14
	ppm	Gd	0.49	4.65
	ppm	Tb	0.20	3.63
	ppm	Dy	0.40	1.49
	ppm	Ho	0.20	5.14
	ppm	Er	0.30	-1.71
	ppm	Tm	0.13	-0.61
	ppm	Yb	0.29	-1.34
	ppm	Lu	0.12	0.41
	ppm	Hf	0.42	5.23
	ppm	Ta	0.38	8.72
	ppm	W*	5.89	-3.84
	ppm	Tl*	0.18	12.48
	ppm	Pb	5.77	0.50
	ppm	Th	0.38	5.63
	ppm	U	0.21	3.96
* = semi quant data only	Unit	Element	*Limits of Quantification*	% Accuracy offset from Standards

Major and Minor Elements from seven wells

	Gross Eagle Ford n=293			Upper Eagle Ford n=51			Middle Eagle Ford n=119			Lower Eagle Ford n=124			PAS Taylor & McLennan 1985
Element	Min	Max	Mean	Min	Max	Mean	Min	Max	Mean	Min	Max	Mean	
Al2O3 (%)	0.87	22.46	8.98	0.87	10.59	6.57	1.76	20.51	10.77	2.46	22.46	8.11	15.40
SiO2 (%)	4.44	62.11	27.68	4.44	38.71	25.07	8.47	62.11	32.21	7.29	41.22	24.33	66.62
TiO2 (%)	0.03	0.83	0.38	0.03	0.48	0.29	0.07	0.83	0.46	0.09	0.72	0.33	0.64
Fe2O3 (%)	0.47	14.03	2.84	0.47	3.96	2.18	0.58	14.03	3.20	0.64	6.04	2.73	5.04(FeO_T)
MnO (%)	0.01	0.09	0.02	0.02	0.05	0.03	0.01	0.04	0.02	0.01	0.09	0.02	0.10
MgO (%)	0.43	3.56	0.88	0.45	1.17	0.85	0.55	3.56	1.06	0.43	1.31	0.70	2.48
CaO (%)	1.24	54.06	26.60	19.61	54.06	30.68	1.24	43.13	22.72	10.25	49.71	28.83	3.59
Na2O (%)	0.07	2.56	0.43	0.14	0.93	0.61	0.21	2.56	0.52	0.07	0.55	0.29	3.27
K2O (%)	0.15	3.10	1.33	0.15	1.79	1.14	0.29	3.10	1.65	0.30	1.93	1.08	2.80
P2O5 (%)	0.03	2.35	0.26	0.05	0.39	0.16	0.03	2.35	0.24	0.05	0.79	0.32	0.15

Trace and Rare Earth Elements

(PAAS from Taylor and McLennan, 1985)

	Gross Eagle Ford n=293			Upper Eagle Ford n=51			Middle Eagle Ford n=119			Lower Eagle Ford n=124			PAAS (ppm) n=23
Element (ppm)	Min	Max	Mean	Min	Max	Mean	Min	Max	Mean	Min	Max	Mean	
Ba	94.70	9577.09	2864.78	1532.96	7379.62	3603.05	130.37	9577.09	2545.26	94.70	6986.37	2875.99	
Be	0.35	3.18	1.41	0.35	1.66	1.02	0.45	3.18	1.69	0.53	2.14	1.29	
Cr	11.55	299.67	94.25	11.55	97.70	64.54	17.55	206.79	102.04	14.92	299.67	98.02	
Sc	0.77	15.87	7.34	0.77	9.09	5.58	1.45	15.87	8.84	1.91	11.28	6.47	
Sr	212.83	1043.01	689.68	340.82	1019.93	777.39	212.83	883.32	687.36	373.45	1043.01	656.58	
Zn	15.78	1344.77	103.31	21.30	270.35	78.75	34.24	1344.77	105.98	15.78	322.01	110.23	
Zr	10.65	222.42	80.50	10.65	114.95	63.62	21.08	222.42	93.29	20.76	144.08	74.43	
V	28.12	1017.77	249.63	40.44	476.58	216.13	48.68	553.46	277.27	28.12	1017.77	237.37	
Co	1.60	13.88	7.50	1.60	10.18	6.00	2.52	13.11	8.39	2.49	13.88	7.18	
Ni	7.60	113.08	48.96	8.15	54.60	35.72	8.51	103.63	52.37	7.60	113.08	51.03	
Cu	5.33	232.36	27.53	8.85	32.49	20.49	5.33	232.36	31.42	8.17	73.15	26.51	

	Gross Eagle Ford n=293			Upper Eagle Ford n=51			Middle Eagle Ford n=119			Lower Eagle Ford n=124			PAAS (ppm) n=23
Element (ppm)	Min	Max	Mean	Min	Max	Mean	Min	Max	Mean	Min	Max	Mean	
Ga	0.92	23.74	10.22	0.92	12.46	7.30	1.99	23.74	12.51	2.60	16.81	9.04	
Rb	5.58	150.50	60.86	5.58	76.57	44.75	11.21	150.50	76.34	16.05	96.12	51.45	
Y	3.08	36.24	15.41	3.08	17.38	11.88	5.14	35.91	16.01	6.24	36.24	16.12	
Nb	0.93	29.03	11.98	0.93	17.00	8.42	1.81	29.03	15.42	2.59	16.96	9.84	
Mo	0.43	85.99	18.37	0.82	29.10	8.87	3.51	85.99	20.98	0.43	58.69	19.84	
Sn	0.00	2.64	0.94	0.00	1.09	0.65	0.04	2.64	1.16	0.05	2.64	0.81	
Cs	0.56	11.34	4.66	0.56	5.82	3.17	0.94	11.34	5.57	1.09	8.39	4.31	
La	3.34	43.54	22.69	3.34	26.77	15.90	5.75	43.54	26.39	7.51	38.51	21.56	38
Pr	0.60	10.87	4.85	0.60	5.71	3.44	1.22	9.82	5.45	1.79	10.87	4.78	8.9
Nd	2.28	43.99	18.05	2.28	21.35	12.83	4.87	36.64	20.02	6.79	43.99	18.05	32
Sm	0.46	9.33	3.42	0.46	4.12	2.48	1.06	6.98	3.71	1.44	9.33	3.48	5.6
Eu	0.27	1.87	0.83	0.27	1.00	0.68	0.47	1.53	0.86	0.37	1.87	0.85	1.1
Gd	0.54	8.13	3.04	0.54	3.41	2.28	0.95	6.24	3.20	1.21	8.13	3.16	4.7
Tb	0.07	1.21	0.45	0.07	0.53	0.34	0.14	0.94	0.48	0.20	1.21	0.47	0.77

	Gross Eagle Ford n=293			Upper Eagle Ford n=51			Middle Eagle Ford n=119			Lower Eagle Ford n=124			PAAS (ppm) n=23
Element (ppm)	Min	Max	Mean	Min	Max	Mean	Min	Max	Mean	Min	Max	Mean	
Dy	0.40	6.50	2.55	0.40	2.97	1.90	0.76	5.38	2.71	1.02	6.50	2.63	4.4
Ho	0.10	1.30	0.53	0.10	0.61	0.40	0.16	1.15	0.56	0.20	1.30	0.55	1.0
Er	0.26	3.26	1.44	0.26	1.61	1.08	0.44	3.19	1.53	0.56	3.26	1.49	2.9
Tm	0.07	0.46	0.22	0.07	0.35	0.18	0.09	0.46	0.23	0.08	0.44	0.23	0.40
Yb	0.24	3.04	1.42	0.24	1.61	1.06	0.43	3.04	1.52	0.47	2.83	1.45	2.8
Lu	0.04	0.48	0.22	0.04	0.25	0.16	0.07	0.48	0.23	0.07	0.43	0.22	0.43
Hf	0.26	6.50	2.34	0.26	3.03	2.00	1.06	6.50	2.56	0.58	4.37	2.24	-
Ta	0.06	1.53	0.69	0.06	0.87	0.50	0.12	1.53	0.84	0.16	1.38	0.60	
Pb	0.49	73.44	4.39	1.73	9.41	3.55	0.85	73.44	5.62	0.49	10.49	3.38	
Th	0.54	25.22	6.40	0.54	7.64	4.45	1.24	19.73	7.44	1.91	25.22	6.10	
U	0.83	15.33	4.73	0.94	5.35	3.15	2.32	10.32	4.64	0.83	15.33	5.48	

Correlation between *Chemostrat, Inc*. and Hand Held ED-XRF cuttings

7 wells; 210 samples matched exact depths

Gross Eagle Ford Formation

	Al2O3 (%)	SiO2 (%)	TiO2 (%)	Fe2O3 (%)	MnO (%)	MgO (%)	CaO (%)	Na2O (%)	K2O (%)	P2O5 (%)	Cr (ppm)	Sr (ppm)	Zn (ppm)	Zr (ppm)	Co (ppm)	Ni (ppm)	Cu (ppm)	Rb (ppm)	Y (ppm)	Nb (ppm)	Mo (ppm)	Sn (ppm)	Pb (ppm)	Th (ppm)	U (ppm)
%SiO2		0.85																							
%Al2O3	0.88																								
%CaO							0.87																		
%MgO						-0.19																			
%Na2O								0.01																	
%K2O																									
%Fe2O3																									
%MnO					0.22																				
%TiO2			0.83																						
%P2O5										0.54															
Cr																									
Cu																	0.35								
Ni																0.28									
Sr												0.72													
Zn													0.28												
Zr														0.83											
Mo																					0.57				
Nb																				0.66					
Th																								0.62	
U																									0.09
Y																			0.10						
Rb																		0.77							
Co															-0.09										
Pb																							-0.07		
Sn																						-0.16			
	Legend:	Poor																							
		Good																							

Appendix C

Hand-held ED-XRF Lower Eagle Ford Data

Mean concentration by well

*ppm concentration

Well	n	%SiO2	%Al2O3	%CaO	%MgO	%Na2O	%K2O	%Fe2O3	%MnO	%TiO2	%P2O5	%SO2	Cr*	Cu*	Ni*	Zn*	Mo*
1																	
2	5	34.52	9.70	41.83	1.41	1.28	1.21	3.51	0.05	0.39	0.46	5.64	20.20	43.80	51.20	60.40	27.00
3	24	33.03	8.79	44.57	1.29	1.24	0.98	3.28	0.05	0.39	0.61	5.77	4.00	43.00	57.83	76.25	26.92
4	32	34.94	10.87	39.76	1.12	1.38	1.24	3.57	0.04	0.38	0.36	6.35	11.69	44.94	59.53	76.22	26.41
5	22	33.91	9.00	43.77	1.29	1.26	1.03	3.22	0.07	0.37	0.33	5.74	0.00	46.95	50.41	71.23	17.95
6	30	33.70	8.74	44.56	1.29	0.95	1.33	3.46	0.04	0.43	0.67	4.84	53.03	42.00	61.13	75.50	26.77
7	29	35.33	10.63	39.32	1.13	1.63	1.22	4.39	0.05	0.39	0.39	5.52	25.41	47.45	60.10	89.62	24.97
8	28	38.15	9.07	36.75	1.06	1.55	1.04	3.79	0.09	0.27	0.37	7.83	4.36	55.29	52.18	101.86	19.11
9	5	33.49	11.39	41.58	1.17	1.24	1.47	3.70	0.04	0.42	0.51	4.98	51.80	43.80	60.40	86.80	22.00
10	26	34.59	10.17	39.41	1.12	1.91	1.05	4.05	0.09	0.28	0.33	7.00	6.54	48.00	57.23	100.19	29.35
11	6	34.54	11.68	40.56	1.14	1.31	1.49	3.86	0.04	0.42	0.39	4.56	70.67	41.83	64.67	84.17	22.50
12	16	32.41	9.86	43.68	1.24	1.33	1.18	3.73	0.05	0.39	0.44	5.69	21.00	46.00	58.69	85.00	19.94
13	28	33.47	11.04	41.87	1.30	1.24	1.46	3.69	0.04	0.42	0.41	5.05	41.11	35.18	60.57	79.14	23.46
14	4	32.83	10.67	41.65	1.25	1.66	1.38	3.84	0.05	0.36	0.44	5.88	26.75	55.50	67.50	91.25	34.25
15	3	32.57	9.11	46.72	1.47	1.34	0.97	3.85	0.04	0.31	0.26	3.36	62.67	33.00	55.67	61.33	23.00
16	26	32.98	10.18	43.69	1.41	1.28	1.31	3.60	0.05	0.41	0.35	4.74	20.96	41.81	58.35	83.04	23.19
17	26	32.85	11.51	42.36	1.26	1.28	1.58	3.77	0.04	0.44	0.39	4.52	61.08	40.85	58.77	86.08	18.77
18	23	40.53	12.65	30.05	1.06	1.47	1.55	3.57	0.07	0.34	0.43	8.28	0.00	54.39	58.00	94.96	9.87
19																	
20	13	39.25	13.09	30.62	1.08	1.22	1.62	4.79	0.04	0.57	0.57	7.14	44.62	56.62	63.46	120.00	9.15
21	13	33.85	10.51	41.92	1.50	1.42	1.28	3.76	0.05	0.43	0.40	4.88	5.38	45.85	20.62	102.77	7.54
22	13	35.87	14.82	34.74	1.19	1.28	1.96	4.39	0.04	0.58	0.40	4.71	72.27	50.35	67.23	112.20	9.07
23	13	39.62	16.49	29.30	1.13	1.24	2.03	4.45	0.04	0.62	0.57	4.52	60.92	42.23	63.23	115.23	5.62
24	2	42.30	16.35	26.67	1.27	1.22	2.37	5.32	0.04	0.70	0.36	3.44	49.50	38.50	46.50	57.00	0.00

Appendix D

Chemostrat, Inc. Raw Data

292 Total samples

Major Elements

Wt. % not normalized

Well	Depth	Formation Top	Al2O3 (%)	SiO2 (%)	TiO2 (%)	Fe2O3 (%)	MnO (%)	MgO (%)	CaO (%)	Na2O (%)	K2O (%)	P2O5 (%)
Well 3	12660	Upper Eagle Ford	3.14	15.97	0.12	1.5	0.05	0.45	38.96	0.5	0.47	0.16
Well 3	12665	Upper Eagle Ford	3.6	15.18	0.14	2.04	0.04	0.53	38.16	0.56	0.55	0.15
Well 3	12670	Upper Eagle Ford	3.36	15.28	0.15	1.63	0.03	0.57	38.02	0.65	0.51	0.19
Well 3	12675	Upper Eagle Ford	4.22	15.04	0.12	1.08	0.03	0.82	38.11	0.53	0.59	0.15
Well 3	12685	Upper Eagle Ford	4.32	18.97	0.18	1.26	0.02	0.59	35.12	0.59	0.73	0.15
Well 3	12690	Upper Eagle Ford	4	18.39	0.17	1.19	0.02	0.57	35.35	0.58	0.69	0.15
Well 3	12695	Upper Eagle Ford	3.87	16.27	0.17	1.22	0.02	0.59	37.01	0.53	0.66	0.13
Well 3	12700	Upper Eagle Ford	4.52	18.52	0.2	1.39	0.02	0.61	35.4	0.54	0.81	0.12
Well 3	12705	Upper Eagle Ford	4.43	18	0.19	1.41	0.02	0.61	34.92	0.53	0.79	0.12
Well 3	12710	Upper Eagle Ford	5.1	19.24	0.21	1.55	0.02	0.74	33.95	0.58	0.86	0.15
Well 3	12715	Upper Eagle Ford	5.04	19.4	0.21	1.59	0.02	0.74	34.01	0.6	0.85	0.14
Well 3	12720	Middle Eagle Ford	4.24	19.98	0.18	1.7	0.04	0.63	34.12	0.57	0.72	0.13
Well 3	12725	Middle Eagle Ford	3.94	18.02	0.17	1.25	0.02	0.62	35.45	0.37	0.71	0.13
Well 3	12730	Middle Eagle Ford	4.91	18.56	0.2	2.09	0.02	0.79	33.1	0.54	0.78	0.16

Well 3	12735	Middle Eagle Ford	1.76	8.47	0.07	0.58	0.02	0.55	43.13	0.22	0.29	0.09
Well 3	12745	Middle Eagle Ford	4.92	22.02	0.21	1.75	0.02	0.68	30.7	0.5	0.8	0.24
Well 3	12750	Middle Eagle Ford	3.99	18.1	0.17	1.43	0.02	0.67	34.74	0.45	0.66	0.14
Well 3	12755	Middle Eagle Ford	5.27	23.37	0.23	1.82	0.01	0.7	29.06	0.47	0.87	0.14
Well 3	12760	Middle Eagle Ford	3.14	14.11	0.14	1.23	0.01	0.63	37.19	0.31	0.52	0.21
Well 3	12765	Lower Eagle Ford	3.55	16.08	0.16	1.42	0.01	0.63	35.48	0.34	0.59	0.19
Well 3	12770	Lower Eagle Ford	4.24	17.79	0.17	1.64	0.01	0.68	34.16	0.37	0.65	0.23
Well 3	12775	Lower Eagle Ford	5.09	20.01	0.2	1.85	0.01	0.65	31.09	0.4	0.82	0.17
Well 3	12780	Lower Eagle Ford	4.62	19.33	0.19	1.65	0.02	0.76	32.66	0.41	0.65	0.59
Well 3	12785	Lower Eagle Ford	4.85	19.34	0.19	1.65	0.01	0.79	31.88	0.42	0.66	0.7
Well 3	12790	Lower Eagle Ford	4.98	19.64	0.23	1.78	0.02	0.76	32.41	0.38	0.65	0.33
Well 3	12800	Lower Eagle Ford	4.25	17.2	0.16	1.31	0.02	0.67	34.71	0.37	0.5	0.65
Well 3	12805	Lower Eagle Ford	4.86	19.46	0.19	1.62	0.02	0.68	32.76	0.41	0.6	0.7
Well 3	12810	Lower Eagle Ford	5.49	21.74	0.21	1.71	0.01	0.8	30.59	0.44	0.69	0.39
Well 3	12815	Lower Eagle Ford	5.19	20.94	0.2	1.6	0.02	0.81	31.48	0.43	0.66	0.41
Well 3	12820	Lower Eagle Ford	5.47	24.45	0.23	1.84	0.01	0.57	28.67	0.28	0.78	0.2
Well 3	12825	Lower Eagle Ford	5.44	23.88	0.22	1.78	0.01	0.6	29.01	0.28	0.77	0.19
Well 3	12830	Lower Eagle Ford	6.46	21.93	0.25	1.95	0.02	0.63	29.53	0.3	0.74	0.3

Well 3	12835	Lower Eagle Ford	7.27	24.61	0.22	1.99	0.01	0.57	28.18	0.25	0.76	0.2
Well 3	12840	Lower Eagle Ford	7.14	24.69	0.22	1.84	0.01	0.57	28.42	0.25	0.78	0.21
Well 3	12845	Lower Eagle Ford	6.09	25.1	0.24	1.91	0.01	0.49	27.87	0.21	0.8	0.19
Well 3	12850	Lower Eagle Ford	6.33	25.01	0.24	1.86	0.01	0.53	28.06	0.22	0.8	0.22
Well 3	12855	Lower Eagle Ford	4.59	21.62	0.19	1.56	0.01	0.48	30.81	0.16	0.65	0.16
Well 3	12860	Lower Eagle Ford	5.74	24.25	0.23	1.96	0.02	0.48	28.1	0.17	0.75	0.22
Well 3	12865	Lower Eagle Ford	5.67	24.4	0.23	1.84	0.01	0.48	28.42	0.18	0.74	0.23
Well 3	12870	Lower Eagle Ford	5.97	22.67	0.24	2	0.02	0.46	28.54	0.17	0.78	0.24
Well 3	12875	Lower Eagle Ford	7.29	24.74	0.28	2.29	0.02	0.51	26.57	0.19	0.92	0.29
Well 3	12880	Lower Eagle Ford	10.23	25.39	0.33	2.79	0.02	0.53	24.42	0.18	0.89	0.79
Well 3	12885	Lower Eagle Ford	8.99	23.76	0.32	2.87	0.02	0.54	25.89	0.17	0.89	0.62
Well 12	13440	Upper Eagle Ford	0.873	5.124	0.031	0.497	0.046	0.497	53.740	0.141	0.146	0.060
Well 12	13450	Upper Eagle Ford	1.216	4.440	0.042	0.472	0.045	0.467	54.057	0.136	0.213	0.047
Well 12	13460	Upper Eagle Ford	5.446	22.330	0.238	1.742	0.023	0.657	35.308	0.537	0.956	0.143
Well 12	13470	Upper Eagle Ford	5.824	23.455	0.251	1.674	0.022	0.668	34.291	0.568	1.029	0.146
Well 12	13480	Upper Eagle Ford	6.042	22.289	0.251	1.757	0.022	0.750	33.847	0.649	0.993	0.167
Well 12	13490	Upper Eagle Ford	6.813	26.605	0.297	1.859	0.022	0.750	31.835	0.650	1.173	0.161
Well 12	13500	Upper Eagle Ford	8.605	29.173	0.338	2.198	0.020	0.961	25.885	0.461	1.587	0.142

Well 12	13510	Upper Eagle Ford	8.187	28.385	0.343	2.446	0.020	0.954	27.219	0.487	1.480	0.173
Well 12	13516	Upper Eagle Ford	8.004	28.406	0.335	2.325	0.021	0.945	29.315	0.541	1.422	0.164
Well 12	13525	Upper Eagle Ford	10.018	34.594	0.414	2.523	0.017	0.988	22.815	0.462	1.778	0.123
Well 12	13535	Middle Eagle Ford	10.485	33.653	0.431	2.558	0.017	1.085	21.809	0.481	1.744	0.140
Well 12	13545	Middle Eagle Ford	9.429	31.239	0.416	2.772	0.015	0.870	24.234	0.458	1.589	0.180
Well 12	13555	Middle Eagle Ford	7.088	25.521	0.302	2.070	0.014	0.701	30.258	0.427	1.129	0.215
Well 12	13565	Middle Eagle Ford	6.952	25.818	0.305	2.277	0.014	0.728	29.728	0.489	1.086	0.195
Well 12	13575	Middle Eagle Ford	6.019	20.939	0.251	1.871	0.016	0.702	33.402	0.455	0.901	0.167
Well 12	13585	Middle Eagle Ford	3.682	14.290	0.151	1.263	0.017	0.587	38.145	0.333	0.541	0.176
Well 12	13595	Middle Eagle Ford	6.189	22.483	0.273	2.258	0.011	0.643	29.390	0.437	0.938	0.213
Well 12	13606	Lower Eagle Ford	5.977	21.593	0.257	2.013	0.014	0.703	31.814	0.413	0.951	0.159
Well 12	13620	Lower Eagle Ford	5.842	23.496	0.246	1.923	0.013	0.599	30.014	0.398	0.952	0.295
Well 12	13630	Lower Eagle Ford	5.940	23.547	0.250	1.920	0.014	0.600	29.072	0.397	0.966	0.291
Well 12	13640	Lower Eagle Ford	6.635	27.587	0.286	2.231	0.015	0.638	27.251	0.500	1.028	0.332
Well 12	13650	Lower Eagle Ford	6.521	27.741	0.280	2.205	0.015	0.621	27.283	0.507	1.016	0.343
Well 12	13660	Lower Eagle Ford	6.659	23.445	0.295	2.282	0.017	0.645	30.533	0.249	1.044	0.279
Well 12	13670	Lower Eagle Ford	6.736	23.659	0.289	2.430	0.018	0.755	29.326	0.307	1.024	0.290
Well 12	13680	Lower Eagle Ford	8.058	26.800	0.320	2.513	0.019	0.735	26.955	0.329	1.197	0.266

Well 12	13690	Lower Eagle Ford	6.923	23.803	0.296	2.411	0.017	0.667	29.771	0.284	1.059	0.329
Well 12	13699	Lower Eagle Ford	7.388	24.969	0.306	2.468	0.017	0.677	28.161	0.298	1.122	0.287
Well 12	13710	Lower Eagle Ford	9.328	27.904	0.359	2.948	0.020	0.881	24.657	0.232	1.283	0.332
Well 12	13720	Lower Eagle Ford	8.823	22.729	0.330	2.888	0.019	0.584	29.347	0.168	1.032	0.696
Well 12	13730	Lower Eagle Ford	12.461	31.239	0.397	3.333	0.016	0.550	20.751	0.200	1.273	0.693
Well 12	13740	Lower Eagle Ford	2.462	7.285	0.093	0.661	0.048	0.446	49.706	0.065	0.323	0.050
Well 12	13750	Lower Eagle Ford	4.251	12.224	0.167	0.968	0.060	0.433	44.031	0.092	0.435	0.088
Well 16	13370	Upper Eagle Ford	4.48	21.48	0.18	1.46	0.04	0.89	35.14	0.51	0.81	0.12
Well 16	13375	Upper Eagle Ford	5.39	20.46	0.27	1.76	0.03	0.75	34.20	0.60	0.98	0.15
Well 16	13380	Upper Eagle Ford	5.26	21.07	0.25	1.68	0.03	0.73	33.50	0.61	0.96	0.14
Well 16	13385	Upper Eagle Ford	5.67	20.28	0.29	2.14	0.03	1.08	32.64	0.63	1.03	0.20
Well 16	13390	Upper Eagle Ford	5.46	19.65	0.25	1.97	0.02	0.82	33.51	0.51	1.04	0.15
Well 16	13395	Upper Eagle Ford	8.07	28.82	0.35	2.34	0.02	1.04	25.68	0.50	1.52	0.15
Well 16	13400	Upper Eagle Ford	7.69	27.84	0.33	2.28	0.02	1.05	27.14	0.49	1.46	0.14
Well 16	13405	Upper Eagle Ford	7.35	27.10	0.34	2.52	0.02	0.96	26.77	0.47	1.41	0.13
Well 16	13410	Upper Eagle Ford	8.70	29.09	0.38	2.75	0.02	1.00	24.23	0.45	1.70	0.15
Well 16	13415	Upper Eagle Ford	8.90	30.60	0.38	2.66	0.02	1.05	23.18	0.48	1.74	0.14
Well 16	13420	Upper Eagle Ford	9.07	31.27	0.41	2.83	0.02	1.17	22.54	0.50	1.67	0.13

Well 16	13425	Upper Eagle Ford	7.47	25.79	0.33	2.39	0.02	1.08	28.17	0.49	1.30	0.13
Well 16	13430	Upper Eagle Ford	5.96	22.09	0.27	2.02	0.02	0.93	32.21	0.48	0.99	0.13
Well 16	13435	Middle Eagle Ford	6.72	25.58	0.31	2.21	0.02	0.92	28.76	0.50	1.13	0.15
Well 16	13440	Middle Eagle Ford	7.69	26.26	0.35	2.44	0.02	0.79	26.78	0.47	1.26	0.15
Well 16	13445	Middle Eagle Ford	7.78	26.51	0.34	2.27	0.02	0.86	26.84	0.48	1.28	0.14
Well 16	13450	Middle Eagle Ford	7.44	26.81	0.33	2.38	0.02	0.88	26.66	0.49	1.39	0.15
Well 16	13455	Middle Eagle Ford	6.34	23.55	0.28	2.16	0.02	0.80	28.98	0.45	1.14	0.17
Well 16	13460	Middle Eagle Ford	6.23	22.44	0.28	2.20	0.01	0.75	28.80	0.54	1.05	0.20
Well 16	13465	Middle Eagle Ford	5.43	19.91	0.25	1.99	0.01	0.71	31.06	0.45	0.90	0.18
Well 16	13470	Middle Eagle Ford	5.50	19.36	0.24	1.97	0.02	0.74	32.57	0.44	0.87	0.20
Well 16	13475	Middle Eagle Ford	4.88	16.73	0.21	1.62	0.02	0.75	35.84	0.41	0.76	0.20
Well 16	13480	Middle Eagle Ford	5.44	20.06	0.24	1.88	0.01	0.63	32.58	0.47	0.90	0.16
Well 16	13485	Middle Eagle Ford	5.94	20.90	0.26	2.14	0.01	0.67	31.31	0.42	1.01	0.16
Well 16	13490	Middle Eagle Ford	5.71	20.86	0.27	2.37	0.01	0.62	30.60	0.42	0.97	0.14
Well 16	13495	Middle Eagle Ford	6.48	22.88	0.29	2.25	0.01	0.71	29.44	0.54	1.06	0.15
Well 16	13500	Lower Eagle Ford	6.14	22.63	0.28	2.28	0.01	0.66	30.22	0.52	1.09	0.14
Well 16	13505	Lower Eagle Ford	7.29	25.86	0.35	2.52	0.02	0.80	26.60	0.51	1.26	0.18
Well 16	13510	Lower Eagle Ford	7.94	24.11	0.32	2.36	0.01	0.79	27.71	0.55	1.36	0.20

Well 16	13515	Lower Eagle Ford	5.80	20.91	0.25	2.03	0.02	0.64	31.93	0.37	1.05	0.23
Well 16	13520	Lower Eagle Ford	5.73	20.27	0.25	2.05	0.02	0.70	33.06	0.41	1.00	0.34
Well 16	13525	Lower Eagle Ford	7.15	24.27	0.30	2.33	0.02	0.76	28.15	0.53	1.19	0.37
Well 16	13530	Lower Eagle Ford	5.90	20.53	0.26	1.96	0.02	0.71	32.12	0.34	1.00	0.29
Well 16	13535	Lower Eagle Ford	6.76	22.95	0.29	2.21	0.02	0.75	29.02	0.33	1.11	0.31
Well 16	13540	Lower Eagle Ford	5.91	20.55	0.25	1.85	0.02	0.69	32.91	0.31	0.94	0.38
Well 16	13545	Lower Eagle Ford	6.92	24.23	0.30	2.28	0.02	0.74	28.39	0.34	1.09	0.32
Well 16	13550	Lower Eagle Ford	7.62	26.78	0.35	2.47	0.02	0.70	25.99	0.36	1.21	0.25
Well 16	13555	Lower Eagle Ford	8.70	25.70	0.37	2.95	0.02	0.76	25.63	0.28	1.27	0.50
Well 16	13560	Lower Eagle Ford	9.23	24.45	0.37	3.21	0.02	0.74	25.95	0.27	1.23	0.67
Well 16	13565	Lower Eagle Ford	8.67	24.66	0.36	2.81	0.02	0.88	26.51	0.27	1.21	0.59
Well 16	13570	Lower Eagle Ford	7.32	23.77	0.30	2.46	0.02	0.74	28.48	0.32	1.11	0.39
Well 16	13575	Lower Eagle Ford	10.37	30.14	0.38	2.75	0.02	0.66	22.09	0.29	1.36	0.26
Well 16	13580	Lower Eagle Ford	9.57	25.83	0.34	2.49	0.02	0.58	25.27	0.22	1.18	0.24
Well 16	13585	Lower Eagle Ford	10.11	26.44	0.35	2.78	0.02	0.60	24.77	0.22	1.18	0.23
Well 16	13590	Lower Eagle Ford	11.29	32.45	0.41	3.03	0.02	0.65	19.97	0.27	1.41	0.18
Well 16	13595	Lower Eagle Ford	10.82	31.49	0.41	2.85	0.02	0.68	20.96	0.31	1.38	0.26
Well 16	13600	Lower Eagle Ford	2.46	7.69	0.10	0.64	0.06	0.46	46.75	0.09	0.30	0.06

Well 16	13605	Lower Eagle Ford	3.24	9.92	0.14	1.04	0.07	0.51	45.11	0.10	0.35	0.06
Well 16	13610	Lower Eagle Ford	3.80	11.26	0.15	1.21	0.06	0.49	42.99	0.11	0.44	0.07
Well 16	13615	Lower Eagle Ford	4.72	13.16	0.18	1.35	0.07	0.50	41.68	0.12	0.50	0.09
Well 16	13620	Lower Eagle Ford	3.85	11.42	0.17	1.22	0.07	0.50	43.47	0.11	0.41	0.07
Well 16	13625	Lower Eagle Ford	4.55	12.87	0.19	1.30	0.07	0.51	42.00	0.12	0.47	0.08
Well 17	13650	Middle Eagle Ford	8.879	30.694	0.375	2.688	0.022	1.091	25.083	0.551	1.582	0.153
Well 17	13660	Middle Eagle Ford	8.410	28.537	0.321	2.335	0.027	1.050	27.509	0.541	1.431	0.127
Well 17	13670	Middle Eagle Ford	8.469	29.030	0.362	2.833	0.022	1.033	26.639	0.538	1.465	0.144
Well 17	13680	Middle Eagle Ford	9.175	30.645	0.404	2.700	0.019	0.983	25.189	0.536	1.587	0.157
Well 17	13690	Middle Eagle Ford	7.616	23.507	0.335	2.538	0.023	0.838	30.264	0.383	1.246	0.462
Well 17	13700	Middle Eagle Ford	7.682	24.194	0.342	2.630	0.018	0.784	29.481	0.434	1.232	0.187
Well 17	13710	Middle Eagle Ford	8.200	24.948	0.350	2.618	0.018	0.784	29.056	0.457	1.303	0.244
Well 17	13720	Lower Eagle Ford	6.387	19.531	0.278	2.088	0.017	0.736	33.415	0.446	0.984	0.276
Well 17	13730	Lower Eagle Ford	5.980	20.924	0.264	1.973	0.016	0.671	33.077	0.436	0.942	0.232
Well 17	13740	Lower Eagle Ford	5.386	18.226	0.232	1.795	0.015	0.642	34.421	0.447	0.770	0.205
Well 17	13750	Lower Eagle Ford	6.049	20.895	0.266	2.056	0.016	0.702	32.835	0.418	0.972	0.182
Well 17	13760	Lower Eagle Ford	6.593	23.275	0.304	2.418	0.013	0.667	30.167	0.381	1.101	0.160
Well 17	13770	Lower Eagle Ford	6.801	22.617	0.297	2.342	0.017	0.773	31.414	0.398	1.122	0.218

Well 17	13780	Lower Eagle Ford	7.489	23.778	0.324	2.711	0.016	0.698	29.133	0.369	1.231	0.232
Well 17	13790	Lower Eagle Ford	7.384	23.671	0.310	2.514	0.016	0.745	30.312	0.358	1.192	0.290
Well 17	13800	Lower Eagle Ford	9.197	26.718	0.357	3.072	0.019	0.994	25.817	0.345	1.360	0.337
Well 17	13810	Lower Eagle Ford	8.762	25.674	0.366	3.066	0.017	0.812	26.832	0.318	1.311	0.356
Well 17	13820	Lower Eagle Ford	9.025	25.403	0.365	3.160	0.019	0.916	26.900	0.263	1.267	0.425
Well 17	13830	Lower Eagle Ford	6.811	18.999	0.289	2.755	0.022	0.820	32.004	0.230	0.919	0.356
Well 17	13840	Lower Eagle Ford	10.689	30.675	0.409	3.098	0.019	0.677	22.956	0.274	1.414	0.286
Well 19	13690	Upper Eagle Ford	4.18	17.98	0.17	2.25	0.03	0.64	38.16	0.55	0.71	0.16
Well 19	13695	Upper Eagle Ford	5.35	20.94	0.22	2.04	0.03	0.74	35.67	0.66	0.93	0.20
Well 19	13700	Upper Eagle Ford	9.48	35.78	0.46	3.96	0.03	1.14	21.74	0.88	1.65	0.17
Well 19	13705	Upper Eagle Ford	8.31	32.85	0.35	2.36	0.02	0.95	25.29	0.93	1.37	0.12
Well 19	13710	Upper Eagle Ford	10.56	38.02	0.47	3.06	0.02	1.10	20.13	0.87	1.79	0.16
Well 19	13715	Upper Eagle Ford	10.37	37.24	0.46	3.30	0.02	1.08	20.29	0.85	1.76	0.15
Well 19	13720	Upper Eagle Ford	10.59	38.71	0.48	3.35	0.02	1.10	19.61	0.89	1.79	0.15
Well 19	13725	Middle Eagle Ford	10.28	34.12	0.44	3.07	0.02	1.20	22.19	0.75	1.74	0.18
Well 19	13730	Middle Eagle Ford	10.26	34.08	0.45	4.11	0.02	1.20	21.78	0.76	1.73	0.19
Well 19	13735	Middle Eagle Ford	10.29	33.69	0.45	3.06	0.02	1.14	22.91	0.76	1.73	0.17
Well 19	13740	Middle Eagle Ford	10.94	35.34	0.47	2.77	0.02	1.17	20.93	0.70	1.85	0.18

Well 19	13745	Middle Eagle Ford	10.83	35.33	0.47	3.14	0.02	1.14	21.21	0.74	1.82	0.20
Well 19	13750	Middle Eagle Ford	10.93	33.43	0.46	3.39	0.03	1.98	21.23	0.55	1.75	0.17
Well 19	13755	Middle Eagle Ford	11.39	32.09	0.51	4.64	0.04	3.56	19.18	0.43	1.74	0.16
Well 19	13760	Middle Eagle Ford	11.05	35.10	0.45	3.35	0.03	1.57	21.10	0.64	1.83	0.15
Well 19	13765	Middle Eagle Ford	11.08	35.31	0.45	3.03	0.02	1.46	20.98	0.63	1.85	0.14
Well 19	13770	Middle Eagle Ford	11.60	36.23	0.48	3.14	0.02	1.36	20.13	0.65	1.92	0.15
Well 19	13775	Middle Eagle Ford	11.36	35.18	0.47	2.87	0.02	1.40	21.06	0.61	1.88	0.14
Well 19	13780	Middle Eagle Ford	11.88	35.93	0.51	2.95	0.02	1.26	20.09	0.62	1.96	0.15
Well 19	13785	Middle Eagle Ford	10.16	34.42	0.43	2.73	0.02	1.17	22.35	0.70	1.67	0.16
Well 19	13790	Middle Eagle Ford	12.06	36.66	0.53	2.91	0.02	1.22	18.99	0.67	1.93	0.15
Well 19	13795	Middle Eagle Ford	12.16	37.20	0.53	3.05	0.02	1.26	19.09	0.65	1.97	0.16
Well 19	13800	Middle Eagle Ford	11.89	35.63	0.50	2.95	0.02	1.17	20.01	0.64	1.92	0.16
Well 19	13805	Middle Eagle Ford	12.23	36.38	0.50	3.23	0.02	1.20	19.00	0.63	1.94	0.15
Well 19	13810	Middle Eagle Ford	11.17	33.61	0.47	3.57	0.03	1.51	21.12	0.53	1.79	0.17
Well 19	13815	Middle Eagle Ford	14.29	41.26	0.60	3.37	0.02	1.34	14.84	0.65	2.27	0.15
Well 19	13825	Middle Eagle Ford	14.38	40.38	0.55	3.05	0.02	1.25	15.71	0.70	2.16	0.16
Well 19	13830	Middle Eagle Ford	14.24	41.01	0.61	4.21	0.02	1.16	14.78	0.57	2.23	0.16
Well 19	13835	Middle Eagle Ford	14.36	40.74	0.58	3.35	0.02	1.13	16.06	0.57	2.22	0.20

Well 19	13840	Middle Eagle Ford	12.95	37.16	0.55	3.83	0.03	1.77	17.77	0.48	2.01	0.17
Well 19	13845	Middle Eagle Ford	13.96	39.03	0.59	3.76	0.02	1.23	16.29	0.48	2.11	0.18
Well 19	13850	Middle Eagle Ford	13.87	37.09	0.59	3.50	0.02	1.39	17.13	0.45	2.07	0.46
Well 19	13855	Middle Eagle Ford	14.34	38.46	0.61	3.55	0.02	1.23	16.30	0.47	2.14	0.46
Well 19	13860	Middle Eagle Ford	14.24	37.21	0.61	3.90	0.02	1.35	17.15	0.48	2.09	0.49
Well 19	13865	Middle Eagle Ford	14.69	37.63	0.64	3.84	0.01	1.03	15.78	0.44	2.13	0.50
Well 19	13870	Middle Eagle Ford	12.80	32.96	0.56	3.63	0.02	0.97	20.43	0.37	1.80	0.58
Well 19	13875	Middle Eagle Ford	11.57	29.52	0.51	3.34	0.02	0.82	23.04	0.32	1.57	0.72
Well 19	13880	Middle Eagle Ford	11.70	29.84	0.50	3.72	0.02	0.91	22.53	0.36	1.58	0.37
Well 19	13885	Middle Eagle Ford	11.14	28.35	0.48	3.42	0.02	0.82	24.11	0.32	1.52	0.46
Well 19	13890	Middle Eagle Ford	9.53	25.05	0.41	2.88	0.02	0.76	27.80	0.29	1.35	0.45
Well 19	13895	Middle Eagle Ford	9.13	25.23	0.40	2.94	0.02	0.76	28.33	0.29	1.35	0.37
Well 19	13900	Middle Eagle Ford	9.56	25.82	0.41	2.88	0.02	0.76	28.12	0.33	1.36	0.28
Well 19	13905	Middle Eagle Ford	8.64	26.25	0.39	3.14	0.02	0.77	27.20	0.30	1.24	0.45
Well 19	13910	Middle Eagle Ford	9.13	27.82	0.41	3.12	0.02	0.71	25.12	0.31	1.28	0.30
Well 19	13915	Lower Eagle Ford	9.11	26.73	0.40	2.73	0.02	0.67	26.40	0.31	1.28	0.28
Well 19	13920	Lower Eagle Ford	8.87	26.16	0.38	3.24	0.02	0.76	26.14	0.29	1.21	0.29
Well 19	13925	Lower Eagle Ford	9.57	27.01	0.40	3.03	0.02	0.82	25.78	0.30	1.28	0.26

Well 19	13930	Lower Eagle Ford	9.29	25.57	0.40	3.09	0.02	0.70	26.46	0.28	1.28	0.32
Well 19	13935	Lower Eagle Ford	10.67	28.36	0.46	3.56	0.02	0.74	24.35	0.28	1.49	0.39
Well 19	13940	Lower Eagle Ford	11.41	30.28	0.47	3.98	0.02	0.78	22.64	0.30	1.56	0.39
Well 19	13945	Lower Eagle Ford	10.97	29.59	0.46	3.85	0.02	0.87	23.86	0.30	1.50	0.53
Well 19	13950	Lower Eagle Ford	10.60	27.72	0.44	5.88	0.02	0.78	23.44	0.26	1.39	0.73
Well 19	13955	Lower Eagle Ford	9.79	26.33	0.42	3.62	0.02	0.72	27.37	0.25	1.31	0.66
Well 19	13960	Lower Eagle Ford	10.18	29.45	0.45	5.27	0.02	1.00	22.76	0.43	1.46	0.33
Well 19	13965	Lower Eagle Ford	10.09	28.39	0.43	3.04	0.02	0.83	24.90	0.37	1.45	0.30
Well 19	13970	Lower Eagle Ford	12.43	32.88	0.46	3.84	0.02	0.83	20.53	0.28	1.48	0.34
Well 19	13975	Lower Eagle Ford	11.71	31.20	0.47	3.57	0.02	0.81	22.63	0.29	1.48	0.37
Well 19	13980	Lower Eagle Ford	10.88	28.76	0.44	3.67	0.02	0.82	24.18	0.29	1.45	0.41
Well 19	13985	Lower Eagle Ford	10.80	29.11	0.45	3.62	0.02	0.80	24.45	0.30	1.42	0.42
Well 19	13990	Lower Eagle Ford	11.15	29.60	0.46	4.02	0.02	0.87	24.39	0.30	1.48	0.42
Well 19	13995	Lower Eagle Ford	10.77	28.01	0.44	3.44	0.02	0.82	25.30	0.29	1.42	0.38
Well 19	14000	Lower Eagle Ford	9.23	25.03	0.39	3.37	0.03	0.83	29.60	0.27	1.27	0.28
Well 20	13660	Upper Eagle Ford	8.823	34.795	0.434	3.238	0.030	1.045	23.507	0.813	1.485	0.150
Well 20	13665	Upper Eagle Ford	9.119	35.346	0.435	3.504	0.025	1.039	22.492	0.832	1.545	0.199
Well 20	13670	Upper Eagle Ford	8.580	33.337	0.380	2.684	0.023	1.007	24.183	0.837	1.423	0.165

Well 20	13675	Upper Eagle Ford	8.612	31.965	0.356	2.843	0.022	0.955	24.815	0.836	1.415	0.150
Well 20	13680	Middle Eagle Ford	8.717	33.221	0.379	2.414	0.021	0.954	23.783	0.911	1.419	0.130
Well 20	13685	Middle Eagle Ford	8.919	35.211	0.400	2.852	0.021	0.976	22.857	0.819	1.481	0.140
Well 20	13690	Middle Eagle Ford	9.924	36.216	0.477	3.710	0.022	1.055	21.148	0.784	1.663	0.269
Well 20	13695	Middle Eagle Ford	11.496	38.766	0.544	3.604	0.021	1.328	17.693	0.755	1.945	0.200
Well 20	13700	Middle Eagle Ford	10.513	34.245	0.473	3.808	0.023	1.279	21.343	0.652	1.790	0.187
Well 20	13705	Middle Eagle Ford	10.991	35.365	0.502	3.240	0.023	1.233	20.346	0.702	1.866	0.180
Well 20	13710	Middle Eagle Ford	10.766	34.168	0.478	3.489	0.025	1.360	21.290	0.589	1.844	0.174
Well 20	13715	Middle Eagle Ford	11.474	36.380	0.503	3.111	0.020	1.168	20.222	0.622	1.954	0.170
Well 20	13720	Middle Eagle Ford	11.947	36.679	0.533	3.041	0.020	1.177	19.616	0.641	2.037	0.154
Well 20	13725	Middle Eagle Ford	11.077	34.689	0.492	3.251	0.021	1.109	20.756	0.577	1.866	0.181
Well 20	13730	Middle Eagle Ford	11.378	35.336	0.486	3.047	0.018	1.128	19.919	0.502	1.929	0.161
Well 20	13740	Middle Eagle Ford	10.505	32.042	0.443	4.452	0.045	2.456	20.329	0.456	1.745	0.184
Well 20	13745	Middle Eagle Ford	12.344	36.109	0.532	3.169	0.021	1.338	18.806	0.483	2.089	0.139
Well 20	13750	Middle Eagle Ford	12.419	37.317	0.544	2.995	0.019	1.229	19.305	0.526	2.054	0.158
Well 20	13755	Middle Eagle Ford	12.032	36.737	0.517	3.414	0.020	1.274	19.136	0.503	1.951	0.154
Well 20	13760	Middle Eagle Ford	12.580	37.433	0.544	3.084	0.019	1.202	18.966	0.474	2.060	0.155
Well 20	13765	Middle Eagle Ford	11.807	36.206	0.519	3.298	0.021	1.242	20.044	0.503	1.953	0.161

Well 20	13770	Middle Eagle Ford	11.668	35.800	0.506	3.875	0.022	1.265	19.812	0.547	1.935	0.161
Well 20	13785	Middle Eagle Ford	12.215	37.530	0.526	3.165	0.022	1.346	19.590	0.614	2.019	0.152
Well 20	13788	Middle Eagle Ford	20.474	62.115	0.522	4.465	0.006	2.823	1.241	2.562	0.736	0.033
Well 20	13790	Middle Eagle Ford	12.312	30.889	0.481	11.833	0.014	0.810	16.317	0.475	1.837	0.328
Well 20	13793	Middle Eagle Ford	13.620	37.805	0.634	3.468	0.022	1.193	20.493	0.564	2.213	0.262
Well 20	13796	Middle Eagle Ford	15.465	42.644	0.685	2.803	0.017	1.154	16.684	0.568	2.573	0.178
Well 20	13799	Middle Eagle Ford	16.087	42.553	0.693	3.103	0.015	1.159	16.124	0.566	2.616	0.130
Well 20	13802	Middle Eagle Ford	16.098	47.271	0.687	3.081	0.017	1.184	13.481	0.573	2.608	0.130
Well 20	13805	Middle Eagle Ford	18.136	50.451	0.760	3.084	0.013	1.279	10.268	0.565	2.960	0.172
Well 20	13808	Middle Eagle Ford	16.055	43.657	0.714	4.123	0.016	1.127	14.031	0.483	2.556	0.230
Well 20	13811	Middle Eagle Ford	14.950	42.442	0.646	4.029	0.022	1.052	16.932	0.506	2.275	0.136
Well 20	13814	Middle Eagle Ford	20.506	52.567	0.831	3.304	0.011	1.429	6.724	0.609	3.101	0.216
Well 20	13816	Middle Eagle Ford	16.902	43.718	0.723	3.506	0.019	1.205	14.334	0.491	2.521	0.111
Well 20	13819	Middle Eagle Ford	11.486	34.383	0.488	3.198	0.021	0.969	23.550	0.439	1.788	0.205
Well 20	13822	Middle Eagle Ford	17.825	44.781	0.771	3.889	0.018	1.231	13.343	0.523	2.575	0.368
Well 20	13825	Middle Eagle Ford	17.042	43.910	0.743	3.192	0.014	1.060	14.215	0.459	2.543	0.078
Well 20	13828	Middle Eagle Ford	15.487	40.194	0.672	3.155	0.018	0.930	18.033	0.401	2.131	0.094
Well 20	13831	Middle Eagle Ford	15.894	40.903	0.666	3.622	0.017	0.905	16.776	0.409	2.168	0.172

Well 20	13834	Middle Eagle Ford	14.564	38.868	0.759	3.193	0.017	0.838	19.438	0.362	1.953	0.262
Well 20	13837	Middle Eagle Ford	14.039	35.405	0.613	3.433	0.020	0.830	20.971	0.354	1.860	0.188
Well 20	13840	Middle Eagle Ford	11.465	26.627	0.503	14.032	0.018	0.656	15.316	0.279	1.353	0.204
Well 20	13842	Middle Eagle Ford	12.419	30.727	0.562	5.256	0.014	0.724	22.577	0.271	1.522	2.345
Well 20	13844	Middle Eagle Ford	10.537	23.822	0.431	2.258	0.019	0.609	28.855	0.214	1.181	0.270
Well 20	13846.4	Middle Eagle Ford	19.670	50.613	0.792	3.589	0.011	1.302	6.186	0.584	3.022	0.127
Well 20	13850	Middle Eagle Ford	10.745	28.970	0.478	4.177	0.021	0.776	23.569	0.244	1.397	0.388
Well 20	13851	Middle Eagle Ford	13.953	36.073	0.609	4.405	0.025	0.997	19.199	0.394	1.925	0.325
Well 20	13854	Middle Eagle Ford	10.216	24.865	0.465	4.448	0.020	0.692	27.634	0.227	1.232	0.731
Well 20	13855	Middle Eagle Ford	11.882	31.289	0.518	3.965	0.019	0.838	21.210	0.273	1.568	0.433
Well 20	13857	Middle Eagle Ford	11.711	26.637	0.517	4.792	0.019	0.731	25.679	0.240	1.415	0.454
Well 20	13860	Middle Eagle Ford	11.550	28.551	0.455	3.559	0.017	0.723	25.294	0.245	1.348	0.247
Well 20	13863	Lower Eagle Ford	8.764	22.638	0.401	3.432	0.020	0.645	30.838	0.200	1.171	0.582
Well 20	13866	Lower Eagle Ford	9.801	24.642	0.433	4.375	0.022	1.312	26.790	0.219	1.255	0.258
Well 20	13869	Lower Eagle Ford	19.584	41.217	0.723	5.288	0.019	1.044	10.250	0.404	1.934	0.237
Well 20	13872	Lower Eagle Ford	15.637	35.223	0.611	4.154	0.018	0.933	17.079	0.350	1.728	0.305
Well 20	13875	Lower Eagle Ford	9.567	26.556	0.435	3.254	0.022	0.785	28.663	0.271	1.296	0.355
Well 20	13876.9	Lower Eagle Ford	9.601	25.331	0.431	3.676	0.018	0.712	28.002	0.228	1.158	0.767

Well 20	13880	Lower Eagle Ford	11.883	32.388	0.532	2.966	0.014	0.823	23.330	0.277	1.453	0.230
Well 20	13883	Lower Eagle Ford	10.746	28.945	0.463	4.048	0.021	0.727	25.496	0.238	1.373	0.206
Well 20	13885	Lower Eagle Ford	10.609	28.207	0.452	3.396	0.018	0.740	24.931	0.215	1.297	0.403
Well 20	13889	Lower Eagle Ford	9.463	26.718	0.428	3.244	0.019	0.670	28.139	0.212	1.253	0.215
Well 20	13892	Lower Eagle Ford	11.819	29.199	0.477	4.279	0.020	0.723	24.486	0.238	1.439	0.195
Well 20	13895	Lower Eagle Ford	8.913	24.217	0.408	3.374	0.018	0.592	30.159	0.190	1.188	0.269
Well 20	13898	Lower Eagle Ford	11.926	32.611	0.545	4.414	0.017	0.722	23.128	0.247	1.615	0.343
Well 20	13901	Lower Eagle Ford	13.342	32.196	0.552	4.351	0.015	0.763	20.383	0.274	1.745	0.403
Well 20	13904	Lower Eagle Ford	11.422	29.472	0.460	4.174	0.019	0.725	25.046	0.231	1.502	0.342
Well 20	13906	Lower Eagle Ford	13.299	35.760	0.570	6.044	0.017	0.829	18.749	0.272	1.759	0.165
Well 20	13909	Lower Eagle Ford	10.950	29.715	0.495	5.282	0.020	0.706	23.871	0.212	1.382	0.765
Well 20	13912	Lower Eagle Ford	11.593	31.902	0.528	3.967	0.020	0.751	24.312	0.241	1.425	0.369
Well 20	13915	Lower Eagle Ford	9.295	27.781	0.416	3.678	0.023	0.788	28.240	0.209	1.228	0.494
Well 20	13918	Lower Eagle Ford	22.458	40.954	0.634	5.116	0.025	0.787	11.691	0.298	1.423	0.161
Well 20	13921	Lower Eagle Ford	10.527	29.290	0.423	4.626	0.019	0.645	25.285	0.215	1.375	0.780
Well 20	13924	Lower Eagle Ford	4.873	14.852	0.195	4.220	0.021	0.514	36.079	0.121	0.648	0.242
Well 20	13927	Lower Eagle Ford	5.066	12.574	0.201	1.584	0.033	0.677	40.981	0.091	0.535	0.059
Well 20	13930	Lower Eagle Ford	11.733	30.869	0.434	3.575	0.018	0.614	25.633	0.244	1.364	0.745

Well 24	14040	Middle Eagle Ford	7.433	24.311	0.434	4.418	0.085	2.659	28.058	0.617	1.340	0.125
Well 24	14100	Middle Eagle Ford	12.853	39.702	0.633	3.957	0.025	1.260	16.748	0.688	2.282	0.164
Well 24	14150	Middle Eagle Ford	12.451	38.465	0.613	4.207	0.026	1.261	16.835	0.691	2.211	0.159
Well 24	14175	Middle Eagle Ford	14.058	36.957	0.625	4.177	0.021	1.006	18.341	0.457	2.088	0.425
Well 24	14190	Lower Eagle Ford	6.054	18.462	0.273	2.168	0.045	1.089	36.570	0.287	0.911	0.213
Well 24	14200	Lower Eagle Ford	7.285	22.524	0.340	2.111	0.065	0.784	33.995	0.266	1.039	0.108
Well 24	14210	Lower Eagle Ford	6.934	21.646	0.324	1.606	0.066	0.754	35.288	0.240	0.959	0.104
Well 24	14220	Lower Eagle Ford	2.949	10.177	0.145	1.808	0.089	0.678	47.016	0.184	0.505	0.384

Trace Elements

ppm

Well	Depth	Formation Top	Ba (ppm)	Be (ppm)	Cr (ppm)	Sc (ppm)	Sr (ppm)	Zn (ppm)	Zr (ppm)	V (ppm)	Co (ppm)	Ni (ppm)
Well 3	12660	Upper Eagle Ford	4219.81	0.51	25.14	2.04	713.67	32.69	33.41	43.64	3.87	11.27
Well 3	12665	Upper Eagle Ford	3085.68	0.6	17.81	2.43	755.18	37.07	39.41	43.5	3.38	10.55
Well 3	12670	Upper Eagle Ford	3658.88	0.63	58.02	3.23	853.44	88.09	33.72	165.44	3.9	30.09
Well 3	12675	Upper Eagle Ford	4041.38	0.56	37.44	2.68	853.03	117.5	49.47	207.41	3.42	31.53
Well 3	12685	Upper Eagle Ford	3481.56	0.66	54.95	3.91	794.69	63.21	43.86	151.79	3.85	28.12
Well 3	12690	Upper Eagle Ford	3539.55	0.57	53.89	3.59	791.06	58.37	44.07	147.54	3.7	26.19

Well 3	12695	Upper Eagle Ford	3643.26	0.62	50.26	3.64	710.74	66.63	38.78	153.51	3.66	25.54
Well 3	12700	Upper Eagle Ford	3361.13	0.69	41.66	4.37	763.04	59.18	45.4	114.98	4.04	21.89
Well 3	12705	Upper Eagle Ford	3549.59	0.67	42.42	4.19	750.45	61.05	43.37	123.68	4.08	23.99
Well 3	12710	Upper Eagle Ford	3005.39	0.65	46.31	4.43	743.39	78.88	47.31	148.55	4.44	28.38
Well 3	12715	Upper Eagle Ford	3151.47	0.68	44.97	4.42	733.72	77.53	52.48	140.87	4.47	25.42
Well 3	12720	Middle Eagle Ford	9577.09	0.65	42.74	3.73	832.68	77.43	50.42	116.09	4.68	20.88
Well 3	12725	Middle Eagle Ford	4225.38	0.75	44.23	3.46	679.2	65.36	41.46	349.99	4.7	34.03
Well 3	12730	Middle Eagle Ford	3661.11	0.79	56.04	4.13	643.53	87.22	48.87	382.86	5.48	38.24
Well 3	12735	Middle Eagle Ford	4807.5	0.45	17.55	1.45	556.26	35.21	21.08	150.27	2.52	18.07
Well 3	12745	Middle Eagle Ford	4319.06	0.9	53.42	3.88	658.24	98.56	54.69	432.61	6.47	49.07
Well 3	12750	Middle Eagle Ford	9515.76	0.84	39.13	3.12	714.37	73.06	44.65	252	4.78	31.98
Well 3	12755	Middle Eagle Ford	3458.15	1.04	52.04	4.28	680.21	134.77	59.54	513.72	7.46	58.52
Well 3	12760	Middle Eagle Ford	4009.04	0.85	33.11	2.8	675.67	77.82	39.74	327.04	5.06	43.17
Well 3	12765	Lower Eagle Ford	4669.22	0.77	39.69	3.01	693.61	92.63	42.26	357.48	5.35	47.96
Well 3	12770	Lower Eagle Ford	3721.33	0.82	52.35	3.43	656.23	73.53	45.02	189.91	4.74	35.31
Well 3	12775	Lower Eagle Ford	4300.1	0.96	47.43	3.98	692.91	96.4	54.96	353.94	6.53	48.09
Well 3	12780	Lower Eagle Ford	4189.7	0.82	53.7	3.7	689.08	62.83	55.26	155.53	4.45	34.04
Well 3	12785	Lower Eagle Ford	3629.88	0.89	49.48	3.85	681.82	72.1	56.01	159.37	4.51	32.31

Well 3	12790	Lower Eagle Ford	4064.8	0.89	59.68	4.05	683.43	89.56	56.97	216.21	5.25	36.28
Well 3	12800	Lower Eagle Ford	4752.86	0.69	38.54	3.08	633.55	57.86	47.72	163.72	3.93	24.63
Well 3	12805	Lower Eagle Ford	5487.76	0.91	46.06	3.89	674.87	72.3	54.26	214.08	4.7	28.77
Well 3	12810	Lower Eagle Ford	3696.79	0.88	53.54	4.05	652.7	78.63	57.48	231.17	5.06	32.45
Well 3	12815	Lower Eagle Ford	3925.4	1	50.57	3.79	673.96	81.21	56.49	222.88	5.13	35.13
Well 3	12820	Lower Eagle Ford	3541.78	1.02	50.96	4.37	690.49	102.55	54.78	379.42	6.69	47.29
Well 3	12825	Lower Eagle Ford	3673.37	0.98	48.49	4.49	691.5	99.35	54.32	369.21	6.79	46.52
Well 3	12830	Lower Eagle Ford	3396.81	1.04	66.88	4.88	627.1	88.81	62.36	173.43	5.39	34.09
Well 3	12835	Lower Eagle Ford	4030.23	0.99	64.28	4	597.17	90.83	64.09	216.61	4.91	36.65
Well 3	12840	Lower Eagle Ford	3464.84	1.08	67.51	4.36	595.96	92.36	68.92	210.44	4.85	37.4
Well 3	12845	Lower Eagle Ford	6220.42	1.12	80.07	4.61	608.26	93.99	62.13	217.52	5.62	44.57
Well 3	12850	Lower Eagle Ford	3642.15	1.08	77.72	4.42	588	98.91	62.84	225.71	5.17	38.72
Well 3	12855	Lower Eagle Ford	3944.36	0.92	56.47	3.71	610.27	118.33	47.42	425.23	5.64	48.25
Well 3	12860	Lower Eagle Ford	5744.25	1.09	78.98	4.68	631.03	91.69	53.62	207.81	5.37	40.19
Well 3	12865	Lower Eagle Ford	6174.7	0.98	77.51	4.66	628.01	93.66	52.69	218.94	5.34	42.46
Well 3	12870	Lower Eagle Ford	4245.46	1.15	80.83	4.7	590.42	91.57	56.54	173.53	5.57	36.25
Well 3	12875	Lower Eagle Ford	3193.85	1.24	83.2	5.63	550.41	99.96	74.62	196.08	5.98	31.41
Well 3	12880	Lower Eagle Ford	4303.45	1.39	117.15	6.61	555.76	138.29	98.18	474.28	6.41	37.67

Well 3	12885	Lower Eagle Ford	3949.94	1.21	118.91	6.36	563.31	148.73	90.43	403.19	5.87	30.37
Well 12	13440	Upper Eagle Ford	3344.210	0.350	11.552	0.771	464.006	21.304	10.653	40.437	1.600	8.147
Well 12	13450	Upper Eagle Ford	4101.206	0.434	16.470	0.917	340.817	37.489	13.370	84.692	1.960	10.452
Well 12	13460	Upper Eagle Ford	3814.171	0.871	93.773	5.034	939.749	211.543	50.199	170.584	4.817	39.897
Well 12	13470	Upper Eagle Ford	3828.766	0.780	93.137	5.199	934.796	52.023	54.974	200.998	4.619	34.671
Well 12	13480	Upper Eagle Ford	3528.108	0.864	88.445	5.136	964.193	71.207	56.083	190.446	4.864	34.521
Well 12	13490	Upper Eagle Ford	4016.555	0.897	91.940	6.148	835.189	48.660	67.126	138.826	5.662	35.142
Well 12	13500	Upper Eagle Ford	3464.863	1.332	68.426	6.906	803.100	93.914	68.103	396.719	6.888	39.372
Well 12	13510	Upper Eagle Ford	2909.278	1.343	69.030	6.684	827.113	76.134	73.526	345.410	7.051	40.678
Well 12	13516	Upper Eagle Ford	2956.955	1.162	79.881	6.557	867.817	270.347	72.538	310.548	6.604	42.059
Well 12	13525	Upper Eagle Ford	3028.957	1.660	79.881	7.941	912.182	114.608	88.027	476.580	8.140	45.518
Well 12	13535	Middle Eagle Ford	4388.242	1.732	82.577	8.202	838.635	104.797	97.907	431.891	8.158	43.409
Well 12	13545	Middle Eagle Ford	2769.166	1.556	79.622	7.773	801.377	109.360	85.842	463.339	8.490	49.094
Well 12	13555	Middle Eagle Ford	2941.387	1.315	71.306	5.696	883.323	97.417	77.379	488.891	7.295	56.997
Well 12	13565	Middle Eagle Ford	3016.308	1.332	75.426	5.813	805.253	128.318	69.420	486.408	8.605	64.331
Well 12	13575	Middle Eagle Ford	4532.247	1.150	64.015	4.574	795.669	92.693	63.591	358.134	6.568	50.958
Well 12	13585	Middle Eagle Ford	4252.022	0.807	45.937	2.814	807.838	67.865	41.253	212.997	4.568	42.445
Well 12	13595	Middle Eagle Ford	3874.497	1.090	71.996	4.741	791.039	159.702	70.233	495.718	9.802	84.965

Well 12	13606	Lower Eagle Ford	3342.264	1.135	67.456	4.807	774.025	107.753	59.958	405.719	7.910	68.925
Well 12	13620	Lower Eagle Ford	4057.421	1.016	83.947	4.816	775.210	80.836	57.587	111.102	5.678	49.512
Well 12	13630	Lower Eagle Ford	4479.704	1.050	83.839	4.857	771.333	83.750	56.533	116.481	5.550	50.079
Well 12	13640	Lower Eagle Ford	4685.008	1.228	91.551	5.448	775.640	84.446	68.312	105.206	5.382	39.864
Well 12	13650	Lower Eagle Ford	4589.654	1.153	91.034	5.412	781.994	88.527	65.776	100.592	5.493	41.449
Well 12	13660	Lower Eagle Ford	4005.852	1.258	104.786	5.790	855.433	87.756	61.067	110.585	5.161	37.273
Well 12	13670	Lower Eagle Ford	4205.318	1.279	101.507	5.609	829.051	88.130	61.539	102.785	5.372	44.169
Well 12	13680	Lower Eagle Ford	3459.025	1.353	98.907	6.003	656.543	97.727	73.241	120.930	5.420	34.072
Well 12	13690	Lower Eagle Ford	3827.793	1.282	101.906	5.761	809.884	90.937	63.767	106.654	5.610	41.760
Well 12	13699	Lower Eagle Ford	3778.170	1.332	102.855	5.908	755.504	89.052	69.080	109.964	5.570	39.693
Well 12	13710	Lower Eagle Ford	3658.490	1.560	126.304	7.271	558.013	123.284	79.750	177.205	6.672	40.742
Well 12	13720	Lower Eagle Ford	3415.240	1.515	129.755	6.761	660.850	188.514	82.966	497.373	6.455	50.904
Well 12	13730	Lower Eagle Ford	3353.940	1.757	140.541	9.436	521.186	147.812	102.254	457.236	8.162	61.344
Well 12	13740	Lower Eagle Ford	4694.738	0.607	14.971	1.912	405.534	15.777	20.758	28.117	2.494	9.501
Well 12	13750	Lower Eagle Ford	3834.604	0.761	24.721	3.457	472.513	27.452	31.274	48.258	4.160	13.620
Well 16	13370	Upper Eagle Ford	5088.99	0.81	54.28	3.76	747.79	71.68	40.05	125.16	4.83	24.14
Well 16	13375	Upper Eagle Ford	4263.26	0.81	86.72	5.08	952.26	65.47	55.09	141.26	4.87	28.98
Well 16	13380	Upper Eagle Ford	4474.20	0.84	78.66	4.84	941.40	66.45	53.58	135.12	4.93	26.43

Well 16	13385	Upper Eagle Ford	7379.62	0.84	77.00	5.29	1019.93	70.07	60.09	141.76	5.33	26.24
Well 16	13390	Upper Eagle Ford	5180.15	0.85	84.31	5.15	952.84	70.95	53.37	132.71	4.57	24.61
Well 16	13395	Upper Eagle Ford	4150.90	1.32	76.32	6.62	867.04	99.26	75.87	339.97	6.68	36.90
Well 16	13400	Upper Eagle Ford	4239.94	1.29	70.88	6.46	852.79	86.85	73.09	327.49	6.39	35.43
Well 16	13405	Upper Eagle Ford	4473.14	1.31	68.99	6.48	821.08	108.39	71.31	327.89	6.51	37.21
Well 16	13410	Upper Eagle Ford	6013.30	1.59	71.18	7.18	724.62	93.12	72.89	407.48	7.77	40.83
Well 16	13415	Upper Eagle Ford	6635.51	1.55	70.36	7.31	852.40	87.50	74.70	355.56	7.79	42.60
Well 16	13420	Upper Eagle Ford	5874.44	1.52	71.16	7.99	781.91	92.52	78.03	418.64	8.77	44.70
Well 16	13425	Upper Eagle Ford	5665.62	1.30	73.69	6.49	800.63	91.81	67.82	390.47	7.47	37.38
Well 16	13430	Upper Eagle Ford	4678.78	1.07	55.46	5.36	728.11	85.46	54.01	365.82	7.22	38.25
Well 16	13435	Middle Eagle Ford	4389.40	1.15	63.41	5.90	776.39	115.07	59.71	456.77	7.78	48.47
Well 16	13440	Middle Eagle Ford	7636.14	1.28	71.70	6.57	815.65	92.50	72.31	446.91	8.12	54.16
Well 16	13445	Middle Eagle Ford	5913.66	1.41	66.32	6.25	780.65	94.02	72.75	450.03	7.66	40.74
Well 16	13450	Middle Eagle Ford	5076.27	1.27	66.37	6.35	815.85	97.01	69.76	356.36	6.92	38.20
Well 16	13455	Middle Eagle Ford	6107.64	1.19	68.04	5.47	800.53	111.98	60.87	422.47	7.39	54.38
Well 16	13460	Middle Eagle Ford	3895.45	1.08	75.43	5.20	772.03	136.33	58.93	452.45	7.66	63.23
Well 16	13465	Middle Eagle Ford	4683.02	1.14	64.98	4.76	773.58	116.92	54.54	380.81	6.73	60.66
Well 16	13470	Middle Eagle Ford	4615.18	1.05	65.67	4.62	769.31	110.24	58.65	337.35	6.48	51.78

Well 16	13475	Middle Eagle Ford	3610.31	0.93	58.68	4.02	817.50	83.67	52.67	265.21	5.41	45.15
Well 16	13480	Middle Eagle Ford	4388.34	1.08	53.71	4.42	757.00	115.89	63.44	421.66	7.22	57.39
Well 16	13485	Middle Eagle Ford	4158.32	1.13	62.68	4.84	791.71	136.13	64.33	492.69	8.24	56.99
Well 16	13490	Middle Eagle Ford	3619.85	1.03	62.46	4.95	818.76	153.29	57.34	553.46	9.19	76.56
Well 16	13495	Middle Eagle Ford	3840.33	1.08	64.57	5.16	811.39	131.09	66.99	508.19	7.88	56.94
Well 16	13500	Lower Eagle Ford	3744.93	1.17	60.30	5.11	804.99	138.90	70.87	507.68	8.22	62.05
Well 16	13505	Lower Eagle Ford	4402.12	1.24	77.12	5.88	731.60	121.95	75.14	415.83	8.24	48.70
Well 16	13510	Lower Eagle Ford	4415.90	1.17	78.47	5.37	729.46	97.49	91.70	151.62	6.08	39.07
Well 16	13515	Lower Eagle Ford	4494.34	1.07	70.54	4.87	743.62	93.51	59.01	195.99	5.72	42.88
Well 16	13520	Lower Eagle Ford	3925.13	1.06	68.79	4.84	779.10	81.39	59.99	169.53	5.35	40.44
Well 16	13525	Lower Eagle Ford	4377.74	1.27	79.60	5.76	741.58	91.62	76.72	143.77	5.78	37.59
Well 16	13530	Lower Eagle Ford	3943.15	1.02	75.15	5.03	751.67	87.95	61.38	158.46	5.20	37.99
Well 16	13535	Lower Eagle Ford	4183.76	1.33	99.82	5.67	781.62	97.82	67.26	159.87	5.32	40.74
Well 16	13540	Lower Eagle Ford	4343.82	1.06	81.93	4.76	755.16	78.18	59.84	123.75	4.98	38.64
Well 16	13545	Lower Eagle Ford	4145.60	1.25	99.56	5.69	800.24	93.84	65.33	139.55	5.53	41.12
Well 16	13550	Lower Eagle Ford	3782.03	1.33	109.05	6.34	725.29	105.82	72.52	209.87	6.29	45.10
Well 16	13555	Lower Eagle Ford	3278.54	1.43	125.65	6.83	650.35	127.60	89.97	232.91	6.86	43.36
Well 16	13560	Lower Eagle Ford	3591.23	1.49	155.28	7.16	651.32	160.89	91.98	358.78	7.13	43.90

Well 16	13565	Lower Eagle Ford	4199.66	1.35	145.51	6.54	689.81	151.33	83.68	310.39	6.69	40.78
Well 16	13570	Lower Eagle Ford	2500.51	1.38	94.75	6.04	676.53	113.22	70.44	284.83	5.84	41.96
Well 16	13575	Lower Eagle Ford	3739.63	1.71	107.02	8.49	570.08	148.66	82.80	482.03	7.12	49.58
Well 16	13580	Lower Eagle Ford	3994.03	1.53	129.32	7.77	603.43	140.24	76.38	690.49	6.95	56.36
Well 16	13585	Lower Eagle Ford	3818.07	1.51	114.25	8.07	565.81	138.18	81.13	569.06	6.33	47.41
Well 16	13590	Lower Eagle Ford	3775.67	1.68	97.15	8.80	480.49	113.63	84.53	507.99	8.14	49.31
Well 16	13595	Lower Eagle Ford	3809.59	1.59	97.93	8.65	521.41	129.55	84.02	453.96	7.95	51.55
Well 16	13600	Lower Eagle Ford	6373.69	0.54	14.92	2.20	434.34	20.69	24.56	30.46	2.81	7.60
Well 16	13605	Lower Eagle Ford	6662.01	0.61	17.39	3.12	443.26	27.44	28.15	35.96	3.63	9.61
Well 16	13610	Lower Eagle Ford	6367.34	0.69	18.51	3.06	442.20	27.60	32.65	41.54	4.22	11.73
Well 16	13615	Lower Eagle Ford	5886.10	0.84	24.06	4.01	472.45	31.15	35.87	55.54	5.28	16.10
Well 16	13620	Lower Eagle Ford	6128.84	0.72	18.78	3.56	443.65	28.21	42.18	40.58	4.33	11.13
Well 16	13625	Lower Eagle Ford	6986.37	0.79	22.07	3.95	457.81	31.61	42.54	47.27	9.43	15.07
Well 17	13650	Middle Eagle Ford	1445.858	1.323	74.615	7.437	761.356	97.489	77.808	359.235	7.770	49.672
Well 17	13660	Middle Eagle Ford	1474.422	1.260	62.704	6.287	668.600	87.114	69.553	288.504	6.488	43.655
Well 17	13670	Middle Eagle Ford	1659.130	1.295	68.221	6.948	768.002	88.497	73.054	352.370	7.606	50.552
Well 17	13680	Middle Eagle Ford	1343.031	1.422	87.885	7.677	796.009	107.814	79.944	303.379	7.633	51.481
Well 17	13690	Middle Eagle Ford	1771.478	1.194	75.461	6.499	745.311	98.176	68.886	256.779	6.843	48.811

Well 17	13700	Middle Eagle Ford	1673.411	1.171	80.817	6.533	822.213	134.055	67.500	377.750	7.874	63.234
Well 17	13710	Middle Eagle Ford	1369.690	1.201	92.205	6.658	786.705	104.988	76.135	243.049	6.872	55.466
Well 17	13720	Lower Eagle Ford	1968.563	0.969	81.592	5.430	826.960	91.343	60.252	200.923	5.790	51.655
Well 17	13730	Lower Eagle Ford	1760.053	0.937	79.911	5.229	831.137	92.413	59.708	224.743	5.809	53.890
Well 17	13740	Lower Eagle Ford	2912.098	0.835	75.400	4.326	812.814	110.236	56.268	178.144	5.096	50.833
Well 17	13750	Lower Eagle Ford	2203.733	0.944	79.790	5.044	789.553	102.233	57.716	271.238	6.483	61.580
Well 17	13760	Lower Eagle Ford	1124.047	1.052	77.746	5.694	762.970	152.929	64.297	537.622	9.563	93.928
Well 17	13770	Lower Eagle Ford	1192.599	1.042	80.878	5.753	815.757	100.456	63.640	256.779	6.857	61.387
Well 17	13780	Lower Eagle Ford	1315.420	1.104	88.902	6.194	792.022	126.688	72.089	173.255	6.805	58.649
Well 17	13790	Lower Eagle Ford	1608.668	1.091	87.674	6.087	762.496	100.911	70.015	207.684	6.921	60.806
Well 17	13800	Lower Eagle Ford	1097.388	1.385	94.531	7.492	699.930	106.704	79.574	154.740	7.758	59.607
Well 17	13810	Lower Eagle Ford	1322.085	1.348	107.217	7.033	699.455	132.037	79.071	189.169	7.600	58.049
Well 17	13820	Lower Eagle Ford	1099.293	1.394	121.313	7.231	636.985	131.532	81.966	218.710	7.295	43.007
Well 17	13830	Lower Eagle Ford	2720.725	1.049	90.735	5.643	736.672	124.770	67.746	304.523	6.832	70.625
Well 17	13840	Lower Eagle Ford	1746.723	1.608	109.432	8.693	547.742	125.779	81.114	438.391	8.892	72.888
Well 19	13690	Upper Eagle Ford	3883.41	0.70	55.96	3.80	846.27	56.89	37.13	213.67	4.09	40.58
Well 19	13695	Upper Eagle Ford	4042.22	0.98	75.32	4.85	922.33	74.81	48.78	257.48	4.97	47.19
Well 19	13700	Upper Eagle Ford	2705.51	1.50	73.81	7.97	663.16	56.82	114.95	146.62	10.18	40.00

Well 19	13705	Upper Eagle Ford	2622.69	1.10	49.22	6.74	719.41	84.97	69.59	298.17	7.04	54.60
Well 19	13710	Upper Eagle Ford	2380.10	1.55	82.49	8.99	625.23	92.98	97.75	216.79	8.32	49.91
Well 19	13715	Upper Eagle Ford	2241.75	1.52	82.69	8.78	624.94	88.83	97.01	224.06	8.28	46.81
Well 19	13720	Upper Eagle Ford	2228.11	1.55	97.70	9.09	619.59	87.99	102.11	237.45	8.39	49.31
Well 19	13725	Middle Eagle Ford	2526.24	1.55	97.40	8.60	705.05	218.99	85.56	249.80	7.70	44.95
Well 19	13730	Middle Eagle Ford	2574.95	1.54	93.56	8.54	681.78	72.62	93.77	243.67	8.33	51.56
Well 19	13735	Middle Eagle Ford	3315.41	1.52	90.56	8.47	699.11	61.93	85.98	243.78	8.26	49.54
Well 19	13740	Middle Eagle Ford	2784.42	1.69	97.73	9.13	685.74	68.35	90.72	266.41	7.93	47.92
Well 19	13745	Middle Eagle Ford	2568.13	1.64	101.03	9.09	688.32	177.40	89.43	263.50	8.20	50.45
Well 19	13750	Middle Eagle Ford	2361.59	1.74	100.37	9.03	674.55	60.74	84.18	253.02	8.14	49.59
Well 19	13755	Middle Eagle Ford	2631.46	1.93	105.17	9.53	616.72	52.37	92.07	204.75	8.88	48.45
Well 19	13760	Middle Eagle Ford	2346.00	1.72	93.36	8.92	671.98	60.95	85.61	253.74	8.81	50.77
Well 19	13765	Middle Eagle Ford	2435.63	1.76	95.81	9.21	679.60	63.93	86.14	253.85	8.21	49.25
Well 19	13770	Middle Eagle Ford	2268.06	1.78	98.27	9.62	675.94	69.24	88.78	248.66	8.31	48.97
Well 19	13775	Middle Eagle Ford	2653.87	1.80	99.17	9.34	695.15	59.44	90.50	254.26	8.03	48.21
Well 19	13780	Middle Eagle Ford	2638.28	1.84	102.92	9.65	684.06	161.35	94.42	243.47	9.13	50.85
Well 19	13785	Middle Eagle Ford	2636.33	1.55	89.59	8.42	705.15	68.91	83.90	243.47	7.56	47.77
Well 19	13790	Middle Eagle Ford	2576.90	1.85	102.93	9.94	675.74	58.78	93.48	237.34	8.35	44.98

Well 19	13795	Middle Eagle Ford	2749.35	1.84	108.30	10.00	686.04	196.45	96.71	242.74	8.58	48.92
Well 19	13800	Middle Eagle Ford	3084.50	1.88	104.47	9.61	707.73	54.36	102.42	235.89	8.12	46.12
Well 19	13805	Middle Eagle Ford	3504.42	1.89	103.55	10.04	709.91	79.30	102.30	242.84	8.99	49.58
Well 19	13810	Middle Eagle Ford	2574.95	1.78	85.89	9.31	775.66	56.09	87.08	258.10	9.56	51.58
Well 19	13815	Middle Eagle Ford	2890.62	2.24	112.08	11.78	628.60	77.51	111.88	235.06	10.06	51.36
Well 19	13825	Middle Eagle Ford	2812.68	2.17	102.41	10.92	655.74	70.95	104.38	283.02	9.78	50.37
Well 19	13830	Middle Eagle Ford	2305.08	2.24	123.55	11.57	607.61	79.14	111.67	230.70	9.44	43.13
Well 19	13835	Middle Eagle Ford	2224.21	2.14	118.25	11.62	650.19	74.73	105.25	321.12	9.62	52.94
Well 19	13840	Middle Eagle Ford	3065.99	2.11	107.46	10.82	670.89	93.97	101.93	228.93	9.50	51.93
Well 19	13845	Middle Eagle Ford	2005.00	2.20	121.71	11.53	648.31	193.36	112.09	255.72	10.31	56.81
Well 19	13850	Middle Eagle Ford	2819.50	2.23	129.82	11.58	665.94	66.37	112.83	235.16	10.08	57.06
Well 19	13855	Middle Eagle Ford	2802.94	2.31	133.71	11.90	656.73	85.63	120.87	229.04	10.64	59.28
Well 19	13860	Middle Eagle Ford	2107.30	2.29	137.61	11.95	634.05	71.78	115.48	233.40	11.73	63.54
Well 19	13865	Middle Eagle Ford	2274.87	2.40	154.05	12.37	600.38	74.74	120.76	205.68	10.90	64.48
Well 19	13870	Middle Eagle Ford	2038.12	2.06	144.53	10.76	706.14	71.87	107.26	244.09	9.93	63.92
Well 19	13875	Middle Eagle Ford	3178.03	1.75	147.56	9.78	729.81	87.59	100.80	238.69	9.49	70.88
Well 19	13880	Middle Eagle Ford	5709.21	1.71	119.22	9.61	731.40	185.28	94.55	207.65	10.00	60.91
Well 19	13885	Middle Eagle Ford	2908.16	1.68	127.01	9.28	714.16	76.93	95.27	201.22	8.66	61.29

Well 19	13890	Middle Eagle Ford	2284.62	1.51	118.90	8.29	769.23	85.27	79.69	145.99	7.87	61.50
Well 19	13895	Middle Eagle Ford	2304.10	1.45	134.04	8.13	736.94	310.92	76.81	193.95	8.46	70.12
Well 19	13900	Middle Eagle Ford	1989.41	1.43	114.46	8.00	727.93	91.95	79.66	186.68	7.77	65.83
Well 19	13905	Middle Eagle Ford	2595.41	1.38	122.25	7.50	720.50	109.99	83.59	161.04	7.26	64.85
Well 19	13910	Middle Eagle Ford	2528.19	1.45	132.09	7.60	687.43	131.03	81.96	312.91	8.41	72.68
Well 19	13915	Lower Eagle Ford	2392.76	1.47	127.12	7.39	707.73	108.30	89.25	174.33	7.32	61.75
Well 19	13920	Lower Eagle Ford	2567.16	1.43	119.98	7.08	682.37	106.30	83.43	172.67	6.61	55.32
Well 19	13925	Lower Eagle Ford	2145.30	1.52	113.81	7.57	682.97	128.24	85.43	235.68	7.77	60.69
Well 19	13930	Lower Eagle Ford	1993.31	1.48	121.49	7.49	715.45	127.25	81.46	330.67	8.29	73.10
Well 19	13935	Lower Eagle Ford	2126.78	1.71	120.09	8.87	685.05	121.96	96.06	164.37	9.58	65.16
Well 19	13940	Lower Eagle Ford	1716.61	1.76	116.63	9.11	648.80	114.08	94.44	152.64	9.07	58.17
Well 19	13945	Lower Eagle Ford	1961.16	1.74	129.71	9.03	693.66	115.98	91.64	158.97	9.70	64.54
Well 19	13950	Lower Eagle Ford	1889.06	1.75	147.56	8.59	624.74	160.75	100.04	282.91	10.50	72.01
Well 19	13955	Lower Eagle Ford	1799.43	1.62	153.29	8.65	727.04	201.53	101.04	461.77	10.29	99.53
Well 19	13960	Lower Eagle Ford	2521.37	1.54	114.46	8.38	669.40	99.82	90.07	212.53	8.18	59.61
Well 19	13965	Lower Eagle Ford	2073.20	1.57	117.06	8.35	690.30	104.61	86.68	226.13	8.45	67.17
Well 19	13970	Lower Eagle Ford	2323.59	1.75	133.82	9.23	574.33	133.23	99.92	401.88	9.79	82.17
Well 19	13975	Lower Eagle Ford	1512.99	1.73	131.12	9.02	609.29	134.62	94.68	285.72	9.78	68.43

Well 19	13980	Lower Eagle Ford	2133.60	1.71	123.22	8.72	643.16	125.95	94.09	225.20	9.60	66.22
Well 19	13985	Lower Eagle Ford	2073.20	1.69	147.99	8.70	647.22	122.76	89.95	239.83	9.82	74.38
Well 19	13990	Lower Eagle Ford	1432.12	1.77	140.31	9.10	638.40	133.53	97.70	267.86	9.44	63.91
Well 19	13995	Lower Eagle Ford	1633.80	1.65	132.20	8.66	651.58	126.05	89.40	234.54	9.31	68.22
Well 19	14000	Lower Eagle Ford	3245.26	1.45	108.41	7.81	673.46	103.61	77.83	227.17	8.06	55.16
Well 20	13660	Upper Eagle Ford	1749.566	1.235	63.873	7.389	709.591	55.563	101.351	124.234	9.255	32.790
Well 20	13665	Upper Eagle Ford	1877.280	1.324	76.479	7.501	686.262	56.748	99.141	179.988	8.501	44.858
Well 20	13670	Upper Eagle Ford	1532.964	1.181	62.430	7.010	695.423	71.683	85.662	219.175	7.899	48.842
Well 20	13675	Upper Eagle Ford	1641.265	1.187	59.337	6.636	691.908	75.841	76.682	287.573	7.055	53.621
Well 20	13680	Middle Eagle Ford	1537.051	1.174	59.941	7.199	706.821	152.349	75.969	308.788	7.199	55.968
Well 20	13685	Middle Eagle Ford	1762.849	1.241	76.234	7.500	677.315	94.268	84.517	284.291	7.231	55.333
Well 20	13690	Middle Eagle Ford	1526.834	1.437	124.227	8.418	643.228	112.778	103.762	270.547	8.712	42.572
Well 20	13695	Middle Eagle Ford	1881.367	1.711	90.717	9.778	574.522	114.328	113.405	214.128	8.624	50.057
Well 20	13700	Middle Eagle Ford	2076.513	1.545	92.536	8.938	659.206	55.244	96.229	213.130	8.071	47.731
Well 20	13705	Middle Eagle Ford	3462.971	1.609	89.274	9.104	667.834	70.689	103.461	198.388	8.220	45.415
Well 20	13710	Middle Eagle Ford	2761.058	1.642	96.506	8.915	662.828	75.157	93.145	221.998	7.671	48.180
Well 20	13715	Middle Eagle Ford	1983.538	1.684	98.297	9.435	674.545	67.790	99.342	219.448	8.060	45.640
Well 20	13720	Middle Eagle Ford	2054.035	1.803	104.143	9.863	660.271	61.289	101.753	215.347	7.978	44.936

Well 20	13725	Middle Eagle Ford	2177.662	1.678	116.024	9.114	666.130	60.705	99.242	225.323	8.044	46.822
Well 20	13730	Middle Eagle Ford	2354.418	1.745	103.766	9.445	687.434	77.282	94.611	228.981	8.250	47.438
Well 20	13740	Middle Eagle Ford	2090.817	1.741	93.621	8.459	618.195	61.708	89.659	205.371	7.439	43.275
Well 20	13745	Middle Eagle Ford	2071.405	1.968	109.706	10.083	665.597	52.262	101.653	226.321	8.374	45.220
Well 20	13750	Middle Eagle Ford	1865.019	1.957	113.666	10.487	693.293	59.292	103.561	206.923	7.980	42.278
Well 20	13755	Middle Eagle Ford	1885.454	1.890	106.406	10.123	673.160	66.285	103.260	193.733	8.455	47.858
Well 20	13760	Middle Eagle Ford	1795.543	1.994	116.212	10.567	677.528	56.885	106.273	214.349	7.897	44.272
Well 20	13765	Middle Eagle Ford	1931.430	1.854	112.346	9.931	685.410	79.707	100.648	219.670	8.011	47.692
Well 20	13770	Middle Eagle Ford	2092.860	1.792	108.292	9.889	679.552	60.158	101.452	204.374	7.959	44.829
Well 20	13785	Middle Eagle Ford	1024.153	1.892	104.332	10.214	587.411	76.972	105.068	213.906	8.154	44.858
Well 20	13788	Middle Eagle Ford	791.568	1.310	22.152	6.277	212.832	86.432	222.420	48.677	4.164	8.513
Well 20	13790	Middle Eagle Ford	218.143	1.785	94.141	9.555	555.986	41.958	113.970	377.443	4.649	29.268
Well 20	13793	Middle Eagle Ford	238.085	2.161	109.943	11.253	704.127	163.077	103.343	345.616	9.755	59.210
Well 20	13796	Middle Eagle Ford	727.688	2.555	119.191	12.813	628.370	75.376	128.971	212.632	9.802	44.524
Well 20	13799	Middle Eagle Ford	380.775	2.472	112.179	11.991	666.811	84.252	134.493	194.381	9.058	39.432
Well 20	13802	Middle Eagle Ford	366.378	2.465	115.532	14.057	611.173	93.275	132.409	204.730	10.870	44.784
Well 20	13805	Middle Eagle Ford	639.173	2.953	157.502	14.088	532.269	72.985	137.618	297.430	10.596	46.703
Well 20	13808	Middle Eagle Ford	615.072	2.654	145.511	12.718	605.891	65.666	138.973	245.238	12.219	55.691

Well 20	13811	Middle Eagle Ford	297.486	2.263	114.618	12.560	638.936	81.797	123.658	176.909	10.646	51.573
Well 20	13814	Middle Eagle Ford	663.381	3.179	188.903	15.870	421.894	86.460	149.391	310.561	12.463	55.286
Well 20	13816	Middle Eagle Ford	1581.373	2.839	133.316	13.403	535.866	65.491	124.700	266.716	10.900	53.955
Well 20	13819	Middle Eagle Ford	232.753	1.752	86.397	10.445	814.391	34.236	84.456	297.652	8.375	54.967
Well 20	13822	Middle Eagle Ford	448.494	2.737	161.160	14.763	572.958	154.100	152.933	249.912	12.108	54.225
Well 20	13825	Middle Eagle Ford	270.825	2.785	172.542	13.488	530.808	77.885	144.702	259.705	12.280	71.159
Well 20	13828	Middle Eagle Ford	480.487	2.354	129.658	13.393	825.181	61.149	133.243	417.283	11.336	65.488
Well 20	13831	Middle Eagle Ford	345.156	2.352	190.326	13.857	531.258	58.997	118.658	302.104	13.112	71.583
Well 20	13834	Middle Eagle Ford	1263.574	2.273	173.355	12.813	632.866	97.764	140.327	178.467	9.892	61.062
Well 20	13837	Middle Eagle Ford	218.143	2.175	128.540	12.286	725.933	57.760	118.554	278.845	9.728	58.256
Well 20	13840	Middle Eagle Ford	176.231	1.630	145.714	10.610	481.915	1344.768	95.530	235.000	5.524	25.844
Well 20	13842	Middle Eagle Ford	409.355	1.888	206.789	11.685	695.810	126.161	128.763	202.060	9.218	72.779
Well 20	13844	Middle Eagle Ford	130.374	1.332	132.300	8.038	766.396	79.369	95.051	363.644	7.901	103.628
Well 20	13846.4	Middle Eagle Ford	501.709	3.043	181.180	15.058	389.860	94.924	149.078	296.428	12.950	57.532
Well 20	13850	Middle Eagle Ford	3972.804	1.638	154.587	9.222	648.341	124.084	94.109	181.429	8.526	62.496
Well 20	13851	Middle Eagle Ford	4902.269	2.153	124.780	11.622	634.103	87.211	115.741	205.287	10.819	55.411
Well 20	13854	Middle Eagle Ford	869.951	1.411	144.291	8.606	779.210	128.542	94.259	130.504	8.971	69.760
Well 20	13855	Middle Eagle Ford	2414.699	1.850	142.330	10.063	607.437	115.969	101.853	180.986	8.941	56.340

Well 20	13857	Middle Eagle Ford	148.504	1.638	138.600	9.017	633.204	141.001	103.135	138.183	9.043	71.621
Well 20	13860	Middle Eagle Ford	154.903	1.520	115.228	10.832	679.737	153.276	103.343	135.957	8.399	64.350
Well 20	13863	Lower Eagle Ford	128.028	1.284	123.357	7.754	710.646	108.848	77.382	108.359	8.521	70.242
Well 20	13866	Lower Eagle Ford	605.260	1.377	130.979	8.100	641.633	129.275	87.008	129.948	8.279	68.584
Well 20	13869	Lower Eagle Ford	187.749	2.139	299.671	9.745	377.496	192.665	144.077	452.560	13.883	101.699
Well 20	13872	Lower Eagle Ford	166.527	1.978	230.161	11.285	474.496	168.757	123.762	392.021	11.397	84.968
Well 20	13875	Lower Eagle Ford	266.239	1.357	138.092	7.818	644.331	120.848	92.207	121.156	7.722	68.343
Well 20	13876.9	Lower Eagle Ford	463.317	1.310	148.356	9.466	742.455	126.436	88.446	216.081	9.200	80.696
Well 20	13880	Lower Eagle Ford	161.621	1.712	217.256	10.280	578.578	176.543	101.114	225.652	8.773	82.518
Well 20	13883	Lower Eagle Ford	311.989	1.535	114.415	8.217	686.705	120.939	109.594	131.172	7.869	58.825
Well 20	13885	Lower Eagle Ford	2288.007	1.628	147.516	8.451	659.739	142.411	97.936	259.463	8.036	61.509
Well 20	13889	Lower Eagle Ford	318.388	1.413	121.426	7.781	652.087	130.375	93.988	135.289	7.628	55.247
Well 20	13892	Lower Eagle Ford	587.238	1.653	116.650	8.819	676.028	156.482	101.447	184.032	10.606	66.038
Well 20	13895	Lower Eagle Ford	166.527	1.281	97.606	7.735	677.039	106.741	84.008	162.220	8.618	59.548
Well 20	13898	Lower Eagle Ford	222.408	1.738	124.475	10.468	679.624	133.672	106.156	158.325	11.884	68.439
Well 20	13901	Lower Eagle Ford	260.694	2.097	216.646	9.707	560.032	233.154	130.742	359.971	10.403	90.397
Well 20	13904	Lower Eagle Ford	144.452	1.764	103.439	9.384	581.612	105.458	92.707	116.371	10.809	67.234
Well 20	13906	Lower Eagle Ford	605.687	2.100	122.544	10.863	590.829	154.833	117.720	133.509	12.706	69.722

Well 20	13909	Lower Eagle Ford	209.291	1.700	147.340	9.274	708.286	137.886	99.530	130.282	11.286	79.047
Well 20	13912	Lower Eagle Ford	277.330	1.725	156.486	10.345	759.428	144.024	94.988	157.991	10.748	69.114
Well 20	13915	Lower Eagle Ford	124.082	1.533	132.198	8.897	611.960	189.276	85.258	134.176	9.371	61.882
Well 20	13918	Lower Eagle Ford	160.875	2.040	102.830	10.420	373.450	123.413	136.472	194.270	13.691	51.525
Well 20	13921	Lower Eagle Ford	154.049	1.726	134.739	9.986	612.410	322.010	110.948	238.116	10.393	61.689
Well 20	13924	Lower Eagle Ford	94.702	1.185	127.320	5.463	1043.010	197.429	54.327	1017.770	4.351	113.078
Well 20	13927	Lower Eagle Ford	113.631	0.669	30.983	5.323	748.412	63.311	49.462	172.347	7.845	37.619
Well 20	13930	Lower Eagle Ford	219.742	2.112	209.532	8.858	658.606	147.596	108.448	669.118	11.763	81.872
Well 24	14040	Middle Eagle Ford	2546.913	0.975	72.481	10.183	856.969	46.690	69.253	136.034	9.798	40.250
Well 24	14100	Middle Eagle Ford	1715.596	1.880	75.923	11.111	671.470	64.978	120.401	180.440	9.277	41.236
Well 24	14150	Middle Eagle Ford	1596.691	1.790	76.897	10.972	679.697	74.147	122.262	179.502	10.052	43.619
Well 24	14175	Middle Eagle Ford	1158.674	2.134	134.731	11.584	625.321	110.621	110.769	205.874	11.547	66.192
Well 24	14190	Lower Eagle Ford	2545.897	0.991	56.763	5.263	562.519	44.696	56.151	113.831	5.354	28.088
Well 24	14200	Lower Eagle Ford	2714.600	1.079	45.832	6.468	553.891	46.334	62.127	85.019	7.262	26.356
Well 24	14210	Lower Eagle Ford	3087.575	1.016	45.471	6.179	549.577	37.226	59.555	86.030	7.365	25.361
Well 24	14220	Lower Eagle Ford	2204.427	0.529	32.603	2.709	511.655	34.590	32.826	66.287	8.176	25.974

Well	Depth	Formation Top	Cu (ppm)	Ga (ppm)	Rb (ppm)	Y (ppm)	Nb (ppm)	Mo (ppm)	Sn (ppm)	Cs (ppm)	La (ppm)	Ce (ppm)
Well 3	12660	Upper Eagle	9.36	3.38	14.27	11.2	3.14	0.82	0.18	1.05	10.1	15.13

		Ford										
Well 3	12665	Upper Eagle Ford	9.01	3.7	18	8.75	3.73	1.4	0.3	1.33	9.27	14.91
Well 3	12670	Upper Eagle Ford	14.03	3.9	18.5	10.38	3.02	5.69	0.33	1.3	9.14	15.1
Well 3	12675	Upper Eagle Ford	16.45	3.99	17.12	10.4	3.65	8.47	0	1.2	13.31	24.83
Well 3	12685	Upper Eagle Ford	17.12	4.59	25.52	9.55	3.41	4.1	0.07	1.85	9.82	18.28
Well 3	12690	Upper Eagle Ford	16.02	4.24	24.35	9.29	3.23	3.5	0.24	1.76	9.53	17.47
Well 3	12695	Upper Eagle Ford	18.49	4.06	23.63	8.45	2.95	3.91	0.27	1.7	8.55	15.83
Well 3	12700	Upper Eagle Ford	14.68	4.8	29.96	9.18	3.7	2.59	0.02	2.33	9.52	17.76
Well 3	12705	Upper Eagle Ford	16.1	4.85	29.47	8.93	3.58	3.24	0.19	2.28	9.2	17.26
Well 3	12710	Upper Eagle Ford	15.43	5.09	30.64	10.7	4.02	4.26	0.07	2.18	10.95	20.6
Well 3	12715	Upper Eagle Ford	17.45	5.39	29.94	10.55	4.06	4.16	0.53	2.14	11.09	20.45
Well 3	12720	Middle Eagle Ford	18.78	4.67	25.62	9.85	3.93	3.51	0.8	1.84	10.28	18.85
Well 3	12725	Middle Eagle Ford	19.69	4.31	29.3	8	5.1	24.01	0.39	2.26	10.72	18.8
Well 3	12730	Middle Eagle Ford	15.97	4.96	29.04	9.72	4.81	28.85	0.04	2.31	12.07	21.64
Well 3	12735	Middle Eagle Ford	14.57	1.99	11.21	5.14	1.81	11.43	0.32	0.94	5.75	9.93
Well 3	12745	Middle Eagle Ford	19.05	5.74	30.64	10.89	6.39	37.84	0.33	2.5	13.63	24.91
Well 3	12750	Middle Eagle Ford	18.09	4.28	25.19	8.21	4.34	20.11	0.25	1.95	9.89	18.18
Well 3	12755	Middle Eagle Ford	18.14	6.07	34.07	11.43	8.72	45.86	0.3	2.81	16.46	29.03
Well 3	12760	Middle Eagle	16.19	3.64	20.48	8.46	4.66	32.53	0.28	1.77	10.5	17.87

		Ford										
Well 3	12765	Lower Eagle Ford	18.36	4.03	23.03	8.94	5.21	35.86	0.39	1.92	11.17	19.28
Well 3	12770	Lower Eagle Ford	16.18	4.43	25.25	10	5.67	25.36	0.4	2.09	12.45	22.34
Well 3	12775	Lower Eagle Ford	20.82	5.41	30.59	11.3	6.48	38.45	0.32	2.62	13.98	25.35
Well 3	12780	Lower Eagle Ford	18.76	4.56	24.39	13.72	5.9	21.47	0.27	2.04	15.99	27.58
Well 3	12785	Lower Eagle Ford	19.09	4.65	24.28	14.49	6.07	22.77	0.47	2.08	16.79	28.59
Well 3	12790	Lower Eagle Ford	16.31	5.4	25.7	13.22	6.65	30.88	0.18	2.26	15.7	26.8
Well 3	12800	Lower Eagle Ford	18.68	4.28	19.22	11.88	4.93	18.57	0.36	1.61	14	23.76
Well 3	12805	Lower Eagle Ford	18.53	4.87	22.39	13.45	5.43	23.6	0.09	1.9	15.55	26.72
Well 3	12810	Lower Eagle Ford	18.99	5.39	27.03	13.04	6.44	28.27	0.41	2.22	16.08	28.26
Well 3	12815	Lower Eagle Ford	16.65	5.22	25.49	13.28	6.06	25.9	0.55	2.09	16.14	28.4
Well 3	12820	Lower Eagle Ford	20.4	6.08	33.22	12.14	7.09	37.91	0.54	2.86	15.47	27.83
Well 3	12825	Lower Eagle Ford	20.11	5.91	31.94	11.81	6.72	38.02	0.34	2.81	14.91	27.05
Well 3	12830	Lower Eagle Ford	19.09	6.36	30.34	15.09	7.35	27.25	0.17	2.61	19.71	35.08
Well 3	12835	Lower Eagle Ford	19.99	6.1	29.59	12.43	7.72	30.06	0.5	2.7	20.67	38.09
Well 3	12840	Lower Eagle Ford	19.38	6.31	30.14	12.74	7.9	29.85	0.22	2.74	21.41	39.36
Well 3	12845	Lower Eagle Ford	21.9	6.71	34.76	12.55	8.37	34.85	0.42	2.98	18.01	31.29
Well 3	12850	Lower Eagle Ford	19.01	6.7	33.72	12.98	8.43	34.07	0.36	2.99	19.22	33.74
Well 3	12855	Lower Eagle	20.14	5.29	28.62	10.22	6.33	35.25	0.32	2.62	13.49	24.78

		Ford										
Well 3	12860	Lower Eagle Ford	19.59	5.98	35.81	11.75	7.04	26.96	0.05	3.17	15.32	27.02
Well 3	12865	Lower Eagle Ford	19.43	6.09	35.52	11.79	7.09	25.38	0.45	3.1	15.36	27.3
Well 3	12870	Lower Eagle Ford	20.03	6.51	37.81	12.83	7.98	21.29	0.72	3.24	17.17	30.44
Well 3	12875	Lower Eagle Ford	15.39	7.7	44.74	16.29	8.91	18.72	0.35	3.99	20.9	38.28
Well 3	12880	Lower Eagle Ford	17.91	9.76	44.13	24.29	9.64	24.87	0.36	3.77	27.02	51.1
Well 3	12885	Lower Eagle Ford	13.36	9.2	42.85	21.91	9.22	19.56	0.49	3.63	25	46.23
Well 12	13440	Upper Eagle Ford	8.855	0.918	5.582	3.081	0.928	1.605	0.344	0.559	3.340	5.091
Well 12	13450	Upper Eagle Ford	11.393	1.249	8.208	3.367	1.499	2.921	0.119	0.752	3.834	6.253
Well 12	13460	Upper Eagle Ford	20.228	5.852	35.135	11.018	5.189	3.102	0.871	2.453	11.489	21.835
Well 12	13470	Upper Eagle Ford	20.470	5.815	36.325	10.839	5.762	2.774	0.405	2.582	11.890	23.581
Well 12	13480	Upper Eagle Ford	21.292	5.698	33.195	10.988	5.489	3.199	0.700	2.480	12.141	23.780
Well 12	13490	Upper Eagle Ford	28.035	7.390	43.136	12.818	7.547	2.140	1.030	3.093	14.196	27.481
Well 12	13500	Upper Eagle Ford	24.154	9.533	63.979	11.933	10.593	21.501	0.964	4.747	18.246	33.855
Well 12	13510	Upper Eagle Ford	23.358	9.824	63.899	13.136	12.386	21.032	0.746	4.735	20.181	37.636
Well 12	13516	Upper Eagle Ford	21.167	8.583	55.628	12.192	10.779	16.340	0.778	4.316	17.424	32.648
Well 12	13525	Upper Eagle Ford	25.594	11.343	76.071	13.216	17.000	22.277	0.912	5.821	23.269	42.593
Well 12	13535	Middle Eagle Ford	22.652	11.283	74.811	13.952	18.878	24.194	0.677	5.654	24.753	45.316
Well	13545	Middle Eagle	22.669	10.614	71.671	13.803	14.516	28.947	0.861	5.459	22.186	40.808

12		Ford										
Well 12	13555	Middle Eagle Ford	28.947	8.173	50.367	12.709	10.705	33.262	0.652	4.007	18.778	34.124
Well 12	13565	Middle Eagle Ford	27.838	7.851	48.327	13.335	10.854	44.798	0.713	3.760	18.647	34.065
Well 12	13575	Middle Eagle Ford	21.149	6.504	37.215	10.939	8.733	30.243	0.526	3.071	15.419	27.292
Well 12	13585	Middle Eagle Ford	22.043	4.115	21.743	8.404	5.321	18.441	0.497	1.771	10.797	18.913
Well 12	13595	Middle Eagle Ford	30.530	7.028	39.206	12.709	10.434	47.521	0.379	3.287	17.504	31.371
Well 12	13606	Lower Eagle Ford	27.955	6.714	38.676	11.227	9.350	37.485	0.432	3.099	15.549	27.960
Well 12	13620	Lower Eagle Ford	26.729	6.540	39.466	13.713	8.598	20.175	0.566	3.236	17.625	31.541
Well 12	13630	Lower Eagle Ford	25.808	6.565	40.096	13.693	9.030	20.808	0.615	3.239	17.795	31.790
Well 12	13640	Lower Eagle Ford	17.429	7.091	41.926	15.036	8.513	15.657	0.298	3.615	18.808	33.935
Well 12	13650	Lower Eagle Ford	18.735	7.122	41.006	15.086	8.459	15.942	0.661	3.490	18.336	33.426
Well 12	13660	Lower Eagle Ford	14.684	7.380	45.037	15.115	9.929	14.667	0.229	3.870	19.590	34.982
Well 12	13670	Lower Eagle Ford	16.150	7.351	43.566	15.036	9.378	14.984	0.896	3.646	19.088	34.244
Well 12	13680	Lower Eagle Ford	13.593	8.537	52.218	15.851	12.190	10.832	0.683	4.471	22.437	40.209
Well 12	13690	Lower Eagle Ford	16.606	7.732	45.947	16.458	9.985	15.218	0.904	4.060	21.184	39.232
Well 12	13699	Lower Eagle Ford	15.149	8.085	49.257	15.951	10.733	12.780	0.509	4.171	21.053	37.626
Well 12	13710	Lower Eagle Ford	16.115	9.695	61.919	16.746	11.788	12.260	0.778	5.357	23.640	44.159
Well 12	13720	Lower Eagle Ford	17.420	9.071	48.607	22.772	9.490	22.205	0.728	3.929	24.392	44.818
Well	13730	Lower Eagle	22.848	13.062	63.609	24.612	10.154	19.319	0.966	5.521	29.264	55.152

12		Ford										
Well 12	13740	Lower Eagle Ford	11.366	2.756	16.292	6.244	2.587	1.022	0.549	1.090	7.508	13.436
Well 12	13750	Lower Eagle Ford	10.999	4.568	23.083	9.768	3.968	0.972	0.588	1.702	12.802	23.701
Well 16	13370	Upper Eagle Ford	14.88	5.25	30.87	9.44	5.28	1.89	0.90	2.13	11.21	19.52
Well 16	13375	Upper Eagle Ford	15.66	6.03	34.50	11.51	7.28	1.55	0.65	2.31	13.96	27.01
Well 16	13380	Upper Eagle Ford	14.46	5.46	33.05	11.08	6.66	1.60	0.56	2.14	12.73	24.58
Well 16	13385	Upper Eagle Ford	14.57	5.95	34.31	12.60	7.01	2.35	0.83	2.29	14.23	28.02
Well 16	13390	Upper Eagle Ford	12.67	6.06	38.42	12.33	6.09	1.37	0.73	3.00	14.30	28.44
Well 16	13395	Upper Eagle Ford	13.86	9.12	59.46	12.77	13.30	15.79	1.06	4.28	19.35	36.01
Well 16	13400	Upper Eagle Ford	13.86	8.36	56.22	12.43	12.38	14.79	0.71	4.02	19.35	36.12
Well 16	13405	Upper Eagle Ford	13.87	8.10	54.26	11.87	12.49	14.05	0.70	4.06	18.67	34.61
Well 16	13410	Upper Eagle Ford	22.01	9.80	71.84	13.04	11.74	25.48	0.78	5.69	20.49	38.39
Well 16	13415	Upper Eagle Ford	23.02	10.17	71.91	12.76	12.87	21.06	0.86	5.63	20.80	37.61
Well 16	13420	Upper Eagle Ford	23.39	10.36	68.63	13.02	12.99	29.10	0.89	5.02	20.90	38.65
Well 16	13425	Upper Eagle Ford	18.33	8.06	50.46	11.63	10.02	21.27	0.93	3.73	17.27	31.97
Well 16	13430	Upper Eagle Ford	20.88	6.17	39.31	10.13	7.38	22.32	0.60	2.84	14.41	26.12
Well 16	13435	Middle Eagle Ford	23.83	7.65	46.00	11.26	8.80	28.07	0.71	3.46	16.30	30.06
Well 16	13440	Middle Eagle Ford	22.75	8.71	51.25	15.49	10.49	27.95	0.57	3.81	21.00	35.42
Well	13445	Middle Eagle	14.78	8.65	52.03	13.82	10.65	25.00	0.45	3.98	20.12	34.99

16		Ford										
Well 16	13450	Middle Eagle Ford	15.76	8.55	56.59	12.47	10.21	20.17	0.75	4.28	18.58	34.10
Well 16	13455	Middle Eagle Ford	23.39	7.09	47.77	12.10	8.28	33.64	0.70	3.77	16.42	30.23
Well 16	13460	Middle Eagle Ford	25.84	6.75	41.86	12.06	8.19	44.87	0.41	3.25	15.66	28.68
Well 16	13465	Middle Eagle Ford	29.33	5.92	36.21	11.47	7.65	37.71	0.32	2.82	14.76	26.94
Well 16	13470	Middle Eagle Ford	26.94	6.18	34.20	11.79	7.37	32.99	0.72	2.48	15.59	28.71
Well 16	13475	Middle Eagle Ford	23.65	5.17	29.27	11.08	7.24	27.01	0.17	2.17	15.01	26.06
Well 16	13480	Middle Eagle Ford	26.64	6.13	34.55	11.48	9.12	36.43	0.40	2.60	16.67	29.07
Well 16	13485	Middle Eagle Ford	17.60	6.63	39.39	12.31	9.78	43.95	0.32	3.08	16.78	30.30
Well 16	13490	Middle Eagle Ford	25.87	6.35	37.52	11.87	8.86	53.44	0.57	3.03	16.54	30.37
Well 16	13495	Middle Eagle Ford	20.04	6.96	40.55	11.86	9.63	43.91	0.44	3.16	17.08	30.79
Well 16	13500	Lower Eagle Ford	22.65	6.95	42.67	13.84	10.65	46.64	0.55	3.18	17.58	31.88
Well 16	13505	Lower Eagle Ford	17.81	8.02	47.99	13.40	12.19	37.91	0.56	3.96	19.59	36.01
Well 16	13510	Lower Eagle Ford	16.52	7.78	47.23	15.56	10.61	21.09	0.70	3.52	21.89	40.75
Well 16	13515	Lower Eagle Ford	15.35	6.20	40.11	13.12	7.39	21.79	0.55	3.40	16.82	29.95
Well 16	13520	Lower Eagle Ford	17.04	6.31	37.14	13.10	6.99	17.87	0.61	3.14	16.10	28.90
Well 16	13525	Lower Eagle Ford	16.36	7.58	45.65	16.69	9.21	15.77	0.29	3.77	21.48	38.79
Well 16	13530	Lower Eagle Ford	16.76	6.80	38.30	14.40	8.59	19.83	0.67	3.22	18.34	32.60
Well	13535	Lower Eagle	19.62	7.45	44.89	15.55	9.83	20.54	0.93	3.66	20.97	37.18

16		Ford										
Well 16	13540	Lower Eagle Ford	19.14	6.32	37.01	14.95	8.15	15.11	0.09	3.02	20.24	36.53
Well 16	13545	Lower Eagle Ford	17.74	7.48	44.94	15.94	9.84	17.01	0.33	3.81	20.93	37.91
Well 16	13550	Lower Eagle Ford	20.88	8.44	51.56	15.68	10.78	22.97	0.46	4.33	21.07	37.82
Well 16	13555	Lower Eagle Ford	15.99	9.20	56.45	20.65	12.62	16.38	0.37	4.53	27.87	51.10
Well 16	13560	Lower Eagle Ford	14.78	9.66	52.98	23.69	11.18	16.58	0.52	4.28	27.25	50.04
Well 16	13565	Lower Eagle Ford	15.63	8.95	51.62	21.30	12.29	17.14	0.55	4.06	25.25	47.29
Well 16	13570	Lower Eagle Ford	12.97	8.33	49.03	16.51	9.42	20.00	0.61	4.13	21.38	39.02
Well 16	13575	Lower Eagle Ford	20.08	11.72	70.39	17.95	9.72	23.68	0.65	6.57	24.89	46.33
Well 16	13580	Lower Eagle Ford	19.15	11.02	61.49	18.63	8.43	29.23	0.50	5.33	23.00	42.79
Well 16	13585	Lower Eagle Ford	18.30	11.24	62.15	18.24	8.31	26.39	0.54	5.68	23.34	43.82
Well 16	13590	Lower Eagle Ford	20.19	12.39	76.84	16.89	10.10	26.58	0.60	7.28	24.86	47.08
Well 16	13595	Lower Eagle Ford	22.00	11.95	72.72	18.34	10.21	27.33	0.93	6.70	25.73	49.38
Well 16	13600	Lower Eagle Ford	8.58	2.60	16.05	7.39	2.66	0.87	0.39	1.09	8.97	16.56
Well 16	13605	Lower Eagle Ford	8.17	3.80	18.74	9.54	3.36	0.43	0.50	1.29	11.35	22.55
Well 16	13610	Lower Eagle Ford	8.65	4.37	23.96	9.68	3.98	0.80	0.71	1.68	12.10	23.14
Well 16	13615	Lower Eagle Ford	10.60	5.17	26.42	11.21	4.68	1.67	0.40	2.07	15.18	28.85
Well 16	13620	Lower Eagle Ford	10.05	4.39	21.55	10.65	3.99	0.52	0.60	1.60	13.70	26.16
Well	13625	Lower Eagle	9.51	5.01	25.47	11.80	4.52	0.70	0.57	2.02	14.92	29.02

16		Ford										
Well 17	13650	Middle Eagle Ford	33.981	11.318	68.193	13.236	13.539	20.959	2.066	4.883	22.205	40.852
Well 17	13660	Middle Eagle Ford	28.566	10.176	58.336	12.045	11.161	17.596	1.697	4.224	20.186	37.625
Well 17	13670	Middle Eagle Ford	33.723	10.586	63.462	12.397	13.508	21.928	2.453	4.564	21.280	39.573
Well 17	13680	Middle Eagle Ford	34.288	11.621	69.967	14.042	15.427	22.570	1.788	5.045	23.919	44.655
Well 17	13690	Middle Eagle Ford	34.996	9.539	55.981	15.811	10.921	22.009	1.704	4.084	22.604	41.197
Well 17	13700	Middle Eagle Ford	36.699	9.333	54.010	13.724	9.943	29.887	1.825	4.007	19.776	36.640
Well 17	13710	Middle Eagle Ford	34.479	9.795	55.711	14.734	10.837	22.610	1.298	4.030	21.690	40.003
Well 17	13720	Lower Eagle Ford	35.063	7.545	41.103	13.497	8.079	25.515	0.998	2.971	17.821	31.569
Well 17	13730	Lower Eagle Ford	36.105	7.308	39.609	13.792	8.192	25.688	1.920	2.915	17.768	32.313
Well 17	13740	Lower Eagle Ford	34.536	6.513	31.516	11.875	7.224	27.095	1.275	2.411	16.223	28.090
Well 17	13750	Lower Eagle Ford	37.254	7.401	41.145	13.112	8.558	31.223	1.515	3.224	18.178	31.506
Well 17	13760	Lower Eagle Ford	47.740	8.347	47.328	13.361	10.305	53.685	2.640	4.005	18.599	34.282
Well 17	13770	Lower Eagle Ford	42.861	8.173	47.027	13.849	9.656	26.636	1.350	3.681	19.009	34.827
Well 17	13780	Lower Eagle Ford	38.526	8.807	50.202	15.516	10.430	22.366	1.970	4.301	20.996	38.327
Well 17	13790	Lower Eagle Ford	39.990	8.821	49.943	15.188	9.572	22.651	1.481	4.295	20.155	37.562
Well 17	13800	Lower Eagle Ford	41.129	10.889	59.249	20.338	11.599	16.536	1.771	5.327	26.389	50.920
Well 17	13810	Lower Eagle Ford	33.599	10.537	59.695	17.490	12.068	19.257	1.694	5.386	24.308	45.126
Well	13820	Lower Eagle	24.901	10.781	60.173	19.578	11.223	13.835	1.037	5.640	25.706	48.689

17		Ford										
Well 17	13830	Lower Eagle Ford	41.033	8.182	42.441	16.311	8.455	22.366	1.460	3.615	20.071	36.797
Well 17	13840	Lower Eagle Ford	42.698	13.437	76.680	19.373	10.148	28.685	1.921	8.388	26.116	51.088
Well 19	13690	Upper Eagle Ford	21.44	4.73	29.60	8.64	5.20	4.68	0.60	1.89	12.02	18.34
Well 19	13695	Upper Eagle Ford	26.14	6.02	38.27	10.35	6.57	4.71	0.71	2.40	13.70	22.86
Well 19	13700	Upper Eagle Ford	22.36	11.23	67.65	16.81	15.30	2.77	1.09	4.38	26.57	50.52
Well 19	13705	Upper Eagle Ford	30.59	9.36	51.82	12.67	8.54	15.08	0.96	3.68	19.15	33.62
Well 19	13710	Upper Eagle Ford	28.75	12.29	76.18	16.95	14.80	10.05	1.06	5.19	26.51	49.07
Well 19	13715	Upper Eagle Ford	27.97	12.19	75.42	17.05	14.80	10.25	0.89	5.21	26.12	48.42
Well 19	13720	Upper Eagle Ford	28.43	12.46	76.57	17.38	15.24	8.91	0.96	5.24	26.77	49.55
Well 19	13725	Middle Eagle Ford	27.29	12.27	77.22	16.25	14.31	13.40	1.43	5.25	25.29	48.02
Well 19	13730	Middle Eagle Ford	27.66	12.12	76.30	15.92	14.52	13.43	1.29	5.22	27.29	47.27
Well 19	13735	Middle Eagle Ford	29.36	12.24	76.37	15.49	14.16	11.96	1.33	5.19	26.55	47.17
Well 19	13740	Middle Eagle Ford	28.08	13.02	82.92	16.63	15.40	13.96	1.32	5.73	28.07	50.56
Well 19	13745	Middle Eagle Ford	29.81	12.85	82.09	16.38	14.93	15.41	1.33	5.61	28.53	49.66
Well 19	13750	Middle Eagle Ford	25.76	13.12	82.89	15.15	16.39	16.27	1.40	5.84	27.31	48.29
Well 19	13755	Middle Eagle Ford	24.66	13.72	85.13	14.95	18.02	14.71	1.37	6.14	29.03	50.19
Well 19	13760	Middle Eagle Ford	30.28	12.91	81.92	15.62	15.08	17.34	1.44	5.55	26.27	48.35
Well	13765	Middle Eagle	25.74	13.17	84.96	15.78	16.14	16.69	1.37	5.86	27.17	50.57

19		Ford										
Well 19	13770	Middle Eagle Ford	28.46	13.65	88.36	15.74	17.03	16.26	1.48	6.06	28.34	51.58
Well 19	13775	Middle Eagle Ford	28.35	13.32	87.45	15.42	16.98	16.08	1.45	6.00	29.36	51.60
Well 19	13780	Middle Eagle Ford	32.67	14.13	90.99	15.77	18.17	17.33	1.53	6.23	28.94	53.77
Well 19	13785	Middle Eagle Ford	27.19	12.07	76.03	14.95	14.31	13.46	1.17	5.19	24.75	45.21
Well 19	13790	Middle Eagle Ford	28.39	14.17	89.12	16.15	18.37	13.63	1.49	6.10	29.33	52.66
Well 19	13795	Middle Eagle Ford	29.26	14.22	91.97	16.34	19.20	15.33	1.47	6.25	29.58	54.14
Well 19	13800	Middle Eagle Ford	27.64	14.18	90.27	16.22	18.49	15.14	1.42	6.16	29.83	52.75
Well 19	13805	Middle Eagle Ford	30.11	14.46	92.01	16.61	19.48	17.13	1.37	6.25	30.12	55.97
Well 19	13810	Middle Eagle Ford	26.76	13.34	84.28	14.27	16.53	17.81	1.19	5.80	27.48	48.66
Well 19	13815	Middle Eagle Ford	31.39	17.18	109.69	18.45	20.33	15.75	1.74	7.54	34.07	62.84
Well 19	13825	Middle Eagle Ford	37.46	17.19	103.53	17.01	18.88	19.99	1.87	7.25	32.67	59.95
Well 19	13830	Middle Eagle Ford	25.96	16.90	108.03	18.66	20.56	14.51	1.34	7.75	34.45	62.76
Well 19	13835	Middle Eagle Ford	31.63	16.67	106.05	18.51	18.59	21.59	1.45	7.65	33.09	60.41
Well 19	13840	Middle Eagle Ford	28.85	15.67	98.28	16.96	19.61	18.11	1.39	7.20	30.98	57.42
Well 19	13845	Middle Eagle Ford	29.91	17.14	106.68	18.27	22.28	17.74	1.26	7.89	34.86	61.77
Well 19	13850	Middle Eagle Ford	30.77	16.76	104.19	20.82	21.75	15.56	1.36	7.75	38.15	67.62
Well 19	13855	Middle Eagle Ford	31.78	17.56	109.37	20.91	22.69	14.35	1.44	8.09	39.47	72.09
Well	13860	Middle Eagle	33.39	17.24	106.05	20.38	21.14	16.11	1.44	7.70	36.01	64.26

19		Ford										
Well 19	13865	Middle Eagle Ford	35.91	17.81	109.89	21.83	21.89	14.59	1.36	8.18	38.63	68.23
Well 19	13870	Middle Eagle Ford	34.87	15.47	93.54	21.69	19.27	15.81	1.06	6.83	35.65	62.01
Well 19	13875	Middle Eagle Ford	36.81	13.62	80.08	24.48	15.30	20.91	0.89	5.98	33.86	61.83
Well 19	13880	Middle Eagle Ford	35.91	13.56	78.69	19.00	14.89	17.62	1.22	5.77	28.84	53.61
Well 19	13885	Middle Eagle Ford	32.46	12.94	75.31	20.33	14.02	18.08	0.93	5.73	30.07	54.01
Well 19	13890	Middle Eagle Ford	35.02	11.13	67.61	19.07	12.13	16.69	0.86	5.30	26.13	46.77
Well 19	13895	Middle Eagle Ford	38.61	10.74	67.02	18.99	11.70	21.80	0.85	5.40	25.42	44.86
Well 19	13900	Middle Eagle Ford	36.79	10.89	63.95	17.35	12.36	22.78	0.83	5.09	25.00	45.21
Well 19	13905	Middle Eagle Ford	35.01	10.04	62.60	18.98	11.96	17.30	0.82	5.13	25.72	46.56
Well 19	13910	Middle Eagle Ford	36.11	10.78	66.11	16.96	12.80	28.32	0.80	5.46	25.82	44.43
Well 19	13915	Lower Eagle Ford	32.21	10.74	64.74	17.08	12.78	19.58	0.83	5.23	25.38	43.63
Well 19	13920	Lower Eagle Ford	24.28	10.22	60.55	16.25	12.62	16.61	0.71	5.08	23.71	42.16
Well 19	13925	Lower Eagle Ford	32.68	11.09	64.60	16.72	12.95	17.82	0.76	5.26	25.23	44.44
Well 19	13930	Lower Eagle Ford	36.77	10.57	63.92	17.35	12.42	24.93	1.04	5.35	25.17	44.95
Well 19	13935	Lower Eagle Ford	33.11	12.41	77.14	20.56	14.19	10.30	0.98	6.49	29.06	54.02
Well 19	13940	Lower Eagle Ford	28.41	13.16	79.63	20.41	14.12	9.73	0.89	6.79	29.47	55.23
Well 19	13945	Lower Eagle Ford	32.43	12.71	78.03	21.19	14.01	11.02	1.02	6.59	29.78	54.90
Well	13950	Lower Eagle	25.44	12.75	73.45	24.54	12.70	18.76	1.06	6.06	29.95	56.60

19		Ford										
Well 19	13955	Lower Eagle Ford	46.47	11.69	68.24	25.26	11.57	27.40	0.94	5.45	31.82	56.30
Well 19	13960	Lower Eagle Ford	21.79	11.96	71.08	17.84	13.45	17.19	0.85	5.45	27.01	48.21
Well 19	13965	Lower Eagle Ford	36.51	11.88	72.81	17.93	13.13	16.38	1.02	5.68	27.62	48.19
Well 19	13970	Lower Eagle Ford	36.37	14.22	80.23	19.13	11.86	25.36	1.08	6.83	27.68	50.97
Well 19	13975	Lower Eagle Ford	30.46	13.65	79.03	18.90	13.18	18.51	1.05	6.66	29.14	51.34
Well 19	13980	Lower Eagle Ford	29.82	13.11	76.48	20.01	13.48	15.05	1.33	6.28	29.67	52.86
Well 19	13985	Lower Eagle Ford	34.15	12.80	74.97	20.26	13.90	14.92	0.97	6.24	28.46	52.87
Well 19	13990	Lower Eagle Ford	31.39	12.94	75.27	20.08	13.23	16.59	1.31	6.08	27.81	50.25
Well 19	13995	Lower Eagle Ford	35.00	12.27	71.67	18.90	12.97	18.64	0.91	5.80	27.61	50.29
Well 19	14000	Lower Eagle Ford	27.22	10.59	63.29	16.03	11.13	17.32	1.07	4.94	23.36	43.02
Well 20	13660	Upper Eagle Ford	22.925	9.990	60.806	15.214	14.158	2.392	0.948	3.862	22.228	42.996
Well 20	13665	Upper Eagle Ford	27.716	10.474	62.928	15.848	13.257	7.888	0.816	4.179	22.892	43.479
Well 20	13670	Upper Eagle Ford	27.937	9.758	56.650	14.499	11.141	11.432	0.733	3.874	20.122	39.484
Well 20	13675	Upper Eagle Ford	32.491	9.730	54.939	13.510	9.497	14.713	0.718	3.807	20.283	36.049
Well 20	13680	Middle Eagle Ford	30.443	9.855	55.286	13.395	9.134	15.448	0.711	3.872	22.250	34.678
Well 20	13685	Middle Eagle Ford	29.859	10.155	60.437	14.675	11.130	10.514	0.865	4.233	22.416	38.266
Well 20	13690	Middle Eagle Ford	23.597	11.413	69.936	17.894	15.374	6.954	0.896	4.705	27.642	47.606
Well	13695	Middle Eagle	30.969	13.523	85.938	18.708	18.143	11.082	0.950	5.911	33.355	54.048

20		Ford										
Well 20	13700	Middle Eagle Ford	27.765	12.255	78.201	15.991	16.376	13.542	1.078	5.279	26.977	49.647
Well 20	13705	Middle Eagle Ford	29.976	12.526	79.120	16.087	16.804	11.702	1.027	5.341	25.870	48.583
Well 20	13710	Middle Eagle Ford	27.970	12.517	79.647	15.513	15.441	12.105	1.090	5.432	27.044	47.474
Well 20	13715	Middle Eagle Ford	31.066	13.194	85.886	16.673	15.948	12.845	1.421	5.848	28.151	51.282
Well 20	13720	Middle Eagle Ford	30.998	13.862	88.419	16.506	16.826	12.138	1.317	6.057	28.284	52.303
Well 20	13725	Middle Eagle Ford	29.917	12.875	82.402	16.338	16.072	13.096	1.172	5.630	27.088	50.075
Well 20	13730	Middle Eagle Ford	29.343	13.146	86.561	16.159	16.410	16.166	1.311	5.928	26.335	50.393
Well 20	13740	Middle Eagle Ford	26.460	12.294	78.687	14.484	15.363	13.096	1.197	5.345	23.977	46.278
Well 20	13745	Middle Eagle Ford	29.197	14.269	94.362	15.776	19.506	14.566	1.389	6.512	31.085	54.333
Well 20	13750	Middle Eagle Ford	29.537	14.337	93.802	16.518	19.753	11.942	1.375	6.544	29.591	53.686
Well 20	13755	Middle Eagle Ford	28.710	13.959	90.129	16.446	18.999	12.628	1.245	6.290	28.561	53.653
Well 20	13760	Middle Eagle Ford	29.489	14.472	94.446	17.021	20.114	13.673	1.393	6.640	34.905	55.749
Well 20	13765	Middle Eagle Ford	27.882	13.475	88.271	16.590	17.884	14.000	1.098	6.061	31.152	52.358
Well 20	13770	Middle Eagle Ford	23.227	13.320	86.160	16.135	17.727	13.488	0.833	5.947	28.838	50.569
Well 20	13785	Middle Eagle Ford	35.751	13.862	86.836	16.697	16.860	13.183	1.238	6.077	28.162	51.458
Well 20	13788	Middle Eagle Ford	37.603	23.141	37.799	27.248	19.467	6.366	2.371	3.019	42.486	84.313
Well 20	13790	Middle Eagle Ford	5.332	13.283	80.651	19.271	18.180	24.724	0.714	5.744	35.814	65.744
Well	13793	Middle Eagle	35.452	15.954	99.687	16.215	18.742	21.596	1.283	7.174	30.016	57.370

20		Ford										
Well 20	13796	Middle Eagle Ford	29.974	18.155	117.156	19.817	23.371	11.852	1.887	8.238	34.722	64.637
Well 20	13799	Middle Eagle Ford	23.983	18.423	117.679	17.976	22.225	10.857	1.754	8.636	33.718	60.899
Well 20	13802	Middle Eagle Ford	28.197	18.691	118.724	22.123	21.165	14.804	1.891	8.963	37.561	70.501
Well 20	13805	Middle Eagle Ford	35.037	21.744	142.978	20.089	22.841	14.256	2.211	10.544	36.557	64.933
Well 20	13808	Middle Eagle Ford	36.705	19.016	122.906	18.385	26.918	15.294	1.818	9.136	36.262	63.157
Well 20	13811	Middle Eagle Ford	27.151	17.121	107.329	20.408	21.121	14.629	1.599	8.022	34.678	65.404
Well 20	13814	Middle Eagle Ford	42.311	23.744	150.505	19.612	24.106	21.934	2.344	11.338	39.374	70.074
Well 20	13816	Middle Eagle Ford	44.197	19.772	122.801	14.567	23.393	29.403	1.854	9.439	30.868	53.336
Well 20	13819	Middle Eagle Ford	31.484	13.130	80.734	14.420	15.044	22.611	1.195	5.842	25.550	49.028
Well 20	13822	Middle Eagle Ford	34.297	21.007	126.983	23.873	29.027	14.104	1.949	9.870	43.545	84.061
Well 20	13825	Middle Eagle Ford	41.384	19.686	125.310	14.260	27.773	22.518	1.734	9.427	30.638	47.877
Well 20	13828	Middle Eagle Ford	38.896	17.667	103.859	14.226	28.919	30.978	1.524	7.717	28.695	49.554
Well 20	13831	Middle Eagle Ford	48.905	17.791	108.793	14.192	19.986	35.810	1.399	8.015	27.592	45.225
Well 20	13834	Middle Eagle Ford	41.009	16.729	98.715	18.465	26.075	4.914	1.356	7.222	33.270	59.156
Well 20	13837	Middle Eagle Ford	30.556	15.810	92.443	14.192	24.355	15.808	1.126	6.828	27.188	46.551
Well 20	13840	Middle Eagle Ford	9.304	12.623	69.141	12.817	13.118	85.989	0.705	5.250	21.237	37.387
Well 20	13842	Middle Eagle Ford	41.364	13.609	78.006	35.906	16.255	18.235	0.819	5.822	42.966	73.329
Well	13844	Middle Eagle	232.360	10.211	61.415	15.135	16.752	30.022	2.644	4.229	25.179	44.863

20		Ford										
Well 20	13846.4	Middle Eagle Ford	42.588	23.180	147.264	17.260	23.252	22.868	2.254	11.122	36.262	62.916
Well 20	13850	Middle Eagle Ford	35.283	12.149	73.620	19.426	13.832	19.204	0.670	5.955	26.734	48.264
Well 20	13851	Middle Eagle Ford	66.908	16.202	97.178	17.056	19.813	19.916	1.222	7.372	30.737	53.259
Well 20	13854	Middle Eagle Ford	40.150	11.293	64.165	21.987	12.318	12.027	0.789	5.045	28.378	50.059
Well 20	13855	Middle Eagle Ford	29.051	13.281	79.457	19.988	15.723	15.774	0.743	6.126	28.173	52.950
Well 20	13857	Middle Eagle Ford	36.893	13.341	68.378	19.533	13.118	16.030	1.106	5.333	27.024	49.050
Well 20	13860	Middle Eagle Ford	44.424	14.384	67.782	24.066	13.302	14.466	1.253	5.517	31.457	66.796
Well 20	13863	Lower Eagle Ford	40.515	9.943	62.492	20.442	10.622	13.521	0.811	5.298	24.786	47.461
Well 20	13866	Lower Eagle Ford	42.272	10.642	64.729	16.681	10.977	20.184	0.852	5.369	22.056	40.577
Well 20	13869	Lower Eagle Ford	73.146	16.805	96.123	15.476	16.547	58.694	1.258	8.225	26.587	46.452
Well 20	13872	Lower Eagle Ford	62.812	15.169	86.819	18.135	14.492	45.811	1.121	7.322	25.648	48.261
Well 20	13875	Lower Eagle Ford	44.848	10.967	65.586	18.896	12.242	22.623	0.828	5.364	24.939	44.435
Well 20	13876.9	Lower Eagle Ford	46.319	10.824	60.694	23.089	12.264	27.618	0.806	4.901	29.088	55.101
Well 20	13880	Lower Eagle Ford	58.242	15.858	77.065	15.976	15.065	35.273	1.521	6.677	26.762	45.225
Well 20	13883	Lower Eagle Ford	39.044	12.116	68.838	16.783	13.886	8.181	0.981	5.847	23.202	43.986
Well 20	13885	Lower Eagle Ford	36.539	11.955	66.685	19.294	13.595	19.803	0.624	5.611	27.664	48.187
Well 20	13889	Lower Eagle Ford	37.821	10.967	66.266	15.431	14.697	9.428	0.865	5.631	22.635	39.558
Well	13892	Lower Eagle	41.512	13.216	74.023	17.249	13.086	8.574	1.010	6.150	24.928	46.376

20		Ford										
Well 20	13895	Lower Eagle Ford	29.875	10.536	64.834	16.044	13.129	3.435	1.107	5.374	23.257	43.591
Well 20	13898	Lower Eagle Ford	35.205	13.551	89.129	21.419	16.298	2.832	1.200	7.465	29.284	59.518
Well 20	13901	Lower Eagle Ford	55.241	15.121	84.404	22.180	15.984	37.700	1.410	6.840	29.481	52.547
Well 20	13904	Lower Eagle Ford	33.231	13.532	79.542	19.021	12.048	3.471	1.127	6.945	26.041	48.667
Well 20	13906	Lower Eagle Ford	33.004	15.494	94.325	16.715	16.958	4.549	1.194	8.243	25.659	49.302
Well 20	13909	Lower Eagle Ford	37.248	13.054	78.372	24.203	13.930	7.965	1.003	6.624	30.999	53.939
Well 20	13912	Lower Eagle Ford	38.235	13.006	81.978	20.976	14.946	5.299	1.013	6.796	28.455	52.229
Well 20	13915	Lower Eagle Ford	36.399	13.006	67.959	24.385	12.080	6.365	1.231	5.808	31.971	55.660
Well 20	13918	Lower Eagle Ford	34.475	15.016	68.085	10.088	14.935	5.213	1.089	5.843	20.800	37.716
Well 20	13921	Lower Eagle Ford	48.668	14.078	75.403	36.236	11.756	13.987	1.101	6.096	38.511	83.786
Well 20	13924	Lower Eagle Ford	56.080	7.387	34.841	12.954	3.943	41.283	0.475	2.647	13.506	21.022
Well 20	13927	Lower Eagle Ford	21.357	5.260	29.666	11.129	6.746	7.196	0.491	2.171	17.830	31.139
Well 20	13930	Lower Eagle Ford	37.623	13.848	74.901	19.760	9.581	18.025	0.846	6.078	24.578	41.268
Well 24	14040	Middle Eagle Ford	38.321	9.085	53.322	13.926	13.218	2.933	1.325	3.310	19.440	33.898
Well 24	14100	Middle Eagle Ford	28.788	15.956	100.486	19.539	23.175	2.194	2.059	6.738	33.762	62.049
Well 24	14150	Middle Eagle Ford	27.722	15.709	99.828	19.643	22.975	3.354	1.873	6.553	34.010	61.532
Well 24	14175	Middle Eagle Ford	35.416	17.032	101.936	21.996	20.680	8.581	1.855	7.817	35.161	64.635
Well	14190	Lower Eagle	18.818	7.750	44.323	12.836	7.585	4.051	1.236	3.210	17.041	32.295

24		Ford										
Well 24	14200	Lower Eagle Ford	16.056	9.187	52.512	14.500	9.157	1.116	1.474	3.839	21.743	41.440
Well 24	14210	Lower Eagle Ford	15.770	8.919	50.434	14.293	8.250	0.982	1.459	3.758	21.237	41.037
Well 24	14220	Lower Eagle Ford	13.256	4.311	23.346	8.463	4.233	0.941	0.825	1.620	9.864	17.707

Well	Depth	Formation Top	Pr (ppm)	Nd (ppm)	Sm (ppm)	Eu (ppm)	Gd (ppm)	Tb (ppm)	Dy (ppm)	Ho (ppm)
Well 3	12660	Upper Eagle Ford	1.86	6.85	1.39	0.45	1.47	0.23	1.36	0.3
Well 3	12665	Upper Eagle Ford	1.84	7.06	1.38	0.43	1.4	0.2	1.23	0.27
Well 3	12670	Upper Eagle Ford	1.99	8.01	1.63	0.51	1.62	0.24	1.34	0.29
Well 3	12675	Upper Eagle Ford	2.96	10.88	2.14	0.54	1.95	0.26	1.5	0.31
Well 3	12685	Upper Eagle Ford	2.29	8.47	1.77	0.54	1.68	0.26	1.4	0.32
Well 3	12690	Upper Eagle Ford	2.08	8.11	1.65	0.52	1.66	0.24	1.41	0.29
Well 3	12695	Upper Eagle Ford	1.95	7.56	1.5	0.5	1.57	0.23	1.3	0.27
Well 3	12700	Upper Eagle Ford	2.16	8.34	1.75	0.55	1.65	0.24	1.44	0.3
Well 3	12705	Upper Eagle Ford	2.14	8.03	1.68	0.54	1.76	0.24	1.39	0.3
Well 3	12710	Upper Eagle Ford	2.53	9.67	2.05	0.59	1.9	0.29	1.68	0.34
Well 3	12715	Upper Eagle Ford	2.54	9.77	1.92	0.57	2	0.29	1.56	0.35
Well 3	12720	Middle Eagle Ford	2.27	8.84	1.76	0.85	1.78	0.26	1.46	0.32
Well 3	12725	Middle Eagle Ford	2.27	8.38	1.46	0.57	1.56	0.23	1.26	0.27
Well 3	12730	Middle Eagle Ford	2.63	9.75	1.93	0.63	1.88	0.27	1.48	0.33
Well 3	12735	Middle Eagle Ford	1.22	4.87	1.06	0.47	0.95	0.14	0.76	0.16
Well 3	12745	Middle Eagle Ford	2.98	11.12	2.23	0.68	2.13	0.32	1.68	0.36
Well 3	12750	Middle Eagle Ford	2.1	8.01	1.66	0.76	1.54	0.22	1.27	0.28
Well 3	12755	Middle Eagle Ford	3.42	12.91	2.51	0.65	2.36	0.34	1.78	0.39
Well 3	12760	Middle Eagle Ford	2.2	8.15	1.52	0.54	1.51	0.23	1.32	0.28
Well 3	12765	Lower Eagle Ford	2.32	8.87	1.64	0.62	1.69	0.26	1.36	0.28
Well 3	12770	Lower Eagle Ford	2.79	10.34	1.96	0.6	1.95	0.28	1.57	0.32
Well 3	12775	Lower Eagle Ford	3.08	11.73	2.35	0.71	2.34	0.31	1.8	0.38
Well 3	12780	Lower Eagle Ford	3.39	12.86	2.41	0.79	2.54	0.36	2.12	0.45
Well 3	12785	Lower Eagle Ford	3.55	13.48	2.73	0.72	2.81	0.39	2.12	0.46

Well 3	12790	Lower Eagle Ford	3.42	13.05	2.42	0.79	2.59	0.36	2	0.43
Well 3	12800	Lower Eagle Ford	3.01	11.16	2.25	0.71	2.12	0.32	1.75	0.39
Well 3	12805	Lower Eagle Ford	3.28	12.59	2.48	0.76	2.42	0.35	2.04	0.44
Well 3	12810	Lower Eagle Ford	3.48	12.81	2.5	0.71	2.46	0.36	2.03	0.42
Well 3	12815	Lower Eagle Ford	3.46	13.21	2.62	0.71	2.45	0.37	1.99	0.42
Well 3	12820	Lower Eagle Ford	3.46	13.04	2.51	0.72	2.42	0.35	1.97	0.42
Well 3	12825	Lower Eagle Ford	3.32	12.42	2.46	0.74	2.22	0.33	1.86	0.4
Well 3	12830	Lower Eagle Ford	4.32	16.28	3.19	0.84	2.96	0.43	2.34	0.51
Well 3	12835	Lower Eagle Ford	4.54	16.49	2.92	0.75	2.69	0.37	2.07	0.43
Well 3	12840	Lower Eagle Ford	4.74	17.22	3.17	0.74	2.79	0.39	2.14	0.45
Well 3	12845	Lower Eagle Ford	3.78	13.86	2.57	0.84	2.53	0.35	2.02	0.42
Well 3	12850	Lower Eagle Ford	4.03	15.06	2.79	0.81	2.51	0.39	2.16	0.42
Well 3	12855	Lower Eagle Ford	3.04	11.24	2.08	0.67	2.04	0.3	1.65	0.35
Well 3	12860	Lower Eagle Ford	3.39	12.74	2.44	0.81	2.28	0.34	1.91	0.39
Well 3	12865	Lower Eagle Ford	3.34	12.53	2.49	0.79	2.4	0.33	1.95	0.4
Well 3	12870	Lower Eagle Ford	3.7	13.86	2.72	0.83	2.64	0.37	2.05	0.45
Well 3	12875	Lower Eagle Ford	4.66	17.41	3.31	0.88	3.24	0.47	2.58	0.53
Well 3	12880	Lower Eagle Ford	6.45	24.89	4.9	1.25	4.94	0.67	3.75	0.75
Well 3	12885	Lower Eagle Ford	5.58	21.54	4.23	1.04	4.19	0.59	3.25	0.7
Well 12	13440	Upper Eagle Ford	0.598	2.282	0.461	0.273	0.536	0.072	0.396	0.095
Well 12	13450	Upper Eagle Ford	0.784	2.985	0.492	0.313	0.585	0.085	0.426	0.106
Well 12	13460	Upper Eagle Ford	2.723	10.334	2.022	0.622	1.986	0.297	1.723	0.374
Well 12	13470	Upper Eagle Ford	2.826	10.785	2.100	0.706	2.041	0.305	1.764	0.384
Well 12	13480	Upper Eagle Ford	2.915	11.226	2.176	0.646	2.128	0.304	1.754	0.373
Well 12	13490	Upper Eagle Ford	3.314	12.305	2.519	0.798	2.384	0.356	1.916	0.423
Well 12	13500	Upper Eagle Ford	4.000	14.815	2.840	0.793	2.478	0.376	2.009	0.409
Well 12	13510	Upper Eagle Ford	4.430	16.217	2.990	0.838	2.712	0.401	2.150	0.491
Well 12	13516	Upper Eagle Ford	3.839	14.089	2.788	0.698	2.652	0.362	2.110	0.426
Well 12	13525	Upper Eagle Ford	4.819	17.197	3.384	0.857	2.948	0.411	2.191	0.474
Well 12	13535	Middle Eagle Ford	5.254	18.825	3.450	0.945	3.134	0.462	2.355	0.510

Well 12	13545	Middle Eagle Ford	4.800	17.893	3.364	0.840	2.936	0.440	2.422	0.492
Well 12	13555	Middle Eagle Ford	4.081	14.766	2.714	0.718	2.631	0.375	2.035	0.450
Well 12	13565	Middle Eagle Ford	4.056	15.609	2.859	0.793	2.598	0.398	2.296	0.456
Well 12	13575	Middle Eagle Ford	3.241	12.295	2.317	0.761	2.211	0.311	1.722	0.378
Well 12	13585	Middle Eagle Ford	2.320	8.945	1.580	0.561	1.552	0.235	1.332	0.261
Well 12	13595	Middle Eagle Ford	3.823	14.628	2.760	0.767	2.706	0.389	2.164	0.454
Well 12	13606	Lower Eagle Ford	3.379	12.422	2.385	0.729	2.271	0.308	1.804	0.384
Well 12	13620	Lower Eagle Ford	3.950	15.070	2.875	0.792	2.675	0.402	2.296	0.459
Well 12	13630	Lower Eagle Ford	3.938	14.873	2.917	0.955	2.801	0.407	2.181	0.472
Well 12	13640	Lower Eagle Ford	4.280	15.883	3.236	0.912	3.198	0.437	2.502	0.524
Well 12	13650	Lower Eagle Ford	4.267	16.452	3.288	0.987	2.958	0.449	2.446	0.517
Well 12	13660	Lower Eagle Ford	4.355	16.599	3.336	0.870	3.195	0.451	2.549	0.525
Well 12	13670	Lower Eagle Ford	4.356	15.952	3.135	0.832	3.103	0.447	2.406	0.506
Well 12	13680	Lower Eagle Ford	4.903	18.246	3.345	0.919	3.290	0.471	2.540	0.533
Well 12	13690	Lower Eagle Ford	5.145	19.589	3.833	0.994	3.516	0.530	2.795	0.573
Well 12	13699	Lower Eagle Ford	4.731	17.923	3.394	0.947	3.185	0.471	2.714	0.532
Well 12	13710	Lower Eagle Ford	5.263	19.972	3.733	0.895	3.538	0.472	2.674	0.591
Well 12	13720	Lower Eagle Ford	5.756	22.031	4.321	1.079	4.321	0.622	3.472	0.730
Well 12	13730	Lower Eagle Ford	7.095	27.580	5.401	1.330	5.164	0.749	4.196	0.869
Well 12	13740	Lower Eagle Ford	1.793	6.791	1.438	0.515	1.212	0.200	1.023	0.200
Well 12	13750	Lower Eagle Ford	3.182	11.726	2.458	0.647	2.128	0.322	1.684	0.360
Well 16	13370	Upper Eagle Ford	2.38	8.96	1.68	0.66	1.75	0.26	1.39	0.30
Well 16	13375	Upper Eagle Ford	3.17	12.20	2.37	0.73	2.29	0.36	1.89	0.40
Well 16	13380	Upper Eagle Ford	2.98	11.66	2.18	0.68	2.26	0.31	1.70	0.34
Well 16	13385	Upper Eagle Ford	3.30	12.62	2.35	0.88	2.35	0.36	2.11	0.43
Well 16	13390	Upper Eagle Ford	3.37	12.79	2.38	0.83	2.51	0.38	2.00	0.40
Well 16	13395	Upper Eagle Ford	4.06	14.94	2.83	0.76	2.56	0.39	2.01	0.43
Well 16	13400	Upper Eagle Ford	4.12	15.02	2.82	0.79	2.66	0.37	2.08	0.44
Well 16	13405	Upper Eagle Ford	3.91	14.53	2.70	0.79	2.45	0.38	1.91	0.41

Well 16	13410	Upper Eagle Ford	4.46	16.56	3.06	0.97	2.79	0.41	2.21	0.47
Well 16	13415	Upper Eagle Ford	4.45	15.90	2.99	1.00	2.70	0.37	2.06	0.43
Well 16	13420	Upper Eagle Ford	4.41	16.61	3.25	0.97	2.84	0.41	2.26	0.46
Well 16	13425	Upper Eagle Ford	3.78	13.77	2.51	0.78	2.46	0.34	1.96	0.41
Well 16	13430	Upper Eagle Ford	3.03	10.88	2.18	0.71	2.10	0.29	1.72	0.34
Well 16	13435	Middle Eagle Ford	3.54	13.14	2.39	0.75	2.35	0.34	1.84	0.38
Well 16	13440	Middle Eagle Ford	4.27	15.84	2.85	0.96	2.87	0.40	2.27	0.47
Well 16	13445	Middle Eagle Ford	4.05	14.99	2.74	0.87	2.69	0.38	2.10	0.43
Well 16	13450	Middle Eagle Ford	4.00	14.78	2.84	0.82	2.54	0.38	2.09	0.45
Well 16	13455	Middle Eagle Ford	3.64	13.60	2.61	0.86	2.46	0.36	1.96	0.44
Well 16	13460	Middle Eagle Ford	3.52	13.60	2.52	0.73	2.53	0.38	2.04	0.41
Well 16	13465	Middle Eagle Ford	3.27	12.68	2.48	0.81	2.30	0.34	1.89	0.37
Well 16	13470	Middle Eagle Ford	3.46	13.07	2.55	0.79	2.45	0.37	1.89	0.41
Well 16	13475	Middle Eagle Ford	3.22	11.69	2.29	0.63	2.10	0.33	1.70	0.37
Well 16	13480	Middle Eagle Ford	3.46	12.48	2.49	0.70	2.38	0.34	1.81	0.38
Well 16	13485	Middle Eagle Ford	3.62	13.31	2.62	0.81	2.44	0.35	1.96	0.41
Well 16	13490	Middle Eagle Ford	3.75	14.05	2.75	0.76	2.50	0.37	2.02	0.42
Well 16	13495	Middle Eagle Ford	3.71	14.09	2.65	0.70	2.57	0.36	2.02	0.39
Well 16	13500	Lower Eagle Ford	3.90	14.52	2.90	0.76	2.78	0.41	2.22	0.49
Well 16	13505	Lower Eagle Ford	4.32	16.19	2.90	0.80	2.84	0.42	2.28	0.47
Well 16	13510	Lower Eagle Ford	4.91	18.18	3.48	0.94	3.29	0.46	2.59	0.53
Well 16	13515	Lower Eagle Ford	3.77	13.64	2.80	0.86	2.73	0.40	2.19	0.44
Well 16	13520	Lower Eagle Ford	3.61	13.41	2.65	0.74	2.59	0.37	2.05	0.44
Well 16	13525	Lower Eagle Ford	4.64	17.44	3.30	0.93	3.38	0.47	2.56	0.56
Well 16	13530	Lower Eagle Ford	4.13	15.04	3.02	0.80	2.83	0.41	2.24	0.49
Well 16	13535	Lower Eagle Ford	4.65	17.60	3.32	0.91	3.12	0.47	2.53	0.52
Well 16	13540	Lower Eagle Ford	4.48	17.04	3.29	0.93	3.23	0.44	2.44	0.52
Well 16	13545	Lower Eagle Ford	4.71	17.85	3.48	0.92	3.33	0.48	2.61	0.55
Well 16	13550	Lower Eagle Ford	4.64	17.34	3.25	0.91	3.21	0.46	2.62	0.53
Well 16	13555	Lower Eagle Ford	6.13	22.18	4.57	1.12	4.02	0.59	3.31	0.67
Well 16	13560	Lower Eagle Ford	6.15	23.27	4.49	1.21	4.56	0.66	3.67	0.76
Well 16	13565	Lower Eagle Ford	5.71	22.13	4.34	1.18	4.16	0.60	3.25	0.69

Well 16	13570	Lower Eagle Ford	4.78	17.83	3.37	0.90	3.16	0.48	2.69	0.55
Well 16	13575	Lower Eagle Ford	5.76	22.09	4.08	1.00	3.86	0.58	3.05	0.61
Well 16	13580	Lower Eagle Ford	5.50	21.07	4.18	1.05	3.85	0.57	3.10	0.65
Well 16	13585	Lower Eagle Ford	5.59	21.46	4.20	1.03	3.89	0.56	3.15	0.64
Well 16	13590	Lower Eagle Ford	5.61	21.00	4.02	0.93	3.52	0.51	2.85	0.59
Well 16	13595	Lower Eagle Ford	6.05	23.34	4.51	1.04	4.10	0.58	3.38	0.63
Well 16	13600	Lower Eagle Ford	2.14	8.20	1.61	0.63	1.48	0.22	1.16	0.24
Well 16	13605	Lower Eagle Ford	2.83	11.03	2.31	0.75	2.03	0.30	1.65	0.34
Well 16	13610	Lower Eagle Ford	2.89	11.20	2.15	0.77	1.99	0.29	1.63	0.33
Well 16	13615	Lower Eagle Ford	3.58	13.84	2.87	0.81	2.62	0.37	1.94	0.39
Well 16	13620	Lower Eagle Ford	3.35	12.94	2.64	0.81	2.35	0.34	1.83	0.36
Well 16	13625	Lower Eagle Ford	3.58	14.15	2.72	0.91	2.59	0.37	2.05	0.39
Well 17	13650	Middle Eagle Ford	4.597	16.850	3.190	0.692	2.662	0.399	2.283	0.478
Well 17	13660	Middle Eagle Ford	4.184	15.581	2.894	0.626	2.488	0.355	2.053	0.428
Well 17	13670	Middle Eagle Ford	4.427	16.361	2.985	0.684	2.590	0.383	2.195	0.451
Well 17	13680	Middle Eagle Ford	4.925	18.004	3.376	0.757	2.887	0.418	2.411	0.494
Well 17	13690	Middle Eagle Ford	4.855	18.441	3.448	0.798	3.077	0.446	2.595	0.534
Well 17	13700	Middle Eagle Ford	4.279	15.820	3.017	0.705	2.751	0.395	2.281	0.485
Well 17	13710	Middle Eagle Ford	4.660	17.526	3.344	0.766	2.849	0.429	2.515	0.511
Well 17	13720	Lower Eagle Ford	3.892	14.842	2.867	0.696	2.555	0.377	2.188	0.462
Well 17	13730	Lower Eagle Ford	3.903	15.092	2.922	0.685	2.580	0.393	2.265	0.463
Well 17	13740	Lower Eagle Ford	3.480	13.147	2.563	0.593	2.287	0.339	1.925	0.412
Well 17	13750	Lower Eagle Ford	3.851	14.697	2.737	0.650	2.491	0.361	2.143	0.440
Well 17	13760	Lower Eagle Ford	4.092	15.654	3.009	0.687	2.583	0.383	2.259	0.469
Well 17	13770	Lower Eagle Ford	4.141	15.862	3.025	0.690	2.685	0.394	2.261	0.470
Well 17	13780	Lower Eagle Ford	4.587	17.432	3.353	0.766	2.999	0.458	2.535	0.538
Well 17	13790	Lower Eagle Ford	4.480	17.162	3.350	0.752	2.975	0.443	2.541	0.530
Well 17	13800	Lower Eagle Ford	6.028	23.339	4.551	0.906	4.016	0.601	3.484	0.709
Well 17	13810	Lower Eagle Ford	5.363	20.178	3.775	0.831	3.318	0.499	2.870	0.626

Well 17	13820	Lower Eagle Ford	5.720	21.852	4.245	0.942	3.775	0.573	3.164	0.666
Well 17	13830	Lower Eagle Ford	4.477	17.442	3.381	0.789	3.072	0.451	2.602	0.552
Well 17	13840	Lower Eagle Ford	6.372	25.149	5.109	1.071	4.386	0.631	3.541	0.696
Well 19	13690	Upper Eagle Ford	2.29	8.52	1.81	0.40	1.50	0.24	1.35	0.27
Well 19	13695	Upper Eagle Ford	2.79	10.57	2.00	0.47	1.79	0.28	1.62	0.34
Well 19	13700	Upper Eagle Ford	5.71	21.35	4.12	0.87	3.41	0.52	2.93	0.60
Well 19	13705	Upper Eagle Ford	3.87	14.54	2.86	0.63	2.35	0.38	2.15	0.45
Well 19	13710	Upper Eagle Ford	5.56	20.65	3.96	0.83	3.33	0.51	2.89	0.60
Well 19	13715	Upper Eagle Ford	5.50	20.55	3.92	0.82	3.26	0.51	2.82	0.59
Well 19	13720	Upper Eagle Ford	5.61	20.77	4.08	0.87	3.39	0.53	2.97	0.61
Well 19	13725	Middle Eagle Ford	5.40	20.03	3.74	0.85	3.24	0.49	2.73	0.56
Well 19	13730	Middle Eagle Ford	5.40	19.93	3.81	0.81	3.14	0.50	2.78	0.55
Well 19	13735	Middle Eagle Ford	5.32	19.66	3.76	0.82	3.02	0.48	2.65	0.55
Well 19	13740	Middle Eagle Ford	5.71	21.08	4.02	0.85	3.30	0.51	2.88	0.57
Well 19	13745	Middle Eagle Ford	5.66	20.87	3.84	0.83	3.25	0.50	2.82	0.58
Well 19	13750	Middle Eagle Ford	5.50	19.87	3.72	0.80	3.08	0.46	2.67	0.54
Well 19	13755	Middle Eagle Ford	5.65	20.46	3.68	0.81	3.10	0.48	2.56	0.54
Well 19	13760	Middle Eagle Ford	5.55	20.31	3.92	0.84	3.12	0.48	2.73	0.55
Well 19	13765	Middle Eagle Ford	5.73	20.78	3.95	0.82	3.20	0.49	2.77	0.56
Well 19	13770	Middle Eagle Ford	5.81	21.40	4.02	0.84	3.24	0.50	2.79	0.56
Well 19	13775	Middle Eagle Ford	5.78	20.82	3.86	0.80	3.24	0.48	2.73	0.55
Well 19	13780	Middle Eagle Ford	6.01	22.09	3.98	0.88	3.30	0.49	2.82	0.56
Well 19	13785	Middle Eagle Ford	5.12	18.78	3.51	0.78	2.95	0.46	2.63	0.53
Well 19	13790	Middle Eagle Ford	5.93	21.56	4.04	0.87	3.26	0.51	2.85	0.58
Well 19	13795	Middle Eagle Ford	6.05	22.11	4.10	0.88	3.32	0.51	2.92	0.59
Well 19	13800	Middle Eagle Ford	5.98	21.76	3.98	0.88	3.36	0.51	2.89	0.57
Well 19	13805	Middle Eagle Ford	6.19	22.62	4.13	0.87	3.46	0.52	2.99	0.60

Well 19	13810	Middle Eagle Ford	5.55	20.34	3.74	0.83	3.01	0.46	2.60	0.53
Well 19	13815	Middle Eagle Ford	7.18	25.90	4.71	1.00	3.80	0.60	3.33	0.68
Well 19	13825	Middle Eagle Ford	6.72	24.60	4.61	0.94	3.56	0.54	3.02	0.62
Well 19	13830	Middle Eagle Ford	7.10	25.74	4.82	1.05	3.80	0.59	3.36	0.68
Well 19	13835	Middle Eagle Ford	6.90	25.37	4.77	1.01	3.82	0.59	3.29	0.66
Well 19	13840	Middle Eagle Ford	6.47	23.60	4.43	0.95	3.52	0.54	2.98	0.61
Well 19	13845	Middle Eagle Ford	6.93	25.28	4.58	1.00	3.69	0.58	3.20	0.66
Well 19	13850	Middle Eagle Ford	7.66	27.94	5.24	1.18	4.30	0.65	3.58	0.73
Well 19	13855	Middle Eagle Ford	8.14	30.47	5.61	1.21	4.56	0.67	3.73	0.74
Well 19	13860	Middle Eagle Ford	7.36	27.19	5.11	1.10	4.05	0.62	3.46	0.71
Well 19	13865	Middle Eagle Ford	7.79	28.41	5.21	1.09	4.35	0.67	3.73	0.77
Well 19	13870	Middle Eagle Ford	7.11	26.24	4.89	1.07	4.15	0.64	3.68	0.73
Well 19	13875	Middle Eagle Ford	7.23	27.57	5.29	1.21	4.63	0.71	3.99	0.82
Well 19	13880	Middle Eagle Ford	6.25	23.28	4.48	1.00	3.69	0.59	3.23	0.66
Well 19	13885	Middle Eagle Ford	6.30	23.89	4.50	1.02	3.87	0.60	3.43	0.71
Well 19	13890	Middle Eagle Ford	5.61	21.36	4.31	0.91	3.51	0.56	3.19	0.64
Well 19	13895	Middle Eagle Ford	5.55	21.25	4.21	0.94	3.54	0.55	3.24	0.63
Well 19	13900	Middle Eagle Ford	5.31	19.94	3.89	0.87	3.25	0.51	2.90	0.59
Well 19	13905	Middle Eagle Ford	5.63	21.43	4.16	0.91	3.61	0.55	3.16	0.66
Well 19	13910	Middle Eagle Ford	5.29	19.82	3.88	0.82	3.23	0.50	2.86	0.60
Well 19	13915	Lower Eagle Ford	5.26	19.72	3.73	0.80	3.28	0.49	2.86	0.58
Well 19	13920	Lower Eagle Ford	4.97	18.68	3.53	0.79	3.06	0.47	2.67	0.56
Well 19	13925	Lower Eagle Ford	5.30	19.59	3.77	0.81	3.16	0.49	2.72	0.57
Well 19	13930	Lower Eagle Ford	5.43	20.52	3.93	0.86	3.34	0.52	2.88	0.61
Well 19	13935	Lower Eagle Ford	6.26	23.34	4.61	1.00	3.85	0.62	3.44	0.70
Well 19	13940	Lower Eagle Ford	6.35	23.78	4.70	0.98	3.85	0.60	3.46	0.72
Well 19	13945	Lower Eagle Ford	6.34	23.74	4.62	0.98	3.96	0.60	3.46	0.73

Well 19	13950	Lower Eagle Ford	6.63	25.29	5.00	1.08	4.29	0.67	3.88	0.82
Well 19	13955	Lower Eagle Ford	6.68	25.74	5.12	1.12	4.41	0.69	3.97	0.83
Well 19	13960	Lower Eagle Ford	5.63	20.98	4.05	0.91	3.41	0.52	3.01	0.61
Well 19	13965	Lower Eagle Ford	5.65	21.05	3.88	0.90	3.44	0.53	2.99	0.61
Well 19	13970	Lower Eagle Ford	6.09	23.44	4.50	0.92	3.69	0.57	3.33	0.68
Well 19	13975	Lower Eagle Ford	6.10	22.89	4.32	0.90	3.68	0.58	3.22	0.68
Well 19	13980	Lower Eagle Ford	6.27	23.71	4.63	0.95	3.74	0.60	3.36	0.70
Well 19	13985	Lower Eagle Ford	6.17	23.03	4.48	0.93	3.83	0.58	3.30	0.70
Well 19	13990	Lower Eagle Ford	5.99	22.68	4.35	0.90	3.66	0.58	3.21	0.69
Well 19	13995	Lower Eagle Ford	5.87	22.06	4.25	0.91	3.48	0.56	3.11	0.65
Well 19	14000	Lower Eagle Ford	5.06	19.05	3.99	0.79	3.01	0.51	2.64	0.56
Well 20	13660	Upper Eagle Ford	4.823	17.605	3.331	0.739	2.949	0.453	2.544	0.534
Well 20	13665	Upper Eagle Ford	4.921	18.217	3.462	0.766	3.029	0.458	2.584	0.544
Well 20	13670	Upper Eagle Ford	4.504	16.557	3.086	0.700	2.725	0.417	2.425	0.490
Well 20	13675	Upper Eagle Ford	4.168	15.387	2.945	0.656	2.611	0.387	2.174	0.465
Well 20	13680	Middle Eagle Ford	3.990	14.873	2.854	0.636	2.522	0.381	2.135	0.460
Well 20	13685	Middle Eagle Ford	4.357	16.096	2.990	0.680	2.700	0.407	2.328	0.490
Well 20	13690	Middle Eagle Ford	5.335	19.388	3.591	0.823	3.313	0.498	2.851	0.602
Well 20	13695	Middle Eagle Ford	6.141	22.121	4.074	0.927	3.570	0.525	3.049	0.634
Well 20	13700	Middle Eagle Ford	5.587	20.243	3.788	0.859	3.287	0.488	2.748	0.565
Well 20	13705	Middle Eagle Ford	5.508	20.159	3.728	0.900	3.308	0.482	2.694	0.558
Well 20	13710	Middle Eagle Ford	5.423	19.800	3.652	0.825	3.210	0.472	2.619	0.550
Well 20	13715	Middle Eagle Ford	5.784	21.783	4.066	0.897	3.489	0.513	2.863	0.583
Well 20	13720	Middle Eagle Ford	5.833	21.667	3.987	0.879	3.377	0.513	2.852	0.589
Well 20	13725	Middle Eagle Ford	5.689	20.781	3.778	0.851	3.292	0.493	2.761	0.572
Well 20	13730	Middle Eagle Ford	5.752	21.098	3.854	0.883	3.382	0.492	2.796	0.565
Well 20	13740	Middle Eagle Ford	5.217	18.808	3.453	0.774	2.996	0.440	2.459	0.512

Well 20	13745	Middle Eagle Ford	6.006	21.615	3.961	0.852	3.387	0.486	2.718	0.570
Well 20	13750	Middle Eagle Ford	6.051	21.952	3.896	0.885	3.391	0.499	2.766	0.578
Well 20	13755	Middle Eagle Ford	6.086	21.847	4.015	0.861	3.435	0.493	2.796	0.582
Well 20	13760	Middle Eagle Ford	6.228	22.427	4.002	0.870	3.502	0.516	2.881	0.592
Well 20	13765	Middle Eagle Ford	5.869	21.161	4.078	0.854	3.383	0.492	2.742	0.574
Well 20	13770	Middle Eagle Ford	5.666	20.559	3.795	0.849	3.254	0.484	2.689	0.554
Well 20	13785	Middle Eagle Ford	5.780	20.834	3.877	0.818	3.332	0.482	2.783	0.578
Well 20	13788	Middle Eagle Ford	9.448	34.534	6.251	1.254	5.467	0.825	4.621	0.953
Well 20	13790	Middle Eagle Ford	7.029	24.648	4.396	1.024	3.971	0.579	3.228	0.663
Well 20	13793	Middle Eagle Ford	6.602	24.134	4.427	0.995	3.718	0.531	2.898	0.609
Well 20	13796	Middle Eagle Ford	7.411	26.912	4.895	1.016	4.202	0.618	3.510	0.730
Well 20	13799	Middle Eagle Ford	6.857	24.941	4.438	1.020	3.827	0.548	3.043	0.654
Well 20	13802	Middle Eagle Ford	8.126	30.099	5.650	1.155	4.878	0.713	3.907	0.793
Well 20	13805	Middle Eagle Ford	7.475	26.545	4.737	1.025	3.935	0.613	3.397	0.740
Well 20	13808	Middle Eagle Ford	6.959	24.522	4.309	0.989	3.656	0.553	3.153	0.669
Well 20	13811	Middle Eagle Ford	7.461	27.384	5.077	1.094	4.354	0.632	3.578	0.737
Well 20	13814	Middle Eagle Ford	8.026	28.768	4.834	0.963	3.953	0.587	3.467	0.746
Well 20	13816	Middle Eagle Ford	5.848	20.108	3.192	0.729	2.706	0.412	2.457	0.554
Well 20	13819	Middle Eagle Ford	5.612	20.832	3.806	0.882	3.278	0.487	2.617	0.541
Well 20	13822	Middle Eagle Ford	9.820	36.641	6.982	1.449	5.892	0.848	4.455	0.882
Well 20	13825	Middle Eagle Ford	4.960	16.166	2.507	0.514	2.062	0.331	2.147	0.504
Well 20	13828	Middle Eagle Ford	5.403	18.557	3.231	0.659	2.704	0.418	2.503	0.541
Well 20	13831	Middle Eagle Ford	5.144	17.854	2.959	0.617	2.466	0.381	2.316	0.513
Well 20	13834	Middle Eagle Ford	6.913	24.941	4.548	0.917	3.653	0.556	3.206	0.682
Well 20	13837	Middle Eagle Ford	5.091	17.728	3.101	0.637	2.513	0.387	2.353	0.518
Well 20	13840	Middle Eagle Ford	4.487	16.156	2.909	0.603	2.524	0.383	2.258	0.491
Well 20	13842	Middle Eagle Ford	9.013	34.177	6.590	1.534	6.242	0.937	5.376	1.151

Well 20	13844	Middle Eagle Ford	5.230	18.745	3.419	0.783	3.048	0.459	2.671	0.545
Well 20	13846.4	Middle Eagle Ford	6.996	23.882	3.656	0.713	3.052	0.471	2.795	0.655
Well 20	13850	Middle Eagle Ford	5.694	21.477	4.046	0.990	3.495	0.544	3.050	0.644
Well 20	13851	Middle Eagle Ford	5.994	21.240	3.727	0.936	3.243	0.484	2.802	0.614
Well 20	13854	Middle Eagle Ford	5.905	22.289	4.155	1.024	3.856	0.581	3.348	0.718
Well 20	13855	Middle Eagle Ford	6.193	22.902	4.350	0.951	3.721	0.561	3.176	0.680
Well 20	13857	Middle Eagle Ford	5.933	22.478	4.244	0.895	3.706	0.559	3.134	0.676
Well 20	13860	Middle Eagle Ford	8.152	31.619	6.473	1.167	5.587	0.842	4.654	0.916
Well 20	13863	Lower Eagle Ford	6.012	23.641	4.751	1.085	4.334	0.621	3.430	0.710
Well 20	13866	Lower Eagle Ford	4.927	18.431	3.591	0.829	3.110	0.484	2.766	0.578
Well 20	13869	Lower Eagle Ford	5.574	19.878	3.268	0.640	2.837	0.429	2.579	0.581
Well 20	13872	Lower Eagle Ford	6.037	22.708	4.216	0.860	3.559	0.542	3.139	0.672
Well 20	13875	Lower Eagle Ford	5.390	20.108	3.874	0.887	3.348	0.512	2.971	0.621
Well 20	13876.9	Lower Eagle Ford	6.797	26.545	5.307	1.257	4.677	0.704	3.843	0.786
Well 20	13880	Lower Eagle Ford	5.332	18.840	3.307	0.689	2.861	0.432	2.498	0.537
Well 20	13883	Lower Eagle Ford	5.215	19.615	3.717	0.772	3.214	0.481	2.811	0.593
Well 20	13885	Lower Eagle Ford	5.784	21.625	4.099	0.900	3.634	0.533	2.989	0.616
Well 20	13889	Lower Eagle Ford	4.706	17.089	3.233	0.707	2.724	0.409	2.411	0.517
Well 20	13892	Lower Eagle Ford	5.560	20.695	3.896	0.819	3.367	0.488	2.794	0.586
Well 20	13895	Lower Eagle Ford	4.989	18.651	3.570	0.772	3.070	0.460	2.580	0.551
Well 20	13898	Lower Eagle Ford	6.718	25.161	4.793	1.049	4.253	0.643	3.608	0.740
Well 20	13901	Lower Eagle Ford	6.218	22.635	4.206	0.946	3.877	0.597	3.447	0.768
Well 20	13904	Lower Eagle Ford	5.637	20.832	3.995	0.827	3.488	0.540	3.021	0.648
Well 20	13906	Lower Eagle Ford	5.506	19.846	3.488	0.670	2.916	0.464	2.676	0.594
Well 20	13909	Lower Eagle Ford	6.431	24.019	4.491	1.043	4.148	0.627	3.650	0.791
Well 20	13912	Lower Eagle Ford	6.214	23.662	4.390	0.964	3.907	0.586	3.405	0.722
Well 20	13915	Lower Eagle Ford	6.469	23.966	4.394	0.936	4.123	0.625	3.667	0.796

Well 20	13918	Lower Eagle Ford	4.100	13.986	2.223	0.419	1.789	0.274	1.639	0.355
Well 20	13921	Lower Eagle Ford	10.872	43.990	9.335	1.872	8.127	1.208	6.504	1.296
Well 20	13924	Lower Eagle Ford	2.794	10.715	2.100	0.500	1.918	0.296	1.782	0.398
Well 20	13927	Lower Eagle Ford	3.473	12.927	2.366	0.539	2.119	0.314	1.786	0.377
Well 20	13930	Lower Eagle Ford	5.310	20.580	3.935	0.892	3.526	0.538	3.123	0.650
Well 24	14040	Middle Eagle Ford	3.939	14.392	2.782	0.669	2.489	0.390	2.268	0.493
Well 24	14100	Middle Eagle Ford	7.045	25.661	4.727	1.073	4.005	0.591	3.439	0.703
Well 24	14150	Middle Eagle Ford	7.002	25.661	4.743	1.073	3.997	0.596	3.448	0.705
Well 24	14175	Middle Eagle Ford	7.459	27.718	5.144	1.099	4.369	0.653	3.770	0.787
Well 24	14190	Lower Eagle Ford	3.983	15.415	3.052	0.645	2.646	0.386	2.219	0.448
Well 24	14200	Lower Eagle Ford	5.039	19.396	3.776	0.748	3.233	0.468	2.733	0.538
Well 24	14210	Lower Eagle Ford	4.995	19.478	3.765	0.758	3.168	0.479	2.709	0.537
Well 24	14220	Lower Eagle Ford	2.246	8.811	1.700	0.369	1.569	0.220	1.347	0.276

Well	Depth	Formation Top	Er (ppm)	Tm (ppm)	Yb (ppm)	Lu (ppm)	Hf (ppm)	Ta (ppm)	Pb (ppm)	Th (ppm)	U (ppm)
Well 3	12660	Upper Eagle Ford	0.86	0.15	0.88	0.13	1.53	0.25	3.9	3.26	3.05
Well 3	12665	Upper Eagle Ford	0.69	0.12	0.67	0.11	1.76	0.29	3.24	3	1.96
Well 3	12670	Upper Eagle Ford	0.8	0.14	0.74	0.12	1.6	0.21	2.75	2	2.43
Well 3	12675	Upper Eagle Ford	0.85	0.14	0.77	0.12	2.03	0.31	3.72	5.42	4.08
Well 3	12685	Upper Eagle Ford	0.86	0.15	0.85	0.12	1.77	0.26	2.22	3.17	2.73
Well 3	12690	Upper Eagle Ford	0.8	0.15	0.84	0.12	1.78	0.23	1.78	2.71	2.66
Well 3	12695	Upper Eagle Ford	0.76	0.14	0.77	0.11	1.73	0.22	2.21	2.45	2.26
Well 3	12700	Upper Eagle Ford	0.81	0.15	0.76	0.13	1.83	0.24	2.13	2.7	1.85
Well 3	12705	Upper Eagle Ford	0.81	0.14	0.77	0.12	1.8	0.25	2.05	2.67	1.85
Well 3	12710	Upper Eagle Ford	0.91	0.16	0.92	0.14	1.83	0.32	1.73	3.54	2.45
Well 3	12715	Upper Eagle Ford	0.9	0.17	0.91	0.14	2.03	0.32	2.5	3.5	2.56
Well 3	12720	Middle Eagle Ford	0.84	0.15	0.85	0.14	2.04	0.29	8.7	3.02	2.48
Well 3	12725	Middle Eagle Ford	0.74	0.13	0.72	0.12	1.66	0.28	2.14	2.75	4.39
Well 3	12730	Middle Eagle Ford	0.87	0.15	0.87	0.12	1.83	0.31	2.02	3.3	4.75
Well 3	12735	Middle Eagle Ford	0.44	0.09	0.43	0.07	1.1	0.12	2.81	1.24	2.32

Well 3	12745	Middle Eagle Ford	1	0.16	0.94	0.14	1.95	0.38	7.63	3.34	5.68
Well 3	12750	Middle Eagle Ford	0.74	0.13	0.71	0.11	1.71	0.3	4.56	2.82	3.34
Well 3	12755	Middle Eagle Ford	1.05	0.18	1.01	0.15	2.08	0.49	1.81	4.03	7.29
Well 3	12760	Middle Eagle Ford	0.74	0.13	0.68	0.11	1.53	0.26	1.78	2.37	4.85
Well 3	12765	Lower Eagle Ford	0.78	0.12	0.73	0.12	1.57	0.31	1.58	2.57	5.2
Well 3	12770	Lower Eagle Ford	0.88	0.16	0.87	0.13	1.69	0.34	1.09	3.1	3.77
Well 3	12775	Lower Eagle Ford	1	0.18	0.99	0.14	1.93	0.4	1.35	3.75	5.87
Well 3	12780	Lower Eagle Ford	1.19	0.2	1.13	0.18	2.04	0.38	1.72	3.87	4.88
Well 3	12785	Lower Eagle Ford	1.27	0.21	1.19	0.18	1.99	0.4	1.47	4.22	5.21
Well 3	12790	Lower Eagle Ford	1.19	0.19	1.1	0.18	1.98	0.4	1.36	3.76	5.26
Well 3	12800	Lower Eagle Ford	1.03	0.18	1.01	0.16	1.84	0.33	3.78	4.22	4.53
Well 3	12805	Lower Eagle Ford	1.13	0.19	1.14	0.17	1.93	0.37	3.68	4.46	5.16
Well 3	12810	Lower Eagle Ford	1.2	0.19	1.2	0.18	2.06	0.45	2.13	5.11	5.3
Well 3	12815	Lower Eagle Ford	1.12	0.19	1.08	0.17	1.97	0.38	2	4.75	5.11
Well 3	12820	Lower Eagle Ford	1.08	0.19	1.05	0.16	1.99	0.43	1.95	4.09	6.53
Well 3	12825	Lower Eagle Ford	1.07	0.18	1.06	0.16	2.01	0.44	1.63	4.14	6.48
Well 3	12830	Lower Eagle Ford	1.35	0.22	1.33	0.2	2.26	0.52	3.39	5.75	5.54
Well 3	12835	Lower Eagle Ford	1.13	0.2	1.14	0.18	2.61	0.65	3.01	9.69	5.75
Well 3	12840	Lower Eagle Ford	1.18	0.21	1.15	0.17	2.67	0.62	2.27	8.89	5.71
Well 3	12845	Lower Eagle Ford	1.1	0.2	1.17	0.16	2.13	0.56	1.9	4.98	4.34
Well 3	12850	Lower Eagle Ford	1.17	0.2	1.09	0.17	2.25	0.6	1.85	5.72	4.76
Well 3	12855	Lower Eagle Ford	0.89	0.16	0.9	0.13	1.76	0.38	2.13	3.49	4.86
Well 3	12860	Lower Eagle Ford	1.11	0.19	1.06	0.16	1.98	0.45	2.28	4.25	3.89
Well 3	12865	Lower Eagle Ford	1.07	0.19	1.07	0.16	1.97	0.45	2.03	4.14	3.9
Well 3	12870	Lower Eagle Ford	1.15	0.19	1.18	0.17	2.1	0.5	2.26	4.62	3.91
Well 3	12875	Lower Eagle Ford	1.47	0.23	1.43	0.22	2.51	0.55	1.59	5.53	4.37
Well 3	12880	Lower Eagle Ford	2.09	0.3	1.88	0.28	3.33	0.72	2.09	7.39	11.83
Well 3	12885	Lower Eagle Ford	1.83	0.28	1.84	0.28	2.98	0.67	2.49	6.67	10.25
Well 12	13440	Upper Eagle Ford	0.264	0.073	0.237	0.037	0.262	0.065	2.968	0.537	0.940
Well 12	13450	Upper Eagle Ford	0.266	0.083	0.279	0.057	0.343	0.104	5.116	0.819	1.069
Well 12	13460	Upper Eagle Ford	0.953	0.192	0.947	0.149	1.428	0.350	2.934	3.143	2.747
Well 12	13470	Upper Eagle Ford	1.012	0.168	0.987	0.149	1.585	0.392	3.345	3.353	2.361

Well 12	13480	Upper Eagle Ford	1.090	0.184	1.032	0.149	1.679	0.393	3.482	3.647	2.937
Well 12	13490	Upper Eagle Ford	1.112	0.197	1.190	0.167	2.003	0.525	3.895	3.941	2.261
Well 12	13500	Upper Eagle Ford	1.137	0.187	1.133	0.187	2.019	0.615	4.672	5.673	4.176
Well 12	13510	Upper Eagle Ford	1.224	0.219	1.189	0.188	2.072	0.691	3.697	5.989	4.282
Well 12	13516	Upper Eagle Ford	1.104	0.165	1.085	0.170	1.975	0.599	3.270	5.301	3.934
Well 12	13525	Upper Eagle Ford	1.269	0.211	1.232	0.196	2.343	0.873	3.819	7.038	4.511
Well 12	13535	Middle Eagle Ford	1.352	0.201	1.394	0.221	2.497	0.927	4.637	7.507	4.629
Well 12	13545	Middle Eagle Ford	1.313	0.208	1.356	0.211	2.268	0.761	2.765	6.572	6.042
Well 12	13555	Middle Eagle Ford	1.223	0.191	1.220	0.195	2.062	0.575	73.436	5.323	7.644
Well 12	13565	Middle Eagle Ford	1.217	0.366	1.218	0.185	1.893	0.597	2.560	5.088	8.011
Well 12	13575	Middle Eagle Ford	1.005	0.179	1.030	0.148	1.628	0.478	2.765	4.373	5.387
Well 12	13585	Middle Eagle Ford	0.742	0.129	0.734	0.104	1.061	0.301	3.059	2.688	3.717
Well 12	13595	Middle Eagle Ford	1.123	0.171	1.219	0.181	1.842	0.559	2.802	4.562	8.737
Well 12	13606	Lower Eagle Ford	1.068	0.150	1.053	0.150	1.567	0.493	1.800	4.273	7.080
Well 12	13620	Lower Eagle Ford	1.281	0.200	1.234	0.177	1.570	0.480	2.289	4.640	4.064
Well 12	13630	Lower Eagle Ford	1.234	0.176	1.156	0.177	1.552	0.500	2.772	4.724	4.078
Well 12	13640	Lower Eagle Ford	1.360	0.195	1.286	0.202	1.883	0.526	2.344	5.198	5.015
Well 12	13650	Lower Eagle Ford	1.359	0.201	1.257	0.196	1.792	0.496	2.941	5.074	4.989
Well 12	13660	Lower Eagle Ford	1.411	0.210	1.364	0.213	1.697	0.550	2.300	5.223	4.000
Well 12	13670	Lower Eagle Ford	1.333	0.206	1.285	0.202	1.727	0.541	1.932	5.323	4.103
Well 12	13680	Lower Eagle Ford	1.413	0.212	1.553	0.209	2.114	0.684	1.773	7.267	4.007
Well 12	13690	Lower Eagle Ford	1.433	0.225	1.407	0.213	1.854	0.541	2.062	5.785	4.575
Well 12	13699	Lower Eagle Ford	1.425	0.217	1.459	0.234	1.956	0.628	1.932	6.293	4.166
Well 12	13710	Lower Eagle Ford	1.527	0.234	1.565	0.239	2.354	0.729	2.257	7.303	4.611
Well 12	13720	Lower Eagle Ford	1.916	0.287	1.849	0.276	2.294	0.558	1.743	6.133	10.999
Well 12	13730	Lower Eagle Ford	2.266	0.357	2.163	0.326	3.184	0.723	3.411	9.233	14.697
Well 12	13740	Lower Eagle Ford	0.560	0.075	0.471	0.068	0.583	0.160	6.160	1.906	0.981

Well 12	13750	Lower Eagle Ford	0.881	0.121	0.861	0.120	0.909	0.247	5.588	3.139	1.151
Well 16	13370.00	Upper Eagle Ford	0.85	0.14	0.78	0.13	1.84	0.40	4.11	3.00	1.91
Well 16	13375.00	Upper Eagle Ford	1.12	0.18	1.07	0.16	2.08	0.47	3.45	3.34	2.00
Well 16	13380.00	Upper Eagle Ford	0.97	0.18	1.01	0.15	2.17	0.44	3.77	3.20	2.07
Well 16	13385.00	Upper Eagle Ford	1.13	0.19	1.06	0.16	2.12	0.47	3.42	3.53	2.48
Well 16	13390.00	Upper Eagle Ford	1.16	0.19	1.10	0.16	2.08	0.40	3.52	3.44	2.21
Well 16	13395.00	Upper Eagle Ford	1.17	0.19	1.18	0.18	2.59	0.70	2.57	5.57	3.48
Well 16	13400.00	Upper Eagle Ford	1.17	0.19	1.09	0.17	2.36	0.66	3.22	5.30	3.52
Well 16	13405.00	Upper Eagle Ford	1.15	0.20	1.15	0.17	2.45	0.66	2.70	5.19	3.29
Well 16	13410.00	Upper Eagle Ford	1.20	0.35	1.26	0.18	2.51	0.66	3.97	6.05	4.39
Well 16	13415.00	Upper Eagle Ford	1.25	0.20	1.19	0.17	2.42	0.69	3.71	6.18	4.15
Well 16	13420.00	Upper Eagle Ford	1.22	0.21	1.21	0.19	2.63	0.72	3.54	6.30	5.35
Well 16	13425.00	Upper Eagle Ford	1.10	0.20	1.13	0.17	2.34	0.58	3.75	5.00	4.28
Well 16	13430.00	Upper Eagle Ford	0.88	0.17	0.94	0.14	1.94	0.42	3.52	3.72	4.28
Well 16	13435.00	Middle Eagle Ford	1.04	0.18	1.06	0.17	2.11	0.48	3.58	4.43	5.39
Well 16	13440.00	Middle Eagle Ford	1.22	0.20	1.24	0.19	2.42	0.58	2.84	5.42	5.60
Well 16	13445.00	Middle Eagle Ford	1.23	0.21	1.16	0.17	2.48	0.61	3.90	5.49	5.50
Well 16	13450.00	Middle Eagle Ford	1.18	0.20	1.14	0.19	2.41	0.58	3.67	5.14	4.54
Well 16	13455.00	Middle Eagle Ford	1.14	0.20	1.16	0.17	2.09	0.51	2.89	4.43	6.54
Well 16	13460.00	Middle Eagle Ford	1.12	0.19	1.12	0.17	2.09	0.50	2.03	4.15	7.52
Well 16	13465.00	Middle Eagle Ford	1.04	0.17	1.09	0.16	2.00	0.44	1.92	3.82	6.09
Well 16	13470.00	Middle Eagle Ford	1.11	0.18	1.08	0.15	2.09	0.46	3.14	4.15	5.20
Well 16	13475.00	Middle Eagle Ford	1.05	0.16	0.91	0.14	1.90	0.41	1.87	3.79	5.00
Well 16	13480.00	Middle Eagle Ford	0.98	0.18	1.01	0.16	2.09	0.48	2.40	4.11	7.03
Well 16	13485.00	Middle Eagle Ford	1.14	0.18	1.16	0.17	2.19	0.51	2.32	4.41	8.30
Well 16	13490.00	Middle Eagle Ford	1.13	0.19	1.16	0.17	2.09	0.52	2.54	4.18	9.84
Well 16	13495.00	Middle Eagle Ford	1.04	0.20	1.01	0.16	2.33	0.54	2.58	4.51	8.06
Well 16	13500.00	Lower Eagle Ford	1.26	0.22	1.34	0.19	2.33	0.61	2.47	4.49	8.53
Well 16	13505.00	Lower Eagle Ford	1.25	0.20	1.22	0.19	2.53	0.73	2.74	5.58	7.33
Well 16	13510.00	Lower Eagle Ford	1.43	0.22	1.42	0.21	3.11	0.70	2.64	6.97	5.36
Well 16	13515.00	Lower Eagle Ford	1.20	0.20	1.19	0.18	2.09	0.46	1.49	4.44	5.33
Well 16	13520.00	Lower Eagle Ford	1.17	0.21	1.14	0.18	2.13	0.42	2.12	4.29	5.00

Well 16	13525.00	Lower Eagle Ford	1.52	0.25	1.48	0.22	2.57	0.63	2.44	6.43	5.47
Well 16	13530.00	Lower Eagle Ford	1.30	0.22	1.33	0.19	2.19	0.52	2.35	4.85	4.74
Well 16	13535.00	Lower Eagle Ford	1.42	0.25	1.41	0.20	2.30	0.59	2.58	5.72	4.69
Well 16	13540.00	Lower Eagle Ford	1.31	0.22	1.27	0.19	2.16	0.52	2.59	5.21	4.16
Well 16	13545.00	Lower Eagle Ford	1.42	0.24	1.39	0.20	2.33	0.60	2.32	5.75	4.55
Well 16	13550.00	Lower Eagle Ford	1.44	0.24	1.48	0.21	2.49	0.65	3.06	5.75	4.88
Well 16	13555.00	Lower Eagle Ford	1.83	0.28	1.78	0.25	3.02	0.73	2.49	6.90	5.84
Well 16	13560.00	Lower Eagle Ford	2.02	0.30	2.02	0.31	3.05	0.68	2.14	6.73	8.68
Well 16	13565.00	Lower Eagle Ford	1.80	0.29	1.73	0.28	2.83	0.70	2.45	6.66	7.54
Well 16	13570.00	Lower Eagle Ford	1.50	0.22	1.49	0.22	2.50	0.59	1.82	5.77	7.40
Well 16	13575.00	Lower Eagle Ford	1.69	0.27	1.68	0.25	2.71	0.67	2.48	7.78	7.74
Well 16	13580.00	Lower Eagle Ford	1.72	0.26	1.81	0.25	2.67	0.61	2.33	6.87	11.11
Well 16	13585.00	Lower Eagle Ford	1.79	0.25	1.69	0.25	2.90	0.60	2.46	6.95	8.98
Well 16	13590.00	Lower Eagle Ford	1.65	0.26	1.69	0.24	2.94	0.72	2.74	7.81	6.37
Well 16	13595.00	Lower Eagle Ford	1.70	0.29	1.75	0.26	2.88	0.72	2.94	7.49	7.48
Well 16	13600.00	Lower Eagle Ford	0.60	0.11	0.53	0.09	1.26	0.17	6.60	2.10	0.96
Well 16	13605.00	Lower Eagle Ford	0.86	0.13	0.80	0.11	1.43	0.22	4.56	2.66	0.83
Well 16	13610.00	Lower Eagle Ford	0.88	0.15	0.79	0.12	1.63	0.27	6.25	3.40	1.12
Well 16	13615.00	Lower Eagle Ford	0.97	0.17	0.95	0.14	1.59	0.30	5.22	3.78	1.41
Well 16	13620.00	Lower Eagle Ford	0.95	0.16	0.92	0.14	1.80	0.26	5.75	3.45	0.99
Well 16	13625.00	Lower Eagle Ford	1.08	0.19	1.02	0.14	1.75	0.31	5.47	3.95	1.16
Well 17	13650	Middle Eagle Ford	1.270	0.200	1.260	0.194	2.013	0.721	10.138	6.340	4.008
Well 17	13660	Middle Eagle Ford	1.146	0.173	1.148	0.171	1.940	0.627	9.429	6.218	3.462
Well 17	13670	Middle Eagle Ford	1.193	0.180	1.188	0.181	1.986	0.707	10.460	6.183	3.881
Well 17	13680	Middle Eagle Ford	1.347	0.202	1.331	0.189	2.155	0.796	6.822	6.622	3.728
Well 17	13690	Middle Eagle Ford	1.426	0.216	1.300	0.203	1.764	0.592	5.563	5.430	4.923
Well 17	13700	Middle Eagle Ford	1.291	0.196	1.274	0.185	1.785	0.554	4.549	5.289	5.749
Well 17	13710	Middle Eagle Ford	1.409	0.204	1.329	0.205	1.939	0.610	4.426	5.849	5.386
Well 17	13720	Lower Eagle Ford	1.227	0.187	1.183	0.177	1.518	0.447	3.737	4.328	5.519
Well 17	13730	Lower Eagle Ford	1.245	0.183	1.220	0.178	1.454	0.456	7.745	4.141	4.808

Well 17	13740	Lower Eagle Ford	1.111	0.165	1.088	0.167	1.430	0.409	6.916	3.910	4.237
Well 17	13750	Lower Eagle Ford	1.222	0.188	1.144	0.172	1.443	0.482	6.119	4.270	5.244
Well 17	13760	Lower Eagle Ford	1.259	0.190	1.248	0.187	1.689	0.559	5.566	4.664	8.765
Well 17	13770	Lower Eagle Ford	1.290	0.198	1.223	0.188	1.653	0.536	4.655	4.871	5.074
Well 17	13780	Lower Eagle Ford	1.489	0.214	1.382	0.210	1.915	0.604	4.808	5.458	5.218
Well 17	13790	Lower Eagle Ford	1.432	0.210	1.364	0.212	1.840	0.563	4.520	5.350	5.204
Well 17	13800	Lower Eagle Ford	1.931	0.283	1.802	0.270	2.350	0.770	5.839	7.583	5.270
Well 17	13810	Lower Eagle Ford	1.656	0.244	1.568	0.238	2.199	0.698	5.286	7.001	5.110
Well 17	13820	Lower Eagle Ford	1.804	0.276	1.726	0.263	2.292	0.684	3.698	6.639	5.455
Well 17	13830	Lower Eagle Ford	1.456	0.220	1.360	0.212	1.850	0.525	7.180	5.136	6.904
Well 17	13840	Lower Eagle Ford	1.855	0.280	1.761	0.259	2.324	0.696	9.737	7.181	9.511
Well 19	13690	Upper Eagle Ford	0.75	0.12	0.72	0.12	1.06	0.33	6.40	2.590	2.635
Well 19	13695	Upper Eagle Ford	0.92	0.14	0.88	0.14	1.22	0.42	9.41	3.214	3.102
Well 19	13700	Upper Eagle Ford	1.53	0.23	1.57	0.23	3.03	0.87	6.85	7.268	2.650
Well 19	13705	Upper Eagle Ford	1.16	0.18	1.17	0.18	2.04	0.55	4.60	5.586	4.526
Well 19	13710	Upper Eagle Ford	1.55	0.25	1.61	0.23	2.71	0.83	5.89	7.545	3.560
Well 19	13715	Upper Eagle Ford	1.59	0.23	1.58	0.23	2.72	0.83	4.93	7.246	3.514
Well 19	13720	Upper Eagle Ford	1.61	0.24	1.61	0.25	2.83	0.85	5.02	7.640	3.558
Well 19	13725	Middle Eagle Ford	1.50	0.23	1.47	0.23	2.34	0.78	7.51	7.115	3.383
Well 19	13730	Middle Eagle Ford	1.47	0.22	1.49	0.23	2.60	0.79	6.05	7.085	3.296
Well 19	13735	Middle Eagle Ford	1.50	0.22	1.46	0.22	2.40	0.79	7.30	7.070	3.314
Well 19	13740	Middle Eagle Ford	1.53	0.23	1.60	0.23	2.54	0.85	7.32	7.618	3.323
Well 19	13745	Middle Eagle Ford	1.56	0.24	1.56	0.22	2.49	0.82	6.59	7.380	3.496
Well 19	13750	Middle Eagle Ford	1.42	0.22	1.46	0.22	2.42	0.87	7.26	7.801	3.293
Well 19	13755	Middle Eagle Ford	1.44	0.23	1.46	0.23	2.63	0.95	7.32	8.000	3.029
Well 19	13760	Middle Eagle Ford	1.47	0.22	1.45	0.23	2.50	0.85	7.92	7.931	3.334
Well 19	13765	Middle Eagle Ford	1.49	0.23	1.49	0.23	2.51	0.88	9.66	7.828	3.327

Well 19	13770	Middle Eagle Ford	1.53	0.24	1.52	0.22	2.53	0.90	8.26	8.215	3.225
Well 19	13775	Middle Eagle Ford	1.48	0.22	1.48	0.22	2.55	0.90	9.76	8.019	3.192
Well 19	13780	Middle Eagle Ford	1.52	0.23	1.52	0.22	2.72	0.98	7.58	8.481	3.226
Well 19	13785	Middle Eagle Ford	1.43	0.20	1.41	0.21	2.42	0.80	5.53	7.147	3.231
Well 19	13790	Middle Eagle Ford	1.54	0.24	1.55	0.24	2.72	0.98	5.56	8.408	3.094
Well 19	13795	Middle Eagle Ford	1.56	0.23	1.60	0.23	2.81	1.00	6.31	8.659	3.273
Well 19	13800	Middle Eagle Ford	1.52	0.23	1.56	0.23	2.76	0.97	6.07	8.524	3.194
Well 19	13805	Middle Eagle Ford	1.59	0.24	1.62	0.24	2.78	1.00	6.77	8.887	3.275
Well 19	13810	Middle Eagle Ford	1.39	0.21	1.36	0.21	2.38	0.89	8.29	7.724	3.541
Well 19	13815	Middle Eagle Ford	1.80	0.27	1.82	0.27	3.17	1.12	8.71	10.537	3.538
Well 19	13825	Middle Eagle Ford	1.69	0.26	1.69	0.25	3.14	1.10	10.36	10.836	4.294
Well 19	13830	Middle Eagle Ford	1.80	0.29	1.80	0.28	3.16	1.13	6.88	10.132	3.811
Well 19	13835	Middle Eagle Ford	1.81	0.27	1.73	0.27	3.01	1.05	7.23	9.845	4.303
Well 19	13840	Middle Eagle Ford	1.66	0.25	1.59	0.25	2.84	1.03	6.21	9.062	3.414
Well 19	13845	Middle Eagle Ford	1.78	0.28	1.81	0.27	3.18	1.16	4.40	10.172	3.965
Well 19	13850	Middle Eagle Ford	1.93	0.28	1.91	0.28	3.05	1.10	4.31	9.983	4.247
Well 19	13855	Middle Eagle Ford	1.98	0.29	1.98	0.29	3.24	1.17	5.45	10.227	4.418
Well 19	13860	Middle Eagle Ford	1.95	0.29	1.97	0.30	3.12	1.12	4.27	9.974	4.265
Well 19	13865	Middle Eagle Ford	2.11	0.31	2.12	0.32	3.41	1.15	5.32	10.803	5.411
Well 19	13870	Middle Eagle Ford	2.04	0.30	1.99	0.31	3.09	1.00	3.77	9.497	5.733
Well 19	13875	Middle Eagle Ford	2.14	0.31	2.01	0.31	2.75	0.83	3.34	7.992	7.919
Well 19	13880	Middle Eagle Ford	1.78	0.27	1.78	0.27	2.70	0.83	8.74	8.019	6.051
Well 19	13885	Middle Eagle Ford	1.87	0.27	1.82	0.28	2.65	0.82	4.32	7.959	6.596
Well 19	13890	Middle Eagle Ford	1.73	0.25	1.72	0.26	2.21	0.71	4.22	6.963	5.786
Well 19	13895	Middle Eagle Ford	1.74	0.26	1.65	0.26	2.11	0.67	3.43	6.222	5.468
Well 19	13900	Middle Eagle Ford	1.61	0.24	1.55	0.25	2.26	0.72	2.73	6.688	5.101
Well 19	13905	Middle Eagle Ford	1.73	0.26	1.62	0.25	2.04	0.69	2.88	6.283	4.577

Well 19	13910	Middle Eagle Ford	1.59	0.24	1.61	0.23	2.21	0.73	3.57	6.381	5.630
Well 19	13915	Lower Eagle Ford	1.61	0.24	1.63	0.24	2.50	0.74	2.94	6.969	4.481
Well 19	13920	Lower Eagle Ford	1.51	0.23	1.50	0.22	2.23	0.71	3.15	6.747	4.299
Well 19	13925	Lower Eagle Ford	1.55	0.23	1.56	0.24	2.33	0.74	3.16	6.805	4.785
Well 19	13930	Lower Eagle Ford	1.62	0.24	1.55	0.23	2.22	0.70	3.14	6.548	6.120
Well 19	13935	Lower Eagle Ford	1.95	0.30	1.91	0.29	2.71	0.83	4.91	7.713	5.134
Well 19	13940	Lower Eagle Ford	1.92	0.29	1.93	0.29	2.81	0.88	3.64	8.633	5.301
Well 19	13945	Lower Eagle Ford	1.98	0.29	1.88	0.29	2.62	0.86	4.44	8.688	5.262
Well 19	13950	Lower Eagle Ford	2.25	0.33	2.11	0.34	2.82	0.77	4.73	7.623	6.865
Well 19	13955	Lower Eagle Ford	2.29	0.33	2.23	0.33	2.58	0.69	2.53	6.985	9.383
Well 19	13960	Lower Eagle Ford	1.67	0.25	1.65	0.25	2.58	0.79	2.54	7.230	4.725
Well 19	13965	Lower Eagle Ford	1.68	0.25	1.64	0.26	2.43	0.76	3.77	7.411	5.189
Well 19	13970	Lower Eagle Ford	1.87	0.28	1.87	0.28	3.05	0.79	3.22	8.858	8.167
Well 19	13975	Lower Eagle Ford	1.86	0.28	1.83	0.29	2.80	0.80	3.85	8.434	7.743
Well 19	13980	Lower Eagle Ford	1.89	0.28	1.90	0.28	2.74	0.84	4.31	8.826	6.495
Well 19	13985	Lower Eagle Ford	1.92	0.29	1.88	0.28	2.67	0.84	3.39	8.891	5.793
Well 19	13990	Lower Eagle Ford	1.85	0.29	1.85	0.29	2.75	0.79	5.88	8.142	6.137
Well 19	13995	Lower Eagle Ford	1.77	0.27	1.78	0.27	2.49	0.79	4.04	7.894	6.335
Well 19	14000	Lower Eagle Ford	1.54	0.23	1.52	0.23	2.11	0.63	8.42	6.620	5.325
Well 20	13660	Upper Eagle Ford	1.428	0.209	1.378	0.211	2.643	0.758	4.006	5.979	2.196
Well 20	13665	Upper Eagle Ford	1.531	0.218	1.466	0.223	2.551	0.752	2.171	6.064	3.790
Well 20	13670	Upper Eagle Ford	1.343	0.201	1.318	0.199	2.236	0.651	2.470	5.781	3.917
Well 20	13675	Upper Eagle Ford	1.268	0.177	1.195	0.183	2.028	0.570	2.197	5.550	4.273
Well 20	13680	Middle Eagle Ford	1.270	0.177	1.166	0.183	2.002	0.569	2.226	5.537	4.544
Well 20	13685	Middle Eagle Ford	1.359	0.197	1.314	0.203	2.191	0.656	2.582	5.943	3.808
Well 20	13690	Middle Eagle Ford	1.674	0.235	1.562	0.231	2.663	0.840	3.454	6.655	3.666
Well 20	13695	Middle Eagle Ford	1.752	0.251	1.661	0.254	2.907	0.967	2.951	7.812	4.034

Well 20	13700	Middle Eagle Ford	1.553	0.224	1.486	0.221	2.453	0.860	3.370	7.116	3.104
Well 20	13705	Middle Eagle Ford	1.559	0.227	1.458	0.230	2.573	0.904	3.732	7.106	3.128
Well 20	13710	Middle Eagle Ford	1.490	0.213	1.415	0.218	2.356	0.838	3.251	6.957	3.007
Well 20	13715	Middle Eagle Ford	1.616	0.235	1.567	0.231	2.565	0.883	3.796	7.655	3.166
Well 20	13720	Middle Eagle Ford	1.586	0.242	1.571	0.231	2.568	0.915	4.087	7.595	2.992
Well 20	13725	Middle Eagle Ford	1.562	0.229	1.545	0.236	2.484	0.872	3.402	7.358	3.058
Well 20	13730	Middle Eagle Ford	1.560	0.226	1.518	0.223	2.344	0.868	4.012	7.440	2.971
Well 20	13740	Middle Eagle Ford	1.384	0.208	1.357	0.205	2.241	0.800	5.233	6.848	2.678
Well 20	13745	Middle Eagle Ford	1.563	0.227	1.499	0.225	2.558	1.002	5.049	8.046	2.871
Well 20	13750	Middle Eagle Ford	1.586	0.235	1.552	0.238	2.606	1.017	4.136	8.079	2.836
Well 20	13755	Middle Eagle Ford	1.571	0.229	1.568	0.230	2.576	0.979	4.091	8.013	2.902
Well 20	13760	Middle Eagle Ford	1.640	0.236	1.545	0.245	2.686	1.050	4.233	8.397	2.994
Well 20	13765	Middle Eagle Ford	1.594	0.232	1.522	0.226	2.545	0.952	2.751	7.694	3.051
Well 20	13770	Middle Eagle Ford	1.559	0.224	1.497	0.229	2.505	0.924	2.337	7.531	2.880
Well 20	13785	Middle Eagle Ford	1.566	0.237	1.527	0.232	2.616	0.888	4.041	7.739	2.971
Well 20	13788	Middle Eagle Ford	2.612	0.380	2.546	0.389	6.495	1.511	30.748	19.731	6.661
Well 20	13790	Middle Eagle Ford	1.806	0.259	1.715	0.263	2.589	1.006	3.302	7.693	4.034
Well 20	13793	Middle Eagle Ford	1.619	0.233	1.556	0.231	2.707	1.049	4.432	8.388	4.891
Well 20	13796	Middle Eagle Ford	1.986	0.287	1.905	0.295	3.365	1.288	4.564	10.006	3.123
Well 20	13799	Middle Eagle Ford	1.758	0.259	1.741	0.262	3.376	1.259	5.351	10.174	3.437
Well 20	13802	Middle Eagle Ford	2.159	0.306	2.049	0.315	3.512	1.234	6.295	11.418	3.954
Well 20	13805	Middle Eagle Ford	2.050	0.323	2.088	0.335	3.734	1.309	5.805	11.639	3.806
Well 20	13808	Middle Eagle Ford	1.853	0.278	1.930	0.298	3.422	1.390	4.999	10.287	3.204
Well 20	13811	Middle Eagle Ford	1.986	0.287	1.902	0.295	3.187	1.206	5.707	9.787	3.587
Well 20	13814	Middle Eagle Ford	2.149	0.322	2.257	0.335	3.814	1.383	6.048	13.129	4.134
Well 20	13816	Middle Eagle Ford	1.653	0.251	1.783	0.266	3.301	1.317	6.265	10.925	3.884
Well 20	13819	Middle Eagle Ford	1.438	0.211	1.380	0.205	2.132	0.822	5.371	6.874	4.419

Well 20	13822	Middle Eagle Ford	2.329	0.332	2.145	0.331	3.791	1.532	6.442	12.783	4.872
Well 20	13825	Middle Eagle Ford	1.630	0.256	1.860	0.288	3.533	1.437	4.176	11.418	3.167
Well 20	13828	Middle Eagle Ford	1.584	0.243	1.751	0.264	3.422	1.456	4.289	10.505	6.041
Well 20	13831	Middle Eagle Ford	1.541	0.248	1.761	0.287	3.044	1.088	3.143	9.846	5.141
Well 20	13834	Middle Eagle Ford	1.956	0.292	1.962	0.307	3.602	1.294	3.001	10.621	4.238
Well 20	13837	Middle Eagle Ford	1.538	0.231	1.693	0.263	2.962	1.208	2.957	8.118	4.592
Well 20	13840	Middle Eagle Ford	1.367	0.211	1.487	0.231	2.335	0.729	0.849	6.786	4.790
Well 20	13842	Middle Eagle Ford	3.187	0.460	3.042	0.483	2.803	0.855	1.369	8.187	7.626
Well 20	13844	Middle Eagle Ford	1.521	0.240	1.576	0.257	2.363	0.753	23.957	8.283	9.217
Well 20	13846.4	Middle Eagle Ford	1.937	0.309	2.133	0.327	3.700	1.338	7.278	13.003	3.661
Well 20	13850	Middle Eagle Ford	1.811	0.264	1.738	0.269	2.372	0.790	1.608	6.853	4.589
Well 20	13851	Middle Eagle Ford	1.770	0.262	1.791	0.267	2.936	1.067	3.730	9.046	4.437
Well 20	13854	Middle Eagle Ford	1.962	0.289	1.922	0.294	2.198	0.665	1.470	6.315	6.129
Well 20	13855	Middle Eagle Ford	1.866	0.270	1.785	0.265	2.542	0.876	1.874	7.718	4.636
Well 20	13857	Middle Eagle Ford	1.877	0.274	1.847	0.280	2.755	0.798	1.936	8.246	10.321
Well 20	13860	Middle Eagle Ford	2.396	0.345	2.301	0.339	2.838	0.886	1.712	9.207	9.898
Well 20	13863	Lower Eagle Ford	1.879	0.257	1.662	0.252	1.790	0.593	1.152	5.546	4.738
Well 20	13866	Lower Eagle Ford	1.616	0.236	1.582	0.238	2.127	0.614	1.290	5.890	4.260
Well 20	13869	Lower Eagle Ford	1.693	0.259	1.788	0.281	4.370	1.050	3.218	11.177	5.385
Well 20	13872	Lower Eagle Ford	1.904	0.275	1.831	0.287	3.414	0.926	3.052	9.114	5.623
Well 20	13875	Lower Eagle Ford	1.755	0.248	1.700	0.256	2.180	0.690	1.197	6.081	4.078
Well 20	13876.9	Lower Eagle Ford	2.099	0.292	1.911	0.288	2.110	0.674	1.280	6.009	6.882
Well 20	13880	Lower Eagle Ford	1.597	0.229	1.683	0.260	2.503	0.971	3.967	7.645	4.803
Well 20	13883	Lower Eagle Ford	1.609	0.236	1.629	0.235	2.921	0.811	2.441	7.930	4.004
Well 20	13885	Lower Eagle Ford	1.744	0.253	1.622	0.249	2.459	0.787	1.312	7.352	5.010
Well 20	13889	Lower Eagle Ford	1.475	0.218	1.465	0.227	2.119	0.724	2.651	6.111	4.017
Well 20	13892	Lower Eagle Ford	1.634	0.238	1.659	0.249	2.542	0.774	2.312	7.214	5.070

Well 20	13895	Lower Eagle Ford	1.559	0.226	1.565	0.240	2.047	0.670	2.890	5.658	3.181
Well 20	13898	Lower Eagle Ford	2.062	0.301	2.011	0.312	2.573	0.914	3.125	7.913	3.793
Well 20	13901	Lower Eagle Ford	2.109	0.323	2.106	0.343	3.138	0.993	3.007	9.441	8.804
Well 20	13904	Lower Eagle Ford	1.835	0.271	1.850	0.289	2.352	0.798	2.433	7.709	4.907
Well 20	13906	Lower Eagle Ford	1.675	0.257	1.805	0.278	3.157	1.110	2.650	10.056	4.122
Well 20	13909	Lower Eagle Ford	2.168	0.314	2.179	0.334	2.421	0.798	1.691	7.559	5.901
Well 20	13912	Lower Eagle Ford	2.018	0.290	1.971	0.298	2.478	0.859	2.228	7.714	5.064
Well 20	13915	Lower Eagle Ford	2.243	0.330	2.256	0.344	2.216	0.666	2.519	5.682	4.053
Well 20	13918	Lower Eagle Ford	1.054	0.165	1.140	0.179	4.161	1.384	9.775	25.220	4.049
Well 20	13921	Lower Eagle Ford	3.259	0.435	2.825	0.434	2.789	0.681	3.118	7.075	8.969
Well 20	13924	Lower Eagle Ford	1.134	0.167	1.201	0.189	1.174	0.239	0.492	2.657	11.192
Well 20	13927	Lower Eagle Ford	1.049	0.155	1.140	0.176	1.200	0.281	0.999	2.894	5.754
Well 20	13930	Lower Eagle Ford	1.873	0.282	1.967	0.308	2.938	0.616	2.294	6.331	15.328
Well 24	14040	Middle Eagle Ford	1.337	0.202	1.281	0.201	2.012	0.751	6.988	4.721	2.424
Well 24	14100	Middle Eagle Ford	1.921	0.278	1.882	0.283	3.357	1.320	8.471	9.322	2.520
Well 24	14150	Middle Eagle Ford	1.928	0.279	1.879	0.275	3.403	1.289	8.987	9.137	2.525
Well 24	14175	Middle Eagle Ford	2.151	0.316	2.110	0.326	3.466	1.188	5.106	10.139	5.405
Well 24	14190	Lower Eagle Ford	1.211	0.170	1.121	0.165	1.655	0.454	7.148	4.786	2.980
Well 24	14200	Lower Eagle Ford	1.451	0.209	1.351	0.201	1.922	0.558	10.491	5.966	1.765
Well 24	14210	Lower Eagle Ford	1.442	0.205	1.362	0.198	1.826	0.509	10.387	5.732	1.691
Well 24	14220	Lower Eagle Ford	0.756	0.103	0.643	0.094	0.895	0.239	7.782	2.376	2.283

Appendix E

Activation Laboratories Ltd. (ActLabs) Raw Data

Bentonite Major Elements

Well	Analyte Symbol	Depth-Core Lab	Formation Top	SiO2	Al2O3	Fe2O3(T)	MnO	MgO	CaO	Na2O	K2O	TiO2	P2O5	LOI	Total
	Unit Symbol			%	%	%	%	%	%	%	%	%	%	%	%
	Detection Limit			0.01	0.01	0.01	0.001	0.01	0.01	0.01	0.01	0.001	0.01		0.01
	Analysis Method			FUS-ICP	FUS-ICP	FUS-ICP	FUS-ICP	FUS-ICP	FUS-ICP	FUS-ICP	FUS-ICP	FUS-ICP	FUS-ICP	FUS-ICP	FUS-ICP
20	2N	14067.75 - 14067.95	Middle Eagle Ford	43.76	26.15	6.67	0.005	0.84	0.66	1.84	2.98	0.385	0.15	15.62	99.06
12	7L	13701.40 0 13701.60	Lower Eagle Ford	38.57	19.26	3.29	0.013	0.9	12.95	1.25	1.62	0.472	0.71	20.31	99.35
8	11H	13090.45 - 13091.35	Lower Austin Chalk	49.65	26.15	2.55	0.008	2.4	0.75	0.97	5.18	0.258	0.11	11.98	100
19	1F	13814.4	Middle Eagle Ford	39.53	23.87	12.18	0.009	0.7	1.38	1.44	1.89	0.479	0.31	16.67	98.45
12	3L	13399.95 - 13400.15	Lower Austin Chalk	43.55	22.29	5.34	0.022	2.46	6.29	1.52	3.98	0.442	0.7	13.51	100.1
1	15R	13916.25 - 13916.85	Lower Austin Chalk	47.21	27.89	1.99	0.015	1.16	2.67	1.25	4.11	0.987	0.21	12.56	100.1
1	14R	13914.75 - 13914.90	Lower Austin Chalk	33.62	18.71	17.78	0.023	0.94	2.2	0.78	2.8	0.715	0.09	20.33	97.98

Bentonite Trace Elements

Well	Analyte Symbol	Depth-Core Lab	Formation Top	Au	Ag	As	Ba	Be	Bi	Br	Cd	Co	Cr	Cs	Cu	Hf
	Unit Symbol			ppb	ppm	ppm	ppm	ppm	ppm	ppm	ppm	ppm	ppm	ppm	ppm	ppm
	Detection Limit			1	0.5	1	1	1	2	0.5	0.5	0.1	0.5	0.2	1	0.2
	Analysis Method			INAA	MULT INAA / TD-ICP	INAA	FUS-ICP	FUS-ICP	TD-ICP	INAA	TD-ICP	INAA	INAA	INAA	TD-ICP	INAA
20	2N	14067.75 - 14067.95	Middle Eagle Ford	< 1	< 0.5	13	167	< 1	< 2	< 0.5	< 0.5	12.2	8.7	6	16	4.8
12	7L	13701.40 0 13701.60	Lower Eagle Ford	< 1	0.6	19	642	2	< 2	2.9	0.6	10.3	125	2.5	59	2.8

8	11H	13090.45 - 13091.35	Lower Austin Chalk	< 1	0.5	18	383	1	< 2	2.4	< 0.5	3.9	3	7.7	13	5.4
19	1F	13814.4	Middle Eagle Ford	< 1	0.6	25	347	< 1	< 2	4.2	0.6	28.3	32	4.1	33	3.4
12	3L	13399.95 - 13400.15	Lower Austin Chalk	< 1	0.6	25	203	1	< 2	4.5	< 0.5	12.3	31.5	5.1	26	7.9
1	15R	13916.25 - 13916.85	Lower Austin Chalk	< 1	0.5	12	519	1	2	3	< 0.5	7.5	13.9	5.5	31	7.8
1	14R	13914.75 - 13914.90	Lower Austin Chalk	< 1	1	27	338	< 1	< 2	1	< 0.5	7.7	14.9	3.9	25	10.4

Well Name	Analyte Symbol	Depth-Core Lab	Formation Top	Hg	Ir	Mo	Ni	Pb	Rb	Sb	S	Sc	Se	Sr
	Unit Symbol			ppm	ppb	ppm	ppm	ppm	ppm	ppm	%	ppm	ppm	ppm
	Detection Limit			1	1	2	1	5	10	0.1	0.001	0.01	0.5	2
	Analysis Method			INAA	INAA	TD-ICP	TD-ICP	TD-ICP	INAA	INAA	TD-ICP	INAA	INAA	FUS-ICP
20	2N	14067.75 - 14067.95	Middle Eagle Ford	< 1	< 1	20	63	39	30	2.8	4.95	4.64	< 0.5	459
12	7L	13701.40 0 13701.60	Lower Eagle Ford	< 1	< 1	17	64	12	60	3.5	2.85	7.7	< 0.5	443
8	11H	13090.45 - 13091.35	Lower Austin Chalk	< 1	< 1	5	5	40	100	2.8	2.04	4.45	< 0.5	465
19	1F	13814.4	Middle Eagle Ford	< 1	< 1	122	172	40	20	3.8	10.5	3.28	< 0.5	357
12	3L	13399.95 - 13400.15	Lower Austin Chalk	< 1	< 1	7	43	45	70	1.9	4.27	7.51	< 0.5	481
1	15R	13916.25 - 13916.85	Lower Austin Chalk	< 1	< 1	5	15	< 5	40	2.8	1.39	7.66	< 0.5	567
1	14R	13914.75 - 13914.90	Lower Austin Chalk	< 1	< 1	16	29	8	40	3	13.3	10.2	4.9	353

Well Name	Analyte Symbol	Depth-Core Lab	Formation Top	Ta	Th	U	V	W	Y	Zn	Zr
	Unit Symbol			ppm	ppm	ppm	ppm	ppm	ppm	ppm	ppm
	Detection Limit			0.3	0.1	0.1	5	1	1	1	2
	Analysis Method			INAA	INAA	INAA	FUS-ICP	INAA	FUS-ICP	MULT INAA / TD-ICP	FUS-ICP
20	2N	14067.75 - 14067.95	Middle Eagle Ford	1	22.6	6.2	66	< 1	6	75	87
12	7L	13701.40 0 13701.60	Lower Eagle Ford	0.9	19.3	6.9	188	< 1	19	102	84
8	11H	13090.45 - 13091.35	Lower Austin Chalk	1.8	52.1	9.8	21	< 1	11	69	177
19	1F	13814.4	Middle Eagle Ford	0.7	18.1	0.7	249	5	5	115	91
12	3L	13399.95 - 13400.15	Lower Austin Chalk	0.9	35.8	6.5	104	< 1	18	69	206
1	15R	13916.25 - 13916.85	Lower Austin Chalk	0.9	14	3.1	193	< 1	7	130	120
1	14R	13914.75 - 13914.90	Lower Austin Chalk	0.4	8.1	2.8	174	< 1	10	28	303

Well Name	Analyte Symbol	Depth-Core Lab	Formation Top	La	Ce	Nd	Sm	Eu	Tb	Yb	Lu	Mass
	Unit Symbol			ppm	ppm	ppm	ppm	ppm	ppm	ppm	ppm	g
	Detection Limit			0.05	1	1	0.01	0.05	0.1	0.05	0.01	
	Analysis Method			INAA	INAA	INAA	INAA	INAA	INAA	INAA	INAA	INAA
20	2N	14067.75 - 14067.95	Middle Eagle Ford	3.63	8	4	1.04	0.31	< 0.1	0.46	0.1	1.404
12	7L	13701.40 0 13701.60	Lower Eagle Ford	28.8	59	29	6.91	0.65	0.6	1.39	0.28	1.209
8	11H	13090.45 - 13091.35	Lower Austin Chalk	28.3	65	22	4.32	0.62	0.4	1.03	0.2	1.259
19	1F	13814.4	Middle Eagle Ford	8.53	20	8	1.91	0.21	0.3	0.97	0.13	1.303
12	3L	13399.95 - 13400.15	Lower Austin Chalk	17.2	37	13	3.46	0.56	0.5	1.67	0.28	1.283
1	15R	13916.25 - 13916.85	Lower Austin Chalk/Upper Eagle Ford	3.82	11	5	1.54	0.41	< 0.1	0.57	0.07	1.185
1	14R	13914.75 - 13914.90	Lower Austin Chalk/Upper Eagle Ford	2.96	6	5	1.62	0.52	0.3	0.83	0.12	1.504

References

Activation Laboratories Ltd. (ActLabs), 2013, 4E Research - INAA, Total Digestion - ICP, Lithium Metaborate/Tetraborate Fusion - ICP: http://www.actlabs.com/page.aspx?page=518&app=226&cat1=549&tp=12&lk=no&menu=64 (accessed October 2013).

Adams, R.L., and Carr, J.P., 2010, Regional depositional systems of the Woodbine, Eagle Ford, and Tuscaloosa of the U.S. Gulf Coast: Gulf Coast Association of Geological Societies Transactions, v. 60, p. 3-27.

Adkins, W.S., 1932, The geology of Texas, Part 2, The Mesozoic systems in Texas, *in* Sellards, E. H., Adkins, W.S., and Plummer, F.B., The University of Texas Bulletin, v. 1, no. 3232, p. 239-516.

Adkins, W.S., and Lozo, F.E., 1951, Stratigraphy of the Woodbine and Eagle Ford, Waco area, Texas: Dallas, Southern Methodist University, Fondren Science Series, v. 4, p. 101-161.

Algeo, T.J., Morford, J., and Cruse, A., 2012, New applications of trace metals as proxies in marine paleoenvironments: Chemical Geology, v. 306-307, p. 160-164.

Algeo, T.J., and Rowe, H., 2012, Paleoceanographic applications of trace-metal concentration data: Chemical Geology, v. 324-325, p. 6-18.

Arthur, M.A., and Sageman, B.B., 1994, Marine shales: depositional mechanisms and environments of ancient deposits: Annual Review of Earth and Planetary Sciences, v. 22, p. 499-551.

Arthur, M.A., and Schlanger, S.O., 1979, Cretaceous "oceanic anoxic events" as causal factors in development of reef-reservoired giant oil fields: AAPG Bulletin, no.6, v. 63, p. 870-885.

Barrat, J., 2004, Determination of parental magmas of HED cumulates: the effects of interstitial melts: Meteoritics & Planetary Science, v. 39, no. 11, p. 1767-1779.

Barton, L. L., and Fauque, G. D., 2009, Biochemistry, Physiology and Biotechnology of Sulfate-Reducing Bacteria: Advances in Applied Microbiology, v. 68, p. 41–98.

Blakey, R., 2013, Paleogeographic and tectonic history of North America -- key time slices, scale 1:600, 2 sheets: http://cpgeosystems.com/namkeypaleogeography.html (accessed September 2013).

Bowker, K.A., 2007, Barnett Shale gas production, Fort Worth Basin: issues and discussion: AAPG Bulletin, v. 91, no. 4, p. 523-533.

Bralower, T. J., 2008, Earth science: volcanic cause of catastrophe: Nature, v. 454, p. 285-287.

Breyer, J.A., Busbey, A.B. III, Hanson, R.E., Befus, K.E., Griffin, W.R., Hargrove, U.S., and Bergman, S.C., 2007, Evidence for Late Cretaceous volcanism in Trans-Pecos Texas: The Journal of Geology, v. 115, no. 2, p. 243-251.

British Geological Survey Natural Environment Research Council (NERC), no date, Greenhouse Earth-the story of ancient climate change: http://www.bgs.ac.uk/discoveringGeology/climateChange/greenHouseEarth.html (accessed October 2013).

Brown, C.W., and Pierce, R.L., 1962, Palynologic correlations in Cretaceous Eagle Ford Group, northeast Texas: AAPG Bulletin, v. 46, no. 12, p. 2133-2147.

Brumsack, H.J., 2006, The trace metal content of recent organic carbon-rich sediments; implications for Cretaceous black shale formation: Palaeogeography, Palaeoclimatology, Palaeoecology, v. 232, p. 344-361.

Burdige, D.J., 2007, Preservation of organic matter in marine sediments: controls, mechanisms, and an imbalance in sediment organic carbon budgets?: Chemical Reviews, v. 107, no. 2, p. 467-485.

Calvert, S.E., Bustin, R.M., and Ingall, E.D., 1996, Influence of water column anoxia and sediment supply on the burial and preservation of organic carbon in marine shales: Geochimica et Cosmochimica Acta, v. 60, no. 9, p. 1577-1593.

Calvert, S.E., and Pedersen, T.F., 1993, Geochemistry of recent oxic and anoxic marine sediments: implications for the geological record: Marine Geology, v. 113, p. 67-88.

Calvert, S.E., and Pedersen, T.F., 2007, Elemental proxies for palaeoclimatic and palaeoceanographic variability in marine sediments: interpretation and application: Developments in Marine Geology, v. 1, p. 567-644.

Charvat, W.A., 1985, The nature and origin of the bentonite-rich Eagle Ford rocks, central Texas [M.S. thesis]: Waco, Baylor University, 220 p.

Chazan, G., 2013, The energy visionary and father of fracking [Obituary]: The Financial Times Ltd.: http://www.ft.com/intl/cms/s/0/7aaa99b6-fa06-11e2-98e0-00144feabdc0.html#axzz2gqyXfLli (accessed October 2013).

Cullers, R.L., 1995, The controls on the major-and trace-element evolution of shales, siltstones and sandstones of Ordovician to Tertiary age in the Wet Mountains region, Colorado, U.S.A.: Chemical Geology, v. 123, nos. 1-4, p. 107-131.

Davidson, J., Turner, S., and Plank, T., 2013, Dy/Dy*: Variations arising from mantle sources and petrogenetic processes: Journal of Petrology, v. 54, no. 3, p. 525-537.

Dawson, W.C., 1997, Limestone microfacies and sequence stratigraphy: Eagle Ford Group (Cenomanian-Turonian) north-central Texas outcrops: Gulf Coast Association of Geological Societies Transactions, v. 47, p. 99-105.

Dawson, W.C., 2000, Shale microfacies; Eagle Ford Group (Cenomanian-Turonian) north-central Texas outcrops and subsurface equivalents: Gulf Coast Association of Geological Societies Transactions, v. 50, p. 607-622.

Demaison, G.J., and Moore, G.T., 1980, Anoxic environments and oil source bed genesis: Organic Geochemistry, v. 2, p. 9-31.

Donovan, A.D., and Staerker, T.S., 2010, Sequence stratigraphy of the Eagle Ford (Boquillas) Formation in the subsurface of South Texas and outcrops of West Texas: Gulf Coast Association of Geological Societies Transactions, v. 60, p. 861-899.

Donovan, A.D., Staerker, T.S., Pramudito, A., Weiguo Li, Corbett, M.J., Lowery, C.M., Romero, A.M. and Gardner, R.D., 2012, The Eagle Ford outcrops of West Texas: A laboratory for understanding heterogeneities within unconventional mudstone reservoirs: Gulf Coast Association of Geological Societies, v. 1, p. 162-185.

Dukes, R.T., 2013, Eagle Ford oil output surpasses 600,000 b/d in May: http://eaglefordshale.com/news/eagle-ford-oil-output-surpasses-600000-bd-in-may/ (accessed September 2013).

Elderfield, H., and Greaves, M.J., 1982, The rare earth elements in seawater: Nature, v. 296, p. 214-219.

Eldrett, J.S., Bergman, S., Minisini, D., and Macaulay, C., 2013, An integrated stratigraphy of the Cenomanian-Turonian Eagle Ford Shale, Texas, USA: AAPG Annual Convention and Exhibition, Pittsburgh, Pennsylvania, i*n* Search and Discovery, Abstract no. #90163, 1 p.:

http://www.searchanddiscovery.com/abstracts/html/2013/90163ace/abstracts/eld.htm (accessed November 2013).

Fairbanks, M.D., and Ruppel, S.C., 2012, High resolution stratigraphy and facies architecture of the Upper Cretaceous (Turonian-Cenomanian) Eagle Ford Formation, central Texas: American Association of Petroleum Geologists, Annual Meeting, Long Beach, California *in* Search and Discovery, Article # 10408, 7 p.

Frey, F., 2009, Trace-Element Geochemistry, MIT OpenCourseWare: http://ocw.mit.edu/courses/earth-atmospheric-and-planetary-sciences/12-479-trace-element-geochemistry-spring-2009 (accessed October 2013).

Galloway, W.E., 2008, Depositional Evolution of the Gulf of Mexico Sedimentary Basin: Sedimentary Basins of the World, v. 5, p. 505-549.

Griffin, W.R., 2008, Geochemistry and geochronology of the Balcones Igneous Province, Texas [Ph.D. dissertation]: Dallas, The University of Texas, 241 p.

Harbor, R.L., 2011, Facies characterization and stratigraphic architecture of organic-rich mudrocks, Upper Cretaceous Eagle Ford Formation, South Texas [M.S. thesis]: Austin, The University of Texas, 195 p.

Hentz, T.F., and Ruppel, S.C., 2010, Regional lithostratigraphy of the Eagle Ford Shale: Maverick Basin to East Texas Basin: Gulf Coast Association of Geological Societies Transactions, v. 60, p. 325-337.

Herrin, E., 1957, Correlation by spectrographic analysis of bentonite in the Gulf series of Dallas area, Texas: Field & Laboratory, v. 25, no. 1, p. 5-16.

Hetzel, A., März, C., Vogt, C., and Brumsack, H., 2011, Geochemical environment of Cenomanian-Turonian black shale deposition at Wunstorf (northern Germany): Cretaceous Research, v. 32, no. 4, p. 480-494.

Hildred, G., Ratcliffe, K., and Schmidt, K., 2011, Application of Inorganic Whole Rock Geochemistry to Shale Resource Plays; an Example from the Eagle Ford Shale Formation, Texas, HGS Northsiders Luncheon Meeting: Houston Geological Society Bulletin, v. 53, no. 8, p. 31-42.

Hill, R.T., 1901, Geography and geology of the Black and Grand prairies, Texas: United States Geological Survey Annual Report, v. 21, Part 7, 666 p.

Horowitz, A.J., 1991, A primer on sediment-trace element chemistry: Chelsea, Michigan, Lewis Publishers, 136 p.

Howard Weil Incorporated, 2011, Eagle Ford Shale-not all areas are created equal: http://www.howardweil.com/docs/Reports/OtherReports/EagleFordShale06-01-11.pdf (accessed October 2013).

Hughes, E.N., 2011, Chemostratigraphy and paleoenvironment of the Smithwick Formation, Fort Worth Basin, San Saba County, Texas [M.S. thesis]: Arlington, The University of Texas, 105 p.

Hunter, B.E., and Davies, D.K., 1979, Distribution of volcanic sediments in the Gulf Coastal province-significance to petroleum geology: Transactions - Gulf Coast Association of Geological Societies, v. 29, p. 147-155.

Jarvis, I., and Jarvis, K.E., 1992, Plasma spectrometry in the earth sciences; techniques, applications and future trends: Chemical Geology, v. 95, nos. 1-2, p. 1-33.

Jianwei Wang, and Yang Liu, 2011, Well performance modeling of Eagle Ford Shale oil reservoirs, North American Unconventional Gas Conference and Exhibition, The Woodlands, TX: http://www.onepetro.org/mslib/app/Preview.do?paperNumber=SPE-144427-MS# (accessed September 2013).

Kato, Y., Yamaguchi, K.E., and Ohmoto, H., 2006, Rare earth elements in Precambrian banded iron formations: Secular changes of Ce and Eu anomalies and evolution of atmospheric oxygen: Geological Society of America Memoirs, v. 198, p. 269-289.

Kauffman, E.G., 1977, Geological and biological overview: Western Interior Cretaceous basin: The Mountain Geologist, v. 14, nos. 3-4, p. 75-99.

Kearns, T.J., 2011, Chemostratigraphy of the Eagle Ford Formation [M.S. thesis]: Arlington, The University of Texas, 270 p.

Keller, G., 2005, Impacts, volcanism and mass extinction: random coincidence or cause and effect?: Australian Journal of Earth Sciences, v. 52, p. 725-757.

Kerr, A.C., 1998, Oceanic plateau formation: a cause of mass extinction and black shale deposition around the Cenomanian-Turonian boundary?: Journal of the Geological Society of London, v. 155, p. 619-626.

Kerr, A.C., White, R.V., Thompson, P. M. E., Tarney, J., and Saunders, A.D., 2003, No oceanic plateau— no Caribbean plate? The seminal role of an oceanic plateau in Caribbean plate evolution, *in* Bartolini, C., Buffler, R.T., and Blickwede, J., eds., The Circum-Gulf of Mexico and the Caribbean: Hydrocarbon habitats, basin formation, and plate tectonics: AAPG Memoir 79, p. 126-168.

Kuroda, J., Ogawa, N.O., Tanimizu, M., Coffin, M.F., Tokuyama, H., Kitazato, H., and Ohkouchi, N., 2007, Contemporaneous massive subaerial volcanism and late cretaceous Oceanic Anoxic Event 2: Earth and Planetary Science Letters, v. 256, p. 211-223.

Kuypers, M.M., Pancost, R.D., Nijenhuis, I.A., and Sinninghe Damste, J.S., 2002, Enhanced productivity led to increased organic carbon burial in the euxinic North

Atlantic basin during the late Cenomanian oceanic anoxic event: Paleoceanography, v. 17, no. 4, 1051, p. 3.1-3.13.

LeBas, M.J., LeMaitre, R.W., Streckeisen, A., and Zanettin, B., 1986, A chemical classification of volcanic rocks based on the total alkali-silica diagram: Journal of Petrology, v. 27, p. 745-750 *in* Carr, M., 2013, Igpet [computer software]: Rutgers University, New Jersey.

Lezin, C., Andreu, B., Pellenard, P., Bouchez, J., Emmanuel, L., Faure, P., and Landrein, P., 2013, Geochemical disturbance and paleoenvironmental changes during the early Toarcian in NW Europe: Chemical Geology, v. 341, p. 1-15.

Lock, B.E., Peschier, L., and Whitcomb, N., 2010, The Eagle Ford (Boquillas Formation) of Val Verde County, Texas-A window on the South Texas play: Gulf Coast Association of Geological Societies Transactions, v. 60, p. 419-434.

MacLeod, N., 2013, The great extinctions: what causes them and how they shape life: Buffalo, New York, Firefly Books, 208 p.

Matsutsuyu, R., 2011, South Texas Eagle Ford Shale geology-regional trends, recent learnings, future challenges, Hart Energy's Developing Unconventional Gas Conference, San Antonio, Texas: http://www.momentumog.com/documents/DUGEagleford2011Presentation.pdf (accessed May 2013).

Mazumdar, A., Banerjee, D.M., Schidlowski, M., and Balaram, V., 1999, Rare-earth elements and Stable Isotope Geochemistry of early Cambrian chert-phosphorite assemblages from the Lower Tal Formation of the Krol Belt (Lesser Himalaya, India): Chemical Geology, v. 156, p. 275-297.

McDonough, W.F., and Sun, S.S., 1995, The composition of the Earth: Chemical Geology, v. 120, p. 223-253.

Mcgarity, H.A., 2013, Facies and stratigraphic framework of the Eagle Ford Shale in South Texas [M.S. thesis]: Houston, University of Houston, 105 p.

McLennan, S.M., 1989, Rare earth elements in sedimentary rocks; influence of provenance and sedimentary processes: Reviews in Mineralogy, v. 21, p. 169-200.

Ming-Jung Jiang, 1989, Biostratigraphy and geochronology of the Eagle Ford shale, Austin chalk, and lower Taylor marl in Texas based on calcareous nannofossils. (Volumes I and II) [Ph.D. dissertation]: College Station, Texas A&M University, 524 p.

Moran, L.M., 2013, High resolution geochemistry of the Cretaceous Eagle Ford Shale, Bee County, Texas [M.S. thesis]: Arlington, The University of Texas, 56 p.

Moreman, W.L., 1942, Paleontology of the Eagle Ford group of North and central Texas: Journal of Paleontology, v. 16, no. 2, p. 192-220.

Mort, H.P., Adatte, T., Föllmi, K.B., Keller, G., Steinmann, P., Matera, V., Berner, Z., and Stüben, D., 2007, Phosphorus and the roles of productivity and nutrient recycling during oceanic anoxic event 2: Geology, v. 35, p. 483-486.

Pearce, T.J., Besly, B.M., Wray, D.S., and Wright, D.K., 1999, Chemostratigraphy: a method to improve interwell correlation in barren sequences-a case study using onshore Duckmantian/Stephanian sequences (West Midlands, U.K.): Sedimentary Geology, v. 124, p. 197-220.

Poulson, R.L., Siebert, C., McManus, J., and Berelson, W.M., 2006, Authigenic molybdenum isotope signatures in marine sediments: Geology, v. 34, no. 8, p. 617-620.

Railroad Commission of Texas, 2013, Wells completed and permitted in the Eagle Ford Shale Play, scale 1:40, 1 sheet: http://www.rrc.state.tx.us/eagleford (accessed August 2013).

Railroad Commission of Texas, 2013, Eagle Ford information: http://www.rrc.state.tx.us/eagleford (accessed September 2013).

Reaser, D.F. and Dawson W.C, 1995, Geologic Study of Upper Cretaceous (Cenomanian) Buda Limestone in Northeast Texas with Analysis of some Regional Implications: Gulf Coast Association of Geological Societies Transactions, v. 45, p. 495-502.

Rollinson, H.R., 1993, Using geochemical data: evaluation, presentation, interpretation, Harlow, Essex, England; New York, Longman Scientific & Technical; Copublished in the U.S. with J. Wiley & Sons, 352 p.

Ross, C.S., Miser, H.D., and Stephenson, L.W., 1929, Water-laid volcanic rocks of early upper cretaceous age in Southwestern Arkansas, Southeastern Oklahoma and Northeastern Texas: Washington, D.C., U.S. Government Printing Office, p. 175-202.

Rowe, H., Hughes, N., and Robinson, K., 2012, The quantification and application of handheld energy-dispersive X-ray fluorescence (ED-XRF) in mudrock chemostratigraphy and geochemistry: Chemical Geology, v. 324-325, p. 122-131.

Rowe, H., Ruppel, S.C., and Moran, L., 2013, A Cenomanian-Age deep continental shelf record of cyclical anoxia, Gulf of Mexico, South Texas: AAPG Annual Convention and Exhibition, Pittsburgh, Pennsylvania, *in* Search and Discovery, Article no. #30284, 31 p.:

http://www.searchanddiscovery.com/documents/2013/30284rowe/ndx_rowe.pdf (accessed November 2013).

Ruppel, S. C., Loucks, R. G., and Frebourg, G. (leaders), 2012, Guide to field exposures of the Eagle Ford-equivalent Boquillas Formation and related Upper Cretaceous Units in southwest Texas: Bureau of Economic Geology field guide, March 8-9, 2012, 151 p.

Sageman, B.B., and Arthur, M.A., 1994, Early Turonian paleogeographic/ paleobathymetric map, Western Interior, U.S., *in* Caputo, M., and Peterson, J., eds., Mesozoic Systems of the Rocky Mountain Region, U.S.: Rocky Mountain Section-SEPM Special Publication, p. 457-470.

Sageman, B.B., and Lyons, T.W., 2003, Geochemistry of fine-grained sediments and sedimentary rocks, *in* Mackenzie, F., ed., Treatise on Geochemistry, v.7, p. 115-158.

Sageman, B.B., Meyers, S.R., and Arthur, M.A., 2006, Orbital time scale and new C-isotope record for Cenomanian-Turonian boundary stratotype: Geology, v. 34, no. 2, p. 125-128.

Salacup, J. M., 2008, The Effects of Sea Level Change on the Molecular and Isotopic Composition of Sediments in the Cretaceous Western Interior Seaway: Oceanic Anoxic Event 3, Mesa Verde, CO, USA [M.S. Thesis]: Amherst, University of Massachusetts Amherst, 108 p.

Schijf, J., 1992, Aqueous geochemistry of the rare earth elements in marine anoxic basins [Ph.D. dissertation]: Rijksuniversiteit, Utrecht, the Netherlands, Geologica Ultraiectina, v. 85, 266 p.

Scott, R.W., 2010, Cretaceous stratigraphy, depositional systems, and reservoir facies of the Northern Gulf of Mexico: Gulf Coast Association of Geological Societies Transactions, v. 60, p. 597-610.

Sethi, P.S., Hannigan, R.E., and Leithold, E.L., 1998, Rare-earth element chemistry of Cenomanian-Turonian shales of the North American Greenhorn Sea, Utah *in* Schieber J., Zimmerle W. and Sethi P.S., eds., Shales and Mudstones: Stuttgart, Germany E. Schweizerbart'sche Verlagsbuchhandlung (Nägele u. Obermüller), p. 195-208.

Sinton, C.W., 1996, A tale of two large igneous provinces: geochronological and geochemical studies of the North Atlantic Volcanic Province and the Caribbean Oceanic Plateau, [Ph.D. dissertation]: Corvallis, Oregon State University, 191 p.

Sinton, C.W., Duncan, R.A., 1997, Potential links between ocean plateau volcanism and global ocean anoxia at the Cenomanian-Turonian boundary: Economic Geology, v. 92, nos. 7-8, p. 836-842.

Smith, R.K., and Gray, W., 2011, Geochemistry and petrogenesis of Mesoproterozoic (~1.1 Ga) magmatic enclaves in granites of the Eastern Llano Uplift, central Texas, USA: Lithos, v. 125, nos. 1-2. p. 463-481.

Surles, M.A. Jr., 1987, Stratigraphy of the Eagle Ford Group (Upper Cretaceous) and its source-rock potential in the East Texas Basin: Baylor Geological Studies Bulletin, no. 45, 57 p.

Taylor, S.R., and McLennan, S.M., 1985, The continental crust, its composition and evolution: an examination of the geochemical record preserved in sedimentary rocks: Oxford; Boston, Blackwell Scientific, 312 p.

Tinnin, B., Hildred, G., and Martinez, N., 2013, Expanding the Application of Chemostratigraphy within Cretaceous Mudrocks: Estimating Total Organic

Carbon and Paleoredox Facies using Major, Minor and Trace Element Geochemistry, Unconventional Resources Technology Conference, Denver, Colorado, p. 1213-1222: http://dx.doi.org/10.1190/urtec2013-123 (accessed August, 2013).

Tribovillard, N., Algeo, T.J., Lyons, T., and Riboulleau, A., 2006, Trace metals as paleoredox and paleoproductivity proxies: an update: Chemical Geology, v. 232, p.12-32.

Tucker, M. E., 2001, Sedimentary petrology: an introduction to the origin of sedimentary rocks: Oxford; Malden, MA, Blackwell Science, 262 p.

Turgeon, S., and Brumsack, H., 2006, Anoxic vs. dysoxic events reflected in sediment geochemistry during the Cenomanian-Turonian boundary event (Cretaceous) in the Umbria-Marche Basin of central Italy: Chemical Geology, v. 234, p. 321-339.

Turgeon, S.C., and Creaser, R.A., 2008, Cretaceous oceanic anoxic event 2 triggered by a massive magmatic episode: Nature, v. 454, p. 323-326.

Tuttle, S., 2010, Oil Resource Plays-Examples and Technology, Houston Chapter – Society of Independent Professional Earth Scientists, Meeting, Houston, Texas: http://www.sipeshouston.org/presentations/Tuttle%27s%20SIPES%20Presentation_Final%20Presentation_09232010.pdf (accessed October 2013).

U.S. Energy Information Administration, 2010, Eagle Ford Shale Play, Western Gulf Basin, South Texas, scale 1:50, 1 sheet: http://www.eia.gov/oil_gas/rpd/shaleusa9.pdf (accessed September 2013).

U.S. Energy Information Administration, 2011, Shale gas and oil plays lower 48 states, scale 1:400, 1 sheet: http://www.eia.gov/oil_gas/rpd/shale_gas.pdf (accessed September 2013).

Vail, P.R., Mitchum, R.M. Jr., and Thompson, S. III, 1977, Seismic stratigraphy and global changes of sea level: Part 3. Relative changes of sea level from coastal onlap: Section 2. Application of Seismic Reflection Configuration to Stratigrapic Interpretation AAPG Memoir 26, p. 63-81.

Walker, J.D., Geissman, J.W., Bowring, S.A., and Babcock, L.E., compilers, 2012, Geologic Time Scale v. 4.0: Geological Society of America: http://www.geosociety.org/science/timescale/timescl.pdf (accessed October 2013).

Waters, J.A., McFarland, P.W., and Lea, J.W., 1955, Geologic framework of the Gulf Coastal Plain of Texas: AAPG Bulletin, v. 39, no.9, p. 1821-1850.

Wedepohl, K.H., 1971, Environmental influences on the chemical composition of shales and clays: Physics and Chemistry of the Earth, v. 8, p. 305-333.

White, W.M., 2013, Geochemistry: Oxford, U.K., Blackwell-Wiley, 672 p.

Wignall, P.B., 2001, Large igneous provinces and mass extinctions: Earth-Science Reviews, v. 53, p. 1-33.

Wilde, P., Quinby-Hunt, M.S., and Erdtmann, B., 1996, The whole-rock cerium anomaly: a potential indicator of eustatic sea-level changes in shales of the anoxic facies: Sedimentary Geology, v. 101, nos. 1-2, p. 43-53.

Wilson, S.A., 2001, U.S. Geological Survey Certificate of Analysis-Green River Shale, SGR-1: U.S. Geologic Survey: http://minerals.cr.usgs.gov/geo_chem_stand/shale.html (accessed March 2013).

Winter, J.D., 2010, Principles of igneous and metamorphic petrology: Upper Saddle River, New Jersey, Pearson Prentice Hall, 702 p.

Workman, S.J., 2013, Integrating depositional facies and sequence stratigraphy in characterizing unconventional reservoirs: Eagle Ford Shale, South Texas [M.S. thesis]: Kalamazoo, Western Michigan University, 153 p.

Yan Zheng, Anderson, R.F., van Geen, A., and Kuwabara, J.S., 2000, Authigenic molybdenum formation in marine sediments: a link to pore water sulfide in the Santa Barbara Basin: Geochimica et Cosmochimica Acta, v. 64, no. 24, p. 4165-4178.

Yao Tian, Ayers, W.B., and McCain, W.D. Jr., 2012, Regional analysis of stratigraphy, reservoir characteristics, and fluid phases in the Eagle Ford Shale, South Texas: Gulf Coast Association of Geological Societies Transactions, v. 62, p. 471-483.

Biographical Information

Shariva Darmaoen was born in Paramaribo, Suriname and moved to the U.S.A in 1996. After graduating from high school, Shariva travelled around the world as a flight attendant for a small charter company. Impressed by the natural beauty of different countries and their intriguing cultures, she decided to study geology and geography in college. She obtained a Bachelor of Science degree in Geology from Florida Atlantic University in December 2011 with a minor in geography and GIS. In January 2012, Shariva entered the Graduate School at the University of Texas at Arlington to pursue a Master of Science in Geology degree. Her personal research interests include the development of hydrocarbon plays; particularly oil and gas development of the Eagle-Ford Shale and other OAE 2 black shales. Her future plans are to work as a Petroleum Geologist.

Contact e-mail: sdarmaoen@gmail.com